

DOCTORAL THESIS

Development of a co-culture model of the human lungs for toxicity testing and identification of biomarkers of inhalation toxicity

Rachel Willetts

If you have discovered material in AURA which is unlawful e.g. breaches copyright, (either yours or that of a third party) or any other law, including but not limited to those relating to patent, trademark, confidentiality, data protection, obscenity, defamation, libel, then please read our takedown policy at <http://www1.aston.ac.uk/research/aura/aura-take-down-policy/> and contact the service immediately eprints@aston.ac.uk.

**Development of a co-culture model of the human lungs for
toxicity testing and identification of biomarkers of inhalation
toxicity**

Rachel S Willetts

Doctor of Philosophy

Aston University

2011

This copy of this thesis has been supplied on the condition that anyone who consults it is understood to recognise that its copyright rests with its author and that no quotation from this thesis and no information derived from it may be published without proper acknowledgement.

Summary

The airway epithelium is the first point of contact in the lung for inhaled material, including infectious pathogens and particulate matter, and protects against toxicity from these substances by trapping and clearance via the mucociliary escalator, presence of a protective barrier with tight junctions and initiation of a local inflammatory response. The inflammatory response involves recruitment of phagocytic cells to neutralise and remove and invading materials and is often modelled using rodents. However, development of valid *in vitro* airway epithelial models is of great importance due to the restrictions on animal studies for cosmetic compound testing implicit in the 7th amendment to the European Union Cosmetics Directive. Further, rodent innate immune responses have fundamental differences to human. Pulmonary endothelial cells and leukocytes are also involved in the innate response initiated during pulmonary inflammation. Co-culture models of the airways, in particular where epithelial cells are cultured at air liquid interface with the presence of tight junctions and differentiated mucociliary cells, offer a solution to this problem. Ideally validated models will allow for detection of early biomarkers of response to exposure and investigation into inflammatory response during exposure. This thesis describes the approaches taken towards developing an *in vitro* epithelial/endothelial cell model of the human airways and identification biomarkers of response to exposure to xenobiotics. The model comprised normal human primary microvascular endothelial cells and the bronchial epithelial cell line BEAS-2B or normal human bronchial epithelial cells. BEAS-2B were chosen as their characterisation at air liquid interface is limited but they are robust in culture, thereby predicted to provide a more reliable test system. Proteomics analysis was undertaken on challenged cells to investigate biomarkers of exposure.

BEAS-2B morphology was characterised at air liquid interface compared with normal human bronchial epithelial cells. The results indicate that BEAS-2B cells at an air liquid interface form tight junctions as shown by expression of the tight junction protein zonula occludens-1. To this author's knowledge this is the first time this result has been reported. The inflammatory response of BEAS-2B (measured as secretion of the inflammatory mediators interleukin-8 and -6) air liquid interface mono-cultures to *Escherichia coli* lipopolysaccharide or particulate matter (fine and ultrafine titanium dioxide) was comparable to published data for epithelial cells. Cells were also exposed to polymers of "commercial interest" which were in the nanoparticle range (and referred to particles hereafter). BEAS-2B mono-cultures showed an increased secretion of inflammatory mediators after challenge. Inclusion of microvascular endothelial cells resulted in protection against LPS- and particle- induced epithelial toxicity, measured as cell viability and inflammatory response, indicating the importance of co-cultures for investigations into toxicity. Two-dimensional proteomic analysis of lysates from particle-challenged cells failed to identify biomarkers of toxicity due to assay interference and experimental variability. Separately, decreased plasma concentrations of serine protease inhibitors, and the negative acute phase proteins transthyretin, histidine-rich glycoprotein and alpha₂-HS glycoprotein were identified as potential biomarkers of methyl methacrylate/ethyl methacrylate/butylacrylate treatment in rats.

Key words Co-culture, air-liquid interface, lipopolysaccharide, titanium dioxide and proteomics

Dedication

I would like to dedicate this thesis to Katie Bodley for getting me through the last 10 years. I love you xx

Acknowledgements

Firstly I would like to thank my supervisors Prof Helen R Griffiths and Dr Lindsay J Marshall for their continual support and endless patience. I would also like to thank Dr Phil Carthew, Dr Samantha Fletcher and Dr Leona Merrola for their support and academic discussion during my PhD. I would like to thank Dr Andrew Devitt and Liz Torr for assistance in fluorescent microscopy, Prof Yvonne Parrie and Dr Malou Henrikeson for assistance in particle sizing and Zeta potential measurements, Prof Peter A Lambert for assistance in LPS isolation and Dr Chris Dunston for assistance in peptide digestion. I would also like to thank all my colleagues in labs 331 and 358 for their support during the last 4 years.

LC-MS/MS was completed by Dr Cleidiane G Zampronio and colleagues at Brimingham University *through the Birmingham Science City Translational Medicine: Experimental Medicine Network of Excellence project*, with support from Advantage West Midlands (AWM). *In vivo* particle treatment was conducted by Dr Birgit Gaiser.

On a personal note I would like to thank Chris for all the laughs, brummie insults and for letting my hide in “his office” during melt downs, I would not have got through the last 4 years without you. My Dad and Step-Mother Helen, for all their support, special thanks to Helen for all the help with science revision. My partner Dave for putting up with all my mad stressful rants during the writing of this thesis, and my son Oliver, for all the smiles and cuddles (even when I missed your bed time).

And finally, thank you Katie, for everything!

List of Contents

Title Page	1
Thesis summary	2
Dedication	3
Acknowledgements	4
List of Contents	5
List of Figures	14
List of Tables	18
Abbreviations	19
Chapter 1: Introduction	23
1.1: Structure of the respiratory system	24
1.1.1: Airways epithelium	24
1.1.2: Cytokeratin profiles of airways epithelium	27
1.1.3: Tight junctions	28
1.1.4: Mucin	29
1.2: Inflammation	30
1.2.1: Inflammatory respiratory diseases	30
1.2.2: Role of airways epithelium in innate immune response	32
1.2.3: Role of the endothelium in the innate immune response	34
1.2.4: Role of leukocytes in the innate immune response	34
1.2.4.1: Neutrophils and the innate immune response	35
1.3: LPS and PM induce innate immune response in airways epithelium	37
1.3.1: LPS	37
1.3.1.1: General structure	37
1.3.1.2: LPS/TLR signalling	39
1.3.2: Particles	39
1.3.3: PM induced ROS and inflammatory signalling	39
1.3.4: Glutathione and redox homeostasis	40

1.4: IL-8 and IL-6 in airway pathologies	42
1.5: PM and airway pathologies and links to CVD	43
1.6: Animal models of respiratory pathologies	44
1.6.1: Immunological variance between human and animal lung Immunity	44
1.7: Epithelial cell models	45
1.7.1: Inflammatory responses of airway epithelium <i>in vitro</i> to LPS exposure	47
1.8: Titanium dioxide	47
1.8.1: Inflammatory and cytotoxic effects of TiO ₂ on airways epithelium <i>in vitro</i>	48
1.8.2: Cellular uptake of TiO ₂	49
1.8.3: Translocation of TiO ₂ particles	49
1.9: Co-culture	50
1.10: Biomarkers	51
1.11: Proteomics	52
1.11.1: Two Dimensional electrophoresis	52
1.11.2: Statistical analysis of spot expression changes between treatments	53
1.11.3: Digestion of proteins of interest	54
1.11.4: Mass Fingerprinting using mass spectrometry	54
1.12: Challenges in airway proteomics	56
1.13: Aim and objectives	57
Chapter 2: Materials and Methods	58
2.1: Materials	58
2.1.1: General Consumables	58
2.1.2: Particles	58
2.1.3: Antibodies	59
2.2: Methods	60
2.2.1: Cell culture	60

2.2.1.1: Epithelial cell culture	60
2.2.1.2: Epithelial culture on Transwell® inserts	61
2.2.1.3: HPMEC culture	61
2.2.1.4: Co-culture of BEAS-2B cells and HPMEC cells	61
2.2.2: TER	62
2.2.3: FITC-dextran permeability measurements	62
2.2.4: Endotoxin determination of LPS and particle by LAL assay	62
2.2.5: IL-8/IL-6 Enzyme-linked immunosorbent assay (ELISA)	63
2.2.6: CellTiter-Blue® viability assay	64
2.2.7: Effect of LPS or particle treatment on BEAS-2B TER	64
2.2.8: Statistical Analysis	65
Chapter 3	66
3.1: Rational	67
3.2: Introduction	68
3.3: Methods	70
3.3.1: Characterisation of epithelial cell and endothelial cell cultures	70
3.3.2: TER and FITC-dextran permeability measurements	70
3.3.3: Mucin identification using antibodies to muc5AC	71
3.3.4: Barrier integrity of BEAS-2B cultured in endothelial cell culture media	71
3.3.5: Co-culture of BEAS-2B cells and HPMEC cells	71
3.4: Results:	72
3.4.1: Submerged populations of BEAS-2B express both epithelial cell markers cytokeratin 5 and cytokeratin 8	72
3.4.2: BEAS-2B cultured at ALI express both basal and differentiated epithelial cell markers	74
3.4.3: BEAS-2B cultured at ALI express the tight junction protein ZO-1 at the site of cell-cell contact	76
3.4.4: TER of BEAS-2B increases significantly and FITC-dextran	

permeability decreases significantly during culture at ALI	78
3.4.5: NHBE cultured at ALI secrete Muc5AC	81
3.4.6: Evidence for EMT in NHBE cultures	83
3.4.7: Expression of VWF in HPMEC cells	85
3.4.8: BEAS-2B cultured at ALI in endothelial cell medium	
maintain barrier integrity	87
3.5: Discussion	89
3.6: Conclusion	93
Chapter 4:	95
4.1: Rationale	96
4.2: Introduction	97
4.3: Methods	99
4.3.1: LPS isolation from <i>P. aeruginosa</i> and <i>B. cepacia</i>	99
4.3.2: LPS endotoxin content determination by LAL assay	100
4.3.3: Cell culture	100
4.3.3.1: BEAS-2B and HPMEC cell mono-cultures	100
4.3.3.2: Co-culture of BEAS-2B cells and HPMEC cells	100
4.3.4: LPS treatment	100
4.3.5: IL-8/IL-6 ELISA	101
4.3.6: CellTiter-Blue [®] assay	101
4.3.7: Barrier integrity measurements using ZO-1 staining	101
4.3.8: Statistical Analysis	102
4.4: Results	103
4.4.1: Endotoxin content of LPS isolates	103
4.4.2: <i>E. coli</i> and <i>P. aeruginosa</i> S:10 induce IL-6 secretion from	
submerged cultures of BEAS-2B	105
4.4.3: Viability of submerged BEAS-2B is not effected by	
LPS-challenge	108
4.4.4: BEAS-2B at ALI mount an inflammatory response after	

apical <i>E. coli</i> LPS challenge	110
4.4.5: Viability of BEAS-2B cultured at ALI is not affected by LPS challenge	112
4.4.6: BEAS-2B barrier remains intact with LPS stimulation	114
4.4.7: Apical <i>E. coli</i> LPS treatment disrupts ZO-1 localisation in BEAS-2B cultured at ALI	116
4.4.8: IL-8 secretion is increased significantly from LPS challenged HPMEC	118
4.4.9: Stimulation with <i>E. coli</i> LPS does not affect HPMEC viability	120
4.4.10: IL-8 and IL-6 secretion from BEAS-2B/HPMEC co-culture is not effected by <i>E. coli</i> LPS challenge	122
4.4.11: BEAS-2B/HPMEC co-culture viability is not affected by <i>E. coli</i> LPS challenge	124
4.5: Discussion	126
4.6: Conclusion	132
Chapter 5:	133
5.1: Rationale	134
5.2: Introduction	135
5.3: Methods	137
5.3.1: Particles	137
5.3.2: Epithelial cell culture of Transwell® inserts	137
5.3.3: Co-culture of BEAS-2B and HPMEC	137
5.3.4: Endotoxin content determination of particle by LAL assay	137
5.3.5: Zeta potential and particle size	137
5.3.6: Particle treatment of BEAS-2B cells in mono- or co-culture	138
5.3.7: CellTiter-Blue® viability assay	138
5.3.8: IL-8/IL-6 ELISA	139
5.3.9: Isolation of primary human neutrophils with a discontinuous percoll™ gradient	139

5.3.10: Respiratory burst assay	140
5.3.11: GSH-Glo™ GSH assay for quantification of reduced GSH	140
5.3.12: Statistical Analysis	141
5.4: Results	142
5.4.1: Particle characteristics	142
5.4.2: S2429901 induces increased IL-6 secretion to the apical and basolateral compartment of BEAS-2B cultured at ALI	145
5.4.3: S2429901 reduces the priming effect of IL-8 on fMLP induced respiratory burst in neutrophils	148
5.4.4: UFTiO ₂ decreases BEAS-2B viability but other particles have no effect	150
5.4.5: UFTiO ₂ results in a loss of cellular GSH content in BEAS-2B	152
5.4.6: Particles have no effect on BEAS-2B barrier integrity	154
5.4.7: Particle treatment does not induce an inflammatory response in HPMEC	156
5.4.8: TiO ₂ and UFTiO ₂ reduce HPMEC viability	158
5.4.9: Particle treatment does not induce oxidative stress in HPMEC	160
5.4.10 S2429901, but none of the other particles tested, induces IL-6 secretion to the apical compartment of the BEAS-2B/HPMEC co-culture	162
5.4.11: BEAS-2B/HPMEC co-culture viability is not affected by particle exposure	165
5.5: Discussion	167
5.6: Conclusion	173
Chapter 6:	174
6.1: Rationale	175
6.2: Introduction	176
6.3: Methods	178
6.3.1: Endotoxin content of particles by LAL assay	178

6.3.2: TiO ₂ depletion from TiO ₂ -treated BEAS-2B cell lysates or BSA samples	178
6.3.3: Proteomic analysis	178
6.3.4: Analysis of protein spots by Progenesis SameSpots	179
6.3.5: Polymer treated rats	180
6.3.6: BCA assay for protein determination	181
6.3.7: Proteomic analysis of pooled plasma	182
6.3.8: Protein digestion from gel pieces	182
6.3.9: LC-MS/MS	183
6.4: Results	184
6.4.1: Development of an optimal method of particle clearance from cell lysates	184
6.4.2: 2-DE analysis following centrifugation for removal of TiO ₂ resulted in areas of protein loss from gels	186
6.4.3: Proteomic analysis of lysates from TiO ₂ and UFTiO ₂ -treated BEAS-2B resulted in poorly resolved gels	188
6.4.4: Proteomic analysis of BEAS-2B cultured at ALI	190
6.4.5: 2-DE analysis of pooled plasmas identified a total of 80 spots with differential expression	192
6.4.6: PCA analysis of protein spots from plasmas of rats treated with differing doses of polymer 020310 or MM/EM/BA	194
6.4.7: Differentially expressed protein spots in positive control MM/EM/BA-treated animals compared to negative control animals	196
6.4.8: Effect of polymer 020310-dose on the rat plasma proteome following 9 weeks recovery or 22 weeks recovery	199
6.4.9: MS/MS identification of significantly altered spots from polymer treated rats	202
6.5: Discussion	210

List of Figures

Chapter 1

- Figure 1.1:** The morphology of the respiratory epithelium 26
- Figure 1.2:** The structure of epithelial tight junctions 29
- Figure 1.3:** Role of neutrophils in the innate immune response 36
- Figure 1.4:** Structure of LPS 38
- Figure 1.5:** Inflammatory signalling induced by LPS and PM 41
- Figure 1.6:** PCA analysis plot 54
- Figure 1.7:** Schematic of b and y ions 55

Chapter 3

- Figure 3.1:** Schematic diagram of BEAS-2B/HPMEC 69
- Figure 3.2:** Submerged populations of BEAS-2B express both epithelial cells markers cytokeratin 5 and cytokeratin 8 73
- Figure 3.3:** BEAS-2B cultured at ALI express both basal and differentiated epithelial cell markers 75
- Figure 3.4:** BEAS-2B cultured at ALI express the tight junction protein ZO-1 at the site of cell-cell contact 77
- Figure 3.5:** TER of BEAS-2B, but not NHBE, increases significantly and FITC-dextran permeability decreases significantly during culture at ALI 79
- Figure 3.6:** NHBE cultured at ALI secrete muc5AC 82
- Figure 3.7:** Evidence for EMT in NHBE cultures 84
- Figure 3.8:** Expression of VWF in HPMEC cells 86
- Figure 3.9:** BEAS-2B cultured at ALI in endothelial cell medium maintain barrier integrity 88

Chapter 4

- Figure 4.1:** *E. coli* and *P. aeruginosa* S:10 induce IL-6 secretion from submerged cultures of BEAS-2B 107
- Figure 4.2:** Viability of submerged BEAS-2B is not effected by LPS-challenge 109

Figure 4.3: BEAS-2B at ALI mount an inflammatory response after apical <i>E. coli</i> LPS challenge	111
Figure 4.4: Viability of BEAS-2B cultured at ALI is not affected by LPS challenge	113
Figure 4.5: BEAS-2B barrier remains intact with LPS stimulation	115
Figure 4.6: Apical <i>E. coli</i> LPS treatment disrupts ZO-1 localisation in BEAS-2B cultured at ALI	117
Figure 4.7: IL-8 secretion is increased significantly from LPS challenged HPMEC	119
Figure 4.8: LPS stimulation does not affect HPMEC viability	121
Figure 4.9: IL-8 and IL-6 secretion from BEAS-2B/HPMEC co-culture is not effected by <i>E. coli</i> LPS challenge	123
Figure 4.10: BEAS-2B/HPMEC co-culture viability is not affected by <i>E. coli</i> LPS challenge	125
 Chapter 5:	
Figure 5.1: S2429901 induces increased IL-6 secretion to the apical and basolateral compartment of BEAS-2B cultured at ALI	147
Figure 5.2: S2429901 induces the priming effect of IL-8 on fMLP induced respiratory burst in neutrophils	149
Figure 5.3: UFTiO ₂ decreases BEAS-2B viability but TiO ₂ and particles have no effect	151
Figure 5.4: UFTiO ₂ results in a loss of cellular GSH content in BEAS-2B	153
Figure 5.5: Particles have no effect on BEAS-2B barrier integrity	155
Figure 5.6: Particle treatment does not induce an inflammatory response in HPMEC	157
Figure 5.7: TiO ₂ and UFTiO ₂ reduce HPMEC viability	159
Figure 5.8: Particle treatment does not induce oxidative stress	

in HPMEC	161
Figure 5.9: S2429901 induces IL-6 secretion to the apical compartment of the BEAS-2B/HPMEC co-culture	164
Figure 5.10: BEAS-2B/HPMEC co-culture viability is not affected by particle exposure	166
Chapter 6:	
Figure 6.1: 2-DE analysis following centrifugation for removal of TiO ₂ resulted in areas of protein loss from gels	187
Figure 6.2: Proteomic analysis of lysates from TiO ₂ and UFTiO ₂ -treated BEAS-2B resulted in poorly resolved gels	189
Figure 6.3: Proteomic analysis of BEAS-2B cultured at ALI treated with test particles	191
Figure 6.4: 2-DE analysis of pooled plasmas identified a total of 80 spots confirmed as protein spots	193
Figure 6.5: Differentially expressed protein spots in positive control MM/EM/BA-treated animals compared to negative control animals	197
Figure 6.6: Effect of polymer 020310-dose on the rat plasma proteome following 9 weeks recovery or 22 weeks recovery	200
Figure 6.7: MS/MS identification of significantly altered spots from polymer treated rats	203
Chapter 8	
Figure 8.1: Schematic diagram of proposed adhesion assay	231
Chapter 10	
Figure 10.1: Cytokeratin filaments are detected with an antibody dilution of 1:250	257
Figure 10.2: Optimising fixing and blocking conditions	259
Figure 10.3: Determining the specificity of the immunohistochemical method	261

Figure 10.4: Heat denaturing or deglycosylation is not required for muc5AC detection by dot blot	265
Figure 10.5: HRP-conjugated sheep anti-mouse secondary antibody at a dilution of 1:1000 cross reacts with serum free airway epithelial cell medium	267
Figure 10.6: HRP-conjugated sheep anti-mouse secondary antibody diluted 1:5000 shows minimal cross reaction with serum free airway epithelial cell medium	269
Figure 10.7: HRP-conjugated sheep anti-mouse secondary antibody diluted 1:5000 allows for detection of 1.25µg muc5AC	271
Figure 10.8: UFTiO ₂ treated IL-8 is not detected by IL-8 ELISA	275
Figure 10.9: Particle-treated IL-6 is detected by IL-6 ELISA	277
Figure 10.10: S2218600 and S2429901 reduce the CellTiter-Blue [®] signal significantly	279
Figure 10.11: The presence of particles does not affect TER acquisition	281
Figure 10.12: The lucigenin signal is not affected by particles	283
Figure 10.13: Effect of particle treatment on GSH	285

List of Tables

Chapter 1

Table 1.1: Airway epithelial cells and inflammatory mediator secretion	33
---	----

Chapter 4

Table 4.1: Endotoxin content of LPS isolates	104
---	-----

Chapter 5:

Table 5.1: Preparation of Percoll™ solutions for a discontinuous gradient	139
Table 5.2: Particle characteristics	144
Table 5.3: Titanium dioxide Zeta charge analysis	144

Chapter 6:

Table 6.1: Analysis design for rat plasma samples	181
Table 6.2: Recovery of BSA after treatments with TiO ₂ , 1% (v/v) Tween-20 and 1mM DTT and separation through 100kDa cut off filters	185
Table 6.3: Protein recovery from <100kDa fraction of filtered lysates	185
Table 6.4: Polymer 020310-treatment-sensitive spots that showed a significant expression change by ANOVA (P<0.05) and statistical power analysis (>0.8)	195
Table 6.5: Protein identifications for Spot 134	204
Table 6.6: Protein identification for Spot 125	205
Table 6.7: Protein identification for Spot 426	206
Table 6.8: Protein identification for Spot 368	207
Table 6.9: Protein identification for Spot 151	208
Table 6.10: Spots chosen for protein identification	214

Abbreviations

2-DE	two-dimensional electrophoresis
ALI	air-liquid interface
AP-1	activator protein-1
BAL	bronchial/bronchio-alveolar lavage
<i>B. cepacia</i>	<i>Burkholderia cepacia</i>
BSA	bovine serum albumin
BSF-2	B-cell stimulatory factor
BSO	L-buthionine sulfoxamine
C/EBP β	CCAAT/enhancer binding protein β
CF	Cystic Fibrosis
CFTR	Cystic Fibrosis transmembrane conductance regulator
CID	collision induced dissociation
COPD	chronic obstructive pulmonary disease
CVD	cardiovascular disease
DAPI	4',6-diamidino-2-phenylindole
DEP	diesel exhaust particles
DTT	dithiothreitol
ECIS	electrical cell substrate impedance sensing
ECL	enhanced chemiluminescent substrate
ECM	extracellular matrix
<i>E. coli</i>	<i>Escherichia coli</i>
EDTA	ethylenediaminetetraacetic acid
ELISA	Enzyme-linked immunosorbent assay
EM	emission
EMT	epithelial to mesenchymal transition
ESI	electrospray ionisation
EU	endotoxin unit

EX	excitation
FCS	foetal calf serum
FEV ₁	forced expiratory volume in one second
FGF	fibroblast growth factor
FITC	fluorescein isothio-cyanate
fMLP	N-formyl-methionine-leucine-phenylalanine
FSP	fibroblast specific protein
GM-CSF	granulocyte macrophage colony stimulating factor
GSH	reduced glutathione
GST	glutathione-S-transferase
HGF	hepatocyte growth factor
HPLC	high performance liquid chromatography
HPMEC	human pulmonary microvascular cells
HRP	horse radish peroxidase
HUVEC	human umbilical endothelial cells
IFN γ	interferon γ
IL	interleukin
IPF	idiopathic pulmonary fibrosis
IPG	immobilised pH gradients
JAM	junctional adhesion molecule
Kdo	2-keto-deoxyoctonic acid
LAL	limulus ameocyte lysate
LBP	LPS binding protein
LC-MS/MS	liquid chromatography-mass spectrometry/mass spectrometry
LPS	lipopolysaccharide
MALDI	matrix-assisted laser desorption ionisation
MCP	monocyte chemotactic species
M-CSF	macrophage colony stimulating factor
MDDC	monocyte derived dendritic cells

MDM	monocyte derived macrophages
MyD88	myeloid differentiation primary response gene 88
<i>mz</i>	mass to charge ratio
MAPK	mitogen-activated protein kinase
MDNCF	monocyte-derived neutrophil chemotactic factor
MM/EM/BA	methyl methacrylate/ethyl methacrylate/butylacrylate
MUC	mucin
NF-κB	nuclear factor-κB
NHBE	normal human bronchial epithelial cells
NP	nanoparticle
OPD	o-phenylenediamine
<i>P. aeruginosa</i>	<i>Pseudomonas aeruginosa</i>
PAMP	pathogen associated molecular patterns
PBS	phosphate buffered saline
PCA	principle component analysis
pI	iso-electric point
PM	particulate matter
PM _{2.5}	PM with a mean diameter <2.5μm
PM ₁₀	PM with a mean diameter <10μm
pNA	p-nitroaniline
PRR	pattern recognition receptors
PTM	post-translational modification
QAEM	quiescent airway epithelial cell medium
RANTES	regulated upon activation, normal T cell expressed and secreted
RNS	reactive nitrogen species
ROFA	residual oil fly ash
ROS	reactive oxygen species
SD	standard deviation
SDS	sodium dodecyl sulfate

SEM	standard error of the mean
Serpin	serine protease inhibitor
sIgA	secretory immunoglobulin A
SP	surfactant protein
TER	transepithelial electrical resistance
TGF	transforming growth factor
TiO ₂	titanium dioxide
TLR	toll like receptor
TNF α	tumour necrosis factor α
TOF	time of flight
TTBS	Tris buffered saline with 0.05% (v/v) Tween-20
UFTiO ₂	ultrafine titanium dioxide
VEGF	vascular endothelial growth factor
v/v	volume/volume
VWF	Von Willebrand Factor
w/v	weight/volume
ZO	Zonula Occludens

Chapter 1. Introduction

Host defences against foreign materials, such as pathogens, toxic chemicals and particulates are achieved by a range of innate physicochemical, humoral and cell mediated mechanisms. In mammals, the mucosal and epithelial surfaces are the first point of contact of exposures and are therefore often specialised to defend against insult and are able to initiate an immune response after noxious exposure.

The airway epithelium secretes antimicrobial peptides and mucus which work with cilia to protect the airways from pathogenic invasion (Tortora and Graboswki, 1993). Airway epithelial cells are anchored to a basement membrane that is enriched in extracellular matrix proteins, termed the extracellular matrix (ECM), which supports epithelial cell attachment, survival and morphology. Comprised of adhesive glycoproteins (including fibronectin and laminin), structural proteins (including collagen and elastin) and proteins involved in ECM homeostasis (for example hyaluronan) (Schulz & Wysocki, 2009) the ECM also functions in epithelial cell wound repair. ECM-mediated epithelial wound repair is aided by the ability of the ECM to sequester growth factors including fibroblast growth factor (FGF)-2 and vascular endothelial growth factor (VEGF) (Schulz & Wysocki, 2009) and other mediators such as cytokines including tumour necrosis factor (TNF)- α (Vaday & Lider, 2000). The growth factor hepatocyte growth factor (HGF) is also sequestered by the ECM and functions in epithelial cells proliferation and differentiation (Ito *et al.*, 2005) and has anti-inflammatory properties (Skibinski *et al.*, 2007).

Ambient air contains noxious material such as pathogens and particulates from several sources including; endotoxins such as LPS which is shed from gram negative bacteria, combustion particulates and particulates liberated from cleaning products and cosmetic products. Endotoxin levels emitted from humidifiers alone are up to $0.39\mu\text{g}/\text{m}^3$, and it is estimated that cleaning products contribute to >32 tonnes volatile organic particulates worldwide per day (Nazaroff & Weschler, 2004). Further, the UK acceptable air pollution levels of respirable PM with a mean diameter of $10\mu\text{m}$ (PM₁₀) is $50\mu\text{g}/\text{m}^3$ (DEFRA). The average adult respire 12,000 litres of air per day (Rogers, 2007),

protective mechanisms in the airways are therefore required to prevent airways damage after inhalation exposure.

1.1. Structure of the respiratory system

The respiratory system comprises of a conducting portion and a respiratory portion. The conducting portion includes the trachea, bronchi and terminal bronchioles and transfers inspired air into the alveolar region of the lungs. The trachea divides into the primary bronchi which enter the lung and further divide into smaller secondary bronchi, which again divide into smaller (tertiary) bronchi and then bronchioles (Tortora & Grabowski, 1993). This division continues and is termed the bronchial tree; the last “branches” are the terminal bronchioles. The respiratory portion includes the bronchioles, alveolar ducts and alveoli, and is where gas exchange occurs (Tortora & Grabowski, 1993). Structurally the trachea is composed of hyaline cartilage, smooth muscle fibres and elastic connective tissue which provide firm support to prevent collapse. The supportive incomplete rings of cartilage become cartilage sheets in the bronchi which are replaced entirely by smooth muscle in the bronchioles. The terminal bronchioles further divide into the respiratory bronchioles and alveolar ducts (Tortora & Grabowski, 1993). A protective epithelial cell layer lines the entire respiratory tract, the morphology of the epithelial layers changes throughout the respiratory tract and reflects a change in function.

1.1.1 Airway epithelium

The tracheal and bronchial epithelium is formed of pseudostratified differentiated muco-ciliary epithelial cells (Tortora & Grabowski, 1993), anchored to the basement membrane by a basal epithelial cell layer. The basal epithelial cells also act as cell progenitors which are able to differentiate and replace muco-ciliary epithelial cells during injury (Erjefalt *et al.*, 2007; Lazard *et al.*, 2009; Plopper *et al.*, 1992). The morphology of the epithelium alters throughout the respiratory tract (Figure 1.1), secretory and ciliated epithelial cells predominate the upper airways and are absent in the bronchioles. Goblet cells synthesise, store and secrete mucin granules which absorb water to form the mucus layer covering the upper respiratory tract. This mucus is

cleared by the beating action of cilia from ciliated cells (Fahy & Dickey, 2010). Submucosal glands are also present in the upper airways and contains serous and mucus secreting cells. The serous cells secrete antimicrobial proteins (Reviewed in Fahy & Dickey, 2010). Simple cuboidal epithelial cells and secretory Clara cells are present in the bronchioles (Tortora & Grabowski, 1993). Clara cells are also secretory cells and function to detoxify xenobiotics and produce surfactant (a fluid layer comprising phospholipids and apoproteins covering epithelium of bronchioles and alveoli) (Jefferey, 1997). The morphology of the airways epithelium again changes as the bronchioles descend into the alveoli, where Type 1 pneumocytes are abundant with few Type 2 pneumocytes (Tortora & Grabowski, 1993).



Illustration removed for copyright restrictions

Figure 1.1: The morphology of the epithelium alters throughout the respiratory tract. (A) The upper respiratory tract is lined with differentiated pseudostratified columnar muco-ciliary epithelial cells attached to the basement membrane by a layer of basal epithelial cells. (B) Excess mucous production within the upper respiratory tract is a consequence of either mucous cell hypersecretion or mucous cell metaplasia (Rogers, 2007). (C) simple cuboidal epithelial cells of the (D) Type 1 squamous epithelial cells predominate the epithelium of the alveoli.

The differentiation state of epithelial cells can be characterised by their expression of cytokeratins. The epithelium of the upper airways is the first point of contact for inhaled material, and protects the lungs against noxious insult. The morphology of the muco-ciliary epithelium represents this role, allowing for a muco-ciliary escalator to clear inhaled material from the lungs (Mills *et al.*, 2009) (see below). The differentiated epithelium also forms tight junctions, which prevent access of xenobiotics to the underlying tissue (Niessen, 2007).

1.1.2 Cytokeratin profiles of airways epithelium

Epithelial cells can be characterised by expression of discrete epithelial cell-specific markers, cytokeratins (Iyonaga *et al.*, 1997; Moll *et al.*, 1982; Purkis *et al.*, 1990). Cytokeratins are intermediate cytoskeleton filaments which serve to provide physical support for the cells. The expression profile in both normal and tumorous epithelia was characterised by Moll *et al.*, (1982) who described cytokeratins 1-6 as large basic cytokeratins that are expressed in stratified epithelia, cytokeratins 7 and 8 as having intermediate size and charge, and are typical of simple epithelia within the trachea. Cytokeratins 9-12 are described as acidic with intermediate or large size, with cytokeratin 12 expression in the cornea and 9-11 in epidermis. Cytokeratins 13-17 are small acidic cytokeratins expressed in trachea and some glands and cytokeratin 19 (a small acidic cytokeratin) is expressed in simple and stratified epithelia (Moll *et al.*, 1982).

In vitro, primary airway epithelial cells cultured at air-liquid interface (ALI) form multiple cell layers, with the lower cell layer showing positive staining for cytokeratins 1, 5, 10 and 14 (Endres *et al.*, 2005). Further, Pohl *et al.*, (2009) characterised basal cell populations of NHBE in cells cultured at ALI by expression of cytokeratin 14. The airways epithelium *in vivo* can be described as containing pseudo-columnar differentiated cells with a cytokeratin expression pattern of 7, 8, 13 and 19 with cytokeratin 5 and 14 expressed in the basal population (Iyonaga *et al.*, 1997). Cytokeratin expression patterns therefore form a useful tool for identifying the

differentiation status of epithelial cells in *in vitro* culture, where the aim is to culture populations of epithelial cells that have morphologies representative *in vivo* cells.

1.1.3 Tight junctions

Areas of fused membranes between adjoining epithelial cells have been observed in a number of epithelial cell types including toad bladder epithelium (Choi, 1961). Farquhar and Palade, (1963) using rodent epithelial models, were the first authors to identify these junctions as “tight junctions” and as the most apical of the three epithelial cell junction complexes (tight junctions, adherens junctions and desmosomes). Farquhar and Palade, (1963) observed that these junctions fused the membranes on neighbouring epithelial cells and restrict the passage of proteins solutions through epithelial cell monolayers. As a consequence the tight junctions were given the Latin term “Zonula Occludens” translating to “closing belt”. Freeze-fracture studies of these junctions have led to the identification of structural proteins within these junctions. The first tight junction protein to be identified by this method was termed Zonula Occludens-1 (ZO-1) (Stevenson *et al.*, 1986).

The structure (Figure 1.2) and function of tight junctions has since been intensively studied and reviewed. ZO- proteins act as scaffolding proteins which provide an anchor between actin and the tight junction proteins claudin and occludin (Niessen, 2007). Occludin was the first transmembrane protein identified within the tight junction (Furuse *et al.*, 1993) and has been suggested to have a role in tight junction permeability (Steed *et al.*, 2010). Claudin, a tight junction transmembrane protein, regulates the “tightness” of epithelial cell tight junctions (Furuse *et al.*, 2001). Junctional adhesion molecules (JAMs) play a role in cell migration (Niessen, 2007) for example, leukocyte diapedesis.

Aside from their role in maintaining a physical protective barrier, tight junctions serve to maintain airway homeostasis. Electrolytes such as sodium (Na^+) and chloride (Cl^-) pass through epithelial tight junctions to the airway surface liquid and mucus layers

(Welsh, 1987). These ions have roles in maintaining a hydrated mucus layer. Impaired ion transport (by both the paracellular and transcellular pathways) may lead to thick dehydrated mucus which limits muco-ciliary beat, thereby decreasing mucus clearance (Tarran, 2004) and increasing pathogenic colonisation and inflammation.

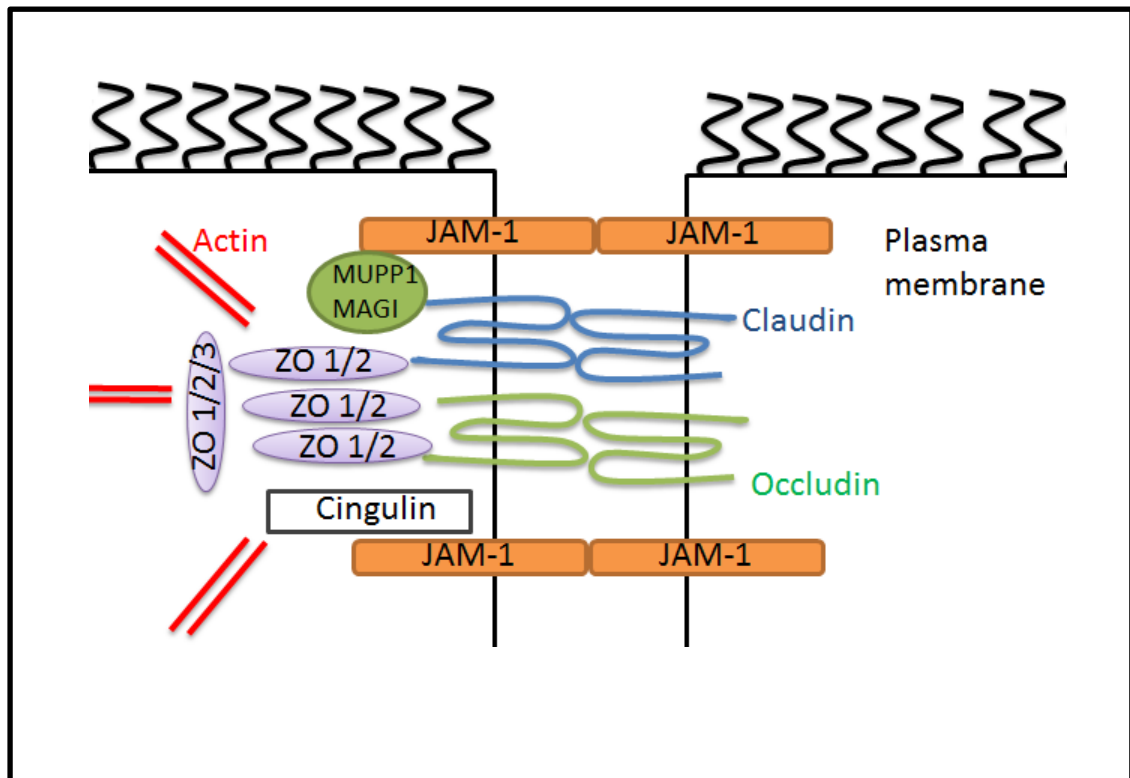


Figure 1.2: The structure of epithelial tight junctions. The epithelial tight junction is composed of the transmembrane proteins occludin, claudin (involved in size selectivity of the tight junction), and ZO which provides structural support between cytoskeletal and transmembrane proteins.

1.1.4 Mucin

Synthesised and secreted by goblet cells, mucins are high molecular weight glycoproteins which form a thick mucus film over the epithelium, serving to trap any inhaled particulates and pathogens. Twenty mucin (Muc) proteins have been identified, of which Muc2, Muc5AC, Muc5b and Muc6 encoded by MUC2, MUC5AC, MUC5B and MUC6 genes are gel-forming mucins found in airway epithelial cells (Davis, 2002;

Kim *et al.*, 2007; Mills *et al.*, 1999; Rogers, 2007; Williams *et al.*, 2006). Muc19 has also recently been identified to be a gel forming mucin of the human airway (Williams *et al.*, 2006). The mucus layer serves to trap invading particulates and pathogens, thereby protecting the epithelium. Trapped material is cleared by the beating action of the cilia protruding from the ciliated cells in a process termed the muco-ciliary escalator (Mills *et al.*, 1999). Mucin traps bacteria by adhesion between mucin glycoproteins and bacterial ligands. For example the respiratory pathogen *Pseudomonas aeruginosa* (*P. aeruginosa*) strain PAO1 flagellin protein fLID binds to mucin carbohydrate moieties (Scharfman *et al.*, 2001). Once trapped in the mucin, pathogenic material can be cleared by the muco-ciliary escalator.

1.2 Inflammation

If pathogens/irritants breach mucosal surfaces the innate immune system provokes an inflammatory response at the site of insult in order to neutralise and remove the “non-self” material (Smith, 1994). During microbial invasion, pattern recognition receptors (PRR) on host cells, such as Toll-like receptors (TLR) on epithelial cells, recognise pathogen associated molecular patterns (PAMPs) on the microbe. Circulating dendritic cells and resident macrophages also express PRR (Barton, 2008). Pattern recognition triggers inflammatory mediator secretion by the affected cells/tissue to promote recruitment of innate immune cells such as neutrophils and monocytes (which differentiate into macrophages upon activation). B and T lymphocytes are also recruited by epithelial derived cytokines (Riffo-Vasquez & Spina, 2002). Recruitment of macrophages and neutrophils promotes removal of pathogenic material by phagocytosis (Reviewed in Parihar *et al.*, 2010) and is therefore desirable. However, failure to resolve inflammation can lead to airways damage and can contribute to airways pathologies such as asthma (Murphey & O’Byrne, 2010) and chronic obstructive pulmonary disease (COPD) (Barnes, 2009).

1.2.1 Inflammatory respiratory diseases

Symptoms of respiratory illnesses such as asthma, COPD and cystic fibrosis (CF) are often worsened by chronic inflammation which results in airways tissue damage. As

many as 5.4 million individuals in the UK suffers from asthma (www.asthma.org) and symptoms include breathlessness, wheezing and coughing. There are two principle forms of asthma, allergic (where asthma attacks are induced after allergen exposure e.g. pollen, and non-allergic. T-helper cells infiltrate the airways in abundance and induce inflammation by secretion of chemokines and cytokines. These proinflammatory molecules promote migration and activation of inflammatory cells including eosinophils, mast cells, basophils and leukocytes (Reviewed in Murphey & O'Byrne, 2010). Like asthma, inflammation is observed in COPD which is estimated to affect up to 19% of the adult population aged over 40 years, and is characterised by restricted airflow that is progressive and non-reversible (Ling & van Eeden, 2009). In COPD infiltration of inflammatory cells such as macrophages and neutrophils enhance inflammation impaired respiratory symptoms and fibrosis (Barnes, 2009). Occupational exposures ranging from asphalt workers to domestic cleaning have been associated with increased risk of both asthma and COPD (Medina-Raman *et al.*, 2005; Randem *et al.*, 2004).

Idiopathic pulmonary fibrosis (IPF) is a fatal airways disorder which involves remodelling of the vasculature (Strieter *et al.*, 2007) and airway inflammation (Yamauchi *et al.*, 2010). Epithelial-to-mesenchymal transition (EMT), a process whereby epithelial cells de-differentiate into mesenchymal myofibroblasts is associated with fibrosis (Guarino *et al.*, 2009; Yamauchi *et al.*, 2010). Damaged epithelial cells down-regulate epithelial cell markers such as E-cadherin, ZO-1 and cytokeratin and up-regulate mesenchymal proteins including alpha-smooth muscle actin, vimentin and fibroblast specific protein-1 (FSP1) (Guarino *et al.*, 2009). Transforming growth factor (TGF)- β induces EMT *in vitro* (Guarino *et al.*, 2009; Yamauchi *et al.*, 2010); further, TGF- β induced EMT is enhanced by the pro-inflammatory mediator TNF α , indicating that lung inflammation may drive airway remodelling observed in airway pathologies. In all of the above conditions there is excess inflammatory mediator secretion resulting in immune cell recruitment. Cysteinyl leukotrienes are lipid mediators secreted from many inflammatory cells including eosinophils, neutrophils and macrophages (Monstuschi, 2010). Cysteinyl leukotrienes contribute to airway remodelling (Monstuschi, 2010) and COPD (Drakatos *et al.*, 2009) by promoting fibroblast proliferation and collagen deposition, and smooth muscle proliferation leading to

thickening of the airway wall (Monstuchi, 2010). Leukotriene B₄ also leads to worsening of airway inflammation by acting as a chemoattractant for T cells and neutrophils (Drakatos *et al.*, 2009).

Cystic fibrosis (CF) is a genetic disorder affecting 9000 individuals in the UK (www.cftrust.org.uk). The most common genetic mutation in CF is the loss of phenylalanine in position 508 ($\Delta F508$) in the cystic fibrosis transmembrane conductance regulator (CFTR) protein leading to abnormal chlorine conductance. The respiratory consequences of the mutated CFTR protein is dehydrated airway surface leading to cilia collapse and subsequent build-up of a thick mucus layer. This provides an environment for bacterial colonisation and results in chronic inflammation due to persistent activation of the immune response (Ratjen, 2009).

1.2.2 Role of airways epithelium in innate immune response

As well as providing a protective barrier and muco-ciliary escalator, airway epithelial cells protect against pathogenic colonisation by orchestrating an immune response by secretion of a range of pro-inflammatory mediators (Table 1.1) such as chemokines (interleukin (IL)-8, regulated upon activation, normal T cell expressed and secreted (RANTES) and granulocyte macrophage colony-stimulating factor (GM-CSF)), and cytokines (IL-6 and IL-1 β). Signalling molecules and cytotoxic (such as reactive oxygen species (ROS) and reactive nitrogen species (RNS)) and antimicrobial factors such as β -defensin, lysozyme and lactoferrin are also secreted by epithelial cells during innate immune response (Bals & Hiemstra, 2004; Polito and Proud, 1998; Thompson *et al.*, 1995). The pro-inflammatory mediators IL-8 and IL-6 are increased in bronchial/bronchio-alveolar lavage (BAL) and induced sputum from asthma, COPD and bronchitis sufferers (Garcia-Rio *et al.*, 2010; Jatakanon *et al.*, 1999; Riise *et al.*, 1995) and in asthmatic serum (Fitzpatrick *et al.*, 2010), again indicating a link between excessive inflammatory responses and airway pathology.

Table 1.1: Airway epithelial cell inflammatory mediator secretion. The airways epithelium can secrete a number of inflammatory mediators including colony stimulating factors which promote the differentiation and survival of immune cells, chemotactic cytokines which attract immune cells and multifunctional cytokines and signalling molecules (Bals & Hiemstra, 2004; Polito & Proud, 1998; Thompson *et al.*, 1995). M-CSF; macrophage colony-stimulating factor, MCP; monocyte chemotactic species, SP, surfactant protein, SIgA; secretory immunoglobulin A.



During inflammation epithelial cell-derived cytokines such as IL-1 β induce a conformational change and up-regulation of adhesion molecules on endothelial cells to facilitate recruitment by chemotaxis of circulating leukocytes to clear the pathogenic insult (Rafiee *et al.*, 2003; Yan *et al.*, 2010).

1.2.3 Role of the endothelium in the innate immune response

As well as its role in blood supply the endothelium has a role in inflammatory cell trafficking (Danese *et al.*, 2007). Activation of endothelial cells results in increased expression of adhesion molecules which allow for attachment and extravasation of circulating leukocytes to sites of infection and inflammation (Langer & Chavakis, 2009; Rao *et al.*, 2007). Endothelial cell adhesion molecules capable of interacting with leukocytes include selectins (E-selectin and P-selectin) and major integrin ligands (VCAM-1 and ICAM) (Danese *et al.*, 2007). Leukocytes adhere to the endothelium by a tethering and rolling process. Binding first occurs via adherence of the leukocyte carbohydrates to endothelial selectins. Rolling leukocytes form firm attachments to the endothelial cells (Langer & Chavakis, 2009) and then migrate through the endothelial cell layer via interactions between leukocyte integrins and endothelial junctional adhesion molecules (JAM) (Langer & Chavakis, 2009).

Further, in the event of endothelial challenge endothelial cells themselves secrete inflammatory mediators (Danese *et al.*, 2007). Adherence of platelets to the endothelium, via the endothelial cell specific molecule Von Willebrand factor (VWF) for instance, may also occur during endothelial cells insult. The platelets allow leukocyte adherence to the endothelium through binding of P-selectin on the platelet surface to P-selectin glycoprotein ligand 1 on the leukocytes (Danese *et al.*, 2007).

1.2.4 Role of leukocytes in the innate immune response

Leukocytes, including monocytes, macrophages and neutrophils, play pivotal roles in elimination of “non-self” xenobiotic materials such as pathogens. Upon activation by colony stimulating factors such as GM-CSF, circulating monocytes differentiate into macrophages which phagocytose the infective substances (reviewed in Parihar *et al.*, 2010). Neutrophils, whilst integral in the innate immune response are able to activate the adaptive immune response via release of cytokines and chemokines (for example IL-8) which activate and induce differentiation of B- and T lymphocytes (reviewed in Coscao *et al.*, 2009).

1.2.4.1 Neutrophils and the innate immune response

Daily, the adult human bone marrow produces 10^{11} neutrophils which comprise up to 60% of the total circulating leukocytes (Smith, 1994), and remain in circulation for up to 18 hours before removal by apoptosis. This removal maintains a balance in neutrophil numbers and homeostasis. Circulating neutrophils act as immune surveyors and roll along endothelial cell monolayers allowing for rapid migration into infected areas upon activation (Coscao *et al.*, 2009). Upon activation, rolling neutrophils adhere to endothelium via binding between endothelial ICAM-1 and neutrophil β_2 -integrin, such as LFA-1 (CD11b/CD18). Neutrophils then move through the endothelial cell layer by a process termed diapedesis (Figure 1.3), which involves binding between neutrophil PECAM-1 and endothelial PECAM-1 and neutrophil LFA-1 and endothelial JAM in tight junctions (reviewed in Coscao *et al.*, 2009).

Neutrophils eliminate pathogens via phagocytosis which triggers the neutrophil respiratory burst and degranulation principally into the phagosome. Phagocytosis occurs via binding between Ig-opsonised material and Fc γ neutrophil receptors or via binding between complement C3bi opsonised material and neutrophil CD11b/CD18 (Coscao *et al.*, 2009). The respiratory burst is initiated upon neutrophil activation and involves the formation of NADPH oxidase/cytochrome *b558* which transfers electrons from NADPH to oxygen forming superoxide anion radicals (Coscao *et al.*, 2009). Cytochrome *b558* is formed by the translocation of the p47^{phox}, p67^{phox} and p40^{phox} heterotrimer, along with rac-GTP from the cytosol to the plasma membrane where it binds gp91^{phox} and p22^{phox} to form the cytochrome (Rosario & Fonseca, 2009; Wientjes & Segal, 2005).

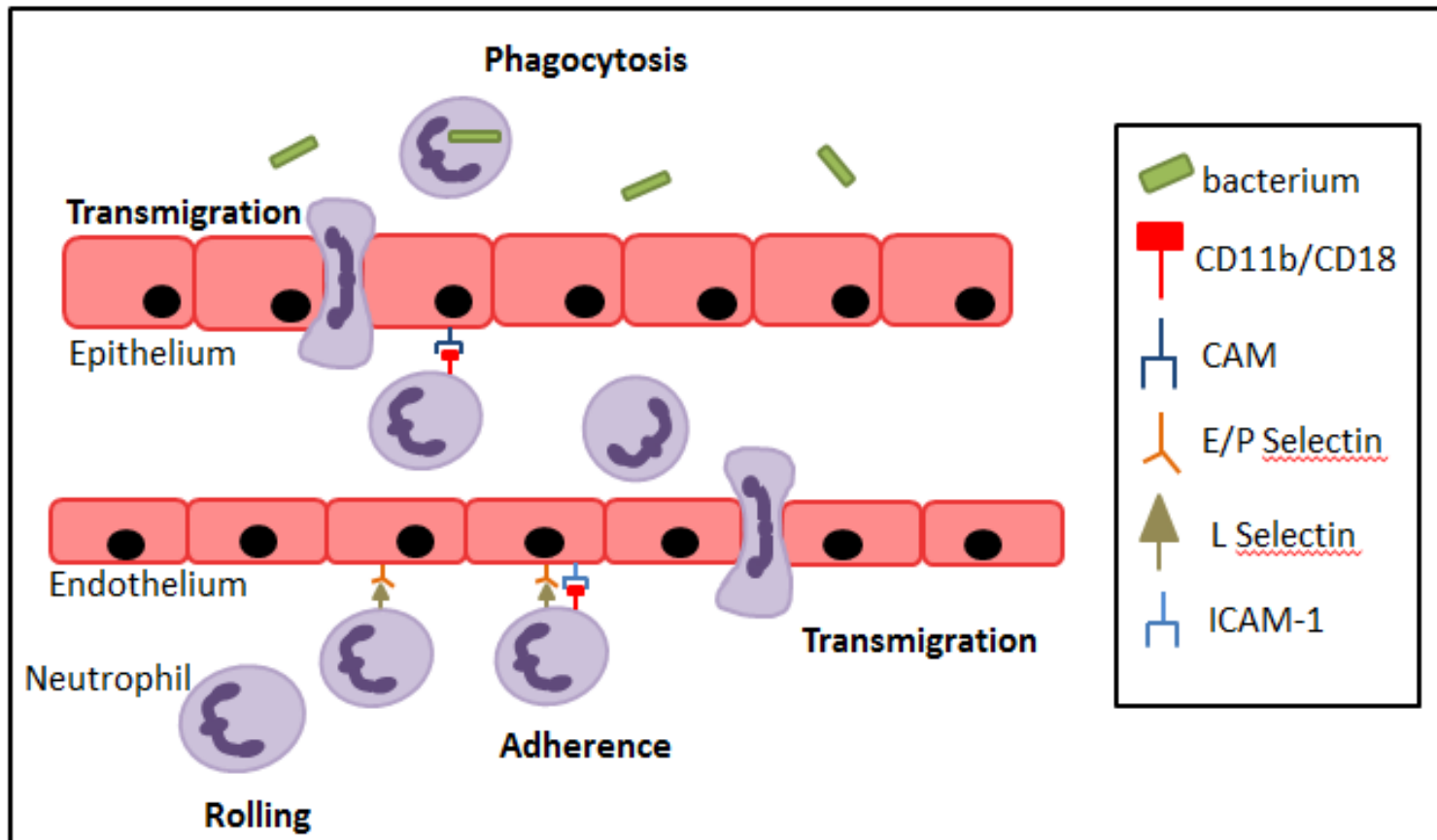


Figure 1.3: Role of neutrophils in the innate immune response. Upon activation neutrophils extravasate through the endothelium to the site of infection. Neutrophils aid to resolve infection by elimination of the pathogen by phagocytosis.

1.3 LPS and PM induce innate immune response in airways epithelium

1.3.1 LPS

LPS is a virulence factor located on the outermost layer of Gram-negative bacterial membranes, and induces an inflammatory response in a broad range of cells including epithelial cells (Rietschel *et al.*, 1994).

1.3.1.1 General structure

LPS has 3 components (Figure 1.4); lipid A, a core region and a polysaccharide region referred to as o-antigen (Haefner-Cavaillon *et al.*, 1998; Rietschel *et al.*, 1994). Lipid A is composed of fatty acids attached to an N-acetylglucosamine dimer, and is the part of LPS responsible for antigenicity (Rietschel *et al.*, 1994). The core oligosaccharide contains a 2-keto-deoxyoctonic acid (Kdo) domain, a sugar specific to LPS, which attached to lipid A. The o-antigen of LPS is composed of repeating oligosaccharides (each comprising 3-7 sugars) and is responsible for the variation of LPS structure between bacterial serotypes and species (Rietschel *et al.*, 1994).

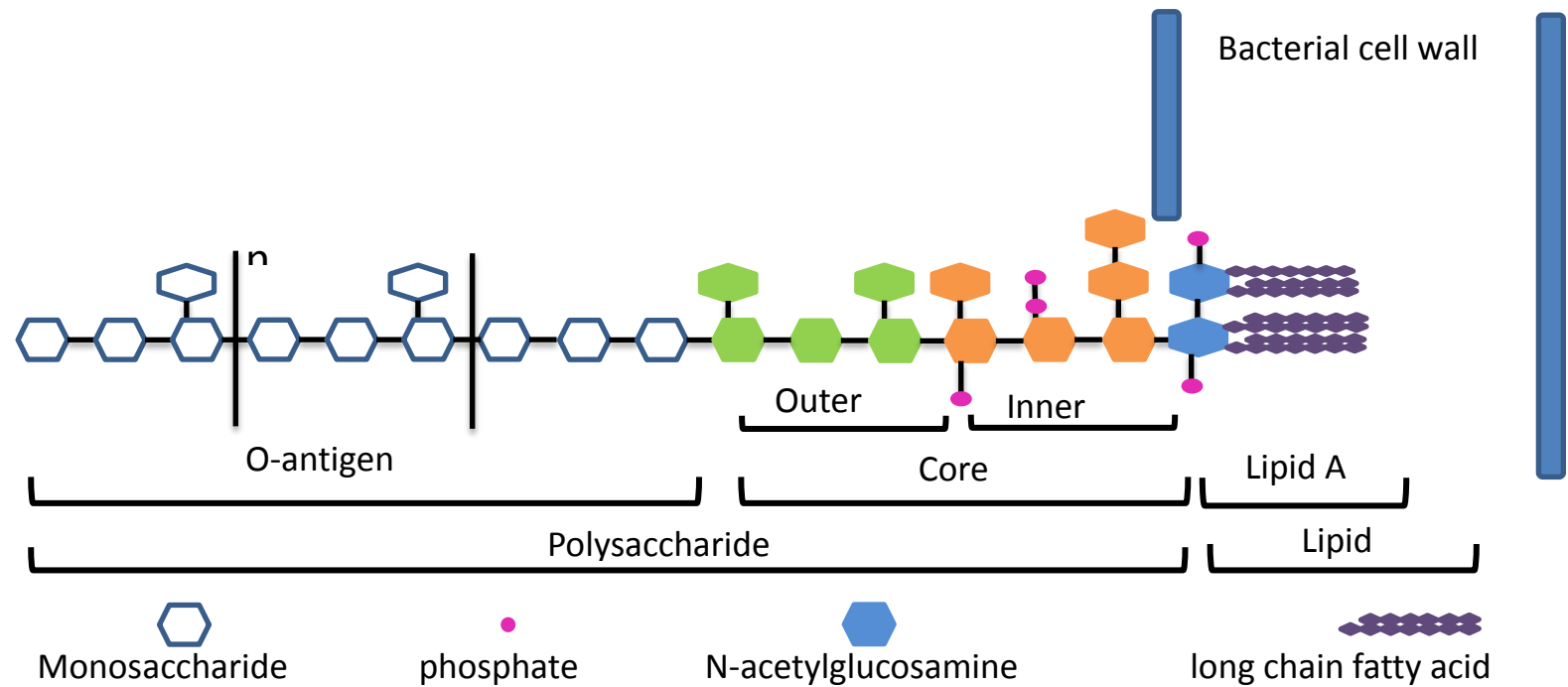


Figure 1.4: Structure of LPS. LPS contains 3 major domains, a Lipid A domain which is responsible for the biological activity of LPS, a core domain which is connected to Lipid A via a Kdo domain, and a polysaccharide usually referred to as O-antigen or O-polysaccharide. The structure of o-polysaccharide varies between bacterial species and serotypes. Image adapted from Tobias *et al.*, (1999).

1.3.1.2 LPS/TLR signalling

TLR's are PRR which bind PAMPs such as LPS (which is recognised mainly by TLR 4). During LPS recognition LPS is bound by LPS-binding protein (LBP) and transferred to CD14 and MD-2. (Lu *et al.*, 2008). After LPS recognition by TLR-4, signalling occurs via 2 pathways; the myeloid differentiation primary response gene 88 (MyD88)-dependent pathway or the MyD88-independent pathway (Figure 1.5). Signalling via the MyD88-dependent pathway results in up-regulation of pro-inflammatory cytokine secretion via a number of transcription factor signalling pathways, including the p38 mitogen-activated protein kinase (MAPK) pathway, which induces activator protein (AP)-1 nuclear translocation (Dunston & Griffiths, 2010). Activation of nuclear factor- κ B (NF- κ B) is also a result of LPS/TLR4 binding. NF- κ B is a dimer of RelA (p65) and p50, in un-activated cells NF- κ B is held in the cytoplasm by inhibitory I κ B proteins which cover nuclear localisation signalling domains (Dunston & Griffiths, 2010). Activation results in degradation of the inhibitory proteins and nuclear translocation of NF- κ B. The MyD88-independent pathway involves up-regulation of Type I interferons which aid in clearance of viral and bacterial pathogens (Perry *et al.*, 2005).

1.3.2 Particles

PM with a diameter of <10 μ m deposit within the respiratory tract and can elicit airway epithelium inflammation and cytotoxicity if ineffectively cleared (Heyder, 2004). Inhalation exposure to particulates may occur from a number of sources including diesel exhaust particulates (DEP) and other combustion derived particulates (Duffin *et al.*, 2007) to particles from workplace exposure such as coal dust particles (Schims and Borm, 1999) or particulates for commercial products such as fine titanium dioxide (TiO₂).

1.3.3: PM induced-ROS and inflammatory signalling

During inflammation, ROS are liberated by epithelial and endothelial cells as mediators of cell signalling (Bals & Hiemstra, 2004 & Polito & Proud, 1998) and by leukocytes during phagocytosis (Coscao *et al.*, 2009). Furthermore, inhaled xenobiotics have the

potential to produce ROS; for example transition metal-containing particulates result in ROS formation by via the Fenton reaction (Carter *et al.*, 1997). PM also induce cellular ROS induction by impairment of mitochondrial electron transfer (Zhao *et al.*, 2009).

1.3.4: Glutathione and redox homeostasis

The tri-peptide thiol glutathione (GSH) protects against excess ROS in the airways and is present in airway surface lining fluid (Biswas & Rahman, 2009). GSH exists both in the reduced (GSH) and oxidised form (GSSG, also known as glutathione disulphide), with reduced GSH accounting for 99% of total cellular glutathione levels. Glutathione peroxidase and peroxiredoxin 6 catalyse the conversion of H₂O₂ to water, resulting in GSH oxidation (GSSG) (Forman *et al.*, 2009). GSSG is reduced to GSH, a reaction catalysed by glutathione reductase, at the expense of NADPH (Harvey *et al.*, 2009). GSH replenishment also occurs via *de novo* synthesis from glutamate, cysteine and glycine. Catalysed by glutamate cysteine ligase (also known as a γ -glutamylcysteine synthetase), the first stage in GSH *de novo* synthesis involves a reaction between cysteine and glutamate to produce γ -glutamylcysteine. Glycine is then added to γ -glutamylcysteine to form GSH, a reaction catalysed by glutathione synthetase (Forman *et al.*, 2009). Up-regulation of glutamate cysteine ligase and other GSH related enzymes by nuclear factor-erythroid 2 p45-related factor 2 (Nrf2) also contributes to GSH *de novo* synthesis. ROS and RNS induce liberation of Nrf2 from Keap1 and translocation of Nrf2 to the nucleus. Nrf2 interacts with target genes through antioxidant response elements (AREs) (Harvey *et al.*, 2009). Nrf2-regulated genes include glutamate cysteine ligase, and other GSH-regulation genes. Nrf2 also has a negative-regulatory role on inflammatory events during LPS induced septicaemia. NADPH oxidase dependant ROS (liberated during the neutrophil respiratory burst during pathogenic clearance) increased TLR4 inflammatory signalling in NRF2^{-/-} macrophages (Kong *et al.*, 2010).

Excessive ROS production leads to depletion of cellular GSH resulting in a redox imbalance and increased levels of GSSG. GSSG induces ubiquitination and phosphorylation of IKK leading to activation of NF- κ B, GSSG also activates AP-1, leading to inflammatory gene up-regulation (Rahman & MacNee, 2000). Furthermore, mitochondrial ROS induces pro-inflammatory signalling via activation of p38 MAPK

signalling cascades (West *et al.*, 2011), NF- κ B and the transcription factor CCAAT/enhancer binding protein beta (C/EBP β) (Zhao *et al.*, 2009) (Figure 1.5). Pro-inflammatory cytokines containing AP-1, NF- κ B or C/EBP β response elements are therefore potentially induced by LPS or PM exposure. The IL-8 gene promoter region contains a NF- κ B element, an AP-1 element and a C/EBP-element and therefore up-regulation of IL-8 gene expression can result from a number of stimuli (Hoffmann *et al.*, 2002). IL-6 is up-regulated by mitochondrial ROS induced C/EBP β activation after PM exposure (Zhao *et al.*, 2009), and is also up-regulated by p38 MAPK pathways (Heinrich *et al.*, 2003).

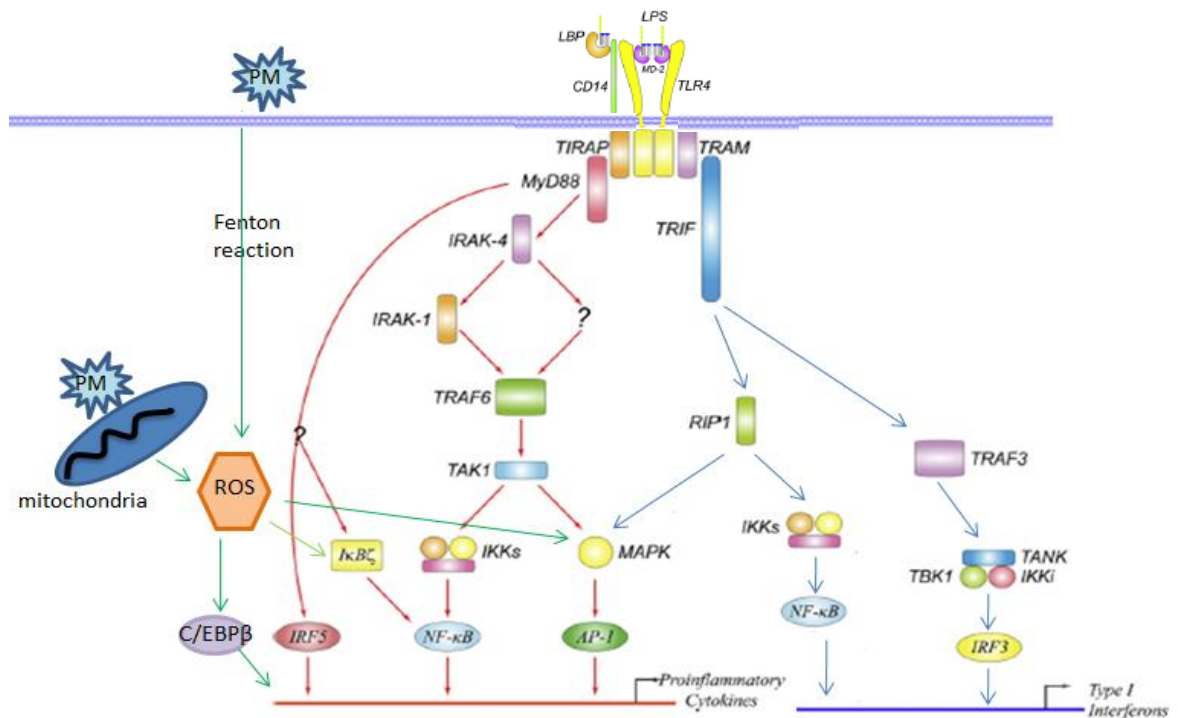


Figure 1.5: Inflammatory signalling induced by LPS and PM. LPS binding to the TLR4 receptor induces pro-inflammatory mediator up-regulation via transcription factors NF- κ B and AP-1. PM exposure results in mitochondrial ROS production which activates C/EBP β , NF- κ B and p38 MAPK signalling. Image adapted from Lu *et al.*, (2008). Blue arrows represent the MyD88-independent pathway, red arrows represent the MyD88-dependent pathway and green arrows represent PM induced inflammatory signalling.

1.4 IL-8 and IL-6 in airway pathologies

Yoshimura *et al.*, (1987) first identified a neutrophil chemotactic mediator in conditioned media of *Escherichia coli* (*E. coli*) LPS stimulated human blood mononuclear cells, termed monocyte-derived neutrophil chemotactic factor (MDNCF). MDNCF is now known as IL-8 (Baggiolini *et al.*, 1989) and has since been extensively studied. After cleavage of the 20 amino acid residue signal sequence from the 99 amino-acid IL-8 precursor, the principal IL-8 variant of 72 amino acids is secreted from immune cells such as neutrophils, whilst non-immune cells such as epithelial cells secrete IL-8-77 (Mikolajczyk-Powlinska *et al.*, 1998). Variants with lengths of 79, 71, 70 and 69 amino acids have also been reported (Nourshargh *et al.*, 1992). IL-8 secretion is observed from a number of different cell types including fibroblasts, epithelial cells and endothelial cells, and induces neutrophil migration, release of storage proteins and respiratory burst (Baggiolini & Clarke-Lewis, 1992).

Kishimoto & Ishizaka, (1973) identified that activated T cells secreted a mediator capable of inducing B cell growth and differentiation. Later, the cDNA of this mediator was identified and the mediator was termed B-cell stimulatory factor (BSF-2) (Hirano *et al.*, 1986). BSF-2 was also independently identified as a hepatocyte stimulating factor (Andus *et al.*, 1987). BSF-2, now known as IL-6, (Kishimoto, 2010) has pro-inflammatory mediator properties including activation of leukocytes (Jones, 2005). IL-6 is also suggested to play a role in leukocyte chemotaxis (Jones, 2005).

Increased secretion of IL-8 and IL-6 contributes to the persistent inflammation in asthma, COPD and bronchitis (Fitzpatrick *et al.*, 2010; Garcia-Rio *et al.*, 2010; Jatakanon *et al.*, 1999; Riise *et al.*, 1995). In a large scale study of COPD (324 COPD sufferers and 110 control individuals) serum levels of IL-8 were found to be significantly greater in COPD subjects than control (after adjustment for age, gender and BMI) whilst serum levels of IL-6 was significantly greater in subjects with severe COPD compared to those with mild COPD (Garcia-Rio *et al.*, 2010). Further IL-8 levels are increased in BAL of chronic bronchitis sufferers compared with control (Riise *et al.*, 1995) and severe asthmatic adults compared to both mild asthmatic adults

and normal control adults (Jatakanon *et al.*, 1999). Increased numbers of neutrophils were also observed in BAL from severe asthmatic compared to control and mild asthmatic adults (Jatakanon *et al.*, 1999) indicating the role of increased IL-8 secretion in asthma. Increased IL-6 is also observed in BAL of asthmatic subjects compared to control (Fitzpatrick *et al.*, 2010). PM exposure has also been linked to decreased respiratory function in asthmatic children (Barraza-Villarreal *et al.*, 2008; Holguin *et al.*, 2007) and increased cardiovascular disease (Nascimento *et al.*, 2001).

1.5 PM and airway pathologies and links to cardiovascular disease

As described above PM induce ROS that in turn promote inflammatory signalling via MAPK and NF- κ B. Exposure to PM in individuals with respiratory illness may therefore worsen disease state by increased inflammation. Significant correlations between impaired respiratory function (measured by forced expiratory volume in one second (FEV₁)) and increased ambient PM_{2.5} (PM with a mean diameter of <2.5 μ m) levels have been observed in asthmatic children (Barraza-Villarreal *et al.*, 2008; Holguin *et al.*, 2007). Further, increased ambient PM_{2.5} levels correlated significantly with increased IL-8 in nasal lavage in both asthmatic and non-asthmatic children (Barraza-Villarreal *et al.*, 2008). PM also induce epidermal growth factor signalling (EGF) in bronchial epithelial cells which also induces epithelial cell proliferation (Sydlick *et al.*, 2006; Tamaoki *et al.*, 2004); it is likely that excessive signalling could potentially lead to airway remodelling and narrowing of the airways.

Inhaled PM have been shown to translocate into the blood stream (Nenmar *et al.*, 2002) and may therefore result in vascular inflammation and pathology. Indeed, PM exposure results in increased microvascular ROS production and impaired vasodilation in coronary arterioles in rats (LeBlank *et al.*, 2010), increased platelet activation (O'Tool *et al.*, 2010), reduced NO synthase levels, increased inflammatory gene expression and endothelial cell death (Yamawaki *et al.*, 2006) in humans. Plasma inflammatory marker concentrations (IL-6, soluble P-selectin and C-reactive protein) in elderly coronary artery disease patients (Delfino *et al.*, 2008) and CVD related hospital patient admissions correlated significantly with ambient PM levels.

Due to the potential for tissue damage, airway remodelling and decreased lung function during airway inflammation, and CVD complications, valid models of airways inflammation are required to help identify mechanisms and inducers inflammatory events and potential inhibitory treatments. Rodent models can be used widely to study inflammatory responses to LPS (Schwartz *et al.*, 2001) and PM (Bermudez *et al.*, 2004) exposure.

1.6 Animal models of respiratory pathologies

Mouse models of asthma often use ovalbumin as a stimulator of pulmonary inflammation, which induces eosinophil infiltration of the lungs and airway remodelling (Nials & Uddins, 2008). House dust mite extract, (which is a more relevant stimulus as it can induce asthmatic symptoms in humans), also induces eosinophil recruitment to the lungs of challenged mice and airway inflammation (Johnson *et al.*, 2004). Rodent models are used to study PM toxicity. Inhalation exposure of hamsters, rats and mice to ultrafine titanium dioxide (UFTiO₂) (variable doses for 6 hours a day, 5 days a week for 13 weeks) induced increasing numbers of macrophages, neutrophils and lymphocytes in BAL of rats and mice indicating the inflammatory potential of this particle *in vivo* (Bermudez *et al.*, 2004). Lung burdens of particles observed after treatment declined during recovery periods for animals. Further, increased burdens in lymph nodes for rats were observed during recovery (Bermudez *et al.*, 2004) indicating clearance of particles. Murine models of CF are also utilised, however, mice bearing CF mutations do not develop spontaneous airway disease (Sheth *et al.*, 2008), possibly due to differences between human and murine immune responses.

1.6.1 Immunological variance between human and animal lung immunity

Whilst animal models are useful to study the effect of a toxicant on multiple organs, and the cross-talk between multiple cell types, the physiology is not entirely representative of humans. For instance, approximately 60% total circulating leukocytes are neutrophils in humans (Smith, 1994), 10-20% in mice (Mestos & Hughes, 2004) and 10-20% in rats (Haley, 2003). Mice also have different TLR2, 3, 9 and 10 expression and activation patterns. For example TLR3 is expressed on both dendritic cells and macrophages in

mice and is activated by LPS, in humans however, TLR3 is expressed on dendritic cells only and is non-responsive to LPS. Mice also do not express the immune mediators caspase 10 (an important mediator in initiation of apoptosis) (Mestos and Hughes, 2004). Rodents do not express the IL-8 gene, the equivalent keratinocyte-derived chemokine (KC) is found in mice and cytokine-induced neutrophil chemoattractants (CINC) are present in rats (Tarrant, 2010). The difference in immune systems between rodents and humans may be important when evaluating the toxicity potential of certain compounds, for example drugs or cosmetics. Further European Regulation (7th Amendment of the European Union Cosmetic Directive, 2003) governing the use of animals in cosmetic studies is now limiting their use for the safety assessment of cosmetic ingredients. The Cosmetic Directive now rules that animal repeat dose testing for cosmetic ingredients will be banned after 2013 (7th Amendment of the European Union Cosmetic Directive, 2003). Due to the differences in human and rodent physiology regarding the immune response and limitations placed on animal testing, valid and robust *in vitro* cell models are required for evaluating toxicity, in particular cosmetic compound toxicity, testing.

1.7 Epithelial cell models

Culture of human primary airway epithelial cells (NHBE) on Transwell[®] inserts at ALI allows for culture of multiple cell layers (as observed *in vivo*). NHBE cells cultured at ALI regain cilia formation, have cytokeratin profiles consistent with airway epithelial cells *in vivo* (de Jong *et al.*, 1993; de Jong *et al.*, 2004), and secrete mucin, lysozyme, lactoferrin and SLP1 (Gray *et al.*, 1996). The trans-epithelial electrical resistance (TER) of NHBE cells at ALI is high ($>800 \Omega \text{cm}^2$, Gray *et al.*, 1996) and tight junctions are formed between neighbouring cells, as determined by immunohistochemical staining of ZO-1 (Coyne *et al.*, 2002). TER measures ion flow throughout the paracellular pathway (Tang & Goodenough, 2003) which is governed by the particular properties of the cells tight junctions. These data indicate that primary airway epithelial cells cultured at ALI are representative of the airway epithelial cells *in vivo*. TER measurements of different epithelial cell lines have shown that electrical resistance, and thus tight junction “tightness”, is variable. For example, values of 700-1000 $\Omega \times \text{cm}^2$

are reached by the airway epithelial cell line Calu-3 (Grainger *et al.*, 2006) and 300-1200 $\Omega \times \text{cm}^2$ are achieved by 16HBE14o⁻ cells (Wan *et al.*, 2000).

Investigations into the transcriptome and apical secretions from primary bronchial epithelial cells cultured at ALI have further shown these cells to be a representative model of the airways epithelium *in vivo* by their expression of mucociliary genes and secretion of mucins (Dvorak *et al.*, 2010; Kesimer *et al.*, 2009). In a study comparing EpiAirway (MatTek) ALI models of airway epithelial cells from healthy non-smoking donors to primary airway epithelial cells obtained from bronchoscopy Dvorak *et al.*, (2011) investigated the transcriptome of both models in relation to ciliary, secretory and basal epithelial cell genes. Expression of cilia-related genes were significantly increased in brushed cell cultures whilst basal cell-related genes showed significantly increased expression in ALI cultures. This is in agreement with histological findings which show that more ciliated cells and fewer basal are found in cells obtained by bronchoscopy. However, both models contained ciliated, secretory and basal cells. Furthermore, over 80% of the genes expressed by both modes had similar expression profiles indicating the relevance of the ALI model compared to epithelial cells *in vivo*. Of the genes that were different, MUC5AC, a major airways mucin, gene expression was increased in brushed cells compared to ALI cells, whilst MUC2 gene expression was observed in brushed cells only (Dvork *et al.*, 2011), suggesting both models have a similar number of secretory cells, the mucin profile of secretions may be different.

Culture of bronchial epithelial cells in spheroids also allows for cellular differentiation (Castillon *et al.*, 2004; Deslee *et al.*, 2007). Here isolated epithelial cells are cultured either under static conditions or under horizontal rotation and form spheres of differentiated epithelial cells. Spheroid models have been shown to contain polarised cells with beating cilia, tight junctions, a basal cell population (Castillon *et al.*, 2004; Deslee *et al.*, 2007), however these models cannot be maintained at ALI or used for co-culture studies.

1.7.1 Inflammatory responses of airway epithelium *in vitro* to LPS exposure

Under submerged conditions BEAS-2B respond to LPS challenge by increasing IL-6 secretion (Schulz *et al.*, 2002). Laan *et al.*, (2004) observe IL-8 secretion from BEAS-2B cells when cultured under submerged conditions after treatment with 1µg/ml *E. coli* LPS and IL-6 secretion has been observed from submerged cultures of BEAS-2B treated with *P. aeruginosa* LPS (Veranth *et al.*, 2008). There has been little research conducted into the response of BEAS-2B cultured at ALI. Inhalation of PM has been implicated in contributing to airways inflammation in existing airway diseases (Barraza-Villarreal *et al.*, 2008; Holguin *et al.*, 2007; Sydlick *et al.*, 2006; Tamaoki *et al.*, 2004). *In vitro* investigations into PM induced inflammation are therefore warranted to investigate the inflammatory potential of these substances to healthy airways epithelium and mechanisms of exacerbation of inflammation in diseased states.

1.8 Titanium dioxide

TiO₂ is used in the cosmetic industry as a component of sun block (Nohynek *et al.*, 2010), in paints as a white pigment (Hext *et al.*, 2005), in the food industry (Lomer *et al.*, 2002) and dentistry (Kim & Ramaswamy, 2009). Workers in TiO₂ production industries are exposed to TiO₂ nanoparticles via inhalation (Boffetta *et al.*, 2006). Reports on TiO₂ exposure have failed to identify definitive links between TiO₂ exposure increased mortality. A large study reported by Boffetta *et al.*, (2004) looking at mortality among TiO₂ workers (15,017 individuals) from 11 European factories failed to identify a statistical link between duration of TiO₂ exposure in workers and all causes of mortality. However, an increase in mortality due to lung cancer in workers in TiO₂ production industries compared to national rates was observed when analysing data against standard mortality ratios, suggesting carcinogenic effects of TiO₂. In another study comprising of both estimated exposure and risk analysis by combining previously published data of TiO₂ airborne distribution in TiO₂ nanoparticle production industries and effects on cell- based models (human dermal fibroblasts), Liao *et al.*, (2008) identified that TiO₂ workers have no significant risk of lung inflammation,

however, a cytotoxic response was likely to be observed with “high” TiO₂ nanoparticle (NP), (10-30nm diameter) exposure.

TiO₂ is classified as a group B carcinogen, i.e, possibly carcinogenic to humans according to the International Agency for Research on Cancer (IARC). Further, *in vitro* studies of TiO₂ exposure suggest detrimental effects on the human airways (Hussain *et al.*, 2010; Park *et al.*, 2008; Singh *et al.*, 2007).

1.8.1 Inflammatory and cytotoxic effects of TiO₂ on airways epithelium *in vitro*

Along with inducing increased mucin secretion from airway epithelial cells, as measured by enzyme-linked lectin assay (Chen *et al.*, 2010) TiO₂, in particular UFTiO₂, can induce an inflammatory response in airway epithelial cells. UFTiO₂ treatment of A549 cells resulted in increased mRNA expression and secretion of IL-8 (Singh *et al.*, 2007). Increased expression (Park *et al.*, 2008) and secretion (Zhao *et al.*, 2009) of IL-8 has been demonstrated with submerged cultures of the bronchial epithelial cells BEAS-2B in response to TiO₂. Directional secretion of these inflammatory mediators has yet to be investigated in epithelial cells cultured at ALI. Since inflammatory mediator gene expression differs between submerged and ALI cultures (Ross *et al.*, 2007) secretion profiles may also differ.

Apoptosis is also a consequence of airway epithelial cell exposure to TiO₂. In terms of cell morphology, 16HBE14o cells undergo membrane blebbing, cell shrinkage and DNA fragmentation after exposure to TiO₂ (40µg/cm² for 4 hours; Hussain *et al.*, 2010). Increased apoptosis (measured by annexin V staining) and protein activity of the apoptotic signalling molecules caspase 3, bax, p53 and caspase 9, along with increased intracellular ROS (Shi *et al.*, 2010) and decreased GSH (Park *et al.*, 2008) levels are observed in submerged cultures of BEAS-2B after TiO₂ exposure.

1.8.2 Cellular uptake of TiO₂

Bhattacharya *et al.*, (2009) demonstrate uptake of TiO₂ into BEAS-2B (engulfment by protruding filopodia from BEAS-2B cell membrane) with localisation of particles to the peri-nuclear region. TiO₂ aggregates have also been identified within vacuoles, vesicles and lamellar bodies of A549 cells (Singh *et al.*, 2007; Stearn *et al.*, 2001). Cellular uptake of TiO₂ may result in further detrimental effects as TiO₂ has been identified to impair respiratory control index, decrease oxygen consumption and disrupt mitochondrial membrane potential (Freyre-Fonseca *et al.*, 2011).

1.8.3 Translocation of TiO₂ particles

Exposure of the airways epithelium to TiO₂ *in vivo* results in inflammation and local epithelial cell apoptosis. Prolonged TiO₂ exposure or lung overload, and therefore prolonged inflammation, may result in widespread airways tissue damage. Rothen-Rutishauser *et al.*, (2007) observe translocation of TiO₂ *in vitro* through multiple cell layers. Using a co-culture model of the airways consisting of monocyte derived macrophages (MDM) seeded apically onto A549 cells (A549 cells were first seeded onto the apical side of a Transwell[®] insert) with monocyte derived dendritic cells (MDDC) underneath the epithelial cells (seeded on the underside of the Transwell[®] insert), cells were exposed apically to TiO₂ (5µg/ml) for 24 hours. TiO₂ was observed in all three cell types indicating particle translocation between cells.

In vivo, TiO₂ particles have been observed in the air spaces, epithelial cells, endothelial cells, basement membrane (within the collagen fibrils) and capillaries of rats 1 hour after inhalation exposure (Geiser *et al.*, 2005; Muhlfeld *et al.*, 2007). Direct exposure of the endothelium to PM initiates an inflammatory response. Ultrafine ambient air particles (4 hour incubation with 100µg/ml) up-regulate gene expression and secretion of IL-8 and IL-6 in human primary pulmonary aortic endothelial cells (Karoly *et al.*, 2007). Further, Qu *et al.*, (2010) observe that primary microvascular endothelial cells exposed to urban air dust (100µg/ml) respond with a time dependant increase in IL-6 secretion.

Owing to the ability of endothelial cells to secrete inflammatory mediators after PM and LPS challenge, and the observation that PM translocate to the endothelium *in vivo*, along with the cytokine induced up-regulation of endothelial cell adhesion molecules, inclusion of endothelial cells into airway models of PM exposure should be considered. A multi-cell model of the airways epithelium and endothelium would allow investigations into whether epithelial cell derived cytokines (induced by PM exposure) act upon the endothelium to further release chemokines for leukocyte recruitment and up-regulate adhesion molecule expression for leukocyte extravasation.

1.9 Co-culture

Multi-cell models such as co-culture models are a step towards bridging the gap between *in vitro* models and *in vivo* systems. These permit the study of several cells responding after a stimulus, for example the collaboration between airways epithelium via cytokine and chemokine secretion, endothelial activation and neutrophil recruitment. Furthermore accessory cells or support cells may aid in target cell growth, differentiation and resistance to challenge. For example, in Parkinson's disease models the inclusion of an astrocyte support monolayer enhances dopaminergic neuronal proliferation and survival (under basal and hydrogen peroxide challenge) in mesencephalic neuronal cultures (Drukarch *et al.*, 1997; Langevold *et al.*, 1995). Regarding the airways, the presence of a fibroblast layer in NHBE cultures increases epithelial cell proliferation under submerged conditions (Skibinski *et al.*, 2007), cilia formation and increased TER (suggesting tight junction formation) in ALI cultures (Pohl *et al.*, 2009).

In terms of airway co-cultures to investigate inflammatory events, epithelial cells have been co-cultured with endothelial cells in order to investigate leukocyte migration, however in these models the epithelial cells are cultured under submerged conditions (Casale & Corolan, 1999; Choudhury *et al.*, 2010) and are therefore not representative of the airways epithelium *in vivo*.

Mogel *et al.*, (1998) developed a co-culture of airway epithelial cells and HUVEC where BEAS-2B cells were cultured on the apical surface of Transwell[®] inserts with ECV304 HUVEC cells in the basolateral compartment. Whilst the orientation of the cells was representative of *in vivo*, the BEAS-B were cultured under submerged conditions rather than at ALI. However, a synergistic effect between the two cells types was observed after apical exposure to 0.15ppm ozone for 90 minutes. Levels of IL-8 and IL-6 were detected in the co-cultures that exceeded the sum of secretion from endothelial cells and epithelial cells monocultures after ozone stimulation.

A potential role for airways co-cultures is the identification of biomarkers of airways toxicity and inflammation following exposure to novel test materials. For example, biomarkers of acute and chronic inflammation of airways, or biomarkers of response to challenge may aid in the assessment of cosmetic compound testing. Ideally, *in vitro* models (required to replace animal cosmetic toxicity studies) exposed to cosmetic compounds will be screened for the presence of these biomarkers.

1.10 Biomarkers

Biomarkers are biological compounds, usually proteins, which reflect and allow detection of pathologic progression (disease states) and pharmacologic processes (drug treatment) (Tarrant, 2010). Biomarkers can be used to investigate the toxicity regarding structural or functional consequences of exposure to compounds such as PM and chemical/cosmetic compounds or bacteria/bacterial products such as LPS. Pathologic biomarkers should be specific and sensitive for toxicological exposure or disease state and be early onset with a practical half-life to allow detection (Tarran, 2004). Once identified (*in vitro* or *in vivo*), biomarkers of human disease must be first validated by comparison to established disease or exposure stages (Tarran, 2004).

Cytokines and chemokines are attractive potential biomarkers as their expression and secretion profiles in inflammation and disease are often intensively investigated.

However, cytokines have short half-lives, significant biological variability between subjects and overlapping expression profiles between similar diseases (Tarran, 2004). Further, cytokines are often bound and carried by serum albumin (Granger *et al.*, 2005), which is more abundant in serum than cytokines by several orders of magnitude. The presence of albumin decreases the resolution of protein separation and sensitivity of protein identification in proteomics (Granger *et al.*, 2005), a method used in the identification of biomarkers. Albumin removal of samples results in loss of cytokines in samples, for example IL-8 detection in albumin-depleted LPS (1ng/ml *E. coli* 0111:B4) blood samples was only 26% of non-albumin depleted samples (Granger *et al.*, 2005).

Despite the pitfalls of the presence or depletion of albumin in samples, proteomics is a powerful tool used for identification of biomarkers. Ostroff *et al.*, (2010), using proteomics methods, identified 12 biomarkers of stage I-III non-small cell lung cancer; including up-regulated levels of MIP-4 and pleiotrophin and decreased expression levels of cadherin-1 in serum. Proteomics has been used to identify decreased levels of heat shock protein-27 in atheroma plaques and the atheroma secretome (Vivanco *et al.*, 2008).

1.11 Proteomics

The global protein changes of a particular treatment on a given proteome (plasma, cell proteome for example) can be identified by proteomics, a method where by proteins are separated using two dimensional electrophoresis, analysed for expression changes using statistics, and identified using mass spectrometry.

1.11.1 Two Dimensional electrophoresis

2-DE (whereby proteins are separated first by the isoelectric point and then by their molecular weight) was first carried out in the 1950's (Isaaq *et al.*, 2008). Proteins are focused according to their isoelectric point on strips with carrier ampholytes in acrylamide to produce gels with immobilised pH gradients (IPG) (Gorg *et al.*, 2004). Proteins are then further separated according to their molecular weight and the resultant

protein map is visualised using protein stains (Gorg *et al.*, 2004). Several protein stains exist including Coomassie blue, silver stain or fluorescent stains such as Flamingo™. Flamingo™ stain is not as sensitive as silver nitrate stains for lower concentration spots (silver nitrate has a sensitivity of 100pg-1ng, Miller *et al.*, 2006) with a sensitivity of 0.5ng to 1µg protein (BioRad), however, silver nitrate can result in varying staining intensities between replicates as it is not an end point stain (Miller *et al.*, 2006) unlike Flamingo™. Once spots have been identified by the software protein expression levels measured as density are compared between treatments.

1.11.2 Statistical analysis of spot expression changes between treatments

To detect differentially expressed proteins between control and treatment groups, densitometry analysis software can be utilised. Progenesis SameSpots (Nonlinear Dynamics, Newcastle Upon Tyne, UK) analysis software used in 2-D analysis, analyses the significance between spot expression profiles. The first step in gel analysis is the selection of a reference gel which has the most spots and spot expression levels in common with all other gels. Progenesis SameSpots then normalises the spot volumes and intensities in all other gels to the reference gel. Any expression differences (up- or down-) are then identified and analysed using ANOVA and a statistical power calculation based on expression variance between gels. Progenesis SameSpots also presents data by principal component analysis (PCA), where by all the spots within a given experiment are shown on a biplot, with the gels. Experimental variation between duplicate gels of the same treatment can be visualised along with differentially expressed proteins between treatments, as shown by clustering of spots. Examination of the spot clustering compared to gel positions can also highlight spot expression profiles.

For example, Figure 1.6 shows a PCA plot for 4 treatment groups. The duplicate gels for the treatment group assigned the orange dots, have a large space between them indicating a large experimental variation. Considering spot expression profiles for spot 20, the treatments designated the orange and blue spots will have a low expression of this spot compared to the treatment with the orange spot.

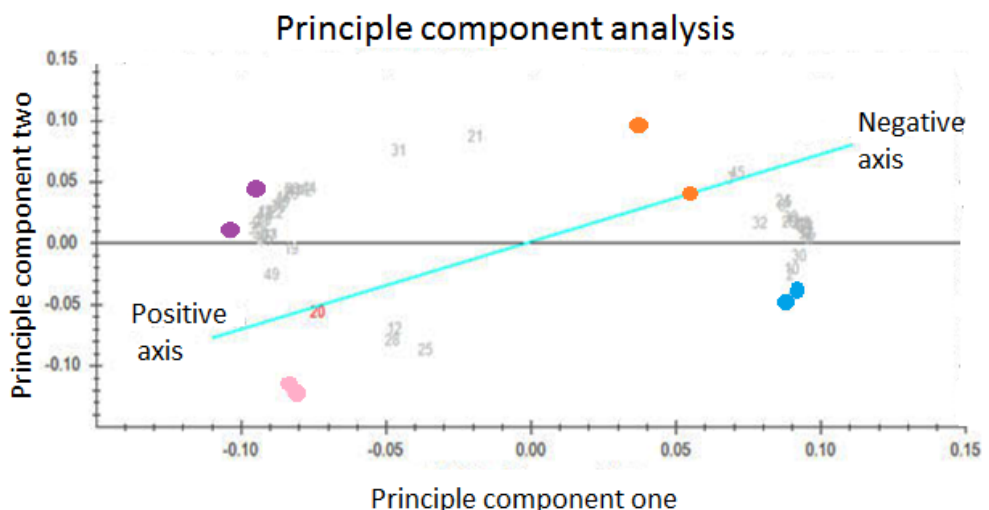


Figure 1.6: PCA analysis plot. PCA plot showing duplicate gels for 4 different treatment groups (coloured dots) and expression profiles of all the proteins spots across all gels. The image and explanation is adapted from [/www.nonlinear.com/products/progenesis/samespots.asp](http://www.nonlinear.com/products/progenesis/samespots.asp).

1.11.3 Digestion of proteins of interest

Once significantly altered spots have been identified across experimental gels the next step is removal of proteins from the gel and peptide digestion. Enzymes such as trypsin are used for peptide digestion as they have known cleavage sites, which is important for identification of protein matches against a database. Peptide masses identified by mass spectrometry are compared against theoretical peptide masses from *in situ* digestion. Peptide masses are governed by the location of cleavage sites within the protein (Canas *et al.*, 2006; Siepen *et al.*, 2006). Trypsin is commonly used as it is low cost and has high cleavage specificity (Siepen *et al.*, 2006).

1.11.4 Mass Fingerprinting using mass spectrometry

The peptide sequences of tryptic digests are determined using mass spectrometry. LC-MS involves separating the peptides first according to their hydrophobicity. The peptides are then ionised using one of 2 methods; matrix-assisted laser desorption ionisation (MALDI) or electrospray ionisation (ESI). ESI has the advantage lower flow rate of peptides to increase sensitivity (Canas *et al.*, 2006; Yates *et al.*, 2009). A heated

capillary aids the removal of ionised droplets from the ionisation source to the mass analyser which determine the mass-to-charge (m/z) ratio of the ion. There are 3 main types of mass analyser; the first is a time of flight (TOF) analyser in which ions are accelerated along the analyser with lighter ions arriving at the detector first (Canas *et al.*, 2006; Yates *et al.*, 2009). The second type is a quadrupole mass analyser. Here, radiofrequency (RF) alternative currents and DC currents are applied to 4 poles, with the DC the frequency of the DC current alternates between the rods causing an oscillating electrical current in the analyser (Canas *et al.*, 2006). Ions are filtered out of the analyser according to their m/z stability (Yates *et al.*, 2009). The third type ion trap in which the ions are separated according to their m/z resonance frequency (Yates *et al.*, 2009). The linear ion trap LTQ has been coupled to an orbitrap mass analyser to produce the LTQ-orbitrap mass spectrometer (Thermo-Scientific) which is capable of tandem mass spectrometry (Yates *et al.*, 2009).

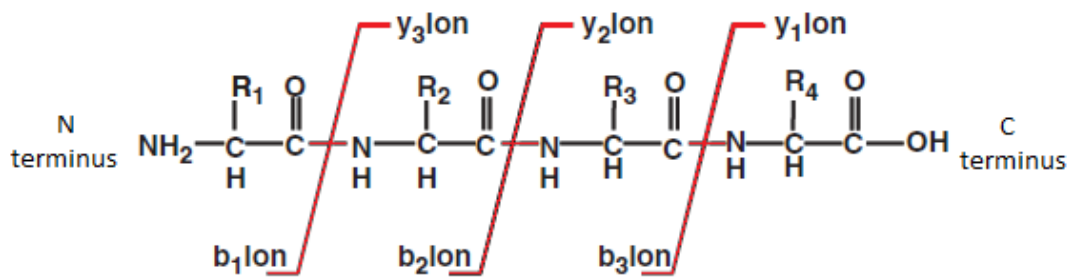


Figure1.7: Schematic of b and y ions. During CID the peptide fragments by splitting of the amide bond resting in b and y ions. Image adapted from Canas *et al.*, 2006.

In tandem mass spectrometry, a full scan is completed on a peak from the liquid chromatograph to identify the parent ion (known as a full ms scan) by the orbitrap (Yates *et al.*, 2009). A zoom scan on of this peak identifies the charge of the ion allowing the mass to be determined. The ion is then selected and fragmented using collision-induced fragmentation (CID). CID results in a spectra of b and y ions which are fragments where the amide bond of the peptide backbone has split during CID (Canas *et al.*, 2006) (Figure 1.7).

The sequence of the peptide can then be determined from these ions, for example if a peptide had the following sequence Ω - κ - β - α - Φ (where the Greek letters represent amino acids to be determined by mass fingerprinting), the b1 ion molecular weight would equal Ω . The b2 ion molecular weight is $\Omega + \kappa$, and so on. During mass fingerprinting the amino acid sequence can be determined by calculating the difference in molecular weight of each ion. Fragmentation occurs in the LTQ ion trap (Yates *et al.*, 2009).

1.12 Challenges in airway proteomics

To enhance the potential for proteomics coupled with mass spectrometry for investigations into global protein changes after airways challenge *in vivo* and identification of biomarkers of airways exposure some challenges need to be overcome. Tissue biopsies from lungs are not readily available (Bharti *et al.*, 2007), furthermore, tissues obtained from biopsies, where mortality was due to respiratory illness, show chronic inflammatory signs, so early responses of exposure cannot be identified. Serum is more readily available and its collection is non-invasive, however, serum proteomics has inherent difficulties owing to the large complexity of serum composition, the presence of abundant proteins and variability between individuals (Bharti *et al.*, 2007). Use of *in vitro* models for identification of biomarkers of response limitations due to removes variability between individuals tissue availability, and once identified, may be used to screen for early lung injury and inflammation.

The aforementioned evidence has provided an overview of our present understanding of particle induced inflammation in the lungs and has highlighted the need for novel *in vitro* techniques to be developed which are relevant physiologically that can provide robust measures of any inflammatory response to unknown particles.

1.13 Aim and objectives

The airways epithelium is the first point of contact for inhaled pathogenic material such as LPS and non-biological compounds such as PM, however, early lung exposure and inflammatory events are difficult to detect. Current *in vitro* models of airways inflammation are limited as the majority do not encompass important immune (neutrophils and macrophages) and non-immune (endothelial cells) cells important in the airways inflammatory response. Whilst animal studies allow detailed examination of mechanisms and cells involved in airways inflammation, they are fundamentally different from humans in their physiology and immunology. Development of robust and valid co-culture models of the airways, in particular where epithelial cells undergo mucociliary differentiation and culture at ALI, may allow detailed toxicity investigations of inhalable toxic material and subsequent identification of biomarkers of response to exposure.

The overall aim of this thesis is to develop a co-culture of the human airways for toxicity testing and identification of novel biomarkers of response to particles.

The specific objectives are;

- 1) To characterise BEAS-2B morphology at ALI compared to NHBE
- 2) To develop an epithelial/endothelial co-culture model
- 3) Investigate inflammatory mediator secretion from this model to LPS (from respiratory and non-respiratory bacterium) and a range of PM
- 4) Determine GSH oxidation and cell viability after LPS/PM challenge
- 5) Identify biomarkers of response using proteomics and LC-MS/MS
- 6) Conduct proteomics and LC-MS/MS on albumin-depleted plasma samples from particle treated rats, where histopathological and transcriptomic analysis was undertaken elsewhere by Carthew *et al.*, (2006).

Chapter 2: Materials and methods

2.1: Materials

2.1.1: General consumables

All reagents were purchased from Sigma (Poole, UK) unless otherwise stated. Cell culture consumables were purchased from Appleton Woods (Birmingham, UK). Penicillin (500,000Uml⁻¹) /streptomycin (500,000µgml⁻¹), foetal calf serum (FCS) gold, amphotericin B and trypsin- ethylenediaminetetraacetic acid (EDTA) were purchased from PAA Laboratories Ltd. (Somerset, UK). BD Falcon Transwell[®] inserts were purchased from VWR (Leicestershire, UK). IPG 3-10 strips, Flamingo[™] protein stain, Criterion 4-20% gradient ready gels and Biolyte 3/10 ampholytes were purchased from BioRad (Hertfordshire, UK). QCL-1000[®] Chromogenic Limulus ameocyte lysate (LAL) endpoint assay kit (Lot GL0969) was purchased from Lonza (Basel, Switzerland). Vectashield hard set mounting medium containing 4',6-diamidino-2-phenylindole (DAPI) was purchased from Vector Laboratories (Peterborough, UK). Immobilon[®] Western Enhanced Chemiluminescent substrate (ECL) was purchased from Millipore (Watford, UK), X-ray film and DeStreak solution was purchased from Amersham Biosciences (Buckinghamshire, UK). Trypsin Gold, ProteaseMAX surfactant Trypsin enhancer, Glutathione-Glo and CellTiter-Blue were purchased from Promega (Southampton, UK). Percoll[™] (1.13g/ml) was purchased from GE Healthcare Bio-Sciences (Buckinghamshire, UK). Nutrient broth and Mueller-Hinton agar were purchased from OXOID LTD. (Basingstoke, UK). Recombinant human IL-8 (Lot BA3109111) was purchased from R&D systems (Oxfordshire, UK), 4 well microscope slides were purchased from C.A. Hendley (Essex) Ltd. (Essex, UK). Phenol, Kodak GBX developer and Kodak GBX fixer and replenisher were purchased from Sigma (Poole, UK). Nunc Maxisorb ELISA plates, microscope slides (1.0-1.2mm thick) and coverslips (0.13-0.17mm thick) were purchased from Fisher Scientific (Loughborough, UK). Immersol[™] immersion oil was purchased from Carl Zeiss Ltd (Hertfordshire, UK). Petri dishes were purchased from Sarstedt Ltd. (Leicester, UK).

2.1.2: Particles

Particles S2219200, S2218600 and S2429901 were provided by Unilever (Colworth) as test particles. S2218600 is an ester derived from a coparticle of methyl vinyl ether and maleic anhydride with butanol. S2218600 is clear yellow suspension and is insoluble in water. The particle was supplied in a vehicle of 74.82% (v/v) water, 22.12% (v/v) ethanol, 1.84% (v/v) diisopropanolamine and 1.22% (v/v) aminomethylpropanol. Upon receipt the particle was made to a stock of 10mg/ml in PBS and stored at -20°C. S2429901 is derived from a coparticle of methyl vinyl ether and maleic anhydride. S2429901 was supplied as a white powder and is water-soluble. S2219200 was provided as an opaque, viscous white suspension in 99.09% (v/v) water and 0.91% (v/v) aminomethylpropanol and is insoluble in water. S2219200 is a high-molecular weight coparticle of methyl- and ethyl methacrylate and butyl acrylate. Upon receipt the particle was made to a stock of 10mg/ml in PBS and stored at -20°C. Fine titanium dioxide (TiO₂, anatase form, lot k342358-48) was purchased from VWR (Leicestershire, UK), ultra-fine titanium dioxide (UFTiO₂, anatase form, Cat 637254) was purchased from Sigma (Poole, UK). Stock concentrations of 10mg/ml particles/particle were prepared in PBS and stored at -20°C prior to use.

2.1.3: Antibodies

Mouse monoclonal anti-cytokeratin 8 (0.5mg/ml ab9023 lot 369887), mouse monoclonal anti-cytokeratin 5 (1mg/ml ab9272 lot 369886), mouse monoclonal anti-mucin5AC (ab3649 clone 45m1), mouse monoclonal anti-VWF (clone 2Q2134, 0.4mg/ml) and mouse monoclonal anti-fibroblast surface antigen clone IB10 (0.2mg/ml) were purchased from Abcam (Cambridge, UK). Mouse IgG kappa (Mopc 21, 5mg m-7894 lot 084k4857), and goat anti-mouse fluorescein isothiocyanate conjugate (FITC F0527 lot 046k6082) were purchased from Sigma. Mouse monoclonal anti-vimentin clone v9 was purchased from GeneTex, Inc (Autogen Bioclear Ltd. Wiltshire, UK). Mouse monoclonal anti-ZO-1 [0.5mg/ml lot 570628A) was purchased from Invitrogen (Paisley, UK). Horseradish peroxidase (HRP) conjugated sheep anti-mouse IgG (NA931V lot 356283) was purchased from Amersham Biosciences (Buckinghamshire, UK).

2.2: Methods

2.2.1: Cell culture

2.2.1.1: Epithelial cell culture

BEAS-2B, passage 22-61 (SV40 transformed normal human bronchial epithelial cells were purchased from American Type Culture Collection (ATCC), LGC Promochem, Middlesex, UK. Product number ATCC-CRL-9609, lot 58121836) and tested negative for mycoplasma. NHBE cells passage 1-3 were purchased from Promocell, Lot 5092901.17 Heidelberg, Germany. BEAS-2B and NHBE were maintained in airway epithelial cell growth medium (Promocell, Heidelberg, Germany) supplemented with 5% (volume/volume v/v) heat inactivated foetal calf serum (Appleton Woods, Birmingham, UK), penicillin/streptomycin (final concentration of 5,000Uml⁻¹/5,000µgml⁻¹ respectively) and manufacturer's supplement (bovine pituitary extract (0.004ml/ml) human recombinant EGF (10ng/ml), human recombinant insulin (5µg/ml), hydrocortisone (0.5µg/ml), epinephrine (0.5µg/ml), triiodo-L-thyronine (6.7ng/ml), transferrin (10µg/ml) and retinoic acid (0.1ng/ml); concentrations listed are final concentrations after supplementation) (Promocell Heidelberg, Germany). BEAS-2B and NHBE were cultured in human placental type IV collagen-coated (Sigma, Poole, UK) 80cm² tissue culture flasks until confluent. Flasks were coated with 10µg/cm² collagen in 3% (v/v) glacial acetic acid for 30 minutes at room temperature. Collagen was then removed and flasks washed 3 times with 5ml PBS

Cells were passaged by washing with PBS followed by incubation with 2.5ml trypsin-EDTA (0.05% trypsin for BEAS-2B, 0.025% trypsin for NHBE) (PAA Laboratories Ltd, Somerset UK) at 37°C (BEAS-2B) or room temperature (NHBE) until 80% of cells were detached. Trypsin was inactivated by addition of 5ml fully supplemented airway epithelial cell culture media. Cells were pelleted by centrifugation at 220xg for 4 minutes, resuspended with 1ml fully supplemented airway epithelial cell media and counted using an improved Neubauer haemocytometer, diluted 1:4 in Trypan blue.

2.2.1.2: Epithelial cell culture on Transwell® inserts

BEAS-2B and NHBE were seeded onto collagen-coated Transwell® inserts (0.65cm diameter, 0.4µm pore size) at 1×10^5 cells/ml in 300µl airway epithelial cell growth medium, with 600µl airway epithelial cell media in the basolateral compartment. On the fourth day of culture, cells were grown at ALI by removal of culture media from the apical compartment, to induce mucociliary differentiation and, basolateral medium was replenished at this point. The basolateral medium was replenished at 4-5 day intervals (cells were cultured on Transwell® inserts for 11-14 days).

2.2.1.3: HPMEC culture

Normal human pulmonary microvascular endothelial cells (HPMEC) were purchased from Promocell (lot 8112001.9 Heidelberg, Germany) and maintained in endothelial cell culture media supplemented with manufacturer's supplement (FCS (0.02ml/ml), endothelial cell growth supplement (0.004ml/ml), recombinant human EGF (0.1ng/ml), heparin (90µg/ml) and hydrocortisone (1µg/ml), concentrations listed are final concentrations after supplementation); and penicillin/ streptomycin (final concentration of 5,000 Uml⁻¹/5,000µgml⁻¹ respectively). HPMEC were cultured in 25cm² tissue culture flasks until confluent. Cells were passaged by washing with 2ml PBS followed by incubation with 1ml trypsin-EDTA (0.04% trypsin) at room temperature until 80% of cells were detached. Trypsin was inactivated by addition of 3ml fully supplemented endothelial cell culture media. Cells were pelleted by centrifugation at 220xg, 4 minutes, resuspended with 1ml fully supplemented endothelial cell medium and counted using a Neubauer haemocytometer.

2.2.1.4: Co-culture of BEAS-2B cells and HPMEC

BEAS-2B cells were cultured on collagen-coated Transwell® inserts as described above. HPMEC were seeded in 24 well culture plates at 5×10^4 cells/well in 1ml endothelial cell culture media overnight. HPMEC media was replenished with 600µl endothelial cell media and BEAS-2B cultured at ALI on Transwell® inserts with a TER

of $>45\Omega\text{cm}^{-2}$ were added to the wells. Cells were left for 4 hours to equilibrate prior to treatments.

2.2.2: TER

Airway epithelial cell medium (300 μl) was added to the apical compartment of cultures grown at ALI and the TER measured using an Epithelial Voltohmmeter with STX2 chopstick electrodes (World Precision Instruments). Measurements were taken 3 times for each well. A blank reading (TER of an empty collagen-coated Transwell[®] insert) was subtracted. TER measurements are expressed as ohms (Ω) x cm^2 .

2.2.3: FITC-dextran permeability measurements

BEAS-2B and NHBE grown at ALI on Transwell[®] inserts were treated apically with 200 μl 40kDa FITC-dextran (1mg/ml stock) for 24 hours, on day 0, 4, 7, 11 and 14 of culture at ALI. The basolateral (B) and apical (A) media were collected after 24 hour incubation; the apical surface of the cells was washed twice with 200 μl PBS and the washes were collected and combined with the apical medium. Fluorescence was determined at an excitation (EX) wavelength of 488nm and emission (EM) wavelength of 520nm using a SpectraMax GeminiXS fluorimeter (Molecular Devices). The cell monolayer permeability was calculated as the basolateral fluorescence as a percentage of total fluorescence $(B/(A+B))*100$.

2.2.4: Endotoxin content determination of LPS and particles by limulus amoebocyte lysate (LAL) assay

In order to determine whether particles contained endotoxin contamination the endotoxin content of particles (200 $\mu\text{g/ml}$ from a 10mg/ml stock, diluted with endotoxin free LAL water) was determined with the QCL-1000[®] Chromogenic LAL Endpoint

assay, according to the manufacturer's instructions. The LAL was also carried out on isolated and purchased LPS to determine endotoxin content.

The principle of the QCL-1000[®] Chromogenic LAL endpoint assay is as follows; a pro-enzyme the limulus ameocyte lysate, is activated in the presence of endotoxin and catalyses the removal of the coloured compound p-nitroaniline (pNA) from a colourless substrate (Ac-Ile-Glu-Ala-Arg-pNA). The amount of pNA released is measured spectrophotometrically (405-410nm) and is proportional to the amount of endotoxin present. Endotoxin standard (25 endotoxin units (EU) EU/ml) was used to create a standard curve with a low standard of 0.1EU/ml and high standard of 1EU/ml. Results are expressed as endotoxin content in EU/ml.

2.2.4: IL-8/IL-6 Enzyme-linked immunosorbent assay (ELISA)

Apical and basolateral media from LPS- or particle-treated cells were analysed for IL-8 or IL-6 by ELISA (IL-8; 900-K18, IL-6; 900-K16, Peprotech, London, UK). A Nunc maxisorb ELISA plate was coated overnight at 4°C with 0.5µg/ml goat-anti human IL-8 or 1µg/ml goat-anti human IL-6 (100µl/well) in 0.05M carbonate/bicarbonate buffer (Sigma, C3041) and subsequently washed 3 times with 200µl wash buffer (0.05% (v/v) Tween-20 in saline, and blotted dry. The plate was then blocked for 1 hour at room temperature with 300µl/well 1% (weight/volume, w/v) BSA in PBS. After blocking the plate was washed 3 times as above and incubated with 100µl/well standards and samples for 2 hours at room temperature. The IL-8 standard curve consisted of recombinant human IL-8 diluted in reagent diluent (0.05% (v/v) Tween-20, 0.1 % (w/v) BSA in PBS) to the following concentrations; 10,000pg/ml, 2000pg/ml, 1000pg/ml, 500pg/ml, 250pg/ml, 125pg/ml, 62.5pg/ml and 0pg/ml. The IL-6 standard curve consisted of recombinant human IL-6 serially diluted in reagent diluent (0.05% (v/v) Tween-20, 0.1 % (w/v) BSA in PBS) with a high standard of 2000pg/ml. The plate was then washed as above and incubated with 100µl/well 0.25µg/ml biotinylated goat anti-human BD-2 IL-8 or 0.25µg/ml biotinylated goat anti-human IL-6 for 2 hours at room temperature, followed by 3 times washing as above and incubation with 100µl/well

avidin-HRP (1:2000) for 30 minutes at room temperature. The plate was washed 3 times as above before incubation with 100µl/well SigmaFast o-phenylenediamine (OPD). Colour development was stopped by addition of 50µl/well 1M HCL and absorbance read using a BioTek EL800 microplate reader (BioTek instruments, Bedfordshire, UK) at 490nm. Sample IL-8 and IL-6 concentration was extrapolated from the standard curve and expressed as pg/sample by correction for sample volume.

2.2.6: CellTiter-Blue[®] viability assay

After LPS- or particle-treatment matter incubation, cell viability was assessed using the CellTiter-Blue[®] viability assay. The principle of the assay is as follows: after treatment cells are incubated with the non-fluorescent CellTiter-Blue[®] solution containing resazurin. Viable cells metabolically reduce resazurin into the fluorescent resorufin, which is released into the culture medium. After incubation with LPS or particles supernatants were removed and cleared at 295xg for 2 minutes and stored at -20°C. Cells were incubated with CellTiter-Blue[®] (diluted 1:5 in appropriate cell culture medium) for 4 hours at 37°C in the dark. For co-culture studies Transwell[®] inserts containing BEAS-2B were removed to separate wells so so that viability of each compartment could be assessed separately. After incubation with CellTiter-Blue[®], supernatants from Transwell[®] inserts were removed to a 96 well plate and fluorescence measured at Ex560nm, Em590nm using a SpectraMax GeminiXS fluorimeter (Molecular Devices). Supernatants from HPMEC cells were measured *in situ*.

2.2.7: Effect of LPS or particle treatment on BEAS-2B TER

Westmoreland *et al.*, (1999) observed that sodium carbonate as a positive control for airway damage induced a significant time dependent reduction in TER, which correlated to loss of viability using MTT. TER was therefore used in the current study to investigate the effects of PM or LPS on the airways epithelium barrier. Triton X-100 was used as a positive control of barrier disruption and did not interfere with volthometry. Prior to LPS or particulate matter challenge airway epithelial cell medium (300µl) was added to the apical compartment of BEAS-2B cultured at ALI and TER

measured using an Epithelial Voltohmmeter with STX2 chopstick electrodes (World Precision Instruments). Measurements were taken 3 times for each well. After treatment of BEAS-2B at ALI with LPS or particles supernatants were collected and the apical surface of cells was washed gently with 100µl airway epithelial cell medium. After washing, fresh airway epithelial cell medium (300µl) was added to the apical compartment of cultures and TER was determined as above. Results are expressed as the TER percentage of control taken before treatment, and the TER percentage of control taken after treatment.

2.2.8: Statistical analysis

Statistical analysis was undertaken using one-way ANOVA with Tukey's post test and represented at mean \pm standard error of the mean (SEM) where experiments were conducted at least 3 times and where with a replicate 3 wells were used per treatment. Standard deviation (SD) was used where there were less than 3 experimental replicates taken, or where in a given replicate the treatments were carried out once only (where stated).

Chapter 3: Suitability of BEAS-2B and NHBE as *in vitro* cell models of the human airways

3.1: Rationale

The bronchial epithelial cell line BEAS-2B are widely used as an *in vitro* model of the human airway epithelium under submerged culture conditions, however, the morphology of these cells at ALI is not well defined. This study aims to compare and contrast the BEAS-2B bronchial epithelial cell line with primary, non-transformed NHBE as *in vitro* models of the human airways cultured at ALI. A suitable culture media for co-culture of epithelial cells at ALI with human primary pulmonary microvascular endothelial cells has also been investigated.

Cells were cultured at ALI on Transwell[®] inserts to induce differentiation and were characterised by measurement of TER and barrier permeability to indicate the presence of a functioning tight barrier. Expression of the tight junction protein ZO-1 and the epithelial cell markers cytokeratin 5 and 8 was also investigated. In this system NHBE failed to form a functioning tight barrier with tight junction protein expression, and cell populations expressed mesenchymal cell markers. BEAS-2B cultured at ALI show cytokeratin expression patterns comparable to the airway epithelium *in vivo*. A functioning tight barrier was formed by BEAS-2B with evidence of tight junction protein expression and distribution to cell margins.

The morphology of BEAS-2B cells, when cultured at ALI, indicates that these cells may be a representative model of the airway epithelium and were used in epithelial/endothelial cell co-culture. Endothelial cell culture media was found to be a suitable culture media for both cell types without effect on BEAS-2B barrier function.

3.2: Introduction

Both the airways epithelium and endothelium are involved in recruitment of leukocytes to the airways after pathogenic or toxic challenge (Bals & Hiemstra, 2004; Danese *et al.*, 2007), co-culture of these cells may therefore be valuable in the study of airways inflammation after challenge. Casale & Coralan, (1999) characterised a model whereby A549 were seeded on the underside of a Transwell[®] insert and human umbilical vein endothelial cells (HUVEC) were seeded in the apical compartment of the insert. Chemoattractants were placed in the basolateral compartment and migration of granulocytes from the apical compartment to the basolateral compartment.

Choudhury *et al.*, (2010) constructed an epithelial/endothelial cell co-culture with 16HBE14o and HUVEC in the same orientation as Casale and Corolan, (1999) to investigate the effect of endothelial cells on epithelial cell membrane permeability. They observed an increased TER in the co-culture model that is greater than the sum of the monoculture TER. Using conditioned media from HUVEC cultures Choudhury *et al.*, (2010) identified that an endothelial cell secreted mediator is responsible for this increase in TER, as conditioned media treatment of 16HBE14o induced an increase in TER to levels observed in the co-culture. This study demonstrates that epithelial cell morphology is influenced by the presence of endothelial cells.

A further example of an epithelial/endothelial cell co-culture where the epithelial cells (in this case H292 epithelial cells) are cultured on the underside of a Transwell[®] insert with HUVEC endothelial cells in the apical compartment is the model described by Mul *et al.*, (2000). Mul *et al.*, (2000) observed that in monoculture negligible amounts of IL-6 are secreted from either cell types, whilst IL-8 is secreted from the epithelial cells only (under unstimulated conditions). In co-culture, however, the basal levels of IL-8 and IL-6 secretion are significantly greater than the epithelial cells alone, highlighting the influence of endothelial cells on epithelial cell cultures.

Little research has been conducted into the morphology of BEAS-2B, a cell line derived from normal epithelial cells, at ALI. Co-culture of these cells at ALI with human pulmonary epithelial cells would be a novel model of the airways *in vivo*. An immediate aim was to therefore characterise the suitability of BEAS-2B cells cultured at ALI as a model of the airways epithelium *in vivo* compared to NHBE cells. Cytokeratin expression profiles (basal epithelial cells express cytokeratins 5 and 14 whilst differentiated pseudo-columnar cells express cytokeratins 7,8,13 and 19 (Iyonaga *et al.*, 1997)), barrier function, tight junction formation and mucin secretion are investigated and directly compared to NHBE cells which undergo mucociliary differentiation. A suitable culture media for construction of an epithelial/endothelial cell co-culture model (Figure 3.1) with epithelial cells at ALI has been investigated.

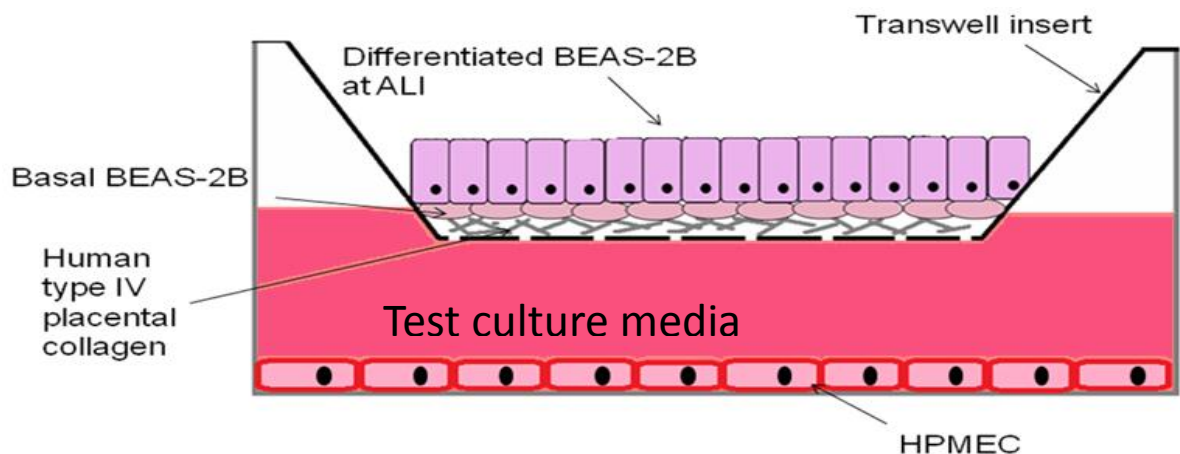


Figure 3.1: Schematic diagram of BEAS-2B/ human pulmonary microvascular endothelial cell co-culture developed in this chapter. BEAS-2B cultured at ALI on Transwell® Inserts in co-culture with HPMEC in the basolateral compartment of the well.

3.3: Methods

3.3.1: Characterisation of epithelial cell and endothelial cell cultures

BEAS-2B and NHBE cells were seeded onto human placental type IV collagen-coated (for collagen coating protocol refer to 2.2.1) ($10\mu\text{g}/\text{cm}^2$) 4-well slides at 5×10^4 cells/ml in $200\mu\text{l}$ airway epithelial cell medium and cultured until confluent, or on Transwell[®] inserts (refer to section 2.2.1.2). Immunohistochemical staining on Transwell[®] inserts was undertaken when a differentiated monolayer was formed as indicated by TER (see section 2.2.2) measurements (when a TER of $>45 \Omega \times \text{cm}^2$ was reached, typically after 11 days of culture at ALI). HPMEC were seeded onto un-coated 4 well slides at 5×10^4 cells/ml in $200\mu\text{l}$ endothelial cell medium. Cells on Transwell[®] inserts and 4 well slides were fixed with $100\mu\text{l}$ 100% methanol (pre-cooled) for 20 minutes at -20°C and washed 3 times with $200\mu\text{l}$ PBS. Cells were then permeabilised with $100\mu\text{l}$ 0.1% (v/v) Triton X-100 in PBS for 30 minutes at room temperature followed by 3 washes with $200\mu\text{l}$ PBS. Cells were then blocked with $100\mu\text{l}$ 1% (v/v) normal goat serum in PBS for 1 hour at room temperature followed by an additional 3 washes with $200\mu\text{l}$ PBS. Cells were incubated with $100\mu\text{l}$ primary mouse monoclonal anti-cytokeratin antibodies, mouse monoclonal anti-fibroblast surface antigen, mouse monoclonal anti-Muc5AC, mouse monoclonal anti-vimentin, mouse monoclonal anti-ZO-1, mouse monoclonal anti-VWF or isotype-matched control in 1% BSA (w/v) in PBS or 1% BSA in PBS alone overnight at 4°C . Cells were then washed 3 times with $200\mu\text{l}$ PBS and incubated with $100\mu\text{l}$ goat anti-mouse FITC-conjugated secondary antibody diluted 1:100 in 1% BSA in PBS for 1 hour at 4°C . Cells were washed a final 3 times with $200\mu\text{l}$ PBS and mounted with hard set mounting medium containing DAPI (1 drop/well/insert) and left to set for 48 hours at 4°C in the dark. Images were taken on a Zeiss Axiovert 200M fluorescent microscope using objective 63 (magnified 63 times) with a DAPI filter (exposures of 5-20ms) and a FITC filter (exposures of 50-150ms). ZO-1 images were taken at the most apical surface of cells.

3.3.2: TER and FITC-dextran permeability measurements

TER and FITC-dextran measurements were undertaken as detailed in sections (2.2.2) and (2.2.3) respectively.

3.3.3: Mucin identification using antibodies to muc5AC

Apical secretions from BEAS-2B or NHBE were collected by gentle pipetting followed by 50µl PBS wash (added to apical secretion). Samples were cleared of cell debris by centrifugation (295xg for 2 minutes) and stored at -20° prior to analysis. Porcine gastric mucin standard, BSA (as a negative control), samples of fully supplemented airway epithelial cell medium and serum-free medium (as blanks), and apical secretions were blotted onto a nitrocellulose membrane using a hybridisation manifold under vacuum (total volume of 50µl/well for each sample). The membrane was subsequently blocked in tris-buffered saline with 0.05% (v/v) Tween-20 (TTBS) with 3% (w/v) BSA prior to overnight incubation with primary mouse monoclonal anti-muc5AC antibody (diluted 1:500 in TTBS with 0.3% (w/v) BSA), at room temperature. The membrane was washed 3 times with TTBS for 15 minutes per wash, prior to incubation with HRP-conjugated sheep anti-mouse antibody (diluted 1:5000 in TTBS with 0.3% (w/v) BSA) for 1 hour 30 minutes at room temperature. After a further 6 times ten minute washes with TTBS the membrane was treated with Immobilon[®] ECL and exposed to film for 3 minutes prior to being visualised with Kodak GBX developer and fixer.

3.3.4: Barrier integrity of BEAS-2B cultured in endothelial cell culture medium

BEAS-2B were cultured on collagen-coated Transwell[®] inserts (as described in section 2.2.1.2). On day 0 of culture at ALI basolateral media was replenished with either 600µl airway epithelial cell media or 600µl endothelial cell culture medium. Barrier integrity was measured during culture at ALI in both culture media using TER and FITC-dextran permeability as described above.

3.3.5: Co-culture of BEAS-2B cells and HPMEC cells

BEAS-2B were co-cultured with HPMEC as described in section 2.2.1.4.

3.4: Results

3.4.1: Submerged populations of BEAS-2B express both epithelial cell markers cytokeratin 5 and cytokeratin 8

In order to identify basal cells within populations of BEAS-2B and NHBE, cells were grown under submerged conditions and expression of the epithelial cell-specific markers, the cytokeratins 5 and 8, has been analysed. The results show that, under submerged conditions BEAS-2B express both the basal cell marker cytokeratin 5 (Figure 3.2A), and the differentiated cell marker cytokeratin 8 (Figure 3.2B). Under submerged conditions NHBE cells showed only non-specific staining (for controls see 10.1.2.3) using antibodies against both the epithelial cell markers cytokeratin 5 (Figure 3.2C) and cytokeratin 8 (Figure 3.2D).

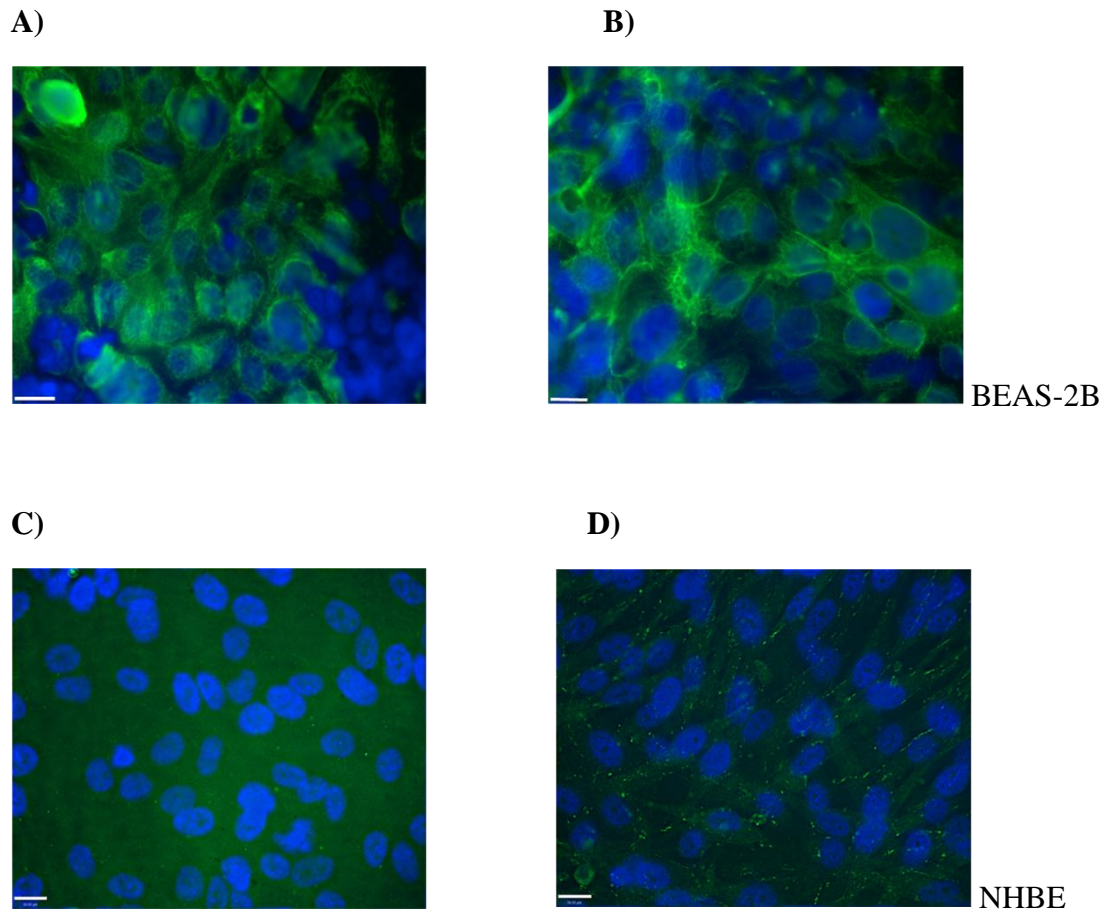


Figure 3.2: Submerged cultures of BEAS-2B express both epithelial cell markers cytokeratin 5 and cytokeratin 8. BEAS-2B (A and B) and NHBE (C and D) were seeded on collagen-coated 4 well slides at a density of 5×10^4 cells/ml and grown to confluence for 3 days. Cells were fixed with 200 μ l pre-cooled methanol, permeabilised with 0.1% Triton X-100 in PBS and blocked with 1% (v/v) normal goat serum in PBS, as described in 3.3.1. Cells were then incubated with mouse-monoclonal antibody to cytokeratin 5 (A and C) or, cytokeratin 8 (B and D) at 1:250 in 1% (w/v) BSA in PBS, overnight at 4°C. Cells were then washed and incubated with FITC-conjugated goat anti-mouse secondary antibody (1:100 in 1% (w/v) BSA in PBS) for 1 hour at room temperature. Cells were mounted in DAPI and images taken using Zeiss Axiovert 200M fluorescent microscope, images are representative of 4 separate experiments for BEAS-2B, bar size is 16 μ m.

3.4.2: BEAS-2B cultured at ALI express both basal and differentiated epithelial cell markers.

In order to investigate whether differentiated populations of BEAS-2B and NHBE, cells were grown on collagen-coated Transwell[®] inserts at ALI, an analysis of the expression profile of the cytokeratins undertaken. Figure 3.2 shows that, when grown at ALI, BEAS-2B express the markers for basal and differentiated epithelial cells (cytokeratin 5 (Figure 3.3A) and cytokeratin 8 (Figure 3.3B) respectively). When cultured at ALI, NHBE cell populations consist of very few cytokeratin 5 positive basal epithelial cells (Figure 3.3C), however, a larger population of cytokeratin 8 positive differentiated epithelial cells was observed (Figure 3.3D and E). Figures 3.3D and E are Z- stack images moving through the multiple cell layers for the same population of NHBE cells, and show that cytokeratin 8 positive, differentiated epithelial cells are dispersed throughout the cell population.

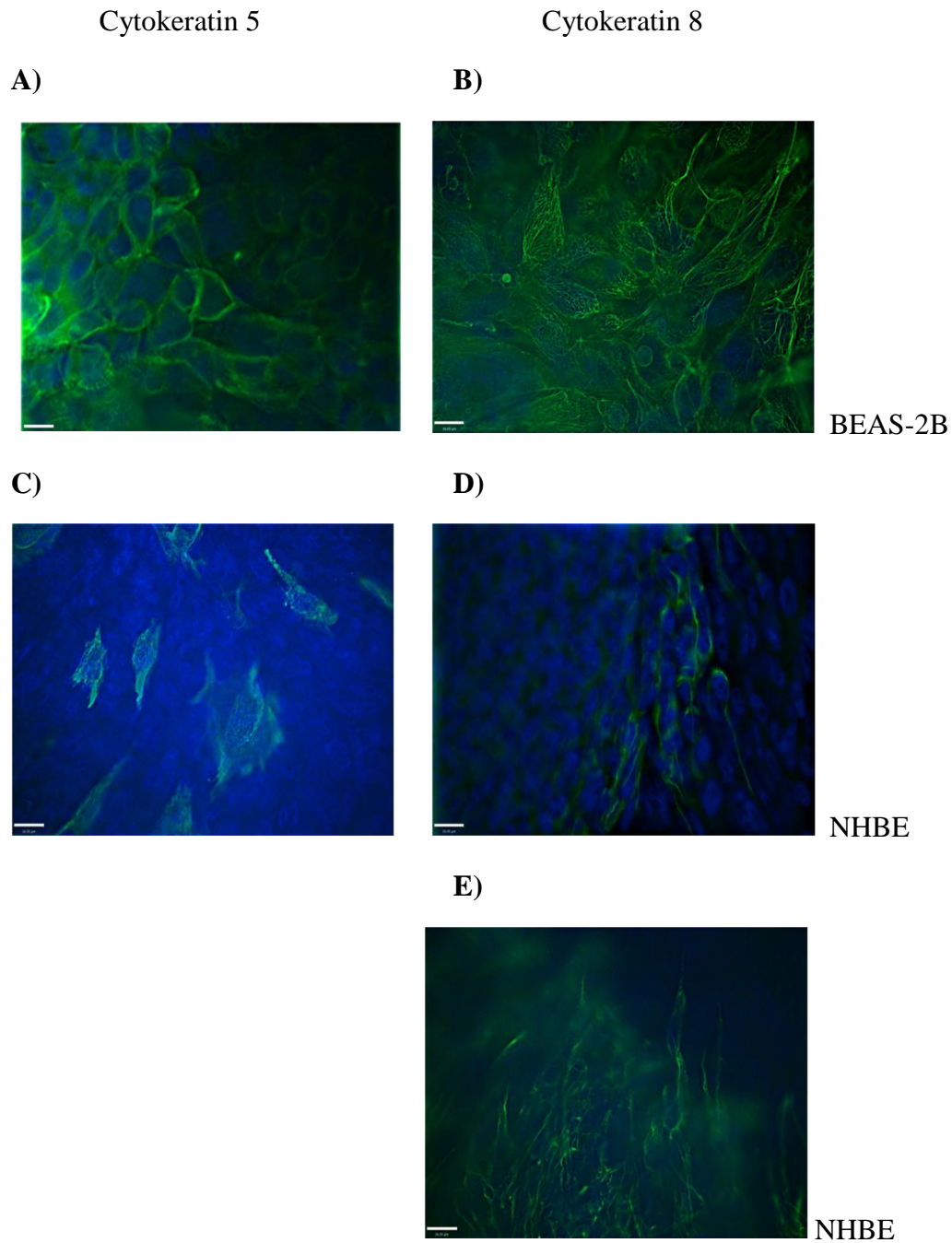


Figure 3.3: BEAS2B cultured at ALI express both basal and differentiated epithelial cell markers. BEAS-2B (A and B) and NHBE (C, D and E) were seeded on collagen-coated Transwell® inserts at a density of 1×10^5 cells/ml and cultured at ALI to induce differentiation. Cells were fixed with 200 μ l methanol at -20°C after which the membranes were excised. Blocking was achieved with 1% (v/v) normal goat serum in PBS and cells were permeabilised with 0.1% (v/v) Triton X-100 in PBS, as described in 3.3.1. Cells were then incubated with mouse-monoclonal antibody to cytokeratin 5 (A and C) or cytokeratin 8 (B, D and E) diluted 1:250 in 1% (w/v) BSA in PBS overnight at 4°C . Cells were washed and incubated with FITC-conjugated goat anti-mouse secondary antibody (1:100 in 1% (w/v) BSA in PBS) for 1 hour at room temperature. Cells were mounted in DAPI and images taken using Zeiss Axiovert 200M fluorescent microscope, images are representative of 4 separate experiments for BEAS2B and 3 separate experiments for NHBE. D and E are images separated from a z-stack whereby D was taken at the bottom of the cell populations and E at the top. Bar indicates 16 μ m.

3.4.3: BEAS-2B cultured at ALI express the tight junction protein ZO-1 at the site of cell-cell contact.

As part of the respiratory defence system, differentiated epithelia produce a tight barrier against pathogens by formation of tight junctions between neighbouring cells. In order to characterise the differentiation of BEAS-2B and NHBE grown at ALI on Transwell[®] inserts, staining for the tight junction protein, ZO-1, was undertaken. An investigation of the expression of ZO-1 was also undertaken on submerged BEAS-2B and NHBE in order to determine whether tight junction formation is specific to cells grown at ALI. Figure 3.4B indicates that BEAS-2B show ZO-1 localisation at the site of cell-cell contact (Figure 3.4B) suggesting tight junction formation in these cells when cultured at ALI. Under submerged conditions BEAS-2B express ZO-1, however, there is no defined localization of the protein to junctions between neighbouring cells (Figure 3.4A). No ZO-1 staining was observed in NHBE cells cultured under submerged conditions (Figure 3.4C), whilst punctate staining was observed when cells cultured at ALI were stained (Figure 3.4D).

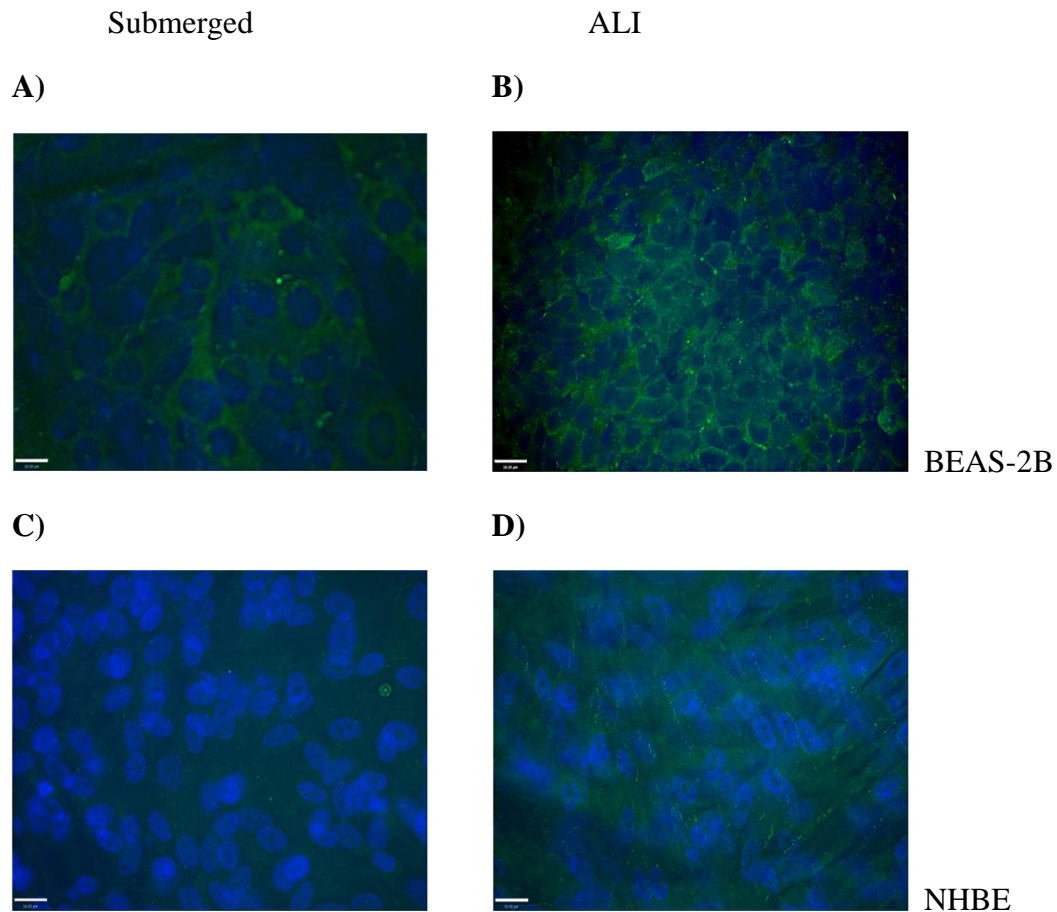


Figure 3.4: BEAS-2B cultured at ALI express the tight junction protein ZO-1 at the site of cell-cell contact. BEAS-2B and NHBE were seeded on collagen-coated 4 well slides until confluent (A and C) or Transwell[®] inserts at ALI until a TER of $45\Omega \times \text{cm}^2$ was reached for BEAS-2B (B) or for 11 days for NHBE (D). Cells were fixed with 200 μl methanol at -20°C . Cells were permeabilised with 0.1% Triton X-100 and blocked with 1% (v/v) normal goat serum in PBS before overnight incubation with mouse-monoclonal antibody to ZO-1 diluted 1:250 in 1% (w/v) BSA in PBS at 4°C . Cells were washed with PBS and incubated for 1 and half hours with FITC-conjugated goat anti-mouse secondary antibody (1 in 100 in 1% (w/v) BSA in PBS) at 4°C . Cells were mounted in DAPI and images taken using Zeiss Axiovert 200M fluorescent microscope. Images are representative of 3 separate experiments. Bar indicates 16 μm .

3.4.4: TER of BEAS-2B increases and FITC-dextran permeability decreases during culture at ALI.

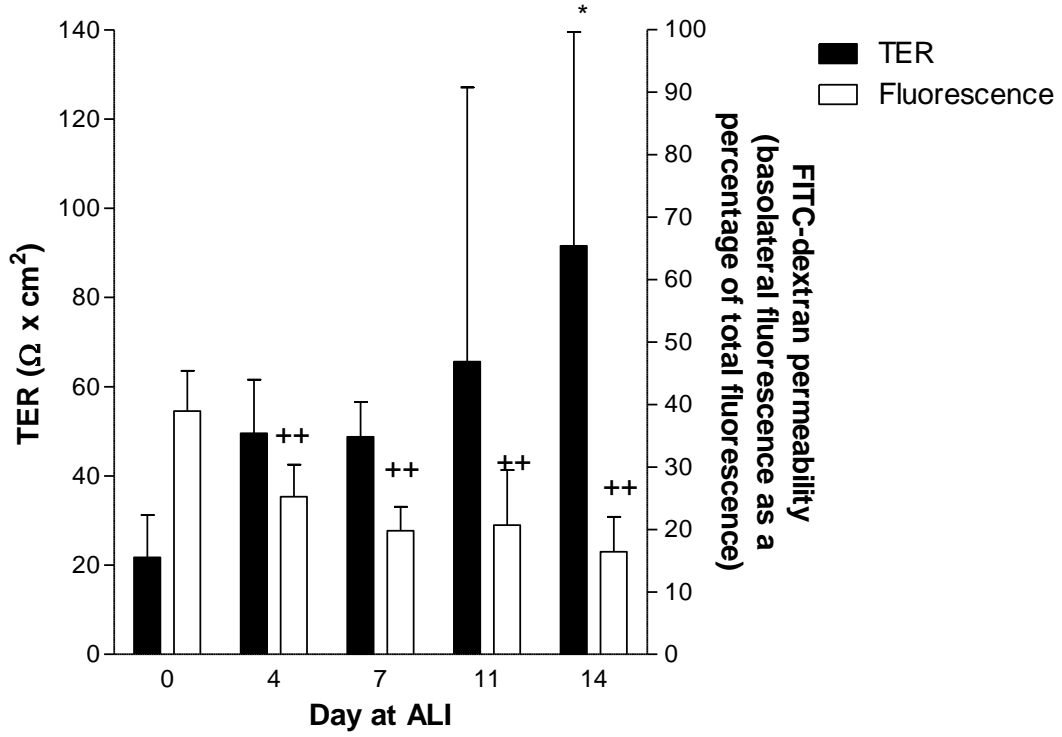
Functional assessment of barrier integrity of epithelial cell cultures on Transwell® inserts can be investigated using TER, which measures the electrical resistance through the paracellular pathway (between apical and basolateral compartments of cells grown on Transwell® inserts). As a tight barrier is formed the electrical resistance increases. Decreased permeability of the epithelial cell monolayer to solutes is also an indicator of barrier formation.

During culture at ALI BEAS-2B form a functioning tight barrier as TER increases with time (Figure 3.5). By day 11 of culture at ALI BEAS-2B have a TER of $79 \pm 26 \Omega \times \text{cm}^2$; however, at this time of culture the TER was extremely variable. By day 14 at ALI, TER was significantly increased compared to day 0 ALI. Permeability of BEAS-2B to 40kDa FITC-dextran significantly decreased ($P < 0.01$) during culture at ALI compared to day 0 ALI, with only $20.7 \pm 3.6\%$ of FITC-dextran permeating the cell monolayer by day 11 of culture at ALI.

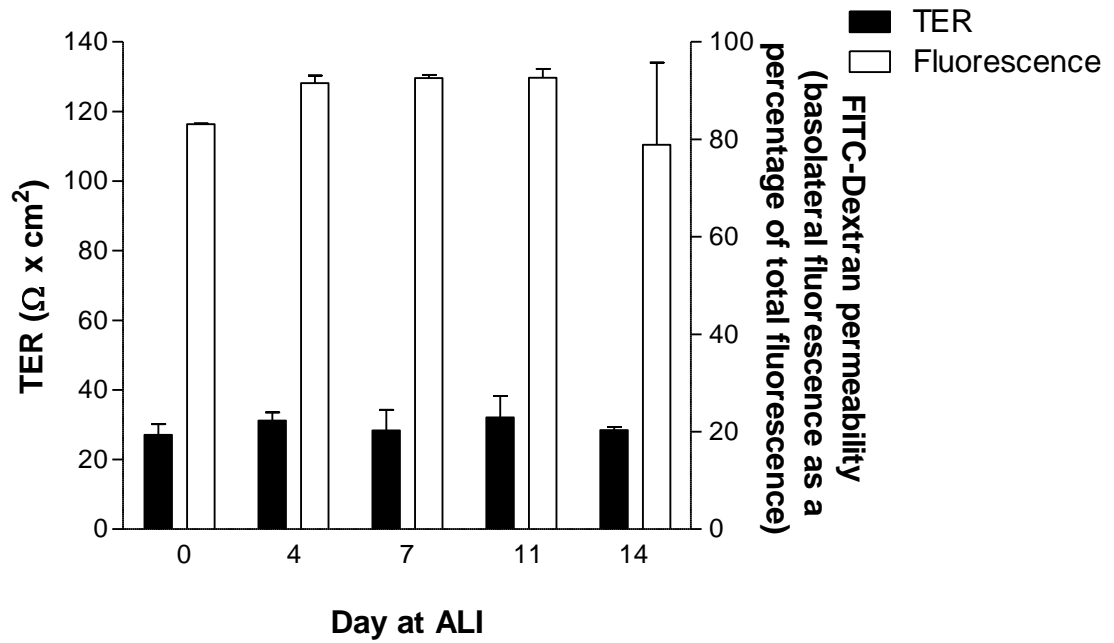
NHBE cells cultured at ALI failed to form a functioning tight barrier as indicated by the lack of increase in TER, or reduction in FITC-dextran permeability, when seeded at the same cell density as BEAS-2B ($1 \times 10^5/\text{ml}$, Figure 3.5B). Indeed the FITC-dextran permeability at day 14 ALI ($78.9 \pm 23.8\%$) was similar to that of a collagen-coated insert without cells ($93 \pm 2.4\%$). TER of these cells at day 0 ALI was $27 \pm 4 \Omega \times \text{cm}^2$; this stayed stable during culture at ALI with cells having a TER of $28 \pm 4 \Omega \times \text{cm}^2$ at day 14 ALI (Figure 5B).

When seeded at the higher cell density of $2.5 \times 10^5/\text{ml}$ NHBE cells again failed to build up a functioning tight barrier with a TER of $20 \pm 12 \Omega \times \text{cm}^2$ on day 0 ALI which showed a non-significant decrease to $12 \pm 7 \Omega \times \text{cm}^2$ by day 11 of culture at ALI. Permeability of NHBE to the solute FITC dextran at day 0 of ALI was $36.7 \pm 3.6\%$, but this did not change significantly ($34.2 \pm 2.2\%$ by day 11 ALI, Figure 3.5C).

A)



B)



C)

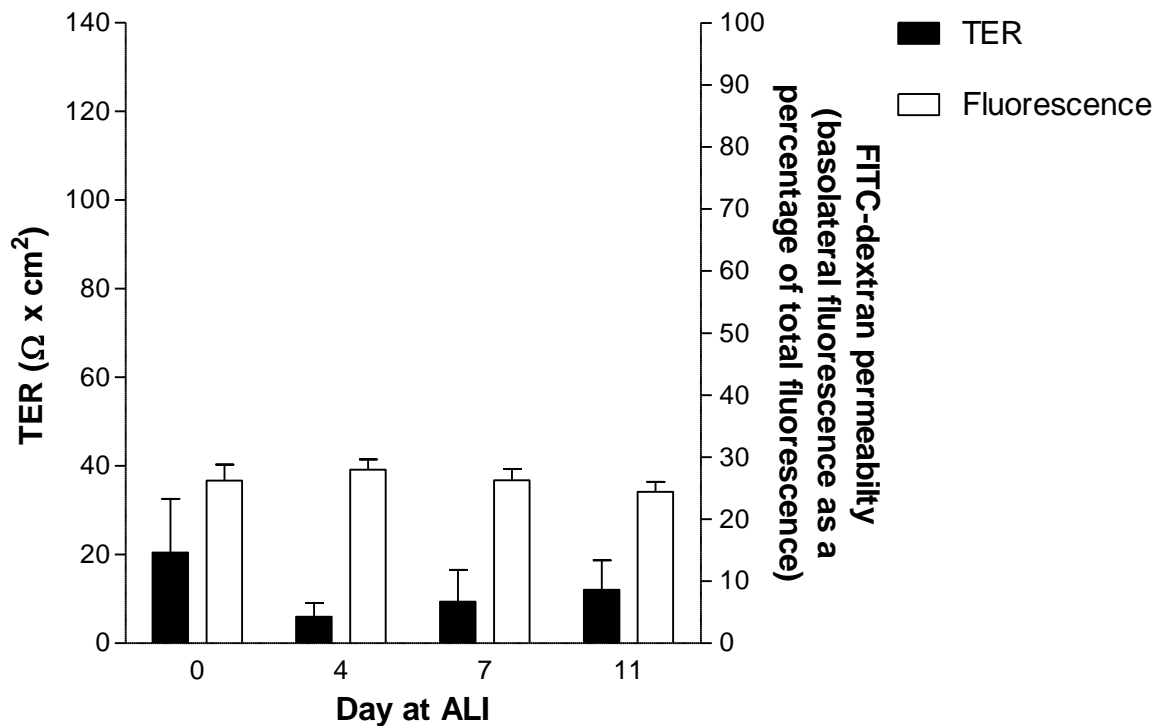


Figure 3.5: TER of BEAS-2B but not NHBE cells increases and FITC-dextran permeability decreases during culture at ALI. BEAS-2B (A) and NHBE (B and C) were seeded on collagen-coated Transwell[®] inserts at a density of $1 \times 10^5/\text{ml}$ (A and B) or $2.5 \times 10^5/\text{ml}$ (C) in $300 \mu\text{l}$ medium. On the fourth day of culture, apical medium was removed and cells were grown at ALI (Day 0). TER measurements were taken at day 0, 4, 7, 11 and 14 of culture (black columns), using an empty Transwell[®] insert as a blank (see section 2.2.2). After TER measurements were conducted, cells were incubated for 24 hours with $200 \mu\text{l}$ FITC-dextran ($1 \text{mg}/\text{ml}$ stock) and fluorescence of apical and basolateral medium was measured at excitation 488nm emission 520nm (see section 2.2.3). FITC-dextran permeability of an empty collagen-coated Transwell[®] insert is $93 \pm 2.4\%$. Permeability is calculated as FITC-dextran in the basolateral compartment as a percentage of total fluorescence (white columns). $N=3$. Data are expressed as mean \pm standard deviation (SD) * $P < 0.05$ compared to TER at day 0 ALI, ++ $P < 0.01$ compared to FITC-dextran in the basolateral compartment permeability at day 0 ALI.

3.4.5: NHBE cultured at ALI secrete muc5AC

The mucociliary escalator plays a vital role in protection of the airways from inhaled pathogens and particulates. In order to determine whether BEAS-2B or NHBE cultured at ALI secrete mucin, apical secretions were gently collected from the apical surface of cells during culture at ALI (up to day 14) and stored at -20°C. Once all samples were collected, apical secretions were pooled, and a dot blot for the major airways mucin muc5AC was performed. The presence of muc5AC in BEAS-2B secretions was not detected, however muc5AC was detected in apical secretions from NHBE apical secretions (Figure 3.6).

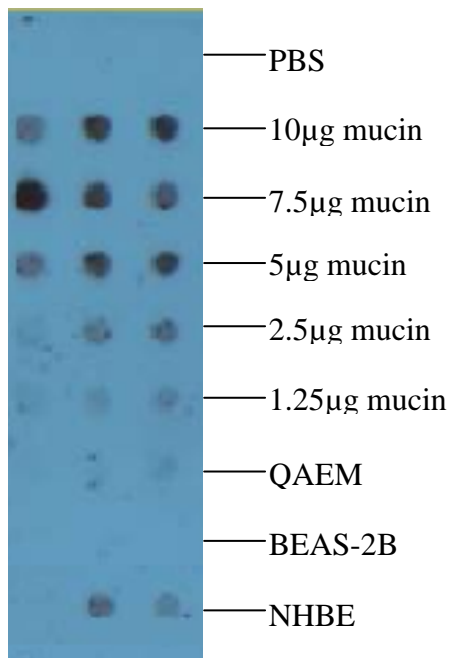


Figure 3.6: NHBE cultured at ALI secrete muc5AC. Apical secretions were collected from BEAS-2B and NHBE cultured at ALI and transferred to nitrocellulose membrane using a hybridization manifold under vacuum. Porcine gastric mucin was used as a standard, BSA, PBS and quiescent airway epithelial cell media (QAEM) serve as negative controls. Membranes were blocked with 3% (w/v) BSA in TTBS prior to incubation with anti-muc5AC antibody overnight (1:500 in 0.3% (w/v) BSA in TTBS). Membranes were incubated with HRP-conjugated sheep anti-mouse secondary antibody (1:5000 in 0.3% (w/v) BSA in TTBS) for 1.5 hours before incubation with ECL and visualisation via exposure to X-ray film for 3 minutes. Image is representative of 3 separate experiments for standard curve and BEAS-2B secretion, and 2 separate experiments for NHBE secretions.

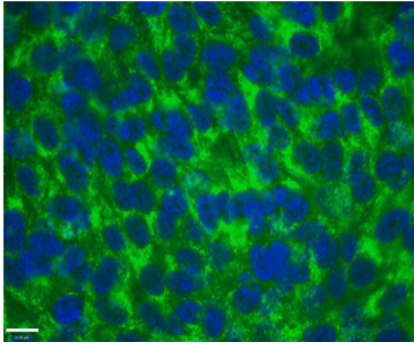
3.4.6: Evidence for epithelial to mesenchymal transition in NHBE cultures.

Since NHBE cells failed to form a functioning tight barrier, measured by both barrier permeability and formation of tight junctions, and had very few epithelial cells in the cell population (as indicated by cytokeratin staining), EMT in NHBE cells was investigated. Cells both under submerged conditions and at ALI were stained for the EMT marker vimentin, and for the fibroblast surface antigen. Cells were also stained with anti-Mmuc5AC, as there is evidence of mucin secretion at ALI, to identify mucus secreting cells and therefore define an epithelial population. Submerged and ALI cells were stained to investigate whether culture condition favours growth of any epithelial cells rather than transformed mesenchymal cells.

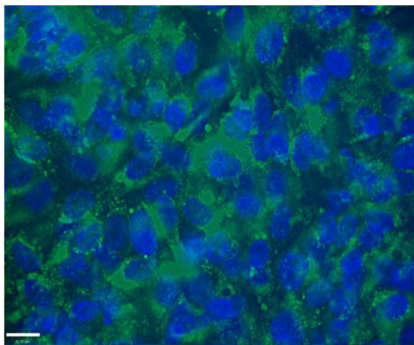
NHBE cells under both culture conditions were positive for fibroblast surface antigen (Figure 3.7A and 3.7B) and the EMT marker vimentin (Figure 3.7C and D). Non-specific staining similar to that observed with isotype control (see section 10.1.2.3) was observed when NHBE cells were stained with antibody against muc5AC, regardless of culture conditions (Figure 3.7E and 3.7F).

Submerged culture

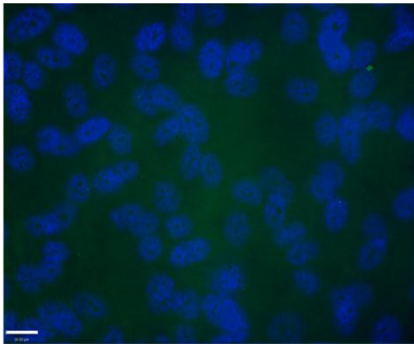
A)



C)

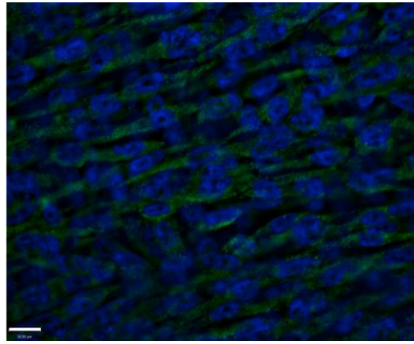


E)

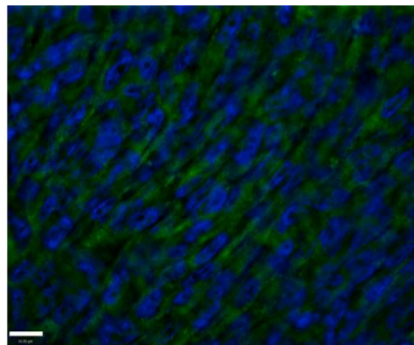


Culture at ALI

B)



D)



F)

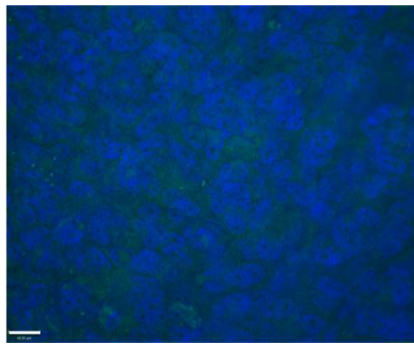


Figure 3.7: Evidence for EMT in NHBE cultures. NHBE were seeded on collagen-coated 4 well slides until confluent (A, C & E) or Transwell[®] inserts at ALI (B, D & F) for 11 days. After fixing, cells were permeabilised with 0.1% (v/v) Triton X-100 and blocked with 1% (v/v) normal goat serum in PBS before overnight incubation with mouse-monoclonal antibody to fibroblast surface antigen (A and B), vimentin (C and C) or muc5AC (E and F), diluted 1:250 in 1% (w/v) BSA in PBS at 4°C. Cells were washed with PBS and incubated for 1 and half hours with FITC-conjugated goat anti-mouse secondary antibody (1:100 in 1% (w/v) BSA in PBS) at 4°C. Cells were mounted in DAPI and images taken using Zeiss Axiovert 200M fluorescent microscope. Images are representative of 3 separate experiments. Bar indicates 16µm.

3.4.7: Expression of VWF in HPMEC cultures.

The purity of primary HPMEC was determined by expression of the specific endothelial cell marker VWF. As HPMEC cells will be used in co-culture experiments they were also examined for expression of the epithelial cell markers cytokeratin 8 and 5, to ensure no epithelial cell contamination. The results show that HPMEC stocks were positive for the endothelial cell marker VWF with localisation consistent that is vesicular (Figure 3.8A) and negative for both epithelial cell markers, cytokeratin 5 (Figure 3.8C) and cytokeratin 8 (Figure 3.8D). HPMEC stained with antibody isotype matched control (IgG1) were negative for cell staining (Figure 3.8B).

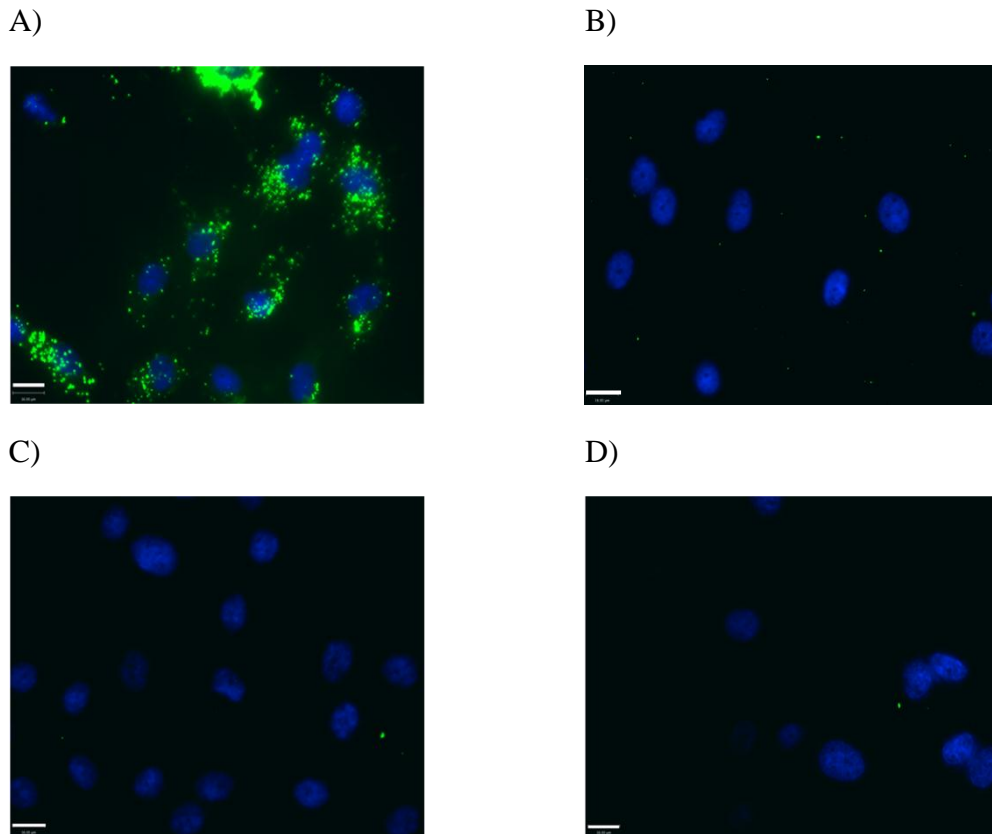


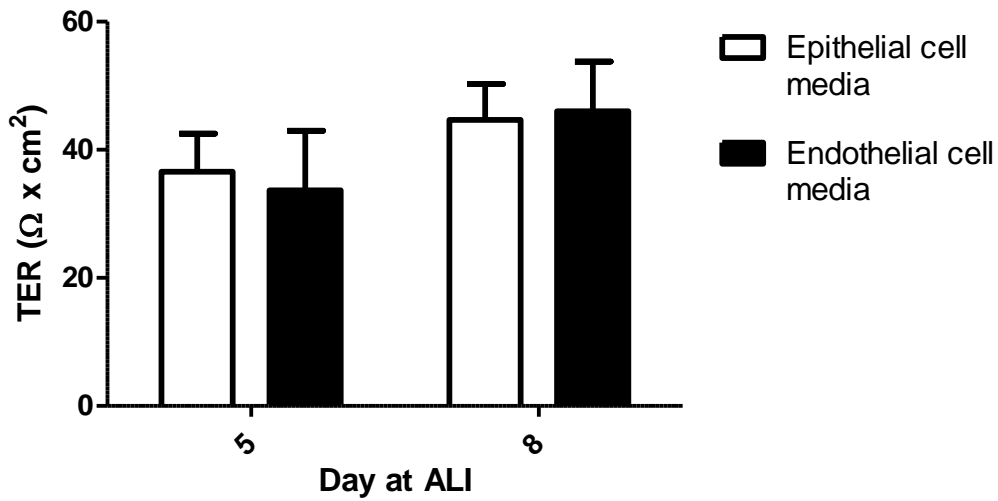
Figure 3.8: Expression of VWF in HPMEC cells. HPMEC were seeded on 4 well slides and cultured until confluent. Cells were fixed with 200 μ l methanol at -20°C , permeabilised with 0.1% (v/v) Triton X-100 and blocked with 1% (v/v) normal goat serum in PBS before overnight incubation with mouse-monoclonal antibody to VWF (A), IgG1 (B) cyokeratin 5 (C) or cyokeratin 8 (D), diluted 1:250 in 1% (w/v) BSA in PBS at 4°C . Cells were washed with PBS and incubated for 1 and half hours with FITC-conjugated goat anti-mouse secondary antibody (1:100 in 1% (w/v) BSA in PBS) at 4°C . Cells were mounted in DAPI and images taken using Zeiss Axiovert 200M fluorescent microscope. Images are representative of 3 separate experiments.

3.4.8: BEAS-2B cultured at ALI in endothelial cell medium maintain barrier integrity.

Once constructed, the co-culture will consist of BEAS-2B cultured at ALI and HPMEC in the basolateral compartment of the 24 well companion plate into which the Transwell[®] insert is submerged (Figure 3.1). In this model the basolateral medium of the Transwell[®] insert will be shared between HPMEC and BEAS-2B, therefore a single medium suitable for both BEAS-2B and HPMEC culture is required. As culture of BEAS-2B at ALI has been shown to be stable it was investigated whether these cells would maintain barrier integrity if cultured with endothelial cell culture medium.

Culture of BEAS-2B in endothelial cell medium for either 5 or 8 days had no significant effect on TER. After 8 days of culture at ALI, TER in epithelial cell medium was $45 \pm 6 \Omega \times \text{cm}^2$ and $46 \pm 8 \Omega \times \text{cm}^2$ in endothelial cell culture medium. Similarly FITC-dextran permeability through the cell layer was unaffected by culture in endothelial cell medium compared to culture in airway epithelial cell medium. FITC-dextran permeability was $13.7 \pm 2\%$ in endothelial cell medium and 16.5 ± 1.7 in airway epithelial cell medium at day 8 of culture at ALI (Figure 3.9).

A)



B)

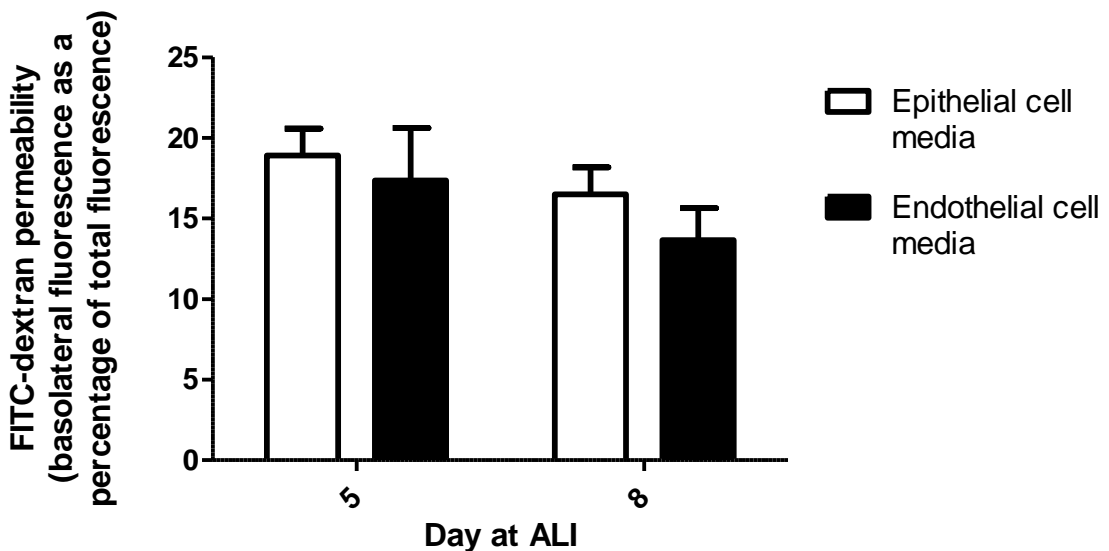


Figure 3.9: BEAS-2B cultured at ALI in endothelial cell medium maintain barrier integrity. BEAS-2B were seeded on collagen-coated Transwell® inserts at a density of $1 \times 10^5/\text{ml}$ in $300\mu\text{l}$ media. On the fourth day of culture, apical medium was removed and cells were grown at ALI (day 0) in either airway epithelial cell culture medium (black bars) or endothelial cell culture medium (clear bars). A) TER measurements were taken at day 5 and 8 of culture, using an empty Transwell® insert as a blank (see section 2.2.2). After TER measurements were conducted cells were incubated for 24 hours with $200\mu\text{l}$ FITC-dextran (B). Apical and basolateral media was then recovered and fluorescence measured at excitation 488nm emission 520nm and expressed as basolateral fluorescence as a percentage of total fluorescence. FITC-dextran permeability of an empty collagen-coated Transwell® insert is $93 \pm 2.4\%$. Results are expressed as FITC-dextran in the basolateral compartment as a percentage of total fluorescence (white columns). $N=4$. Data are expressed as mean \pm SEM.

3.5: Discussion

BEAS-2B cells are widely used under submerged conditions as an *in vitro* model of human airways epithelium, especially in inhalation toxicity studies (Cha *et al.*, 2007; Noah *et al.*, 1995; Petacchia *et al.*, 2009, Veranth *et al.*, 2007). However the morphological features of these cells when cultured at ALI are less well characterised compared to NHBE. The present study has evaluated the differentiation phenotype, and thus suitability of BEAS-2B as a model of the airway epithelium. BEAS-2B differentiation, measured by means of cytokeratin expression, tight junction and barrier formation, and mucin secretion were directly compared to NHBE grown at ALI.

Results from the current study culturing NHBE at ALI failed to replicate those by other authors whereby a pseudostratified ciliated mucus-secreting epithelium with tight junctions have been observed (Keisemer *et al.*, 2009; Lin *et al.*, 2007, Ross *et al.*, 2007; Sajjan *et al.*, 2008). In the current study NHBE cells cultured at ALI failed to form tight junctions as evident by ZO-1 staining and did not show increasing TER whereas Lin *et al.*, (2007) observed a maximal TER of $766 \pm 154 \Omega \times \text{cm}^2$ with these cells. The presence of retinoic acid in cell culture media and culture on a collagen substratum have both been shown to enhance epithelial cell differentiation (Gray *et al.*, 1996, Wu *et al.*, 1997), however, culture conditions in the current study include both retinoic acid as a component of the culture medium and a collagen basement membrane on the Transwell[®] insert.

Initially in the current study NHBE were seeded on the inserts at a density of 1×10^5 cells/ml. Culturing NHBE at a higher seeding density as used by Lin *et al.*, (2007) resulted in a lower percentage permeability of FITC-dextran ($34.19 \pm 2.19\%$) at day 11 of culture at ALI. However, the TER again was low ($12.07 \pm 6.68 \Omega \times \text{cm}^2$). These results suggest that FITC-dextran permeability is at least in part influenced by cell number as at the higher cell density NHBE failed to increase TER and were negative for tight junction staining as measured by ZO-1.

It is possible that the NHBE cells underwent EMT, due to stress, which would explain the lack of tight junction formation and failure of NHBE to produce increasing TER at ALI. EMT was therefore investigated in NHBE submerged and ALI cultures by staining for vimentin and fibroblast surface antigen. Under both culture conditions NHBE cells were positive for both EMT markers. The lack of epithelial cell markers under submerged conditions may indicate that in these conditions mesenchymal cells outgrow epithelial cells whereas culture at ALI allows for some epithelial cell growth as there was presence of few cytokeratin 5 cells with a larger cytokeratin 8 population in NHBE at ALI. Furthermore mucin was observed in apical secretion of NHBE at ALI, despite immunohistochemical analysis failing to show mucin positive cells. The presence of an underlying population of mesenchymal fibroblasts within initial cell cultures which outgrew epithelial cells may account for the presence of vimentin and fibroblast surface antigen positive cells in NHBE cultures, or cells may have undergone EMT due to the stress, possibly as a result of sub-optimal culture conditions.

The current study aimed to characterise the suitability of BEAS-2B at ALI as an *in vitro* model of the human airways by direct comparison to NHBE cells, however, as NHBE cells in the current study contained large populations of mesenchymal cells results obtained with BEAS-2B will be compared to current literature of epithelial cell culture at ALI.

Under submerged conditions, BEAS-2B expressed both the basal epithelial cell marker cytokeratin 5 and the differentiated epithelial cell marker cytokeratin 8. The presence of cytokeratin 8 expression in BEAS-2B cells under submerged conditions suggests that these cells are at least in part differentiated. This may be a consequence of their transformation with the SV40 virus, as transformed cells often do not express the characteristics of primary cells (Forbes and Ehrhardt, 2005). In support of this hypothesis Morris *et al.*, (1985) observe a change in cytokeratin expression in SV40 transformed keratinocytes whereby decreased expression of cytokeratins 5, 10, 14 16 and 20 was observed compared to non-transformed keratinocytes. Furthermore, transformed keratinocytes showed increased expression of cytokeratins 18 and 19 (Morris *et al.*, 1985).

BEAS-2B also express both cytokeratin 5 and 8 when cultured at ALI indicative of a differentiated cell phenotype with a basal cell population. The maintained expression of cytokeratin 5 in BEAS-2B cultured at ALI suggests the presence of a basal cell population indicating that BEAS-2B when cultured at ALI are representative of the respiratory epithelium *in vivo* and are comparable to NHBE cultured on ALI where basal cell populations alongside differentiated mucociliary cells have been observed (Bonnans *et al.*, 2006; Lin *et al.*, 2007). However, the suggestion that BEAS-2B may be partially differentiated anyway means that caution is warranted in analysis of results. Further investigations are required to determine whether BEAS-2B at ALI are indeed pseudo-columnar differentiated epithelial cells. The presence of ciliated cells in BEAS-2B cultures at ALI was not investigated in the current study. Results from a mucin dot blot detecting the mucin muc5AC in apical secretions show that the BEAS-2B did not differentiate into mucus secreting goblet cells. Mucin secretion by BEAS-2B at ALI has not been previously reported, however muc5AC expression in submerged cultured of BEAS-2B was shown to be non-significantly increased by treatment with 50nM retinoic acid whilst untreated cells showed no muc5AC expression (Kuntz *et al.*, 2006). Future work could investigate retinoic acid treatment of BEAS-2B at ALI and electron microscopy to see whether mucociliary differentiation can be induced.

BEAS-2B showed a trend towards increasing TER during culture at ALI with TER reaching significance at day 14 compared to day 0 ALI suggesting that formation of a tight barrier (suggestive of differentiation) occurs over a number of days. Ross *et al.*, (2007) show that mucociliary differentiation of NHBE occurs over a period of 21 days with the absence of cilia at day 6 of ALI culture but the presence of cilia at 12 days ALI culture which may explain the time dependent increase in TER observed here. The results obtained for TER in the current study for BEAS-2B ($91.56 \pm 47.96 \Omega \times \text{cm}^2$) are low, however, TER correlates poorly to permeability tracers (Tang and Goodenough, 2003). Immunohistochemical staining of tight junction proteins was undertaken to give further insight into presence of tight junctions in BEAS-2B cultures.

Petacchia *et al.*, (2009) observed ZO-1 staining in submerged cultures of BEAS-2B at the site of cell-cell contact and Woo *et al.*, (2008) observed ZO-1 staining in aquaporin

5 transfected BEAS-2B at ALI. Results from the current study confirm that under submerged conditions BEAS-2B express ZO-1 however the staining pattern is not localised to sites of cell-cell contact. When cultured at ALI ZO-1 was localised to sites of cell adhesion i.e. sites of tight junctions. To the author's knowledge this is the first time that ZO-1 staining and therefore tight junction formation has been observed in wild type non-challenged BEAS-2B cultured at ALI. As tight junctions are the most apical junctional complex between neighbouring epithelial cells (Neissen, 2007) the sub-cellular localisation ZO-1 may not have occurred at cell junctions in submerged cultures of BEAS-2B as they have not undergone differentiation. It would be interesting to observe whether localisation of ZO-1 to cell junctions occurs in stages of culture at ALI in a similar manner to mucin secretion and cilia formation.

In order to gain a better understanding of the airway inflammation in response to LPS and PM an aim of this study is the construction of an epithelial/endothelial cell co-culture to represent the airways *in vivo*. To this end primary human HPMEC in mono-culture were assessed for purity of culture by staining for the endothelial cell specific marker VWF as described by Middleton *et al.*, (2005). Cells were shown to be positive for staining with VWF, with a punctuate staining pattern. This staining is typical of VWF which is stored in secretory granules termed Weibel-Pallade bodies where it acts as an endothelial cell specific carrier protein for coagulation factor VIII (van den Biggelaar *et al.*, 2009; Rosenberg, 2000). HPMEC populations were negative for the epithelial cell markers cytokeratin 5 and cytokeratin 8, indicating that HPMEC were not contaminated with epithelial cells.

There are only a few pulmonary epithelial/endothelial models characterised in the literature, further these models focus on using the model for investigation of inflammatory cell extravasation, or barrier permeability studies (Casale & Corolan, 1999; Chowdhury *et al.*, 2010). In these models the epithelial cells are under submerged conditions and while this may be appropriate for permeability and infiltration studies, it is not appropriate for the current study which aims to investigate airway inflammation at ALI. In the current study BEAS-2B are cultured in the apical compartment of a Transwell[®] insert at ALI with HPMEC in the basolateral compartment of the companion plate, attached to the companion plate itself. In this model the apical surface

of the endothelial cells is in close proximity to the basolateral surface of the epithelial cells, and although this orientation is not observed *in vivo*, it allows for an ALI epithelial culture. Future work could focus on characterising a model whereby HPMEC are cultured on the underside of the Transwell[®] insert allowing for basolateral-basolateral cell surface contact with ALI culture of epithelial cells.

As the BEAS-2B and HPMEC will be sharing the same culture media whilst in co-culture a suitable media that allows for BEAS-2B barrier integrity and growth of HPMEC is required. Effect of culture media in the study of Casale and Coralan, (1999) or Chowdhury *et al.*, (2010) was not investigated as in both cases the cells used were cell lines rather than primary cells. Whilst the current study has physiological relevance as the endothelial cells are primary human pulmonary cells it has the disadvantage that primary cells are less robust than cell lines and often require specific manufactured culture media. The barrier integrity of BEAS-2B at ALI in endothelial cell culture media was therefore investigated. No differences in either TER or FITC-dextran permeability were observed when BEAS-2B were cultured in epithelial cell culture media or endothelial cell culture media for up to 8 days. Co-culture studies described in later chapters of this thesis will therefore include endothelial cell culture media in the endothelial cell compartment.

3.6: Conclusion

The current study aimed to characterise BEAS-2B cultured at ALI as a model of the airways epithelium *in vivo* compared to NHBE cells at ALI. However, NHBE cultures in the current study failed to undergo differentiation as measured by tight junction formation and barrier integrity. NHBE also contained mesenchymal cell populations, either from contaminant cell outgrowth or EMT. BEAS-2B cultured at ALI produced a low TER consistent with other reports. BEAS-2B also formed tight junctions as measured directly by ZO-1 staining but failed to secrete mucin. Further studies are required to investigate whether cilia are formed by BEAS-2B at ALI. As BEAS-2B formed tight junctions at ALI with indications of the presence of both basal and

epithelial cell populations they were considered a representative model of the airways epithelium *in vivo*.

This study also characterised the purity of HPMEC cultures destined for co-culture studies and confirmed that BEAS-2B retain barrier integrity when cultured in endothelial cell media at ALI. Together BEAS-2B cultured at ALI with HPMEC in co-culture are considered as a representative epithelial/endothelial cell model of the human airways. This model along with BEAS-2B alone at ALI and HPMEC mono-cultures will be used to characterise the effect of LPS and particulate matter exposure in relation to inflammatory mediator secretion and identification of biomarkers of toxicity.

Chapter 4: LPS stimulation

4.1: Rationale

Culture of epithelial cells at ALI on Transwell[®] inserts supports the formation of tight junctions. Physiological barriers are important to defend the airways against invading pathogens. In addition, epithelial cells normally exhibit innate immune response properties after challenge. Therefore the propensity for BEAS-2B cells at ALI to respond to inflammatory stimuli was investigated. BEAS-2B cultured at ALI are sensitive to LPS from *E. coli* and respond with directional secretion of the inflammatory mediators IL-8 and IL-6. ZO-1 localisation to tight junctions in LPS challenged cells was disrupted however the integrity of the epithelial barrier was maintained, as measured by TER. The BEAS-2B/HPMEC did not produce an inflammatory response after *E. coli* LPS challenge. These results suggest that BEAS-2B at ALI, with and without HPMEC, represent a valid model for the study of pathogenic insult to the airways epithelium. The co-culture system requires further development.

4.2: Introduction

The airway epithelium serves to protect the airways from invading pathogens by forming a protective ion and size selective barrier, via tight junctions (Farquhar and Palade, 1963). Epithelial cells cultured on physical supports such as Transwell® inserts at ALI, where the apical surface of cells is free of medium and cells receive nutrients from a basolateral compartment, can differentiate into mucociliary cells (de Jong *et al.*, 2003; Gray *et al.*, 1995) which supports formation of tight junctions. Despite having morphological features representative of *in vivo*, submerged cultures of epithelium are often utilised for the study of airway inflammation after pathogenic challenge.

Koyama *et al.*, (2000) observed that *P. aeruginosa* S:10 LPS induces IL-8 secretion from A549 cells under submerged conditions. Interestingly, *E. coli* 0127:B8 LPS induced IL-8 secretion from A549 cells to a lesser extent. TLR4/LBP bind the Lipid A domain of LPS. Whilst the general structure of LPS is conserved; the degree of phosphorylation of the fatty acids, location of fatty acid acyl group and fatty acid chain length vary between different species (Rietschel *et al.*, 1994) resulting in differing degrees of TLR4 activation and thus different potencies regarding cellular activation. Koyama *et al.*, (2000) also reported that *E. coli* 0111:B4 LPS induced less IL-8 secretion from A549 than *E. coli* 0127:B8 and BEAS-2B responded to *E. coli* 0111:B4 LPS (increased IL-8 secretion) only in the presence of serum, a result mirrored in experiments undertaken by Schulz *et al.*, (2002). However, Schulz *et al.*, (2002) observed that replacement of serum with sCD14, LBP or both failed to result in the increased secretion of IL-8 and IL-6 from BEAS-2B as observed with serum and suggest that LPS induces inflammatory signalling in BEAS-2B in an undefined CD14-independent manner.

ALI models have been used to investigate tight junction integrity. Coyne *et al.*, (2002) observed that the tight junctions of NHBE cells at ALI are disrupted by 72 hour incubation with TNF α and interferon (IFN) γ . Under inflammatory conditions there was a decreased number of tight junctional strands (measured by freeze-fracture electron microscopy) and a loss of ZO-1 and JAM expression and localisation to the tight

junction. It is therefore possible that pathogen-induced inflammation induces disruption in airway epithelial cell tight junctions. Therefore, the aim of the current study was to investigate the use of BEAS-2B cells cultured at ALI as directional models of inflammatory responses of the airway epithelium, measured by phenotype characterisation, barrier function and cytokine secretion after treatment with LPS. The response inflammatory response of the BEAS-2B/HPMEC after LPS-challenge was also characterised to investigate whether presence of HPMEC alters the BEAS-2B inflammatory response.

4.3: Methods

4.3.1: LPS isolation from *P. aeruginosa* and *B. cepacia*

In order to test the response of airway epithelial cell cultures to relevant respiratory pathogens, LPS was isolated from *P. aeruginosa* and *B. cepacia*. *P. aeruginosa* and *B. cepacia*, were cultured on commercial blood agar plates overnight at 37°C. A colony of each bacterium was used to inoculate a 100ml of sterile nutrient broth which was further incubated at 37°C overnight. Following overnight incubation a loop of each inoculated broth was streaked out onto sterile agar plates and incubated at 37°C overnight to check purity of cultures. Inoculated broth (50ml) was then transferred to 2 conical flasks containing 2 litres of sterile nutrient broth each and cultured at 37°C on a shaker for 48 hours after which 10ml was removed from each flask and from this a loop was taken and streaked onto agar plates again to check the cultures for contamination. *P. aeruginosa* and *B. cepacia* were collected by centrifugation of inoculated nutrient broth at 7,871xg for 5 minutes in an Avante JE centrifuge using a JA14 rotor. The pellets were then washed once with 50ml sterile water and pelleted again by centrifugation at 7,871xg for 5 minutes. Bacterial pellets were then re-suspended in 100ml sterile water and an equal volume of 80% (v/v) phenol added and stirred at 80°C for 30 minutes to lyse cells.

The phenol/bacteria mix was centrifuged at 2,298xg for 20 minutes using a Avante JE centrifuge using a JA14 rotor, and the upper phase containing LPS was collected. This LPS phenol mix was dialysed in 5 litres non-sterile water for 4 days with 2 water changes on the first and fourth day. The dialysate was then collected and 10mM magnesium sulphate was added to encourage LPS micelle formation. The LPS was then centrifuged in a Beckman Coulter ultracentrifuge for 4 hours at 109,564xg at 4°C using a 70Ti rotor. The LPS “jelly like” pellet was resuspended in 10ml sterile water, collected into a sterile universal and frozen under liquid nitrogen. The LPS was freeze-dried overnight, weighed, prepared as 10mg/ml stocks in sterile airway epithelial cell culture media and stored at -20°C.

4.3.2: LPS endotoxin content determination by LAL assay

The endotoxin content of LPS isolates was determined using the LAL assay as described in section 2.2.4

4.3.3: Cell culture

4.3.3.1: BEAS-2B and HPMEC mono-culture

For submerged cell studies, BEAS-2B were seeded onto collagen-coated 24 well plates ($10\mu\text{g}/\text{cm}^2$, see section 2.2.1, at 1×10^5 cells/well in 1ml airway epithelial cell culture medium overnight. For ALI studies BEAS-2B were seeded onto collagen-coated Transwell[®] inserts (as detailed in 2.2.1.2). HPMEC (see 2.2.1.3 for complete supplement composition and routine culture) were seeded in 24 well plates (unless otherwise stated) at a density of 5×10^4 cells/well in 1ml endothelial cell medium and cultured overnight.

4.3.3.2: Co-culture of BEAS-2B cells and HPMEC cells

BEAS-2B were co-cultured with HPMEC as described in section in 2.2.1.4.

3.3.4: LPS treatment

BEAS-2B cultured on Transwell[®] inserts with a TER $>45\Omega \times \text{cm}^2$, were treated for 24 hours with LPS isolated from *P. aeruginosa* strain 5ODR, *P. aeruginosa* strain10 (Sigma), *E. coli* strain 0111B (Sigma) or *B. cepacia*, (10-1000ng/ml) in 300 μl airway epithelial cell medium. Control cultures were treated with 300 μl airway epithelial cell medium alone. BEAS-2B or HPMEC seeded in 24 well plates (seeded at 5×10^4 cells/well and cultured overnight) were incubated with LPS at concentrations of (10-1000ng/ml) in 1ml airway epithelial cell medium (BEAS-2B) or endothelial cell medium (HPMEC) for 24 hours. For co-culture studies LPS was added to the apical compartment of Transwell[®] inserts as above. Following the incubation period supernatants were collected separately; (apical and basolateral media were collected for

cells seeded on Transwell[®] inserts, and co-culture studies). Cells were washed twice with 200µl PBS and lysed for 30 minutes with 1% (v/v) Triton X-100 in PBS with 1% protease inhibitor cocktail for 30 minutes on ice. Lysates and supernatants were cleared by centrifugation at 295xg for 2 minutes and stored at -20°C prior to analysis.

4.3.5: IL-8/IL-6 ELISA

Apical and basolateral media from LPS-treated cells were analysed for IL-8/IL-6 by ELISA as described in 2.2.5.

4.3.6: CellTiter-Blue[®] viability assay

After LPS-treatment, cell viability was assessed using the CellTiter-Blue[®] viability assay as detailed in 2.2.6.

4.3.7: Barrier integrity measurements using ZO-1 staining

The barrier integrity of BEAS-2B at ALI after LPS treatment was investigated by visualisation of tight junctions using an antibody against the tight junction protein ZO-1. Cells on Transwell[®] inserts were fixed with 100µl 100% methanol (pre-cooled) for 20 minutes at -20°C and washed 3 times with 200µl PBS. Cells were then permeabilised with 100µl 0.1% (v/v) Triton X-100 in PBS for 30 minutes at room temperature followed by 3 washes with 200µl PBS. Cells were then blocked with 100µl 1% (v/v) normal goat serum in PBS for 1 hour at room temperature followed by an additional 3 washes with 200µl PBS. Cells were incubated with 100µl primary mouse monoclonal anti-ZO-1 or isotype-matched control in 1% BSA (w/v) in PBS or 1% BSA in PBS alone overnight at 4°C. Cells were then washed 3 times with 200µl PBS and incubated with 100µl goat anti-mouse FITC-conjugated secondary antibody diluted 1:100 in 1% BSA in PBS for 1 hour at 4°C. Cells were washed a final 3 times with 200µl PBS and mounted with hard set mounting medium containing DAPI (1 drop/well/insert) and left to set for 48 hours at 4°C in the dark. Images were taken on a Zeiss Axiovert 200M fluorescent microscope using objective 63 with a DAPI filter

(exposures of 5-20ms) and a FITC filter (exposures of 50-150ms). ZO-1 images were taken at the most apical surface of cells and 4 fields of view were analysed for each replicate and 200 cells in each field were counted. The percent of cells with complete tight junctions was analysed by cell counting using Image J software.

4.3.8: Statistical analysis

Statistical analysis was conducted using one-way ANOVA and Tukey's post test. Results are of at least 3 independent experiments and are expressed as mean \pm SEM unless stated otherwise. For Figure 4.3B statistical analysis was conducted using a repeated measures one-way ANOVA and Tukey's post test.

4.4: Results

4.4.1: Endotoxin content of LPS isolates

In order to compare the endotoxin content of isolated LPS compared to commercial strains the LAL assay was undertaken. The results show that the *P. aeruginosa* strain 5ODR had the highest endotoxin content (Table 1; 0.775 ± 0.008 EU/ml) whilst the commercial strain *P. aeruginosa* S:10 had the lowest endotoxin content (0.214 ± 0.029 EU/ml).

Table 4.1: Endotoxin content of LPS. Endotoxin levels were determined in LPS isolates from *P. 5ODR*, *B. cepacia* and the commercial strains *E. coli* 0111B and *P. aeruginosa* S:10. LPS isolates were diluted to 0.05ng/ml and endotoxin content was determined using the LAL assay (see section 2.2.4). Results are from triplicate wells of a a single experiment and expressed as mean \pm SD.

<u>Bacterium</u>	<u>Endotoxin content (EU/ml)</u>
<i>P. aeruginosa</i> Strain 5ODR	0.775 \pm 0.008
<i>B. cepacia</i>	0.273 \pm 0.012
<i>E. coli</i> Strain 0111:B4	0.313 \pm 0.053
<i>P. aeruginosa</i> Strain S:10	0.214 \pm 0.029

4.4.2: *E. coli* and *P. aeruginosa* S:10 induce IL-6 secretion from submerged cultures of BEAS-2B.

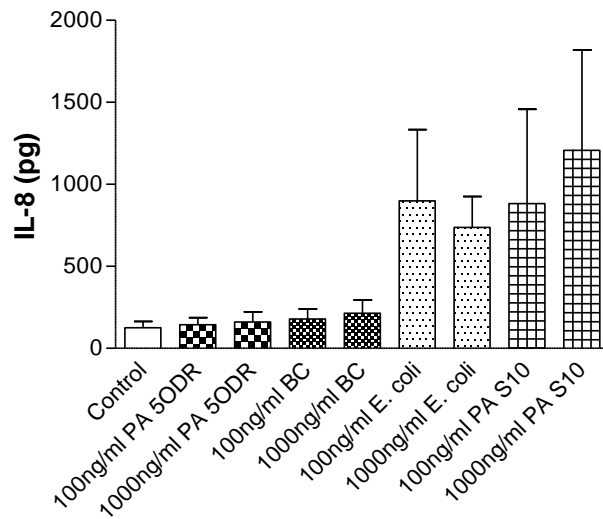
In order to determine the inflammatory response of submerged BEAS-2B to LPS from airways and non-airways pathogens, cells were seeded in 24 well plates and treated for 24 hours with LPS from the airway pathogens *P. aeruginosa* 5ODR and *B. cepacia*, and the non-airways pathogens *E. coli* 0111B and *P. aeruginosa* S:10 for 24 hours. After incubation, supernatants were collected and assayed by ELISA for the pro-inflammatory chemokine IL-8 and the pro-inflammatory cytokine IL-6.

LPS from the respiratory pathogens *P. aeruginosa* 5ODR or *B. cepacia* failed to induce IL-8 or IL-6 secretion from submerged BEAS-2B (control IL-8 secretion 125.53±38.10pg, 1000ng/ml *P. aeruginosa* 5ODR 160.72±66.16pg, 1000ng/ml *B. cepacia* 213.58±82.56pg, control IL-6 secretion 134.48±45.36pg, 1000ng/ml *P. aeruginosa* 5ODR 141.57±72.46pg, 1000ng/ml *B. cepacia* 134.17±82.41pg, Figure 4.1). LPS from *E. coli* increased IL-8 secretion from submerged BEAS-2B however this increase was both dose independent (100ng/ml; 899.76±435.35pg, 1000ng/ml; 737.53±188.76pg) and non-significant compared to control. A non-significant increase in IL-8 secretion was observed from submerged BEAS-2B incubated with *P. aeruginosa* S:10 (100ng/ml 882.55±575.47pg, 1000ng/ml; 1207±612.81pg). Experimental error for IL-8 detection was high (greater than 10%) in *E. coli* and *P. aeruginosa* S:10 treatments (Figure 4.1A).

Over the range of LPS concentrations tested, a dose independent significant increase in IL-6 secretion was observed from *E. coli* LPS-treated BEAS-2B compared to control (control: 134.48±45.36pg, 100ng/ml 632.48±123.1pg P<0.05, 1000ng/ml: 644.48±163.55pg P<0.05) under submerged culture conditions (Figure 4.1B). *P. aeruginosa* S:10 LPS induced a significant but dose independent increase in IL-6 secretion from submerged BEAS-2B (control; 134.48±45.36pg, 100ng/ml 791.12±59.33pg P<0.05, 1000ng/ml 879.37±58.61pg P<0.01).

These results indicate that BEAS-2B do not respond in an inflammatory manner after incubation with LPS from the respiratory pathogens *P. aeruginosa* 5ODR and *B. cepacia*, however, they are responsive to LPS from the non-respiratory *E. coli* and *P. aeruginosa* S:10 pathogens.

A)



B)

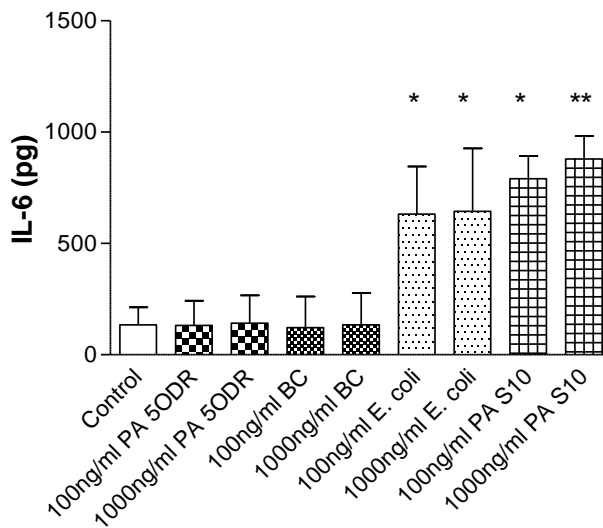


Figure 4.1: *E. coli* and *P. aeruginosa* S:10 induce IL-6 secretion from BEAS-2B significantly. BEAS-2B were seeded on collagen-coated 24 wells plates at a density of 1×10^5 cells/ml. Cells were treated for 24 hours with 100ng/ml or 1000ng/ml LPS from *P. aeruginosa* 5ODR (PA 5ODR), *B. cepacia* (BC), *E. coli* 0111B (*E. coli*) or *P. aeruginosa* S:10 (PA S:10) in fully supplemented airway epithelial cell medium. After treatment supernatants were collected and assayed for IL-8 and IL-6 by ELISA. Results are from 3 separate experiments (triplicate wells per experiment) expressed as mean \pm SEM. * $P < 0.05$ compared to control, ** $P < 0.01$ compared to control.

4.4.3: Viability of submerged BEAS-2B is not affected by LPS challenge.

In order to determine whether lack of an inflammatory response from BEAS-2B cells treated with LPS from airways pathogens was due to epithelial cell death, the effect of LPS treatment on BEAS-2B viability was investigated using the CellTiter-Blue[®] viability assay. Figure 4.2 shows that there was no significant reduction in BEAS-2B viability with any of LPS isolates used at the concentrations tested. Treatment with 1% (v/v) Triton X-100 served as a positive control and reduced BEAS-2B viability to 5.61 ± 0.52 percent of control, $P < 0.001$.

These results suggest that cell death was not responsible for the lack of inflammatory mediator secretion from submerged BEAS-2B treated with LPS from the airways pathogens *P. aeruginosa* 5ODR or *B. cepacia*. Since BEAS-2B respond to *E. coli* LPS by significant increase in IL-6 secretion without effect on cell viability, further experiments were conducted using *E. coli* LPS isolate.

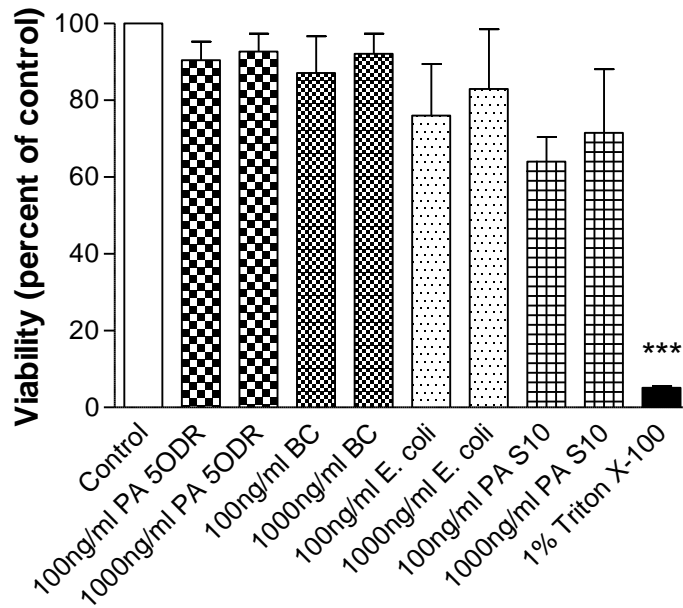


Figure 4.2: Viability of submerged BEAS-2B is not affected by LPS-challenge. BEAS-2B were seeded on collagen-coated 24 wells plates at a density of 1×10^5 cells/ml. Cells were treated for 24 hours with 100ng/ml or 1000ng/ml LPS from *P. aeruginosa* 5ODR (PA 5ODR), *B. cepacia* (BC), *E. coli* 0111:B4 (E. coli) or *P. aeruginosa* S:10 (PA S:10) in fully supplemented airway epithelial cell medium. After treatment supernatants were removed and cells were incubated with CellTiter-Blue[®] (1:5 v/v) in fresh airway epithelial cell culture media for 4 hours. After incubation fluorescence was measured at excitation 560nm, emission 590nm. Results are expressed as mean \pm SEM, n=4. ***P<0.001 compared to control.

4.4.4: *E. coli* LPS induces inflammatory mediator secretion from BEAS-2B at ALI

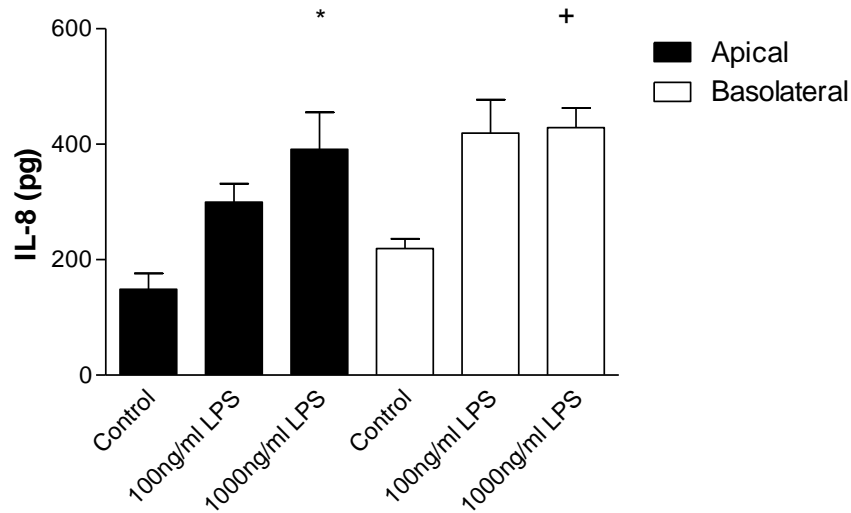
In order to determine whether *E. coli* LPS induces increased inflammatory mediator secretion from BEAS-2B cultured at ALI in a similar manner to submerged cultures, and are therefore a valid epithelial cell model of airways inflammation, cells were cultured at ALI on Transwell[®] inserts and treated apically with *E. coli* LPS for 24 hours. After LPS challenge apical and basolateral supernatants were collected separately and assayed for IL-8 and IL-6 by ELISA.

A significant and dose-dependent increase in IL-8 secretion was observed from BEAS-2B cultured at ALI after *E. coli* LPS challenge (Figure 4.3A). A significant increase in IL-8 secretion in response to 1000ng/ml LPS was observed in both the apical and basolateral compartments (apical control; 148.71±27.55pg, apical 1000ng/ml LPS 391.33±63.82pg (P<0.05). Basolateral control; 291.29±58.20pg, basolateral 1000ng/ml LPS 428.62±34.12pg (P<0.05)).

Compared to control a dose independent significant release in IL-6 secretion was observed into the basolateral compartment of *E. coli* LPS-treated BEAS-2B cultured at ALI (control; 77.06±2.32pg, 100ng/ml; 147.88±10.4pg, 1000ng/ml 145.24±34.44pg, P<0.05). Secretion of IL-6 into the apical compartment from *E. coli* LPS challenged BEAS-2B was non-significantly increased (control; 38.67±23.97pg, 100ng/ml; 74.22±6.34pg, 1000ng/ml 95.19±19.58pg).

These results show that BEAS-2B cultured at ALI are sensitive to apical *E. coli* LPS stimulation, and that IL-6 release from BEAS-2B cultured at ALI is directional.

A)



B)

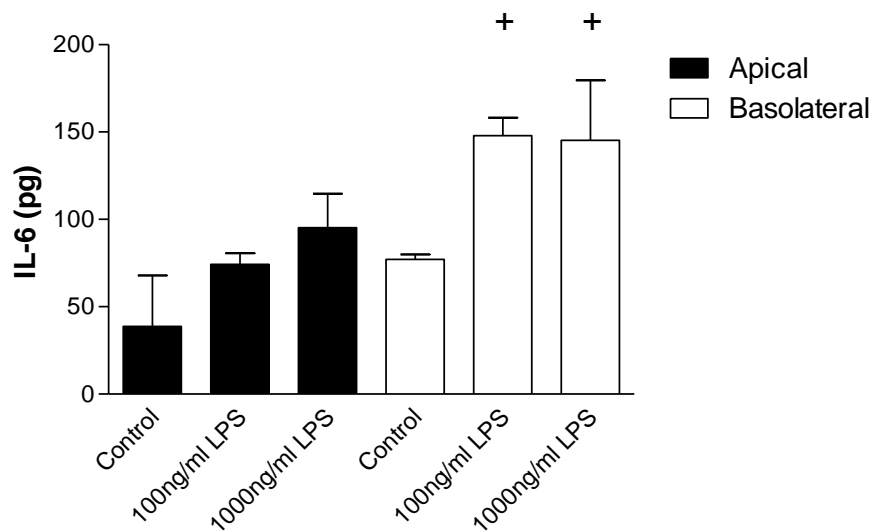


Figure 4.3: *E. coli* LPS induces inflammatory mediator secretion from BEAS-2B at ALI. BEAS-2B seeded on collagen-coated Transwell® inserts (see section 2.2.1.2) were challenged apically for 24 hours with *E. coli* LPS (1000ng/ml or 100ng/ml) in fully supplemented airway epithelial cell medium, or medium alone as a control. After incubation supernatants were collected and assayed for IL-8 or IL-6 secretion by ELISA. Results are expressed as mean \pm SEM, n=3. A) *P<0.05 versus apical control, +P<0.05 versus basolateral control by One-Way ANOVA and Tukey's post hoc test. B) +P<0.05 versus basolateral control by repeated measures One-Way ANOVA and Tukey's post hoc test.

4.4.5: Viability of BEAS-2B cultured at ALI is not affected by LPS-challenge.

In order to determine whether LPS affects the viability of BEAS-2B cultured at ALI, cells were treated with 100ng/ml or 1000ng/ml *E. coli* LPS for 24 hours and viability assessed using the CellTiter-Blue[®] assay; 1% (v/v) Triton X-100 served as a positive control. Neither dose of *E. coli* LPS affected BEAS-2B viability (Figure 4), whereas 1% (v/v) triton X-100 significantly reduced cell viability to $6.32 \pm 1.43\%$ of control ($P < 0.001$)

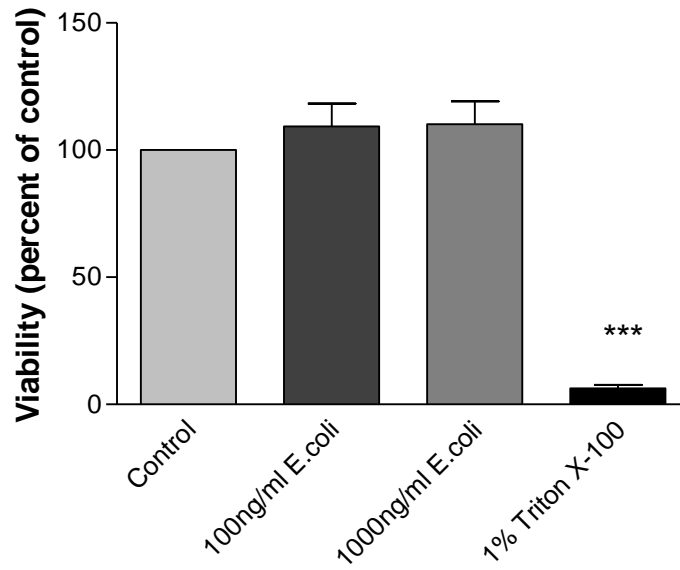


Figure 4.4: Viability of BEAS-2B cultured at ALI is not affected by LPS challenge. BEAS-2B cultured at ALI on Transwell® inserts for 11 days as described in 2.2.1.2, were treated apically for 24 hours with *E. coli* LPS (1000ng/ml or 100ng/ml) or 1% (v/v) Triton X-100 in fully supplemented airway epithelial cell culture medium for 24 hours. After treatment basolateral media was replenished and cells were incubated apically with CellTiter-Blue® for 4 hours. Fluorescence was determined at Ex560nm Em590nm, results are expressed as mean ± SEM, n=4. P<0.001 compared to control.

4.4.6: BEAS-2B barrier remains intact with LPS stimulation.

Maintenance of a tight barrier is an important mechanism whereby the airway epithelium protects against pathogenic infection. In order to determine whether LPS stimulation compromises the integrity of the epithelial tight barrier BEAS-2B cultured at ALI were treated apically with *E. coli* LPS for 24 hours and the change in TER (as a measure of barrier integrity) measured. TER readings were taken for each well before treatment and normalised to pre-treatment control. After treatments TER was measured for each well again and test treatments normalised to control TER at 24 hours. Treatment with 1% (v/v) Triton X-100 for 24 hours served as a positive control for barrier disruption.

E. coli LPS stimulation at either 100ng/ml or 1000ng/ml had no effect on BEAS-2B barrier integrity as measured by TER (106.12±8.57% of control before treatment and 102.53±9.43 percent of control after treatment for 1000ng/ml LPS, (Figure 4.5)). Treatment with 1% (v/v) Triton X-100 significantly reduced TER from 108.5±11.18 percent of control before treatment to 61.45±9.06 percent of control after treatment (P<0.001). These results indicate that apical LPS treatment of BEAS-2B for 24 hours does not compromise barrier integrity, as measured by TER.

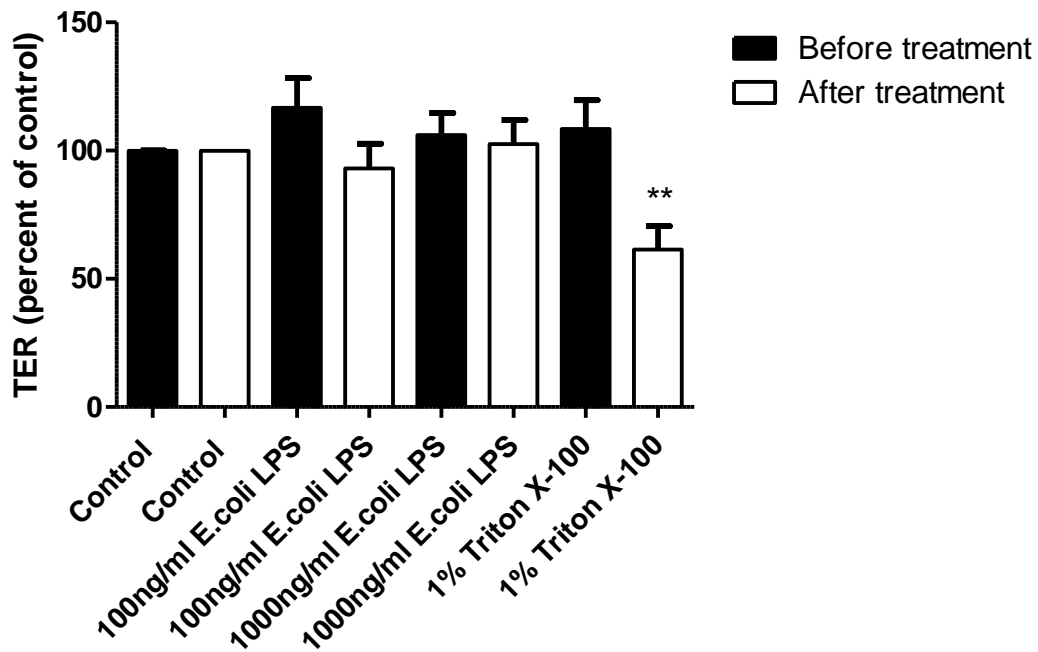
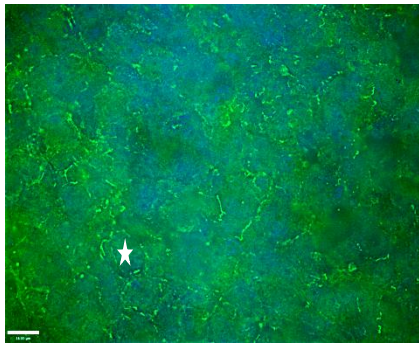


Figure 4.5: BEAS-2B barrier remains intact with LPS stimulation. BEAS-2B were cultured at ALI on Transwell[®] inserts for 11 days as described in section 2.2.1.2. TER was measured and basolateral medium was replenished 4 hours prior to apical treatment with *E. coli* LPS (100ng/ml or 1000ng/ml) or 1% Triton X-100 for 24 hours. After treatment, basolateral medium and apical medium were replenished and TER measured. Results are expressed as TER for each well before treatment (percent of control before treatment) black bars, and TER for each well after treatment (percent of control after treatment) clear bars. Results are expressed as mean \pm SEM, N=3 with 2 Transwell[®] inserts for each replicate. **P<0.01 compared to 1% (v/v) triton X-100 before treatment.

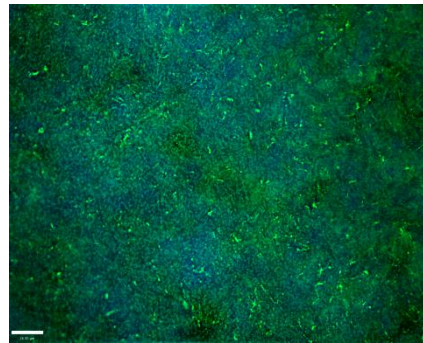
4.4.7: Apical *E. coli* LPS treatment disrupts ZO-1 localisation in BEAS-2B cultured at ALI

As TER is an indirect measure of tight junction formation, ZO-1 staining after LPS treatment was analysed as a direct measure of tight junctions. Figure 4.6 shows that ZO-1 localisation at the site of cell-cell contact as seen with control cells (Figure 4.6A) was not observed following 24 hour treatment with either 100ng/ml or 1000ng/ml *E. coli* LPS (Figure 4.6B and C). When images were analysed by counting the total number of cells with intact tight junctions (ZO-1 staining localised around the whole cell), LPS treatment significantly affected ZO-1 localisation (51±4 percent of control 100ng/ml, 48±7 percent of control P<0.01. Figure 4.6D). These results suggest that although TER is not affected by LPS treatment disruption of ZO-1 localisation may be occurring.

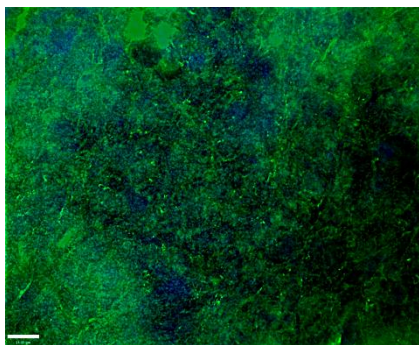
A) Control



B) 100ng/ml LPS



C) 1000ng/ml LPS



D)

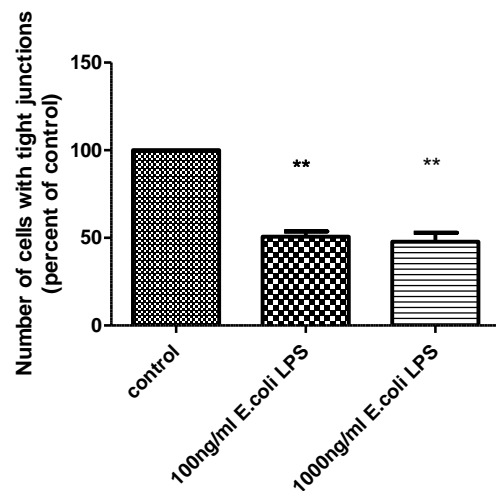


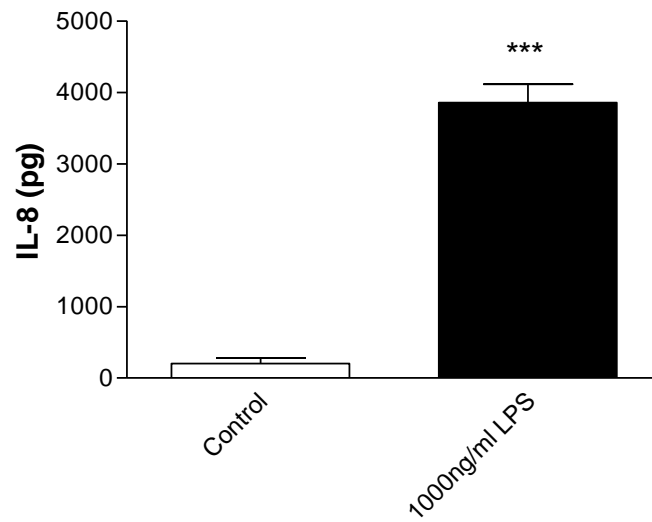
Figure 4.6: Apical *E. coli* LPS treatment disrupts ZO-1 localisation in BEAS-2B cultured at ALI. BEAS-2B cultured on Transwell® inserts at ALI treated with and without 100ng/ml or 1000ng/ml *E. coli* LPS for 24 hours were fixed with pre-cooled methanol, permeabilised with 0.1% (v/v) triton X-100 and blocked with 1% (v/v) goat serum in PBS. Cells were then incubated with mouse monoclonal anti-ZO-1 antibody (1:250) in 1% (w/v) BSA in PBS overnight at 4°C followed by incubation with goat anti-mouse FITC-conjugated secondary antibody (1:100) in 1% (w/v) BSA in PBS. Cells were mounted in mounting medium containing DAPI and visualised using a Zeiss Axiovert 200M fluorescent microscope. Images are representative of 3 separate experiments with 4 fields of view at the most apical surface taken for each replicate. The percent of cells in each field of view with intact ZO-1 localisation around the cell (Figure 6A, star) was analysed using Image J software and expressed as percent of control **P<0.01 compared to control cells. Scale bar indicated 16µm. 200 cells in each image were examined. Results in Figure D are expressed as mean ± SEM.

4.4.8: IL-8 secretion is increased significantly from LPS-challenged HPMEC

The BEAS-2B/HPMEC co-culture model of the airways were challenged apically with *E. coli* to assess the impact of the co-culture on inflammatory response compared to the BEAS-2B monoculture. ZO-1 localisation studies of *E. coli* LPS-treated BEAS-2B suggest possible loss of barrier integrity, and LPS may therefore leak through to the basolateral compartment. Under these conditions HPMEC would directly be challenged with LPS. The response of HPMEC in monoculture to 1000ng/ml *E. coli* LPS for 24 hours was therefore investigated, to assess the contribution of HPMEC to LPS stimulated co-culture inflammatory response (if observed).

E. coli LPS induced IL-8 release significantly from HPMEC (Figure 4.7, 3860 ± 260 pg ($P < 0.001$)) compared to control cells (Figure 4.7, 200 ± 80 pg). A non-significant trend for an increase in IL-6 secretion was observed from HPMEC treated with *E. coli* (Figure 4.7, control: 790 ± 500 , LPS: 2520 ± 1730 pg). Experimental error for *E. coli*-treated HPMEC was greater than 10% (Figure 4.7B).

A)



B)

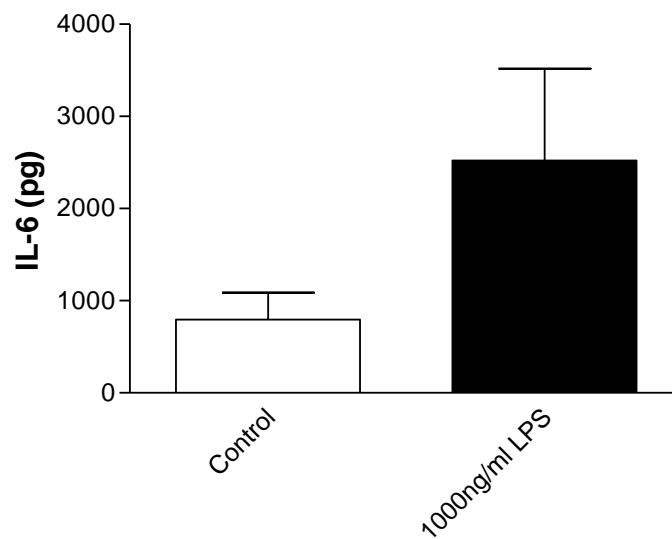


Figure 4.7: IL-8 secretion is increased significantly from LPS challenged HPMEC. HPMEC were cultured on 24 well plates at 0.5×10^5 cells/ml overnight prior to challenge with 1000ng/ml *E. coli* LPS for 24 hours. After incubation supernatants were collected and assayed for IL-8 and IL-6 using ELISA. Results are expressed as mean \pm SD, n=3. ***=P<0.001 compared to control.

4.4.9: Stimulation with *E. coli* LPS does not affect HPMEC viability

In order to assess the effect of *E. coli* LPS on HPMEC viability, the CellTiter-Blue[®] assay was conducted after LPS challenge. Treatment of HPMEC 24 hours with *E. coli* LPS had no effect on HPMEC viability (Figure 4.8, 1000ng/ml LPS: 99.94±6.69 percent of control). Treatment of HPMEC with 1% (v/v) triton X-100 for 24 hours served as a positive control and reduced HPMEC viability to 9.52±7.86 percent of control (Figure 4.8, P<0.001).

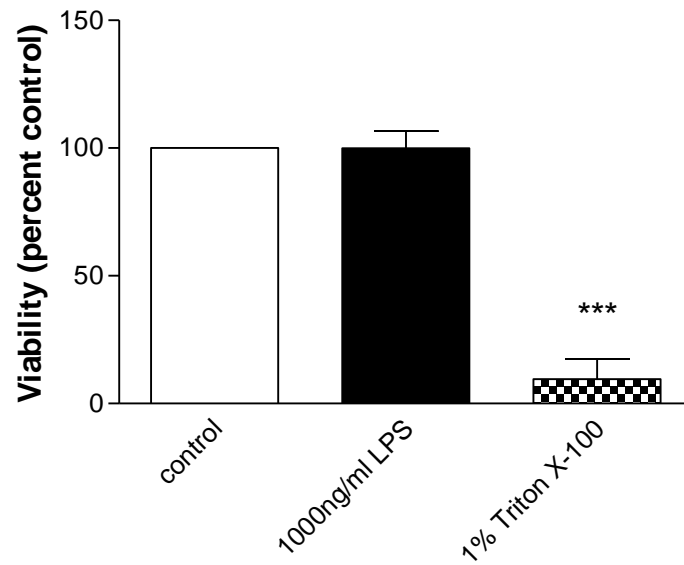
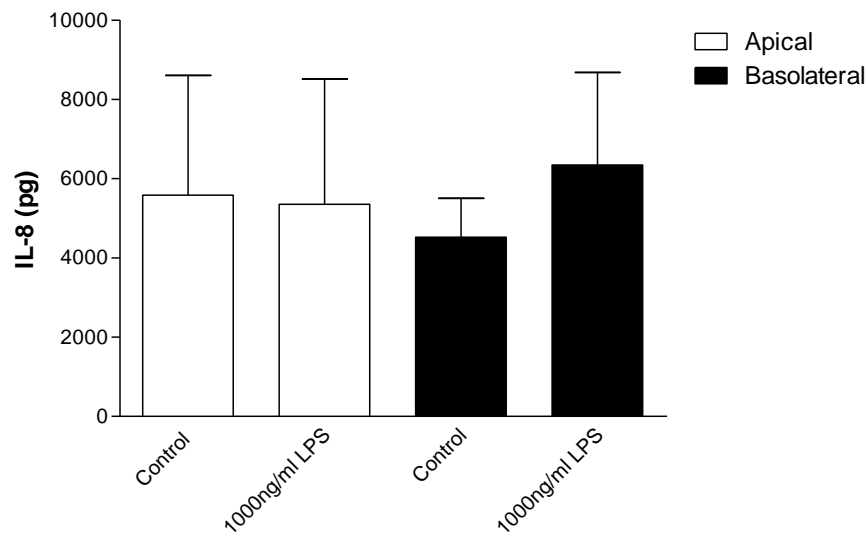


Figure 4.8: Stimulation with *E. coli* LPS does not affect HPMEC viability. HPMEC seeded in 96 well plates at 8000cells/well were treated for 24 hours with 1000ng/ml *E. coli* LPS or 1% (v/v) triton X-100 for 24 hours. After incubation supernatants were removed and cells were incubated with CellTiter-Blue® (1:5 v/v) in endothelial cell culture medium for 4 hours. After incubation fluorescence was measured at excitation 560nm and emission 590nm. Results are expressed as mean \pm SD, n=4, ***P<0.001 compared to control.

4.4.10: IL-8 and IL-6 secretion from BEAS-2B/HPMEC co-culture is not affected by *E. coli*-LPS challenge.

In order to validate the BEAS-2B/HPMEC co-culture as a model of airways inflammation the response of the model to *E. coli* LPS was investigated and compared to the response of BEAS-2B (cultured at ALI) and HPMEC monocultures. BEAS-2B monoculture showed significant IL-8 secretion with 1000ng/ml *E. coli* LPS in both apical and basolateral compartments (Figure 4.3A). Further HPMEC alone showed significant IL-8 secretion after *E. coli* LPS challenge (Figure 4.7A). However, *E. coli* LPS (1000ng/ml) failed to enhance IL-8 secretion from BEAS-2B/HPMEC co-culture in either compartment (Figure 4.9A). Significant directional (into the basolateral compartment) IL-6 secretion was seen from BEAS-2B alone treated with *E. coli* LPS (Figure 4.3B). Similarly, there was a significant increase in IL-6 secretion from the BEAS-2B/HPMEC co-culture to the basolateral compartment for both control and LPS treatment compared to respective apical treatments (Figure 4.9, apical control IL-6: 165.93 ± 38.81 pg, basolateral control IL-6: 916.9 ± 49.4 pg ($P < 0.001$)). IL-6 secretion for LPS treatment compared to control, however, was not significantly increased for either the apical or basolateral compartment.

A)



B)

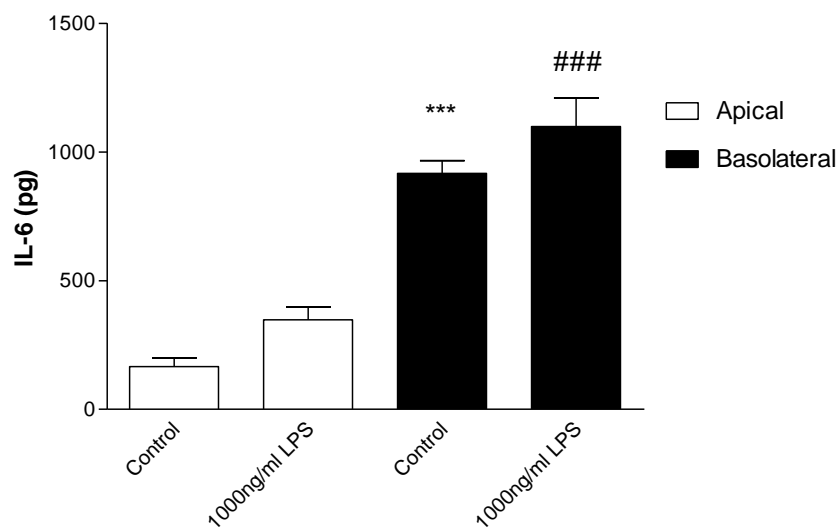


Figure 4.9: IL-8 and IL-6 secretion from BEAS-2B/HPMEC co-culture is not affected by *E. coli* LPS challenge. BEAS-2B/HPMEC co-culture (for details see 2.2.1.4) was treated apically with or without 1000ng/ml *E. coli* LPS for 24 hours. After incubation supernatants were collected and assayed for IL-8 and IL-6 by ELISA. Results are expressed as mean \pm SD, n=4. ***P<0.001 compared to apical control, ###=P<0.001 compared to apical 1000ng/ml LPS.

4.4.11: BEAS-2B/HPMEC co-culture viability is not affected by *E.coli* LPS challenge.

In order to determine whether challenge with LPS from *E. coli* affected viability of either BEAS-2B or HPMEC within the co-culture, the CellTiter-Blue[®] assay was conducted after LPS challenge. *E. coli* LPS (1000ng/ml for 24 hours) had no effect on either BEAS-2B or HPMEC viability in the co-culture model (Figure 4.10). Apical treatment of the BEAS-2B with 1% (v/v) triton X-100 for 24 hours significantly reduced viability of both BEAS-2B (Figure 4.10, 4.45 ± 0.57 percent of control, $P < 0.001$) and HPMEC (7.83 ± 2.6 percent of control, $P < 0.001$).

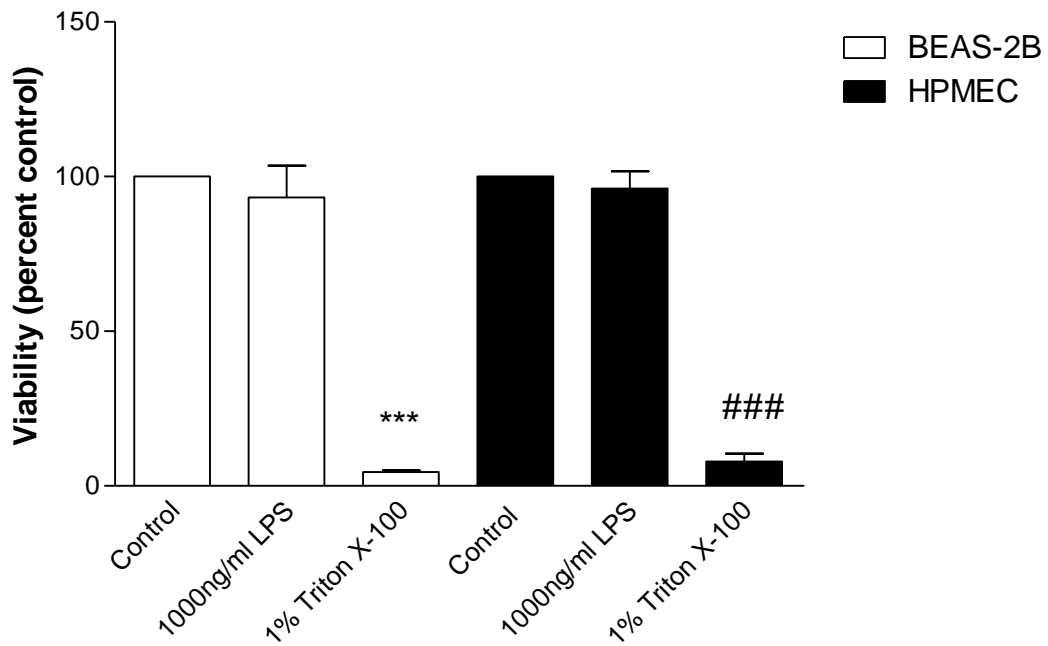


Figure 4.10: BEAS-2B/HPMEC co-culture viability is not affected by *E. coli* LPS challenge. BEAS-2B/HPMEC co-culture (for details see 2.2.1.4) was treated apically for 24 hours with or without 1000ng/ml *E. coli* LPS or 1% (v/v) Triton X-100. After treatment the BEAS-2B on Transwell® inserts were removed to a separate well in the companion plate and both BEAS-2B and HPMEC were incubated with CellTiter-Blue® (1:5 v/v) in airway epithelial cell medium (BEAS-2B) or endothelial cell medium (HPMEC) for 4 hours. After incubation fluorescence was measured at excitation 560nm emission 590nm. Results are expressed as mean \pm SD, n=4. ***=P<0.001 compared to BEAS-2B control, ###=P<0.001 compared to HPMEC control.

4.5: Discussion

The airway epithelium has a number of protective mechanisms in place to help prevent against pathogenic invasion including tight, semi-permeable junctions between neighbouring mucociliary cells (Steed *et al.*, 2010) as well as invoking bacterial elimination indirectly through pro-inflammatory cytokine and chemokine release. Several cell lines of human bronchial epithelial origin have been investigated as models of lung tissue and these include BEAS-2B, Calu-3 and 16HBE14o cells. However, the least studied of these is the BEAS-2B cell line, despite the fact that they are derived from normal epithelial cells. This contrasts with Calu-3 cells which are derived from lung adenocarcinoma cells. Culture at ALI allows for mucociliary differentiation which reflects the morphology of the airways epithelium *in vivo*.

The aim of the current study therefore was to characterise the inflammatory response of BEAS-2B cultured at ALI to LPS compared to a submerged cultures of BEAS-2B. The ALI model was further investigated in terms of barrier integrity and tight junction stability. Once characterised the ALI model was used in construction of a co-culture model with the inclusion of HPMEC to further mimic the airways *in vivo*.

BEAS-2B are bronchial epithelial cells and therefore their response of LPS from respiratory pathogens was first investigated. Submerged BEAS-2B were incubated for 24 hours with 100ng/ml or 1000ng/ml LPS from *P. aeruginosa* strain 5ODR and *B. cepacia*, for comparison LPS from the non-respiratory pathogens *P. aeruginosa* S:10 and *E. coli* 0111:B4 were also used. The LAL assay was conducted to determine the endotoxin levels of each LPS. *P. aeruginosa* 5ODR has the highest endotoxin content whilst the commercial, non-respiratory strain S:10 has the least. A limitation of the current study is that cells were treated with equal concentrations of LPS by mass, rather than endotoxin content. Despite this cells exhibited a higher inflammatory response to *E. coli* 0111:B4 and *P. aeruginosa* S:10, rather than *P. aeruginosa* 5ODR, the isolate with the highest endotoxin content. Indeed, IL-8 and IL-6 secretion remained unchanged from BEAS-2B after treatment with LPS from either of the respiratory pathogens, whilst IL-8 secretion was increased non-significantly, and IL-6 increased

significantly with LPS from either *E. coli* LPS and *P. aeruginosa* S:10 compared to control. Cell viability studies show that the lack of inflammatory response was not due to cell death as none of the LPS strains tested significantly affected cell viability. Seydel *et al.*, (2003) observe that the EU/ml of synthetic LPS compounds did not correlate with inflammatory response from human macrophages and propose that the LAL recognises the lipid A backbone rather than the toxic lipid chains.

The fact that increased IL-6 secretion was observed with LPS from *E. coli* or *P. aeruginosa* S:10 shows that BEAS-2B are responsive to LPS as suggested by their expression of TLR4 (Guillot *et al.*, 2004; Schulz *et al.*, 2002), TLR2 and CD14 (a glycosyl-phosphatidylinositol (GPI)-linked LPS co-receptor (Elson *et al.*, 2007). TLR2/4 and CD14 are both involved in the recognition of LPS (Lu *et al.*, 2008). However, it is unclear as to why BEAS-2B showed no inflammatory response with respiratory strains of LPS. Raoust *et al.*, (2009) report that mouse primary lung epithelial cells with TLR2/4 knockdown still produce the inflammatory mediators KC and IL-6 (albeit at a lower concentration than wild type epithelia cells) in response to 4 hours incubation with *P. aeruginosa* live bacteria (2×10^4 - 10×10^4 bacteria/ 5×10^4 epithelial cells). These results suggest that *P. aeruginosa* LPS is not the sole PAMP employed by *P. aeruginosa* during infection. Guillot *et al.*, (2004) show that TLR-4 is internalised in unstimulated BEAS-2B and suggest this acts to protect the epithelium from promotion of an inflammatory state in response to trace amount of LPS. Since inhaled particles, for example, urban air particulates often contain LPS contamination it is tempting to speculate that the airways minimise inappropriate inflammation in response to low levels of respiratory LPS, and therefore stimulation by other PAMPs are required as a protective mechanism. Further work to investigate this hypothesis could examine whether *P. aeruginosa* 5ODR and *B. cepacia* whole bacteria or increased LPS doses activates an inflammatory state in submerged BEAS-2B.

E. coli LPS has been observed to induce increased IL-8 secretion from a number of airway cell types including A549 (Schulz *et al.*, 2009) and NHBE (Palmberg *et al.*, 1998). Here, submerged BEAS-2B showed a non-significant increase in IL-8 secretion in response to *E. coli* and *P. aeruginosa* S:10 LPS, however, the same concentration of

LPS from *E. coli* O26:B6 induced IL-8 secretion after 2, 6 and 18 hours incubation from BEAS-2B significantly in a study by Laan *et al.*, (2004). The difference may be due to differences in LPS serotype as the O-antigen of LPS can differ in structure between LPS bacteria serotypes and genera (Haeffner-Cavaillon *et al.*, 1998). Significant IL-8 secretion however, was observed in BEAS-2B cultured at ALI with 1000ng/ml LPS into both the apical and basolateral compartments. IL-8 is a potent neutrophil chemo-attractant, and its release in the basolateral compartment mimics *in vivo* IL-8 secretion into the underlying blood vessels to attract circulating leukocytes (Mukaida., 2003). Secretion directed to the apical compartment would allow for a gradient of IL-8 whereby leukocytes attracted to the intima traverse the endothelium to the epithelial cell and site of infection. Incubation of the BEAS-2B ALI model with FITC-dextran at 10kDa, (a similar size to IL-8), shows that the permeability is not affected by 24 hour treatment with 1000ng/ml LPS from *E. coli*. The basolateral IL-8 concentration detected is indeed due to enhanced directed secretion, rather than diffusion of IL-8 through the cell layer due to leakage from the apical compartment or diminished barrier integrity (unpublished data Willetts *et al.*, 2011).

IL-8 secretion after LPS from *E. coli* treatment was altered significantly in BEAS-2B cultured at ALI but not submerged, a large experimental variance was observed in the submerged culture studies which may mask any IL-8 response. Ross *et al.*, (2007) conducted transcriptional analysis of HBEC during differentiation at ALI and found that for a number of genes their expression was increased. IL-8 was one of these genes and showed an increase in expression during the initial 10 days of ALI culture, so it is possible that airway epithelial cells at ALI have increased expression of the necessary genes required to mount an inflammatory response, and may explain the enhanced IL-8 response observed during ALI in the current study. Further, although BEAS-2B are known to express CD14 and TLR receptors their location in cells cultured at ALI is unknown (in submerged BEAS-2B TLR4 is internalised, Guillot *et al.*, 2004), it is possible that differentiated cells may show apical polarised expression of these receptors, making them more available to bind LPS.

Previous studies have shown submerged populations of BEAS-2B to secrete IL-6 in response to $\geq 10\mu\text{g/ml}$ LPS from *E. coli* O55:B5 (Schulz *et al.*, 2002) and 1000 endotoxin units/ml *Pseudomonas* LPS (Veranth *et al.*, 2008). Here, significant IL-6 secretion was observed with both 100ng/ml and 1000ng/ml LPS in submerged BEAS-2B cultures. Furthermore, significant IL-6 secretion was observed in the basolateral compartment of BEAS-2B cultures at ALI with 1000ng/ml LPS. BEAS-2B cultured at ALI therefore respond in a manner similar to that of submerged cultured regarding LPS induced IL-6 secretion.

Pathogenic insult has been shown to induce tight junction disruption in a number of epithelial cell types (Kim *et al.*, 2005; Nazil *et al.*, 2010; Yi *et al.*, 2000). Incubation with *E. coli* LPS (100ng/ml or 1000ng/ml) for 24 hours had no effect on BEAS-2B TER, however, ZO-1 localisation was punctate and fragmented with a significant reduction in the number of cells with complete tight junctions with LPS challenge. In contrast, Nazil *et al.*, (2010), observed a correlation between decreasing TER and ZO-1 mRNA expression and protein localisation at tight junctions in HIV-1 treated primary endometrial epithelial cells.

B. cenocepacia infection of 16HBE14o⁻ cells resulted in decreased TER, and disruption of occludin at tight junctions with unaltered ZO-1 (Kim *et al.*, 2005), lending further support that disruption to ZO-1 localisation and TER may not go hand in hand in tight junction disturbance. Yi *et al.*, (2000) observed that in the human corneal epithelial cell line THCE, *P. aeruginosa* LPS challenge resulted in a decrease in TER at 9 hour of treatment, with TER returning to baseline at 24 hours of treatment, however, ZO-1 localisation remained unchanged and ZO-2 localisation was disturbed. Therefore pathogenic insult may cause transient disruption of some tight junction proteins without completely diminishing tight junction integrity. In the current study, stable TER with perturbed ZO-1 staining in response to LPS at 24hours may indicate the beginning of tight junction disruption, or their composition after repair mechanisms have been induced; no cytotoxicity was observed under these conditions as measured by CellTiter-Blue[®] analysis and lack of apoptotic nuclei in ZO-1 localisation studies.

Tight junctions are composed of several proteins of which the claudin family members are responsible for the ion-selectivity of the tight junction whilst ZO-1 family members act as scaffold proteins (Steed *et al.*, 2010). It is possible therefore that although ZO-1 localisation in BEAS-2B treated with LPS is disrupted, claudin localisation may be unaffected, and therefore TER remains unaffected. Further, the number of cells with ZO-1 disruption was reduced to ~50% of control with either 100ng/ml or 1000ng/ml LPS and such cells may be able to maintain TER. The ZO-1 images were all taken at the most apical surface of cell cultures, as BEAS-2B form several cell layers on the Transwell[®] inserts the underlying cells may help maintain TER also. A limitation of the current study is that barrier integrity studies were undertaken immediately after the LPS treatment, with no investigation into tight junction integrity during the LPS challenge. Electric Cell-Substrate Impedance Sensing (ECIS) allows continuous measurement of electrical resistance of cultures by incorporation of a impedance sensing chip into the culture without removal of cells from an incubated setting (Heijink *et al.*, 2009; Sun *et al.*, 2010). ECIS may therefore be used to monitor the barrier function during LPS treatment, as it has been utilised to show disruption to 16HBE14o⁻ cells treated with Triton X-100, giving similar results to TER (Sun *et al.*, 2010). ECIS along with immunofluorescent staining for tight junction proteins at given time points during LPS treatment would allow for a greater understanding of barrier integrity with pathogenic insult.

As previously mentioned, during inflammation, the endothelium increases expression of adhesion molecules (as a result of increased inflammatory mediator release by epithelial cells) to allow passage of inflammatory cells through the endothelium to the site of infection by attraction to epithelial-released chemokines. Therefore the effect of pathogenic material on endothelial cells alone and an epithelial/endothelial co-culture was investigated. LPS induces a non-cytotoxic (LPS treatment had no effect on HPMEC viability) inflammatory response in HPMEC cells alone. IL-8 secretion in HPMEC cells is significantly increased compared to control. Further, Zhang *et al.*, (2011) observed significant IL-8 secretion from HUVEC treated with LPS from *E. coli* (strain 055:B1). Here HPMEC cells secrete 3856±260pg/ml IL-8, whilst Zhang *et al.*, (2010) reported 7000pg/ml IL-8 secretion in their HUVEC system. The difference in concentration of IL-8 secreted is likely to be due to the fact that the HUVEC in the

study by Zhang *et al.*, (2010) show increased IL-8 secretion under resting conditions (1000pg/ml) compared with the HPMEC cells of the current study which secrete only 200 ± 80 pg/ml suggesting they are already more primed than HPMEC.

The effect of introducing HPMEC into the BEAS-2B ALI model in terms of cytokine secretion after LPS challenge was investigated. Permeability studies in BEAS-2B treated with LPS suggest that the barrier is not permeable to solutes of 10kDa (Willetts *et al.*, 2011) so the HPMEC cells may never come into contact with the LPS which exists as micelles in aqueous solutions with sizes ranging from 200kDa (Jang *et al.*, 2009) to 1000kDa (Magalhaes *et al.*, 2007). It can therefore be assumed that any basolateral secretion of cytokines is from the BEAS-2B cells in response to LPS stimulation or from HPMEC cells in response to BEAS-2B secreted cytokines. In BEAS-2B mono-culture, basolateral IL-8 concentrations increase nearly 100% with 1000ng/ml LPS for 24 hours (control IL-8 secretion of 291.29 ± 58.2 pg, LPS-induced IL-8 secretion 428.62 ± 34.12 pg). The presence of HPMEC does not enhance the LPS-induced increase in IL-8 secretion, which is only increased by 40% in the basolateral compartment of the co-culture (control IL-8 secretion 4520 ± 980 pg, LPS-induced IL-8 secretion 6340 ± 2330 pg). Further, the significant LPS-induced secretion of IL-6 in the basolateral compartment of BEAS-2B at ALI was lost in the co-culture.

Lack of HMPMEC cells due to limited cell doubling of primary populations presented a key restriction to the current study. For HPMEC and co-culture studies, treatments were carried out singly in three independent experiments, rather than the 3 wells for each replicate for BEAS-2B, due to the slow doubling and limited passage of HPMEC. This introduced high levels of variability to results. In fact, IL-6 secretion from LPS stimulated HPMEC in mono-culture was more than 3 times control IL-6 secretion indicating a probable response (control 793.54 ± 509.24 pg, LPS stimulation 2520.79 ± 1725.75). This large variability may mask any small but significant changes in cytokine response from the co-culture. Further work would concentrate on growing numerous cultures of HPMEC from the same primary cell lots to provide a larger HPMEC pool for studies.

The expression of adhesion molecules in HPMEC cells after apical treatment of BEAS-2B with LPS needs investigation to determine whether the current model of inflammation represents inflammatory responses *in vivo*. The presence of the inflammatory mediators secreted from LPS activated epithelial cells such as IL-6 are predicted to induce adhesion molecule up-regulation in HPMEC cells. This may be investigated by stimulation of HPMEC cells with conditioned media from the basolateral compartment of LPS-treated and control BEAS-2B, and comparing the results to HPMEC treated with a positive stimulator of adhesion molecule up-regulation.

4.6: Conclusion

BEAS-2B cultured at ALI respond to *E. coli* LPS challenge in a physiologically relevant manner by directional secretion of IL-6 and IL-8, without loss of viability and with tight barrier maintenance regarding solute permeability. The inflammatory response of the co-culture is less defined owing to high experimental variability. Overall results suggest that BEAS-2B cultured at ALI are an effective model of airway inflammation that may have application in investigating effects of pathogens or particulates. Further investigations into the response of this model to airway pathogens is required.

Chapter 5: Particulate matter exposure

5.1: Rationale

The airways can be exposed to PM from a number of sources including the workplace, pollution or cosmetics. Investigations into any potential health effects from airways PM exposure are therefore warranted. BEAS-2B, a normal human airway epithelial cell line, under submerged conditions have been previously used in the study of PM toxicity under submerged conditions, however, ALI cultures allow for a cell phenotype more representative of *in vivo* conditions. Further, inhaled PM are observed to translocate to the endothelium *in vivo*. The current study aims to characterise the inflammatory, cytotoxic and GSH response of BEAS-2B cultured at ALI in mono-culture and co-culture with HPMEC to UFTiO₂, TiO₂ and test particles S2219200, S2218600 and S2429901.

UFTiO₂ induced a loss of cell viability and GSH (possibly due to ROS production) in BEAS-2B cultured at ALI. Analysis of inflammatory mediator secretion from these cells is complicated due to adsorption of chemokines onto the particle surface. The neutrophil respiratory burst assay was employed to investigate whether particle bound IL-8 remained biologically active. S2429901 induced IL-6 secretion from BEAS-2B cultured at ALI and reduced the ability of IL-8 to prime human primary neutrophils for the fMLP induced respiratory burst, but, had no effect on cell viability, GSH content or barrier integrity. UFTiO₂ induced a significant reduction in BEAS-2B mono-culture viability, however, when in co-culture with HPMEC, BEAS-2B viability was unaffected by UFTiO₂ challenge.

5.2: Introduction

NPs are commonly used in industrial and commercial products; NP-TiO₂ for example is used in numerous areas from cosmetics (Nohynek *et al.*, 2010) to the food industry (Lomer *et al.*, 2002). *In vitro* studies of NP exposure have indicated a link between inflammatory and cytotoxic responses and particulate matter size (Gurr *et al.*, 2005, Singh *et al.*, 2007). Using BEAS-2B as an *in vitro* model of the human lungs the cytotoxic potential of ultrafine (UF, 10nm and 20nm) and fine (200nm) TiO₂ particles was investigated (Gurr *et al.*, 2005). Cellular damage was measured by assessing oxidative DNA damage, lipid peroxidation and levels of ROS. In all cases, the ultrafine particles induced more damage than fine particles (Gurr *et al.*, 2005), providing evidence that smaller particles with larger surface area and increased chemical reactivity are more potent inducers of damage to BEAS-2B than larger diameter particles, with relatively smaller surface areas, of the same material.

Intracellular ROS production has been linked to induction of apoptosis and inflammation after PM exposure. The antioxidant enzyme catalase inhibits TiO₂-induced increase in GM-CSF expression (Hussain *et al.*, 2009), and carbon black (CB) induced DNA fragmentation and caspase activation in 16HBE14o⁻ cells (Hussain *et al.*, 2010). Further, the combustion derived particle residual oil fly ash (ROFA) induced intracellular ROS and increased IL-6 and IL-8 mRNA expression in NHBE. Cytokine expression was inhibited by the ROS scavenger dimethylthiourea and the metal chelator deferoxamine (Carter *et al.*, 1997). The increased intracellular ROS may be a consequence of phagocytosis of particles by cells and activation of NADPH oxidase. In addition, the mitochondrion has been implicated as a major source of this increased ROS. Indeed Zhao *et al.*, (2009) observed significant induction of mitochondrial ROS with 100µg/ml PM₁₀ treatment of submerged primary bronchial epithelial cells and Freyre-Fonseca *et al.*, (2011) observed an increase in ROS in mitochondria isolated from rat whole lung tissue treated with UFTiO₂. NP have been shown to localise to the mitochondrial membrane of epithelial cells *in vitro* (Singh *et al.*, 2007).

Increased inflammatory mediator secretion has also been observed from airway endothelial cells in response to PM. For example; iron oxide and zinc oxide particles induce an increase in IL-8 secretion from human aortic endothelial cells (Gojova *et al.*, 2007). Similarly, Qu *et al.*, (2010) observed a significant increase in IL-6 secretion from human lung microvascular endothelial cells. Furthermore, Geiser *et al.*, (2005) observed the presence of TiO₂ particles in the endothelium of lung sections from rats exposed to TiO₂ aerosol, suggesting that the endothelium should also be considered during PM and NP toxicity testing.

Airway co-culture models of epithelial cells combined with alveolar macrophages (Fujii *et al.*, 2002 & Ishii *et al.*, 2005) or dendritic cells (Rothen-Rutishauser *et al.*, 2008) have been described, but models with endothelial cells are rarely employed. The aim of this study is to therefore characterise the inflammatory, cytotoxic and GSH response of BEAS-2B cultured at ALI in mono-culture or in a co-culture (characterised in chapter 3) with HPMEC after TiO₂ or UFTiO₂ treatment. Further, three particles of unknown composition were also investigated, where *in vivo* work has been completed (in previous unpublished work, Geiser, 2008) elsewhere, to provide insight into the use of both cell models for testing compounds of commercial interest. HPMVEC were treated with particulates in mono-culture to allow possible interaction between the 2 cell types to be investigated when cultured together and challenged with particulates.

5.3: Methods

5.3.1: Particles

Particles S2219200, S2218600 and S2429901 were provided by Unilever (Colworth) as test particles and their composition is described in 2.1.2. TiO₂ was purchased from VWR and UFTiO₂ was purchased from Sigma (Poole, UK). Particles were stored in as stock solutions at a concentration of 10mg/ml in PBS and stored at -20°C.

5.3.2: Epithelial cell culture on Transwell® Inserts

BEAS-2B were seeded onto collagen-coated Transwell® inserts as described in section 2.2.1.2.

5.3.3: Co-culture of BEAS-2B cells and HPMEC cells

BEAS-2B were co-cultured on with HPMEC as described in section 2.2.1.4.

5.3.4: Endotoxin content determination of particles by LAL assay

Bacterial endotoxins can be shed, and bind particulates. In order to determine whether particles were contaminated with a bacterial endotoxin which would influence the response directly, the endotoxin content of particles (200µg/ml from a 10mg/ml stock, diluted with endotoxin free LAL water) was determined with the QCL-1000® Chromogenic LAL Endpoint assay as described in section 2.2.4.

5.3.5: Zeta potential and particle size

In order to determine whether particle size was related to the cellular response, two sizes of particles were used in the current study. TiO₂ was sized in filtered distilled water using a Sympa Helios BI particle analyser. According to manufacturer's details UFTiO₂ has a diameter of 5nm. For zeta analysis particles were diluted in 1.5ml 1mM

Tris-HCl pH 6.8 (20µl from 10mg/ml stock) and analysed using a Brookhaven Zetaplus Zeta potential analyser.

5.3.6: Particle treatment of BEAS-2B cells in mono- or co-culture

Cells were treated with; TiO₂, UFTiO₂, S2219200, S2218600, or S2429901 to investigate size-related effects on cell viability, oxidative and inflammatory response. Stock concentrations of 10mg/ml of particles were prepared in PBS and stored at -20°C. Stock solutions were diluted to a final concentration of 100µg/ml in quiescent (serum-free) airway epithelial cell medium. To remove aggregates particles were vortexed for 2 minutes, sonicated for 30 minutes in a water bath sonicator for 30 minutes and vortexed for another 2 minutes prior to addition to cells. BEAS-2B on Transwell[®] inserts alone and co-cultured with HPMEC were apically treated with 300µl of particles or quiescent medium alone for 24 hours at 37°C. HPMEC mono-cultures seeded in 24 well plates (seeded at 5x10⁴ cells/well and cultured overnight) were treated with 100µg/ml particles in 1ml fully supplemented endothelial cell medium for 24 hours at 37°C. Cells received fully supplemented medium (in the basolateral compartment for BEAS-2B) 4 hours prior to treatment. After treatment apical and basolateral media from BEAS-2B mono-cultures, co-cultures and media from HPMEC cultures were removed, centrifuged to remove particulates at 295xg for 2 minutes and stored at -20°C until required for analysis of IL-8 or IL-6 by ELISA. Cells were washed twice with PBS (200µl) and lysed with 1% (v/v) Triton X-100 in PBS with 1% (v/v) protease inhibitor cocktail for 30 minutes on ice. Lysates were collected, centrifuged at 295xg for 2 minutes to remove particulates and stored at -20°C prior to analysis by proteomics (section 6.2).

5.3.7: CellTiter-Blue[®] viability assay

After particles stimulation, cell viability was assessed using the CellTiter-Blue[®] viability assay as described in section 2.2.6.

5.3.8: IL-8/IL-6 ELISA

Apical and basolateral media from particle-treated cells were analysed for IL-8 or IL-6 by ELISA as detailed in section 2.2.5.

5.3.9: Isolation of primary human neutrophils with a discontinuous Percoll™ gradient

Discontinuous Percoll™ gradients (1.079g/ml and 1.098g/ml), as described in Table 5.1, were prepared by layering 5ml 1.079g/ml Percoll™ on top of 5ml 1.098g/ml Percoll™ in non-sterile 25ml tubes incubated overnight at 4°C.

Table 5.1: Preparation of Percoll™ solutions for a discontinuous gradient

<u>Final Percoll™ density</u>	<u>1.079g/ml</u>	<u>1.098g/ml</u>
Percoll™ (1.13g/ml)	9.85ml	12.41ml
Water	5.9ml	3.34ml
1.5M NaCl	1.75ml	1.75ml

Venous blood (10ml) was collected into 1ml of 4% (w/v) sodium citrate and layered on top of the Percoll™ gradients (5ml blood per gradient). Ethical approval for collection of blood from healthy donors was approved by Aston University. Informed consent was given by each donor, who tested positive for immunity for Hepatitis B. Gradients were centrifuged at 4°C for 8 minutes at 150xg followed by 10 minutes at 400xg. After centrifugation neutrophils were collected from the clear fraction of separated blood and briefly mixed with red cell lysis buffer (0.83% NH₄Cl (w/v), 0.1% KHCO₃ (w/v), 0.004% Na₂EDTA.2H₂O (w/v), 0.25% BSA (w/v) in dH₂O) in a ratio of 1 part cells to 2 parts lysis buffer. Cells were then centrifuged at 350xg for 6 minutes (4°C) and washed with 2ml PBS before being centrifuged at 350xg for 6 minutes (4°C) and re-suspended in 1ml PBS. Cells were counted and viability was determined using trypan blue exclusion. In all cases viability of recovered neutrophils was above 90%.

5.3.10: Respiratory burst assay

IL-8 was pre-treated with 100µg/ml particles (or PBS as a control) for 24 hours at 37°C. A white 96 well plate (Grenier BioOne, Promega, Southampton, UK) was coated with 0.1% (w/v) BSA in PBS (100µl/well) overnight at 4°C. Primary human neutrophils were re-suspended to a concentration of 1×10^6 cells/ml in PBS and 100µl cells were transferred to a BSA-coated 96 well plate (100µl cells/well) along with 40µl of lucigenin (final concentration 100µM) and 40µl PBS. Neutrophils were incubated at room temperature for 30 minutes in the dark. Baseline luminescence was measured for 10 minutes using an Orion II microplate luminometer (Berthold Detection Systems). Cells were stimulated for 15 minutes with 10µl 50ng/ml pre-treated IL-8 (with or without incubation for 24 hours with 100µg/ml particles at 37°C) during this time luminescence was measured. After stimulation with pre-treated IL-8, the respiratory burst was initiated with 1.25µM N-formyl-methionine-leucine-phenylalanine (fMLP) and luminescence recorded until signal returned to baseline.

5.3.11: GSH-Glo™ GSH assay for quantification of reduced GSH

In order to assess the potential of TiO₂, UFTiO₂ and unknown test particles to induce GSH oxidation (and therefore an imbalance in cellular redox state) in BEAS-2B and HMPEC, cells were incubated with particles for 2 hours and reduced GSH (referred to as GSH) content determined using the GSH-Glo™ GSH assay. The principle of this assay is as follows: Cells are incubated with GSH-Glo™ reaction buffer containing Luciferin-NT substrate, glutathione S-transferase (GST) and esterase. GSH converts the Luciferin-NT into luciferin, with GST acting as a catalyst. The reaction is stopped by addition of Luciferin Detection reagent containing luciferase enzyme to convert the luciferin into a luminescent signal.

BEAS-2B were cultured on Transwell® inserts as described in section 2.2.1.2 and HPMEC were cultured in 96 well plates at 0.8×10^4 cells/well until 70% confluent. Cells were treated with 10µM L-Buthionine sulfoximine (BSO) for 24 hours to deplete GSH, or 100µg/ml particles for 2 hours. After particle or BSO incubation, GSH was determined as follows: Cells were incubated for 30 minutes with 100µl GSH-Glo™

reaction buffer containing Luciferin-NT substrate, esterase and GST. After incubation, 100µl Luciferin Detection Reagent luciferase enzyme was added to wells for 15 minutes (no leakage of reaction buffers to the basolateral compartment of Transwell[®] was observed during this time). After incubation with Luciferin Detection Reagent lysates were collected from the Transwell[®] inserts and 96 well plate and removed to a white walled 96 well plate for measurement. Luminescence was measured using an Orion II microplate luminometer (Berthold Detection Systems). The concentration of GSH in cells was extrapolated from a standard curve constructed using GSH (0µM-5µM).

5.3.12: Statistical analysis.

Statistical analysis was conducted using a one-way ANOVA and Tukey's post test except in Figure 5.2B where IL-8 is normalised to 100% and PBS to 0% using a repeated measures one-way ANOVA and Tukey's post test.

5.4: Results

5.4.1: Particle characteristics

One of the aims of this study was to characterise the effects of two size grades of titanium dioxide and particles (S2219200, S2218600 and S2429901) on cell viability, inflammatory and GSH redox state and barrier integrity of BEAS-2B cultured at ALI and the BEAS-2B/HPMEC co-culture system. As the inflammatory response of both BEAS-2B/HPMEC monocultures and co-cultures were being investigated, the presence of endotoxin contamination of test particles was determined using an LAL assay.

UFTiO₂ endotoxin content was initially above the 1EU/ml, data not shown. Treatment in a dry oven 160°C for 4 hours reduced the endotoxin content to a negligible level and only heat treated-UFTiO₂ was used for further study. The results indicate that TiO₂, heat treated-UFTiO₂ (hereafter referred to as UFTiO₂) and test particles contained minimal endotoxin contamination (Table 5.2) as endotoxin levels were below the lowest standard provided with the assay (0.1 EU/ml).

Particle size determination was undertaken so that any size-related effects of titanium particles may be taken into account during analysis of cell responses, and characterise particle size range. Particle sizing of TiO₂ was first undertaken using a Brookhaven Zeta Analysis analyser using a particle sizing program. The size of the particles was found to be 1000nm, however, this is at the upper limits for the analyser accuracy. TiO₂ particles were then sized using a Sympa Helios BI particle sizer (lower limits >1000nm). In two separate preparations the TiO₂ was found to have a diameter of 3000nm, however on the third occasion the size of the particles was 1000nm. Nevertheless, TiO₂ had a mean diameter greater than 1000nm.

UFTiO₂ had a diameter of 5nm according to manufacturer's details. This could not be confirmed as 5nm is below the limits of detection for both the Brookhaven Zeta Analyser and Sympa Helios BI particle sizer. To rule out any charge related effects of titanium particles, the zeta potential of each suspension was analysed. TiO₂ and UFTiO₂

were found to have similar zeta potentials, $-38.91 \pm 8.74 \text{mv}$ and $-33.91 \pm 5.63 \text{mv}$ respectively (Table 3). Particles S2219200, S2218600 and S2429901 were all in the fine NP size category and ranged in size from 168-533nm with particle S2218600 having the largest diameter ($533.7 \pm 213.79 \text{nm}$, Table 5.2).

Table 5.2: Particle characteristics. Endotoxin content of particle (200µg/ml) was determined using the LAL assay, results are from a single experiment (measured in triplicate) and within assay standard deviations are shown. Titanium dioxide was sized using both a Brookhaven Zetaplus Zeta potential analyser using a particle sizing analysis program and a Sympa Helios BI particle sizer. The S2219200, S2218600 and S2429901 were sized using a Brookhaven Zetaplus Zeta potential analyser using a particle sizing analysis program, n=3, results are expressed as mean ± SEM. Ultrafine titanium dioxide is 5nm according to the manufacturer's details.

	TiO ₂	UFTiO ₂	S2219200	S2218600	S2429901
Endotoxin content (EU/ml)	0.078 ± 0.003	<0.001 ± 0.012	0.077±0.001	0.078±0.001	0.094±0.003
Size (nm)	1000-3000	5	168.07±61.67	533.7±213.79	387.3±154.03

Table 5.3: Titanium dioxide Zeta charge analysis. Zeta potential analysis was conducted on TiO₂ and UFTiO₂ diluted in 1mM Tris-HCl pH 6.8 (20µl from 10mg/ml stock) using a Brookhaven Zetaplus Zeta potential analyser, results are expressed as mean ± SEM n=3.

	TiO ₂	UFTiO ₂
Zeta potential (mV)	-38.91 ± 8.74	-33.91 ± 5.63

5.4.2: S2429901 induces increased IL-6 secretion to the apical and basolateral compartment of BEAS-2B cultured at ALI.

UFTiO₂ has been previously shown to significantly increase IL-8 expression and secretion compared to TiO₂ in A549 cells (Singh *et al.*, 2007). In order to determine whether the BEAS-2B airways epithelium model used in this study behaves in a similar manner, cells were exposed apically to TiO₂ and UFTiO₂ (100µg/ml for 24 hours in serum free airway epithelial media) and apical and basolateral secretion of IL-8 was determined using ELISA. Secretion of IL-6 in response to titanium particles was also investigated. There was a significant (P<0.05) decrease in apical secretion of IL-8 following UFTiO₂ treatment (control: 1922.5±164.6pg, UFTiO₂: 1052.5±362.3pg) by ELISA (Figure 5.1A). This apparent reduction is due to loss of detection of UFTiO₂-bound IL-8 (Appendix 3). Basolateral IL-8 secretion was not affected by TiO₂ treatment (Figure 5.1A).

Particles S2219200, S2218600 and S2429901 had no impact on IL-8 secretion to either compartment (Figure 5.1C), There was a non-significant trend towards greater IL-8 secretion in the basolateral compartment under control conditions compared to the apical compartment (Figure 5.1C). IL-6 secretion was not significantly affected by either TiO₂, UFTiO₂ (Figure 5.1B), S2219200 or S221800 (Figure 5.1C). In TiO₂/UFTiO₂-stimulations; basal secretion of IL-6 was directional with significantly greater IL-6 secretion into the basolateral compartment under control conditions compared to the apical compartment (apical control: 13.4±2.8pg, basolateral control: 253.7±18.1pg). However, this effect was not observed in particle studies. Particle S2429901 induced significantly greater IL-6 release in both apical and basolateral compartments compared to control (apical control: 24.85±8.96pg, apical S2429901; 366.71±11.85pg P<0.001. Basolateral control 77±13.8pg, basolateral S2429901 163.8±8.1pg P<0.001, Figure 5.1D).

These results suggest that particles TiO₂, S2219200 and S2218600 are non-inflammatory to BEAS-2B whilst S2429901 is inflammatory regarding IL-6 secretion. No size-related inflammatory mediator effects were observed since increased IL-6 secretion did not correspond to either the largest or smallest test particle within the

range of 168-3000nm. Also, IL-8 secretion from UFTiO₂ treated cells cannot be measured by ELISA due to interference with the assay (see Figure 10.8).

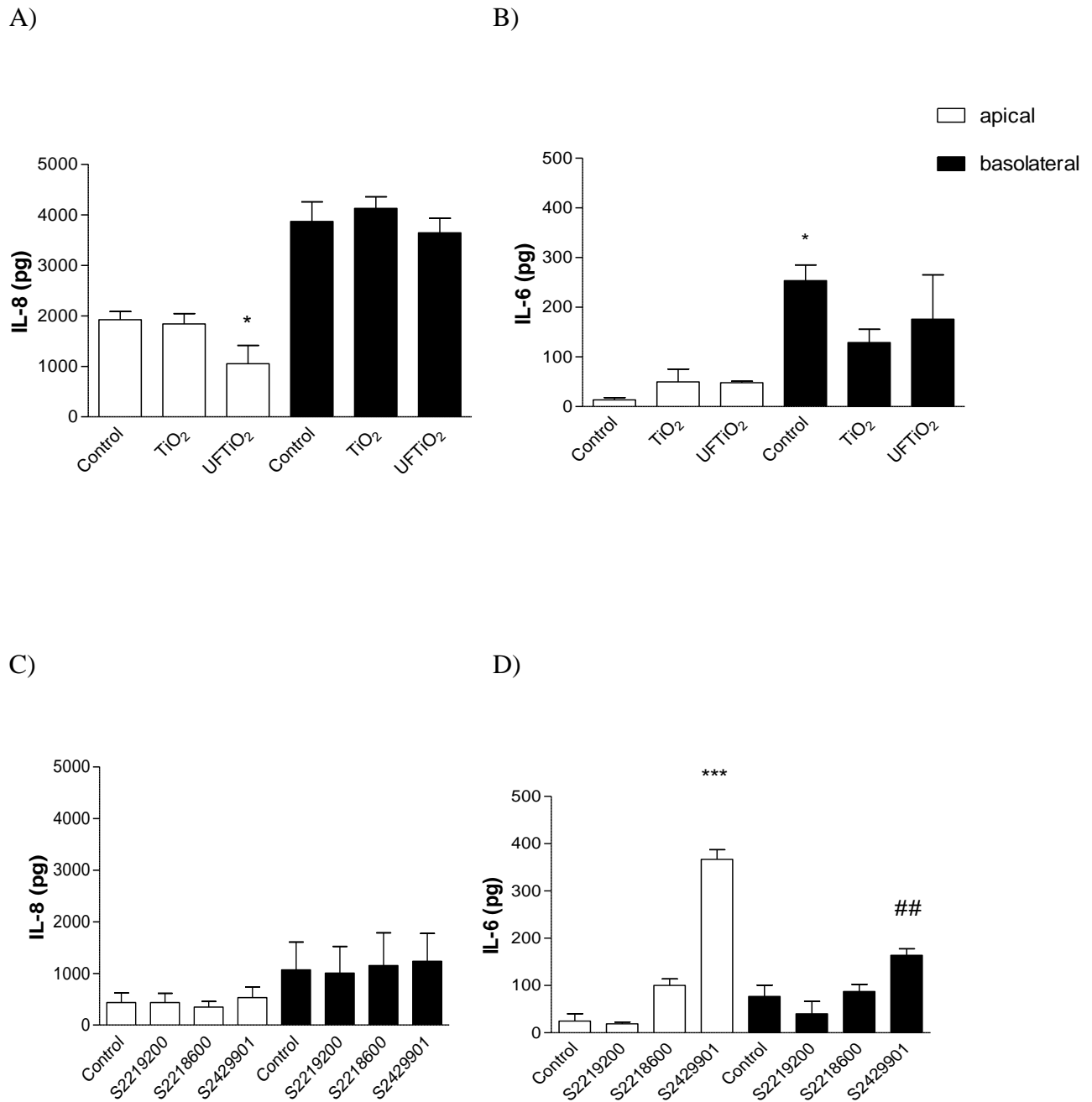


Figure 5.1: S2429901 induces increased IL-6 secretion to the apical and basolateral compartments from BEAS-2B at ALI. BEAS-2B were cultured on Transwell® inserts until a TER of $>45\Omega \times \text{cm}^2$ was achieved (see section 2.2.1.2). BEAS-2B were treated apically with $100\mu\text{g/ml}$ particles in serum free airway epithelial cell medium for 24 hours. After treatment apical and basolateral supernatants were collected, cleared at $295\times\text{g}$ for 2 minutes and stored at -20°C before analysis of IL-8 (A and C) and IL-6 (B and D) secretion by ELISA. Results are expressed as mean \pm SEM, $n=3$. A and B) $*=P<0.05$ compared to apical control. D) $***=P<0.001$ compared to apical control, $##=P<0.01$ compared to basolateral control using one-way ANOVA and Tukey's post test. Clear bars represent secretion to the apical compartment, black bars represent secretion to the basolateral compartment.

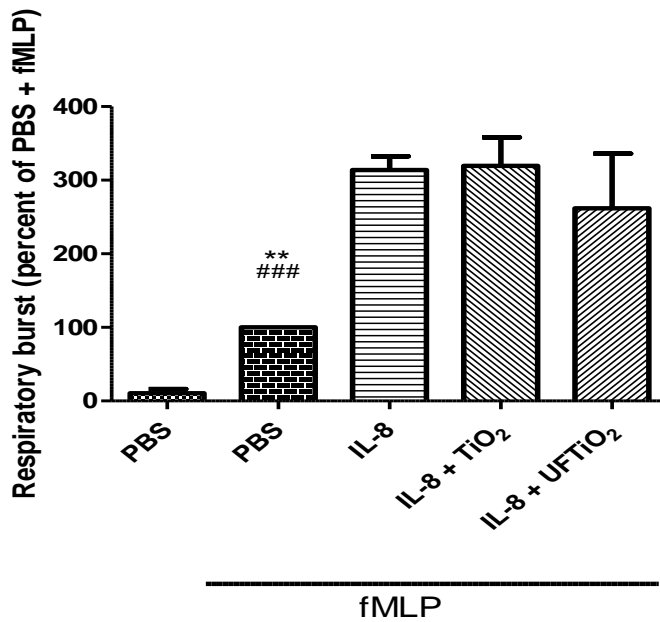
5.4.3: S2429901 reduces the priming effect of IL-8 on fMLP induced respiratory burst in neutrophils.

As UFTiO₂ bound IL-8 is not detected by ELISA (Appendix 3), a method was sought to allow investigations into whether particle-bound IL-8 remains bioactive. IL-8 primes human primary neutrophils for the fMLP induced respiratory burst (Dias *et al.*, 2008). Human recombinant IL-8 was therefore incubated with test particles for 24 hours at 37°C under the same conditions as cell stimulations. Primary human neutrophils were then treated with particle bound IL-8, IL-8 alone as a positive control or PBS (as a negative control) for 15 minutes prior to induction of the respiratory burst by fMLP.

The respiratory burst is induced by fMLP and this effect is enhanced by IL-8 priming. Luminescence is significantly lower when primary human neutrophils are pre-treated with PBS rather than IL-8 (Figure 5.2A and B, 34±3 percent of control P<0.01). TiO₂- and UFTiO₂- bound IL-8 is capable of priming the respiratory burst (IL-8; 306.8±11.1% of PBS + fMLP, TiO₂; 331.9±23.6% of PBS + fMLP; UFTiO₂; 239.4±45.7% of PBS + fMLP, Figure 5.2A). S2219200 and S2219200 also had no impact on the ability of IL-8 to prime the neutrophil respiratory burst (Figure 2B). Particle S2429901 however, resulted in a significant reduction in the respiratory burst priming activity compared to IL-8 alone (IL-8, 306.8±11.1% of PBS + fMLP; S2429901, 218.5±28.8% of PBS + fMLP Figure 5.2B) suggesting that the presence of particle results in loss of IL-8 function.

These results show that although UFTiO₂-bound IL-8 is not detected by ELISA; it remains functional in its ability to prime the neutrophil respiratory burst.

A)



B)

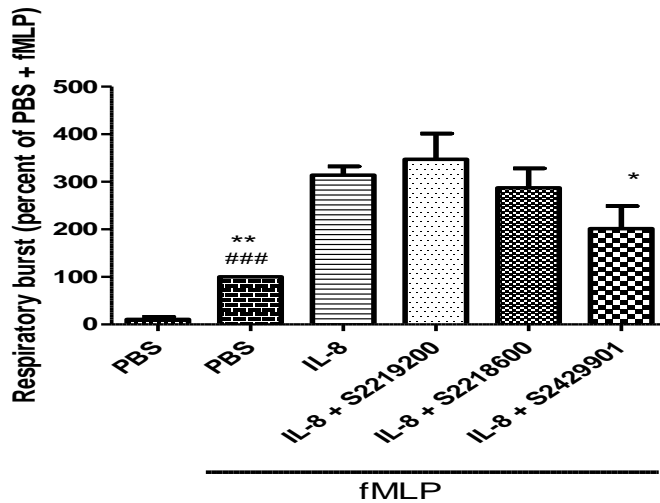


Figure 5.2: S2429901 reduces the priming effect of IL-8 on fMLP induced respiratory burst in neutrophils. Recombinant human IL-8 was incubated for 24 hours at 37°C with 100µg/ml particles. Human primary neutrophils were isolated using a discontinuous Percoll™ gradient (see section 5.3.9) and pre-treated with IL-8 (control) particle bound IL-8 or PBS for 15 minutes in the presence of lucigenin. After pre-treatment with IL-8 respiratory burst was induced using fMLP (see section 5.3.10). Results are expressed as mean ± SEM, n=5, **=P<0.01 compared to IL-8, ###=P<0.001 compared to PBS using one-way ANOVA, *=P<0.05 compared to IL-8 when IL-8+fMLP is normalised to 100% and PBS to 0% using repeated measures one-way ANOVA and Tukey's post test.

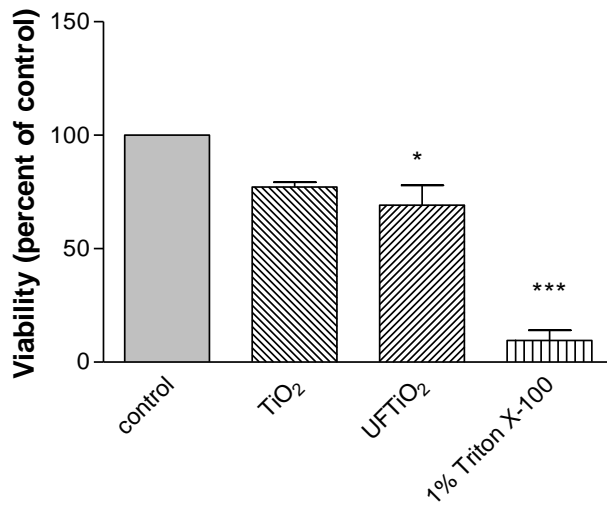
5.4.4: UFTiO₂ decreases BEAS-2B viability but TiO₂ and particles have no effect.

It has been reported that UFTiO₂ is more toxic than TiO₂ to submerged cultures of BEAS-2B (Gurr *et al.*, 2005). In order to determine whether this is observed in the mono- and co-culture model presented in this study, BEAS-2B cultured at ALI were exposed to TiO₂ and UFTiO₂ (100µg/ml for 24hours) and cell viability assessed using the CellTiter-Blue[®] viability assay. The toxic potential of the particles S2219200, S2218600 and S2429901 was also investigated.

Figure 5.3A shows that treatment of BEAS-2B with UFTiO₂ results in a significant loss of cell viability compared to control (69.1±8.8 percent of control, P<0.05) whereas TiO₂ had no significant effect on cell viability. Cells were incubated with 1% (v/v) Triton X-100 as a positive control for cell death, and viability was reduced to 9.5±4.6 percent of control under these conditions (P<0.001, Figure 5.3A).

There was no significant reduction in viability when BEAS-2B were incubated with S2219200 or S2218600 indicating that these particles are not cytotoxic to BEAS-2B cells (Figure 5.3B). Particle S2429901 showed a non-significant trend towards decreasing BEAS-2B viability (Figure 5.3B).

A)



B)

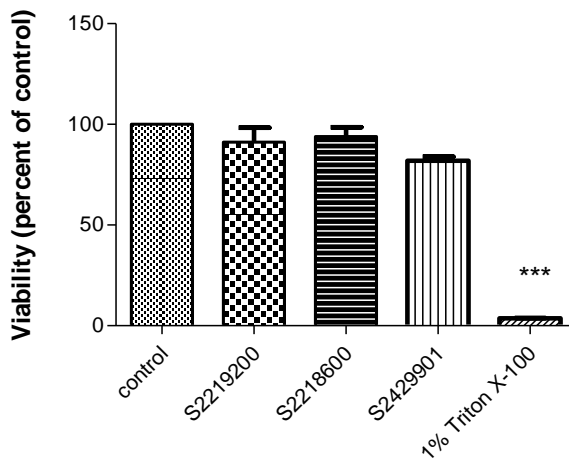


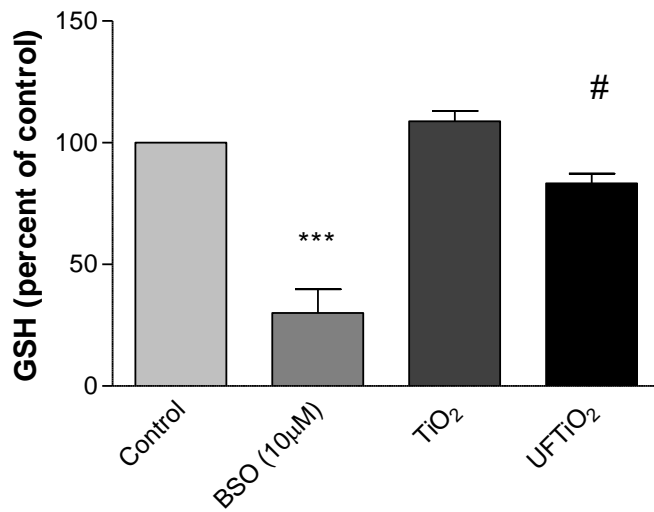
Figure 5.3: UFTiO₂ decreases BEAS-2B viability but TiO₂ and particles have no effect. BEAS-2B cultured on Transwell® inserts until a TER of $>45\Omega \times \text{cm}^2$ was achieved (see section 2.2.1.2) were treated apically with 100 $\mu\text{g}/\text{ml}$ particles or 1% (v/v) Triton X-100 in serum free airway epithelial cell medium for 24 hours. Prior to addition to cells particles were vortexed for 2 minutes, sonicated in a water bath sonicator for 30 minutes and vortexed for a further 2 minutes to remove aggregates. After treatment supernatants were removed and BEAS-2B incubated with CellTiter-Blue® reagent (1:5 v/v in serum free airway epithelial cell medium) for 4 hours in the apical compartment. After incubation, apical media was removed to a 24 well plate and fluorescence measured at ex560nm em590nm. Results are expressed as mean \pm SEM, n=3, *P<0.05 compared to control, ***P<0.001 compared to control using one-way ANOVA and Tukey's post test.

5.4.5: UFTiO₂ results in a loss of cellular GSH content in BEAS-2B at ALI

During oxidative stress, reduced GSH becomes oxidised (GSSG) and excessive ROS production in cells therefore can lead to a loss in GSH levels as GSSG is rapidly exported from cells via p-glycoprotein transporters. Here, GSH levels were measured using the GSH-Glo™ GSH assay. UFTiO₂ has been shown to induce more ROS damage to A549 cells (Singh *et al.*, 2007) and submerged BEAS-2B (Gurr *et al.*, 2005) owing to its larger surface area to mass ratio than TiO₂. It was therefore investigated whether any change in GSH levels was observed in BEAS-2B cultured at ALI with UFTiO₂ compared to TiO₂. The GSH removing potential of S2219200, S2218600 and S2429901 was also investigated. As a positive control for GSH loss, positive control cells were incubated for 24 hours with BSO, an inhibitor of GSH synthesis (Figure 5.4).

Figure 5.4A shows that BSO significantly decreases cellular GSH concentration (control: 32±1µM, BSO: 9±3µM P<0.001) compared to control BEAS-2B at ALI. When control values are normalised to 100% and BSO to 0%, UFTiO₂ treatment results in significant reduction of GSH in BEAS-2B (control: 32±1µM, UFTiO₂: 27±1µM P<0.05). TiO₂, S2219200, S2218600 and S2429901 did not alter GSH levels (Figure 5.4B).

A)



B)

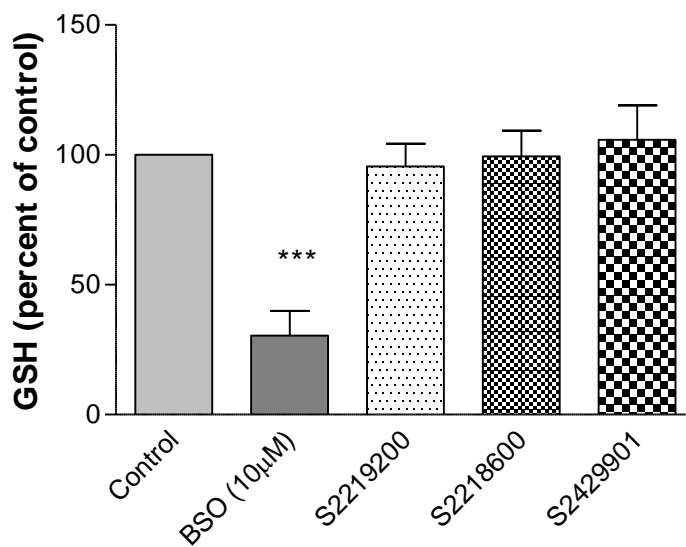


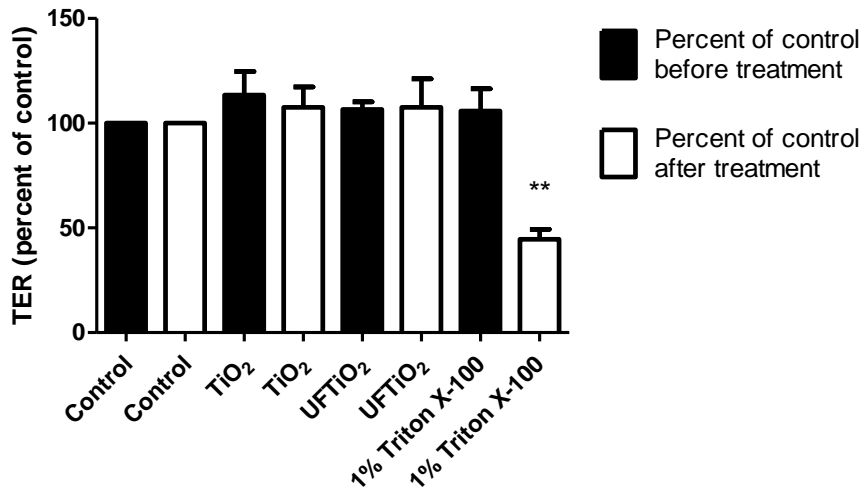
Figure 5.4: UFTiO₂ results in a loss of cellular GSH content in BEAS-2B at ALI. BEAS-2B cultured on Transwell® inserts until a TER of >45Ω x cm² was achieved, were treated apically with 100µg/ml particles for 2 hours or 10µM BSO for 24 hours. After incubation reduced GSH levels were determined using the GSH-Glo™ GSH assay (materials and methods) Results are expressed as mean ± SEM n=3 ***=P<0.001 compared to control, **=P<0.05 compared to control where control is normalised to 100%, BSO normalised to 0% using a repeated measured one-way ANOVA and Tukey's post test.

5.4.6: Effect of particles on BEAS-2B barrier function

A major function of the airways epithelium is the maintenance of a semi-permeable tight barrier against inhaled pathogens and particulates. UFTiO₂ treatment resulted in a loss of BEAS-2B viability and S2429901 was found to induce a pro-inflammatory response in BEAS-2B as measured by increased IL-6 secretion. To determine whether loss of viability or an inflammatory environment influences barrier integrity, TER was analysed. TER measurements were taken before particle treatment and normalised to control. After incubation with particles TER measurements were taken again and normalised to control TER after treatment.

Neither TiO₂, UFTiO₂ (Figure 5.5A) nor particles (Figure 5.5B) compromised barrier integrity as measured by TER. Incubation of BEAS-2B with 1% (v/v) Triton X-100 resulted in a significant loss of barrier integrity (P<0.001) with TER before treatment being 106±11 percent of control and TER after treatment being 45±5 percent of control. These results show that the loss of viability after UFTiO₂-challenge or increased inflammation as a result of S2429901-challenge do not compromise BEAS-2B barrier integrity significantly.

A)



B)

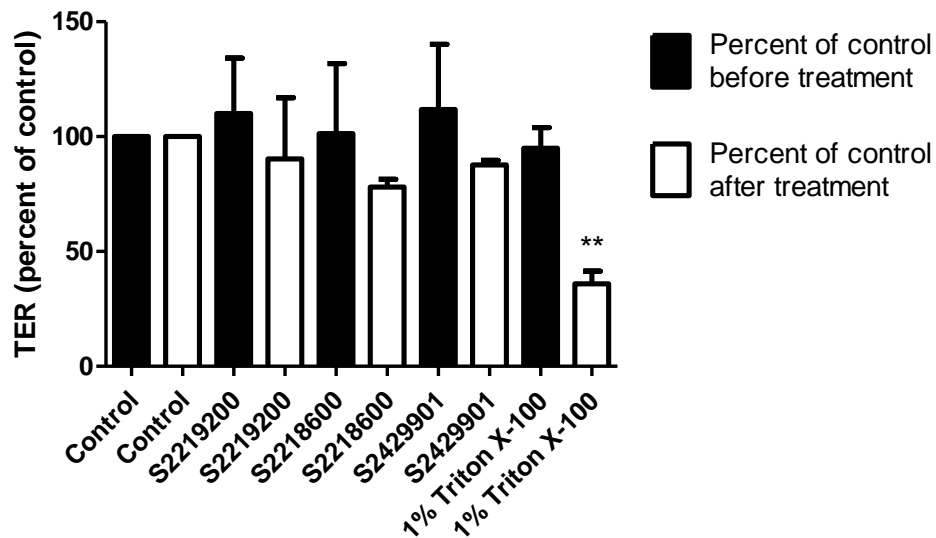


Figure 5.5: Particles have no effect on BEAS-2B barrier integrity. BEAS-2B were cultured on Transwell® inserts until a TER of $>45\Omega \times \text{cm}^2$ was achieved (see section 2.2.1). TER was recorded before apical treatment with $100\mu\text{g/ml}$ particles or 1% (v/v) Triton X-100 in serum free airway epithelial cell medium, or with serum free medium alone (control) for 24 hours and normalised to control (black bars). After incubation culture medium as replenished and TER was recorded again and normalised to control well after treatment (open bars). Results are expressed as mean \pm SEM, from 3 separate experiments with 2 Transwell® inserts per treatment in each experiment $**=P<0.01$ compared to 1% (v/v) Triton X-100 percent of control before treatment using one-way ANOVA and Tukey's post test.

5.4.7: Particle treatment does not induce increased inflammatory mediator secretion from HPMEC

The epithelial barrier is maintained in particle treated BEAS-2B (measured by TER). However, any affect of particle treatment on inflammatory mediator secretion from HPMEC was examined so any contribution of HPMEC cells to inflammation induced by particle could be determined in the event of epithelial barrier disruption. HPMEC alone were exposed to particles for 24 hours, and supernatants were assayed for the inflammatory mediators IL-8 and IL-6.

Figure 6 shows that neither IL-8 secretion (Figure 5.6A) nor IL-6 secretion (Figure 5.6B) was altered after incubation with TiO₂, UFTiO₂ or particles. These results suggest that test particles are non-inflammatory to the endothelium alone.

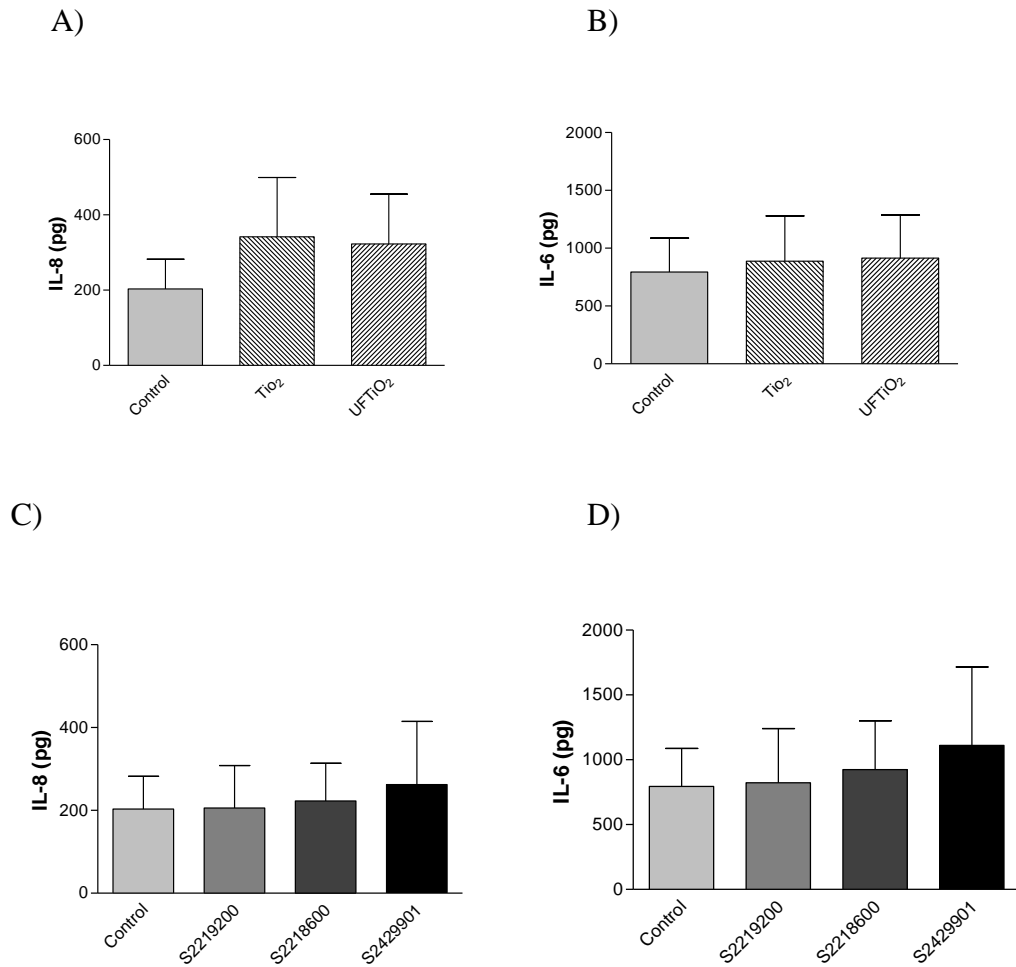


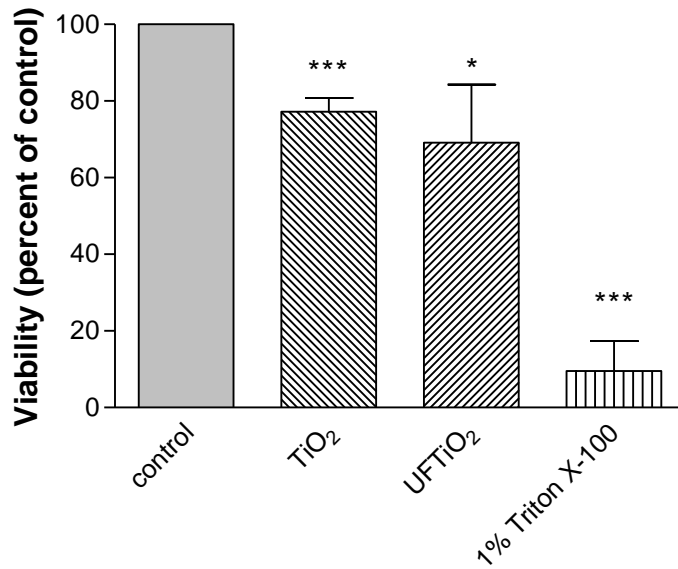
Figure 5.6: Particle treatment does not induce increased inflammatory mediator secretion from HPMEC. HPMEC were seeded in 24 well plates at 5×10^4 cells/well and cultured overnight. Cells were incubated with $100 \mu\text{g/ml}$ particles in fully supplemented endothelial cell medium for 24 hours. Prior to addition to cells particles were vortexed for 2 minutes, sonicated in a water bath sonicator for 30 minutes and vortexed for a further 2 minutes to remove aggregates. After treatment supernatants were collected, cleared at $295 \times g$ for 2 minutes and stored at -20°C until analysis. IL-8 and IL-6 was analysed using IL-8 and IL-6 ELISA respectively. Results are expressed as mean \pm SEM, $n=3$.

5.4.8: TiO₂ and UFTiO₂ reduce HPMEC viability

In order to determine whether the lack of inflammatory response of particle exposed HPMEC was due to loss of cell viability, HPMEC were exposed to 100µg/ml particles or particles for 24 hours, after which the CellTiter-Blue[®] viability assay was performed. As a positive control for loss of viability, cells were incubated with 1% (v/v) Triton X-100.

The results show that both TiO₂ and UFTiO₂ incubation significantly reduced HPMEC viability (TiO₂ 77±1% of control, UFTiO₂; 69.1±4% of control, Figure 5.7A, P<0.05). Treatment with 1% (v/v) Triton X-100 reduced cell viability to 9.5±4.6 percent of control (P<0.001). There was no loss of viability in particle-treated HPMEC (Figure 5.7B).

A)



B)

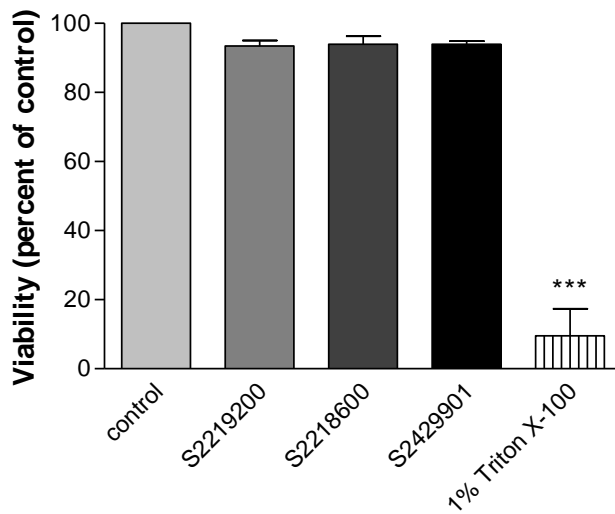
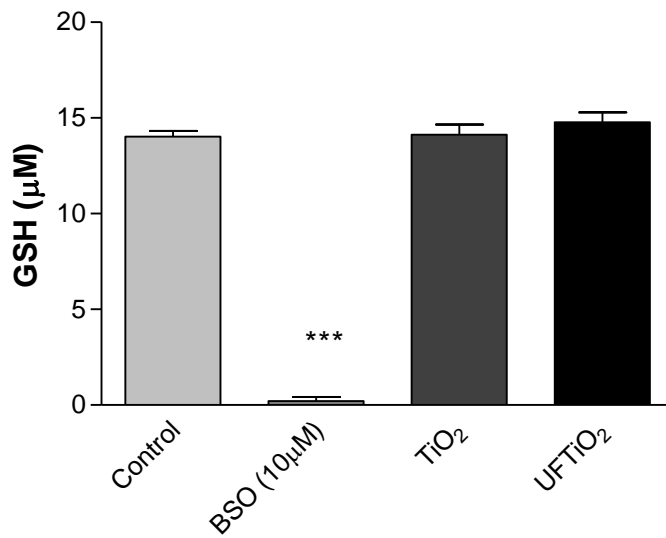


Figure 5.7: TiO₂ and UFTiO₂ reduce HPMEC viability. HPMEC were seeded in 24 well plates at 5×10^4 cells/well and cultured overnight. Cells were incubated with 100 μ g/ml particles in fully supplemented endothelial cell medium for 24 hours after which supernatants were collected and cells were incubated with CellTiter-Blue[®] reagent (1:5 v/v) in fully supplemented endothelial cell media for 4 hours. After incubation fluorescence was measured at ex560nm em590nm. Results are expressed as mean \pm SD n=3, *=P<0.05 compared to control, ***=P<0.001 compared to control using one-way ANOVA and Tukey's post test.

5.4.9: Particles treatment does not induce oxidative stress in HPMEC.

In order to determine whether the loss of cell viability observed with TiO₂ and UFTiO₂ exposed HPMEC may be due to oxidative stress, levels of GSH were investigated in HPMEC-treated with particles for 2 hours. The effect of particles of cellular GSH was also determined. Cells were incubated for 24 hours with BSO which inhibits synthesis of GSH. BSO incubation depleted the HPMEC GSH concentration significantly (Figure 5.8, control; 14±0μM, BSO; 0.2±0.1μM GSH, P<0.001). Neither TiO₂ nor UFTiO₂ had any effect on HPMEC GSH, suggesting that loss of viability with these particles in HPMEC was not due to oxidative stress; there was also no loss of GSH in HPMEC when treated with particles (Figure 5.8).

A)



B)

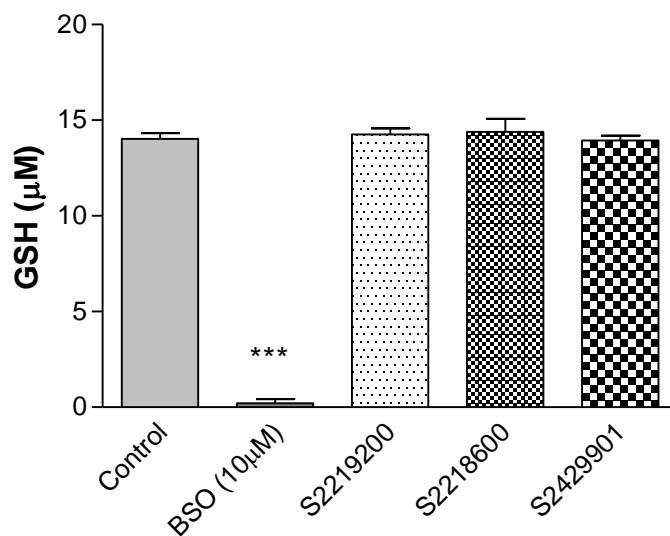


Figure 5.8: Particle treatment does not induce oxidative stress in HPMEC. HPMEC were seeded in a 96 well plate at 8000cells/well and incubated overnight. Cells were treated with 10µM BSO for 24 hours or 100µg/ml particles for 2 hours in fully supplemented endothelial cell medium. After incubation supernatants were removed and GSH content determined using the GSHGlo™-GSH assay. Results are expressed as mean ± SD, n=2, ***=P<0.001 compared to control.

5.4.10: S2429901, but none of the other particles tested, induces IL-6 secretion to the apical compartment of BEAS-2B/HPMEC co-cultures.

An aim of the current study was to expose the BEAS-2B/HPMEC co-culture to TiO₂, UFTiO₂ and particles to determine if the inflammatory response and viability mirror the mono-cultures experiments or whether there was any synergism/antagonism between the two cell types. The inflammatory response of the co-culture after 24 hour apical exposure to 100µg/ml particle was measured by analysis of IL-8 and IL-6 secretion.

Figure 5.9A shows that secretion of IL-8 into the apical compartment was reduced non-significantly compared to control with TiO₂ (control: 5585.3±1509.456pg, TiO₂: 2739.41±767.78pg). Basolateral IL-8 secretion was unaffected by particle treatment, however, a large experimental error was observed during IL-8 detection.

IL-6 secretion into the basolateral control was significantly greater than in the apical compartment (apical control: 165.93±33.82, basolateral control; 920±49.4pg). IL-6 secretion in both the apical and basolateral compartment was un-changed after TiO₂ or UFTiO₂ challenge (Figure 5.9B). These results suggest that TiO₂ and UFTiO₂ are not inflammatory to the airways epithelium. S2219200 and S2218600 were found to be non-inflammatory to BEAS-2B and HPMEC monocultures (Figure 1C-D and 6C-D respectively). S2429901 induced an inflammatory response in BEAS-2B with significantly increased IL-6 secretion after 100µg/ml S2429901 treatment for 24 hours (Figure 5.1D). As with BEAS-2B mono-cultures there was no significant increase in IL-8 secretion from BEAS-2B/HPMEC co-culture model (Figure 5.9C). S2429901 induced IL-6 secretion into the apical compartment of the co-culture model (apical control: 165.9±33.8pg, apical S2429901: 724±24.9pg P<0.01, Figure 5.9D). Again, IL-6 secretion was shown to be directional with significantly greater IL-6 secretion into the basolateral compartment than the apical compartment for both titanium and particle (Figure 5.9B and 5.9D P<0.001).

In order to determine whether there was any synergism or antagonism regarding inflammatory mediator secretion between the BEAS-2B and HMVEC total IL-8 or IL-6 from mono-culture studies were compared the total for co-culture studies (it appears that there is greater IL-8 secretion in co-culture studies for the particle stimulation. However in BEAS-2B mono-cultures there was much lower IL-8 secreted from particle stimulated cells than TiO₂ stimulated cells (Figure 5.1).

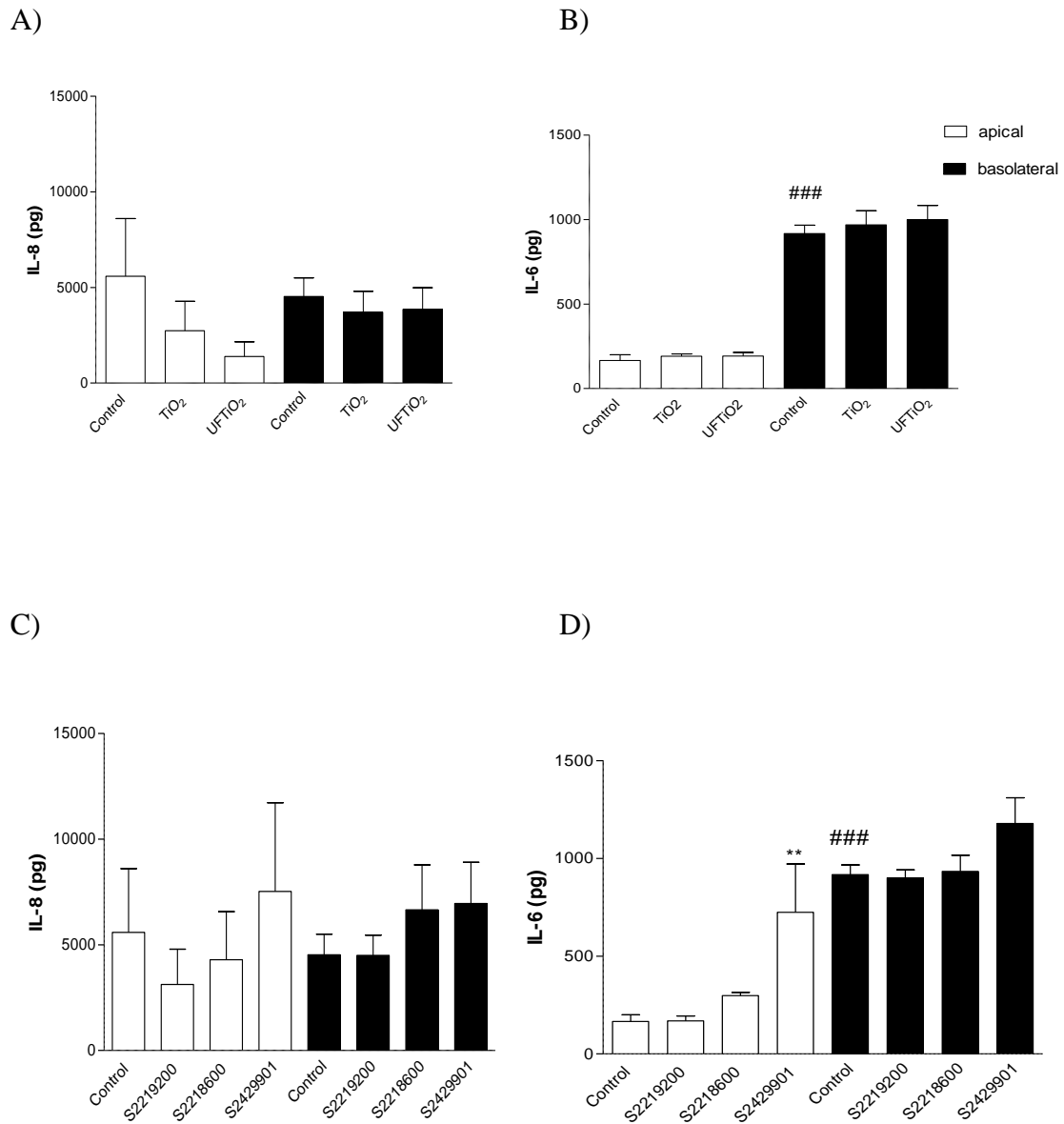
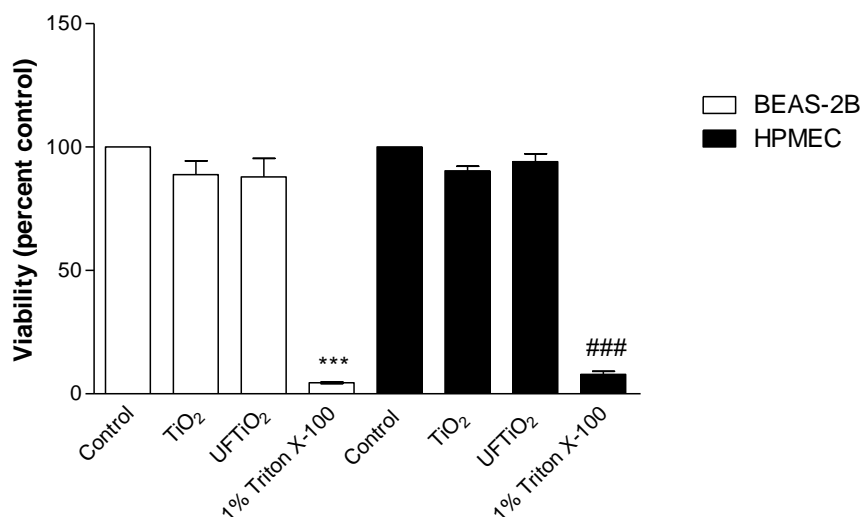


Figure 5.9: S2429901 but none of the other particles tested, induces IL-6 secretion to the apical compartment of the BEAS-2B/HPMEC co-culture. HPMEC were seeded in a companion plate at 5×10^4 cells/well and cultured overnight, after which media was replenished with 600 μ l endothelial cell medium and BEAS-2B previously cultured on Transwell[®] inserts with a TER greater than $45\Omega \times \text{cm}^2$ were placed in the well. The co-culture was treated apically for 24 hours with 100 μ g/ml particles in serum free airway epithelial cell medium, or serum free airway epithelial media alone. After exposure supernatants were collected and cleared at 295xg for 2 minutes and stored at -20°C until analysis by IL-8 and IL-6 ELISA. Results are expressed as mean \pm SEM, $n=4$, $**=P<0.01$ compared to apical control, $###=P<0.001$ compared to apical control. Clear bars represent secretion to the apical compartment, black bars represent secretion to the basolateral compartment.

5.4.11:BEAS-2B/HPMEC co-culture viability is not affected by particle exposure

The particles were previously shown to have no cytotoxic effects on either BEAS-2B (Figure 5.3) or HPMEC (Figure 5.7). However, UFTiO₂ was found to be toxic to both BEAS-2B (Figure 5.3) and HPMEC mono-cultures (Figure 5.7) and TiO₂ was toxic to HPMEC (Figure 5.7). The effect on cell viability of these particles on the BEAS-2B/HPMEC co-culture was therefore investigated in order to determine whether the co-culture responds in a similar manner to the mono-cultures. There was no loss of cell viability with either cell type in the co-culture after TiO₂, UFTiO₂ or particle treatment (Figure 5.10).

These results suggest that the co-culture model is more resistant to particle induced cell death than either cell type alone.



b)

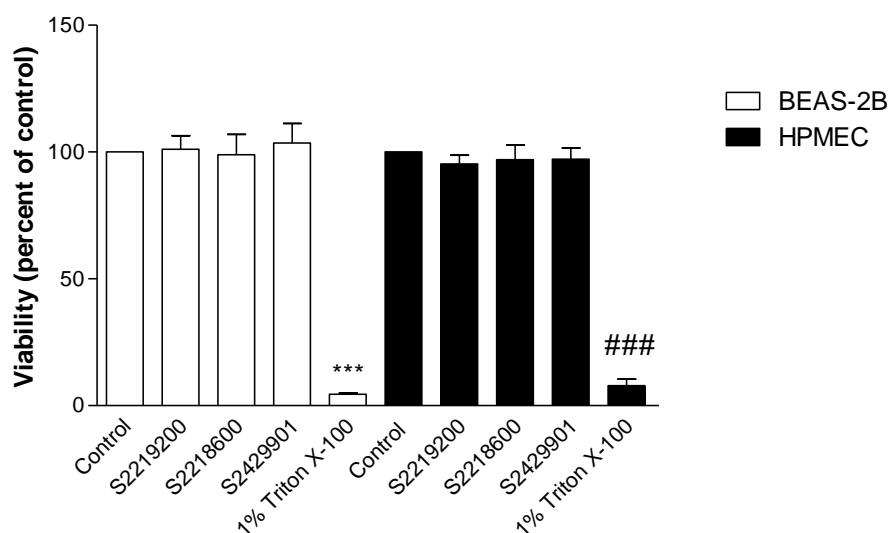


Figure 5.10: BEAS-2B/HPMEC co-culture viability is not affected by particle exposure.

HPMEC were seeded in a companion plate at 5×10^4 cells/well and cultured overnight, after which media was replenished with 600 μ l endothelial cell medium. HPMEC were then combined with BEAS-2B cultured on Transwell[®] inserts with a TER greater than $45 \Omega \times \text{cm}^2$. The co-culture was treated apically for 24 hours with 100 μ g/ml particles in serum free airway epithelial cell medium, or serum free airway epithelial media alone. After incubation BEAS-2B on Transwell[®] inserts were removed to a separate well and incubated with 300 μ l CellTiter-Blue[®] (1:5 v/v in airway epithelial cell media) for 4 hours. HPMEC were incubated with 1ml CellTiter-Blue[®] (1:5 v/v in endothelial cell media) for 4 hours. After incubation fluorescence was measured at excitation 460nm emission 590nm. Results are expressed as mean \pm SD, n=4, ***=P<0.001 compared to apical control, ###=P<0.001 compared to basolateral control.

5.5: Discussion

Most of the research conducted into the inflammatory and cytotoxic effects of NP on the airways *in vitro* has been conducted on submerged mono-cultures of airways epithelial cells (Park *et al.*, 2008; Singh *et al.*, 2007 & Veranth *et al.*, 2007). These do not entirely mimic the *in vivo* airways where epithelial cells are at ALI. Further, since endothelial cells themselves release inflammatory cytokines in response to PM (Gojova *et al.*, 2007) and NP have been observed to translocate to the endothelium (Geiser *et al.*, 2005), co-cultures of epithelial and endothelial cells may provide a better understanding into the toxic and inflammatory effect of NP exposure. The aim of this study was to therefore characterise the inflammatory response of BEAS-2B cultured at ALI and BEAS-2B/HPMEC co-culture model to TiO₂ and UFTiO₂ at 100µg/ml for 24 hours, and any associated toxicity. Particles, dose and incubation period were chosen as they are commonly used in the study of airways inflammation (Ishii *et al.*, 2005; Newland & Richter, 2008; Sakamoto *et al.*, 2007; Veranth *et al.*, 2007). The inflammatory, cytotoxic and oxidative response of cells to S2219200, S2218600 and S2429901, were also undertaken. *In vivo* studies have already been conducted elsewhere (Gaiser, 2008).

Size has been shown to be a determining factor in the cellular response of airway epithelial cells after exposure to PM (Singh *et al.*, 2007). The size of the particles in this study was therefore characterised. TiO₂ was found to be a heterogeneous mix of fine to coarse particles with diameter of 1000nm-3000nm. UFTiO₂ has a diameter of 5nm as per manufacturers details. As direct comparisons between TiO₂ and UFTiO₂ will be made during this study, the charge of particles (zeta potential) was also investigated since zeta particle charge has also been shown to affect cell-particle interaction (Dausend *et al.*, 2008). TiO₂ and UFTiO₂ were found to have a similar negative charge, so charge-related effects of the particles on the cells can be eliminated. S2219200, S2218600 and S2429901 are of unknown composition so charge analysis was not undertaken since any results observed may be due to particle composition. Size determination showed that all three particles are indeed NP as the size range was 168-533nm.

The endotoxin content of particles was determined in order to rule out endotoxin-induced cell responses after particle challenge. The particles were shown to have negligible endotoxin contamination; endotoxin levels were shown to be below the lowest standard in the assay kit (0.1 EU/ml). US Food and Drug Administration (FDA) state that medical devices may contain endotoxin levels of ≤ 0.5 EU/ml (Gorbet and Sefton, 2005). Further, Ishii *et al.*, (2005), reported that endotoxin content of particulate matter up to 6.4EU/ml does not result in an inflammatory response in lung epithelial cells, therefore, any inflammatory response observed here is solely due to the particles themselves.

TiO₂ has been previously shown to induce IL-8 secretion from and increased mRNA expression in airway epithelial cells, (Park *et al.*, 2008; Singh *et al.*, 2007 & Veranth *et al.*, 2007). The results of the present study conversely showed a significant decrease in IL-8 secretion from BEAS-2B treated with UFTiO₂ compared to TiO₂ which was likely to be due to adsorption of IL-8 onto UFTiO₂ resulting in a reduced detection of IL-8 by ELISA (Chapter 10). Whether UFTiO₂ bound IL-8 remains functional was investigated by measuring the ability of particle-bound IL-8 to prime the human primary neutrophil respiratory burst. This analysis has relevance to the present study as increased numbers of neutrophils have been observed in BAL fluid of TiO₂ treated rats (Renwick *et al.*, 2004) possibly due to increased chemokine activity. Neither TiO₂, UFTiO₂, S2219200 or S2218600 affect the ability of IL-8 to prime the neutrophil respiratory burst for enhanced response to fMLP. These results suggest that IL-8 secreted in response to UFTiO₂ remains biologically active, however future work is required to determine whether UFTiO₂ challenged BEAS-2B respond by increased IL-8 production, and a Boydem chemotaxis chamber could be used to determine the chemotactic potential of particle-bound IL-8.

Pre-incubation with S2429901 significantly reduced the priming affect of IL-8. Adsorption studies showed that S2429901 did not significantly reduce IL-8 detection by ELISA (Appendix 3) nor did the presence of this particle affect the luciferase signal of the respiratory burst assay (Chapter 10) or the baseline signal of neutrophils without luciferase. It is therefore not clear as to why there was a reduction in the respiratory

burst priming with S2429901. This particle may have exhibited cytotoxic effects towards primary human neutrophils thereby resulting in loss of the respiratory burst. Further work should investigate the effect of S2429901 on neutrophil viability; previous studies have shown dose-dependent cytotoxicity towards this particle in rat epithelial and fibroblast cell types (Gaiser *et al.*, 2009) and there was a trend towards decreased viability in BEAS-2B cultured at ALI after S2429901 exposure. Taken together these results suggest that particles S2219200, S2218600 and S2429901 do not induce an increase in IL-8 secretion in the airways epithelium, but IL-8 activity may be influenced/inhibited in the presence of S2429901.

Urban air PM₁₀, ROFA and DEP have all been reported to increase IL-6 secretion from airway epithelial cells *in vitro* (Auger *et al.*, 2006; Carter *et al.*, 1997 & Ishii *et al.*, 2005). The current study shows that incubation of BEAS-2B cells either alone or in co-culture with S2429901 results in increased IL-6 secretion. There are several possible explanations for the lack of IL-6 response to TiO₂ that was observed in the current study compared to published data. First, the increased IL-6 secretion in ROFA-treated NHBE was due to the presence of transition metals on the particle surface (Carter *et al.*, 1997) the presence of which have been suggested to induce an inflammatory response via ROS production through the Fenton reaction (Carter *et al.*, 1997). Here, TiO₂ was found to have no effect on GSH suggesting that ROS was not increased. Another possible explanation for the lack of IL-6 response is the difference in cell type. Carter *et al.*, (1997) and Ishii *et al.*, (2005) observe significant IL-6 secretion in response to PM by NHBE cells. Veranth *et al.*, (2007) noted that NHBE secrete far greater basal levels of IL-6 than BEAS-2B, suggesting that the regulatory control of IL-6 expression may also differ. Stimulation of NHBE cells cultured at ALI with particles may therefore result in increased secretion of IL-6, however the aims of the present study are to validate the BEAS-2B cultured at ALI as a model of airways inflammation, rather than a comprehensive analysis of the inflammatory potential of the particles to the airways.

Veranth *et al.*, (2008) also observed that cell culture media influences the IL-6 response of submerged cultures of BEAS-2B when treated with the same particle species. Zhao *et al.*, (2009) reported that submerged cultures of NHBE secrete significant levels of

GM-CSF, IL-6, IL-8 and IL-1 β response to 24 hour treatment with 100 μ g/ml PM₁₀ compared to submerged control cells, whilst the same cells cultured under ALI with the same treatment only show significant secretion in IL-6 compared to control cells cultured at ALI. These results imply that the culture conditions themselves also govern the inflammatory response observed and may explain the discrepancy between this work and published data regarding IL-6 secretion. The closest comparison to the present study is that by Veranth *et al.*, (2007), who treated submerged BEAS-2B cultured in either KGM or LHC-9 media with 100 μ g/ml TiO₂ or UFTiO₂ for 24 hours, and observed no significant increase in IL-6 secretion, a result mirrored in the current study with BEAS-2B cultured at ALI.

TiO₂ has been shown to increase ROS and cell death in NHBE, 16HBE14o (Hussain *et al.*, 2010) and BEAS-2B (Gurr *et al.*, 2005; Park *et al.*, 2008). An important contributor to the toxicity and cell signalling activity of ROS is a change in cellular redox state due to reactions between ROS and thiols on GSH (Forman *et al.*, 2009). Cell viability and GSH content (as a measure of redox stress) were therefore investigated in the current study. Here, BEAS-2B cultured at ALI showed a significant reduction in both cell viability and GSH content with UFTiO₂-treatment compared to control, this response was not observed with TiO₂. Similarly Gurr *et al.*, (2005) observed that UFTiO₂ induced significant oxidative DNA damage, lipid peroxidation, ROS and micronuclei formation in submerged cultures of BEAS-2B. Despite the differences in methods between Gurr *et al.*, (2005) and the current study, they both show increased oxidative stress and cell damage after UFTiO₂ challenge. Further, Park *et al.*, (2008) observed a significant reduction in cellular GSH and viability in submerged BEAS-2B with UFTiO₂. The oxidative and cytotoxic response of BEAS-2B cultured at ALI show good agreement with published data from submerged BEAS-2B, and lend support to BEAS-2B cultured at ALI as a valid model for investigations into PM toxicity.

An important function of airway epithelial cells is to maintain a tight barrier against invading pathogens and toxins. As UFTiO₂ induced a loss of cell viability investigations were carried out to determine if the BEAS-2B cell barrier was compromised by UFTiO₂ and other test particle exposure by analysis of TER. There

was no change in TER with any of the test particles used indicating no loss of barrier integrity. Westmoreland *et al.*, (1999) reported no change in TER after TiO₂ treatment in 16HBE14o, however, they also observed no change in cell viability. The size of the TiO₂ used in the study by Westmoreland *et al.*, (1999) was not reported making comparisons difficult. However, sodium carbonate treatment caused loss of viability which was mirrored with loss of TER. Caraballo *et al.*, (2011) showed that transepithelial electrical conductance in response to PM treatment in rat alveolar epithelial cells, did not mirror permeability changes using lanthium nitrate, a compound reported to not pass through tight junctions under normal conditions. Results reported in this chapter suggest that the BEAS-2B barrier (electrical resistance) was not compromised; further investigations into tight junction integrity by lanthium nitrate permeability or tight junction protein localisation studies would support this finding.

Comparisons into inflammatory mediator secretion between the current BEAS-2B ALI model and other published models are difficult, due to chemokine adsorption onto PM and effects of differing culture conditions and cell types. Nethertheless, the viability and oxidative stress studies are in agreement with those reported for TiO₂ and UFTiO₂ (Gurr *et al.*, 2005; Park *et al.*, 2008). The BEAS-2B ALI model was therefore adopted in a co-culture of the airways by incorporation of a HPMEC cell layer. To this end the contribution of the endothelial compartment to the inflammatory response, endothelial viability and GSH concentration were determined in response to all test particles.

IL-8 or IL-6 secretion from HPMEC alone was not modified with any of the particles tested, compared to control. In contrast Qu *et al.*, (2010) reported a significant increase in IL-6 secretion from human lung blood microvascular endothelial cells (HMVEC-LB1) treated with 100µg/ml urban air PM_{2.5}, and this increase in IL-6 secretion was sustained over 24 hours. In the present study, both TiO₂ and UFTiO₂ reduced HPMEC viability which contrasts with the result obtained from Yu *et al.*, (2010) where TiO₂ treatment had no affect on cell viability. However, Yu *et al.*, (2010) treated cells with a dose of particles ten-fold less than used in this study, and this difference in particle dose may account for the increase in cytotoxicity observed here in response to particles. UFTiO₂ induces greater oxidative stress in airway epithelial cells than TiO₂ (Singh *et*

al., 2007). There was however, no oxidative stress induced in HPMEC exposed to either UFTiO₂ or TiO₂ as measured by GSH levels.

Acute challenge with S2219200, S2218600 and S2429901 did not induce a significant inflammatory response in HPMEC and had no effect on cell viability or GSH suggesting that these particles are non-inflammatory and not cytotoxic to pulmonary endothelial cells. The reduction in IL-8 detection in UFTiO₂ treatment was not observed with HPMEC cells; this is likely to be due to the presence of FBS in the culture media. FBS proteins would bind to the particles thereby inhibiting cytokine binding. Indeed Val *et al.*, (2010) show a reduced adsorption of GM-CSF to particles by inclusion of serum into culture media. A significant loss of IL-8 detection in apical supernatants by ELISA was not observed in UFTiO₂-treatment of the co-culture however, in these experiments there was a lot of variability within the control treatments. TiO₂, S2219200 and S221800 were non-inflammatory to BEAS-2B cells in mono-culture, and were also non-inflammatory in the co-culture model, suggesting that the co-culture model has a similar sensitivity to the mono-cultures.

S2429901 increased IL-6 secretion from BEAS-2B significantly, however, this particle failed to induce an increase in IL-6 secretion in the co-culture. It may be that the presence of the HPMEC cell layer provides protection against airway inflammation *in vitro*. Mogel *et al.*, (1998) reported that co-cultures of endothelial cells and epithelial cells show greater inflammatory mediator secretion in response to stimuli than the mono-cultures combined. Mogel *et al.*, (1998) investigated BEAS-2B cells that were cultured on the apical surface of Transwell[®] inserts with ECV304 HUVEC cell line in the basolateral compartment compared with BEAS-2B in the apical compartment under submerged conditions. The co-culture was exposed to 0.15ppm ozone for 90 minutes without medium in the apical compartment. While the cell orientation and types were very similar to the current study, the synergism observed by Mogel *et al.*, (1998) was not observed here.

The loss of viability with HPMEC cells observed with TiO₂ and UFTiO₂ is not observed in the HPMEC compartment of the co-culture model and this is likely to be due to the presence of the BEAS-2B presenting a physical barrier to protect the endothelium from direct particle exposure. TER suggests that BEAS-2B barrier remained intact during particle treatment. TER measurements were not undertaken on the co-culture after particle treatments. UFTiO₂ has been shown to translocate through cell layers by Rothen-Rutishauser *et al.*, (2008) in a triple cell model of A549 cell on Transwell[®] inserts with alveolar macrophages in direct contact on the apical surface of A549 and monocyte derived dendritic cells on the underside of the insert. Particles added apically in solution were observed in all 3 cell types after 24 hour incubation. A limitation of the present study is that, due to limited expansion of HMVEC cells, the location of particles was not investigated. Future work could include investigation of particle transport through the BEAS-2B epithelial barrier to the endothelial compartment to make further comparisons between the co-culture model and *in vivo* reports of particle localisation within endothelial cells.

5.6: Conclusion

The inflammatory response of the BEAS-2B ALI model in response to titanium is complicated by cytokine adsorption onto particles and varying cytokine responses of cells under different culture conditions. A size-dependent loss of cell viability and GSH (indicative of ROS production) was observed with titanium treated BEAS-2B cultured at ALI, similar to those reported elsewhere in submerged models. The current ALI model presents a closer representation of epithelial cell phenotype *in vivo* and is therefore a compelling model for study of PM induced lung inflammation. The co-culture model requires further investigations however. Investigations into particle translocation within the model would also allow for characterisation and validation of the model when compared to *in vivo* studies.

Chapter 6: Proteomic identification of airway inflammation biomarkers

6.1: Rationale

Proteomics, is the study of all the protein isoforms within a cell, tissue or bodily fluid at a given time, such as plasma. The proteins within these samples undergo expression changes during cellular events, for example during inflammation the plasma proteome shows expression changes in acute-phase protein. Proteomics is therefore a powerful tool which can provides un-biased (global protein expression changes are analysed rather than selecting to identify expression changes of a given protein) analysis of up- and down-regulated proteins and identification of post-translational modifications within a sample. This method may prove useful in the identification of early biomarkers of disease and biomarkers of particulate matter exposure and response. Comparable *in vitro* biomarkers of risk profiles to those observed *in vivo* may be considered to substantiate *in vitro* testing and allow for high throughput and rapid reproducibility.

The current study aims to use proteomics to investigate effects of either TiO₂ or UFTiO₂ on the cell proteome of BEAS-2B differentiated at ALI and to identify early toxicity biomarkers of toxicity on repeat doses of particle exposure in rats.

6.2: Introduction

The Cosmetic Directive now rules that cosmetic testing on animals will be banned after 2013 (7th Amendment of the European Union Cosmetic Directive, 2003). This necessitates development of robust and valid *in vitro* models that represent physiological systems. By comparative analysis between these *in vitro* models and *in vivo* experiments, it is anticipated that common biomarkers of toxicity and disease states may be observed which may subsequently allow for early diagnosis of toxicity and disease from *in vitro* tests alone (Ocak *et al.*, 2009; Matt *et al.*, 2008), or allow exposure profiles to be identified.

Approaches in identification of biomarkers of exposure, response, or disease include genomics and proteomics. Genomics, the study of all the genes in an organism, is a powerful tool, although, mRNA expression and protein expression are not tightly related (Aldred *et al.*, 2004; Ocak *et al.*, 2009); indeed post-translational modifications (PTM), such as phosphorylation, which may act as on/off signals for protein functions are not identified in genomic analysis (Ocak *et al.*, 2009; Matt *et al.*, 2008; Zhou *et al.*, 2005). In contrast, proteomics allows for post-translational modifications to be identified (Zhou *et al.*, 2005 & Lim *et al.*, 2004) and was first described in the early 70's (Rabilloud *et al.*, 2010). Proteomics involves separation of proteins within a sample first by their iso-electric point (pI, the pH at which the proteins have no net charge) followed by separation based on their molecular weight (Matt *et al.*, 2008). The proteins are then visualised using protein stains and digested from the gel with site-directed proteases such as trypsin. Peptide digests are then analysed by mass spectrometry (MS).

Proteomic analysis of UFTiO₂-treated BEAS-2B has identified up-regulation inflammatory and ROS associated proteins including macrophage migration-inhibitory factor (Cha *et al.*, 2007), superoxide dismutase and peroxiredoxin-1 (Ge *et al.*, 2011) and proteins involved in mitochondrial dysfunction, ERK signalling, cell cycle and myc-mediated apoptosis signalling pathways (Ge *et al.*, 2011). However, in these

studies BEAS-2B were cultured under submerged conditions, proteomic analysis of TiO₂ treated BEAS-2B cultured at ALI has not been described previously.

The aim of this study is to identify early biomarkers of toxicity/exposure from model systems exposed to commercially relevant particles. Proteomic analysis was undertaken on lysates from BEAS-2B (cultured at ALI) exposed to both fine and UF-TiO₂ S2219200, S2218600 and S2429901, to identify possible biomarkers of epithelial damage after inhalation exposure. Proteomic analysis was also undertaken on plasmas from rats treated with a methyl vinyl ether/maleic anhydride copolymer (referred to as 020310), which is a water-soluble particle with an average molecular weight of 62,000Da or positive control (a copolymer of methyl methacrylate, ethyl methacrylate and butyl acrylate of a molecular weight of 700,000Da, which is not soluble in water, but can be suspended in aqueous solution), referred to as MM/EM/BA and negative control of saline. Rats were further separated into 9 or 22 week recovery groups for each treatment, whereby plasma samples were collected either 9 or 22 weeks after the last polymer treatment.

6.3: Methods

6.3.1: Endotoxin content by LAL assay.

Endotoxin content of particle stocks were determined using the QCL-1000[®] LAL assay as described in section 2.4.4.

6.3.2: TiO₂ depletion from TiO₂ -treated BEAS-2B cell lysates or BSA samples

PM in cell lysates following cell challenge with particles prevented subsequent proteomic analysis. To overcome this problem a depletion method was sought that would allow removal of particles from cell lysates without removal of protein. Extraction buffers containing the reducing agent dithiothreitol (DTT) (1mM) or DTT plus 1% (v/v) Tween-20 were added to lysates from particle- treated BEAS-2B, or to 5mg/ml BSA, and then samples were vortexed for 2 minutes. “No particle”-treatment served as a control. Lysates were then passed through Microcon[®] YM-100 100KDa cut off filters (Sigma; z648094, Poole, UK) as per manufacturer’s instructions at 14,000xg. Protein content of both <100KDa and > 100KDa fractions was determined using the bicinchoninic acid (BCA) method as detailed in section 6.3.6. To clear particles without filtration, lysates were either left to stand for 1 hour to sediment particles prior to centrifugation at 23800xg for 10 minutes at 15°C (Wang *et al.*, 2005) or centrifugation at 14,000xg for 30 minutes (Cha *et al.*, 2006). Protein concentrations of supernatants were subsequently determined using the BCA assay and proteomic analysis was undertaken.

6.3.3: Proteomic analysis

Cleared cell lysates from particle-treated cells, or un-cleared lysates from particle-treated cells (50µg) were lyophilised and re-suspended in 180µl rehydration buffer (6M urea, 2M thiourea, 2% (w/v) CHAPS, 2% (w/v) SB3-100, 40mM Tris HCl and bromophenol blue to colour) with 2.4µl DeStreak and 1µl ampholyte (biolytes3/10). The resuspended sample (180µl) was loaded in a well of the rehydration plate (Protean IEF, BioRad, Hertfordshire, UK) covered with Criterion IPG strip pH range 3-10,

overlaid with mineral oil and rehydrated overnight at 20°C. Solubilised proteins focused by isoelectric point onto Criterion IPG strip using a ramping program of 500V for 500Vh, 3500V for 3500Vh, 3500V for 90kVh in a Protean IEF Cell (BioRad, Hertfordshire, UK). Gels were then equilibrated for 20 minutes in 7ml equilibrium buffer (6M urea, 20% (v/v) glycerol, 2% (w/v) sodium dodecyl sulphate (SDS), 0.375M Tris-base pH8.8). Proteins were separated in a second dimension by molecular weight on 4-20% Tris-glycine gradient gels for 150 minutes at 90V in BioRad criterion cell tanks (BioRad, Hertfordshire, UK) with TGS running buffer (3.03g Tris HCl pH8.3, 14.4g glycine, 1g SDS). Proteins were detected using Flamingo™ fluorescent protein stain (Linear range of 0.5-100ng, BioRad, Hertfordshire, UK) for 5 hours. Gels were scanned on a Pharos FX™ Plus Molecular Imager (BioRad, Hertfordshire, UK). A thin layer of water was added to gels prior to scanning to allow for removal of dust from the gel surface. Up- or down-regulated protein spots (Significance by ANOVA <0.05 and statistical power >0.8) were identified.

6.3.4: Analysis of protein spots by Progenesis SameSpots

After scanning, analysis of protein spots was conducted using Progenesis SameSpots as follows. Gels are cropped so that an area containing all the proteins spots is collected. A reference image is then selected, the reference image is one where the spot profiles differ the least from all other gels. Damaged areas/saturated areas are then removed and spots are matched by the analysis software. After matching spots in damaged or saturated areas not previously removed can be excluded (Progenesis SameSpots removes spots which have a small spot area but high volume intensity (indicative of a speckle), these parameters can be edited). Spot volumes are then normalised to the reference gel and the user then defines the experimental design, after which, results and statistics for up- or down-regulated spots can be observed.

6.3.5: Polymer treatment of rats

Proteomic analysis was carried out on plasma from polymer treated rats, where polymer treatment was undertaken previously and reported by Carthew *et al.*, (2006). Briefly the 10 week old male Wistar rats were treated on 3 separate occasions (2 week intervals between treatments) with varying doses of polymer 020310, a copolymer of methyl vinyl ether and maleic anhydride (10 rats per group). The high dose group received a total of 12mg/kg polymer 020310 (individual doses of 4mg/kg), the intermediate dose group received a total of 1.2mg/kg polymer 020310 (3 individual doses of 0.4mg/kg) and the low dose group received a total of 0.3mg/kg polymer 02310 (3 individual doses of 0.1mg/kg). A co-polymer of methyl methacrylate/ ethyl methacrylate and butyl acrylate (MM/EM/BA) was used as a positive control (rats received a total dose of 12mg/kg, over 3 treatments with 2 week intervals) and a negative control group received saline. Treatment groups were further divided into 9 week recovery groups (plasma collected 9 weeks after final treatment) and 22 week recovery group (plasma collected 22 weeks after final treatments). All treatments were administered by intratracheal instillation via the oropharynx. Treatments were conducted by, Carthew *et al.*, (2006) and plasma samples were provided by Dr P Carthew (Unilever).

In order to remove the major plasma protein albumin and immunoglobulins from rat plasma samples provided by Carthew *et al.*, (2006), ammonium sulphate was added to plasma (0.277g/ml) and rotated at 4°C for 30 minutes followed by centrifugation at 11337xg for 15 minutes. The resulting pellet was re-dissolved with 3ml of 1mM potassium chloride with 1mM imidazole, pH7. The protein concentration of samples was then determined using the BCA protein assay. Equal concentrations of sample (5mg) were grouped according to treatment. Groups were numbered 1-10 blindly and group IDs were disclosed after spot analysis, Table 6.1. Albumin-depleted plasma-pools were desalted into PBS using 10ml disposable chromatography columns (BioRad, cat 732-2010). The BCA assay was performed (see section 6.3.6) on albumin-depleted desalted plasma-pools to determine final protein concentrations of the groups.

Table 6.1: Analysis design for rat plasma samples

Blinded group	Treatment group
Group 1	Negative control, 9 weeks
Group 2	Negative control, 22 weeks
Group 3	Low dose treatment, 9 weeks
Group 4	Low dose treatment, 22 weeks
Group 5	Mid dose, 9 weeks
Group 6	Mid dose, 22 weeks
Group 7	High dose, 9 weeks
Group 8	High dose, 22 weeks
Group 9	MM/EM/BA, 9 weeks
Group 10	MM/EM/BA, 22 weeks

6.3.6: BCA assay for protein determination.

Protein concentration of rat-plasma samples and cell lysates was determined using the bicinchoninic acid assay. The principle of the assay is as follows: Copper_(II) is dose-dependently reduced to copper_(I) by protein and bicinchoninic acid subsequently forms a purple product in the presence of copper_(I) which can be detected by adsorption at 570nm. Briefly, 10µl samples and standards (0-1mg/ml BSA diluted in distilled water) in a 96 well plate were incubated with 200µl/well working solution of 4% (v/v) copper(II) sulphate diluted 1:50 in bicinchoninic acid) for 30 minutes at 37°C. The plate was then left to equilibrate for 10 minutes at room temperature prior to measurement of absorbance at 570nm. Protein concentrations of samples were extrapolated from the standard curve using BSA as a standard (0-1mg/ml) and expressed as mg/ml.

6.3.7: Proteomic analysis of pooled plasma

Albumin-depleted pooled-plasmas (50µg) were concentrated to a pellet using an eppendorf concentrator plus (Jencons, VWR, West Sussex, UK) and proteomic analysis was undertaken as above

6.3.8: Protein digestion from gel pieces

Gel pieces were excised over a UV light box, removed to Protein LoBind eppendorf tubes (Sigma) and washed with 200µl distilled water for 30 seconds whilst vortexing. Gel pieces were destained twice with 200µl methanol:50mM NH₄HCO₃ (1:1 v/v) with vortexing for 1 minute, followed by dehydration for 5 minutes with 200µl acetonitrile (Fisher scientific, Loughborough, UK):NH₄HCO₃ (1:1 v/v). The supernatant was discarded and gel pieces further dehydrated with 100% acetonitrile for 30 seconds. Gel pieces were dried using an Eppendorf concentrator plus followed by reduction with 100µl 25mM DTT in 50mM NH₄HCO₃ at 56°C for 20 minutes. After incubation the supernatant was discarded and gel pieces were alkylated with 100µl 55mM iodoacetamide in 50mM NH₄HCO₃ at room temperature for 20 minutes in the dark, followed by 2 washes with 400µl distilled water. Gel piece were then dehydrated and dried as before. Peptides were digested from the gel pieces by incubation with 20µl 12ng/µl Trypsin Gold (Promega, Southampton, UK) in 0.01% ProteaseMAX™ Surfactant (Promega):50mM NH₄HCO₃ for 10 minutes. Samples were then overlaid with 30µl 0.01% ProteaseMAX™ Surfactant:50mM NH₄HCO₃ with gentle vortexing for 30 seconds followed by incubation at 50°C for 1 hour. Samples were centrifuged at 12,000xg for 10 seconds and the solution containing the peptide digests was removed to a fresh Protein LoBind eppendorf tube. Trypsin was inactivated by addition of 0.5% trifluoroacetic acid (Fisher scientific, Loughborough, UK). Samples were stored at -20°C until analysis by mass spectrometry.

6.3.9: Liquid chromatography mass spectrometry/mass spectrometry (LC-MS/MS) Experiment

The mass spectrometer used in this research was obtained from the *Birmingham Science City Translational Medicine: Experimental Medicine Network of Excellence* project, with support from Advantage West Midlands (AWM) and performed by Dr Cleidiane G Zampronio. UltiMate[®] 3000 high performance liquid chromatography (HPLC) series (Dionex, Sunnyvale, CA USA) was used for peptide concentration and separation. Samples were trapped on Precolumn Cartridge, Acclaim PepMap 100 C18, 5 μ m, 100A 300 μ m i.d. x 5mm (Dionex, Sunnyvale, CA USA) and separated in Nano Series[™] Standard Columns 75 μ m i.d. x 15 cm, packed with C18 PepMap100, 3 μ m, 100Å (Dionex, Sunnyvale, CA USA). The gradient used was from 3.2% to 44% solvent B (0.1% (v/v) formic acid in acetonitrile) for 30 min. Peptides were eluted directly (~ 300 nL min⁻¹) via a Triversa Nanomate nanospray source (Advion Biosciences, NY) into a LTQ Orbitrap Velos ETD mass spectrometer (ThermoFisher Scientific, Germany). The data-dependent scanning acquisition was controlled by Xcalibur 2.7 software. The mass spectrometer alternated between a full FT-MS scan (m/z 380 – 1600) and subsequent collision-induced dissociation (CID) MS/MS scans of the 20 most abundant ions. Survey scans were acquired in the Orbitrap with a resolution of 30,000 at m/z 400 and automatic gain control (AGC) 1x10⁶. Precursor ions were isolated and subjected to CID in the linear ion trap with AGC 1x10⁵. Collision activation for the experiment was performed in the linear trap using helium gas at normalized collision energy to precursor m/z of 35% and activation Q 0.25. The width of the precursor isolation window was 2 m/z and only multiply-charged precursor ions were selected for MS/MS.

The MS and MS/MS scans were searched against NCBI nr database using Mascot algorithm (Matrix Sciences). Variable modifications were deamidation (N and Q), oxidation (M) and phosphorylation (S, T and Y). The precursor mass tolerance was 5 ppm and the MS/MS mass tolerance was 0.8Da. Two missed cleavages were allowed and were accepted as a real hit protein provided at least two high confidence peptides were identified. Peptides with an Expectation value (E value) of greater than 0.001 were disregarded. Peptide sequences for each protein were searched through uniprot.org blast search to give additional scores and E values.

6.4: Results

6.4.1: Development of an optimal method of particle clearance from cell lysates.

During proteomic analysis of TiO₂-treated BEAS-2B lysates, electrical resistance occurred during the iso-electric focusing stage causing the gels to melt. In order to investigate whether the presence of particles was responsible for the electrical resistance, methods for total clearance of particles from cell lysates were developed.

To optimize the approach for removing particles from cell lysates without losing protein, BSA was used as a target for particles instead of cell lysates. BSA was treated with TiO₂ followed by treatment with the reducing agent DTT (1mM) and the detergent Tween-20 (1% v/v) to remove the bound protein from the particles. The BSA-particle solution was then passed through a 100KDa cut- off filter to remove particles from the solution. A BCA protein assay was conducted on the cleared samples (samples were diluted 1:10 as the detection limits of the BCA is 1mg/ml) in order to determine protein concentration. BSA (5mg/ml) that had not been treated or cleared through the 100kDa cut off filters was used as a control (Table 6.2).

Table 6.2 shows that protein was lost during filtration in the absence of particles, and this could not be fully recovered by addition of 1mM DTT with 1% (v/v) Tween-20. Protein loss was also observed with TiO₂ particle treatment, however, there was a similar protein loss observed with BSA alone, and again protein was not recovered with 1mM DTT plus 1% (v/v) Tween-20.

Table 6.2: Recovery of BSA after treatments with TiO₂, 1% Tween-20 and 1mM DTT and separation through 100kDa cut off filters. BSA (5mg/ml) was treated with either 1mM DTT and 1% (v/v) Tween-20, TiO₂ or 1mM DTT and 1% (v/v) Tween-20 and TiO₂ followed by filtration through 100KDa cut off filters at 14,000xg. Protein content of the filtrate (<100KDa fraction) was determined. Filtered BSA and un-filtered BSA serve as controls. Results are expressed as percent protein recovered. N=3, filtration = cleared through 100KDa cut off filter.

Treatment	Percent protein recovery
None	99.7 ± 0.36
Filtration	59.8 ± 0.43
1mM DTT + 1% Tween + filtration	67.68 ± 0.4
TiO ₂ + filtration	67.94 ± 0.91
TiO ₂ + 1mM DTT + 1% Tween + filtration	66.6 ± 0.85

Protein recovery after filtration was further investigated with lysates from control cells, TiO₂-treated cells or control cell lysates with TiO₂ added prior to filtration (Table 6.3). Protein loss was still evident after using the 100KDa cut off filters; however, there was no significant loss of protein due to particles.

Table 6.3: Protein recovery from <100KDa fraction of filtered cell lysates. BEAS-2B were treated with 100µg/ml TiO₂ for 24 hours (TiO₂ lysate) in airway epithelial cell medium or with airway epithelial cell medium alone (control lysate) at 37°C. Cells were then lysed with 1% Triton-X100 with protease inhibitor cocktail (1%). Lysates as collected or control lysate with addition of 100µg/ml TiO₂ were cleared through 100KDa cut off filter as per manufacturer's instructions. Protein content of <100KDa fraction was determined using BCA assay and percent protein recovery expressed as protein in <100KDa fraction relative to total concentration before filtration. N=2

Condition	Percent protein recovered
Control lysate	48.51 - 71.12
TiO ₂ lysate	47.35 – 54.18
TiO ₂ added to control lysates	52.29 – 56.97

6.4.2: 2-DE analysis following centrifugation for removal of TiO₂ resulted in areas of protein loss from gels.

As filtration methods for removal of particles from cell lysates results in protein loss, centrifugation methods of particle removal from lysates were investigated.

Initially, samples were allowed to stand for 1 hour at room temperature to sediment particles, then centrifuged for 10 minutes at 23800xg at 15°C. Protein recovery from this method was typical for BEAS-2B cell lysates (control lysate 0.530mg/ml, TiO₂-treated 0.411mg/ml) however, during the iso-electric focussing stage of proteomic analysis electrical resistance occurred again resulting in melting of the IPG-strips. Failure of focusing on any single strip e.g. lysates from TiO₂-treated cell, results in damage to all strips being focussed at the same time.

A second alternative centrifugation method for clearing particles from cell lysates was investigated. This method involved centrifugation at 14,000xg for 30 minutes. The protein yield was similar for both control (0.545mg/ml) and TiO₂-treated lysates (0.508mg/ml). During iso-electric focusing electrical resistance did not occur, however, there were some areas on the IPG strip (pH 3-10) where melting had occurred, as a consequence some areas of the 2D gels were protein free (Figure 6.1, boxed area). Since this method allowed iso-electric focusing to run without electrical resistance, it was adopted to permit proteomic analysis of lysates from particle-treated differentiated BEAS-2B.

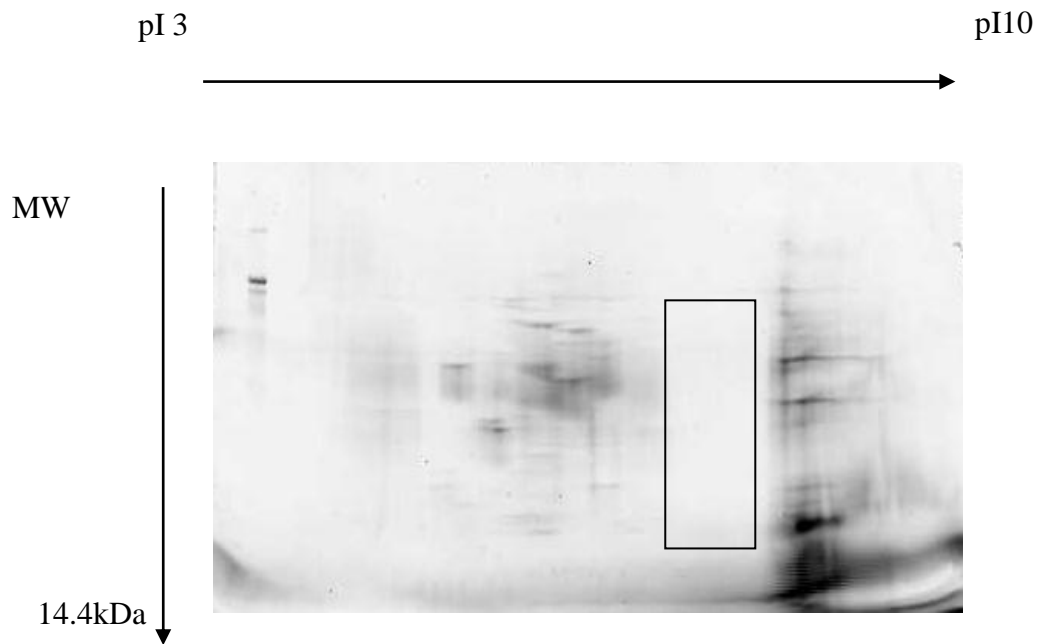


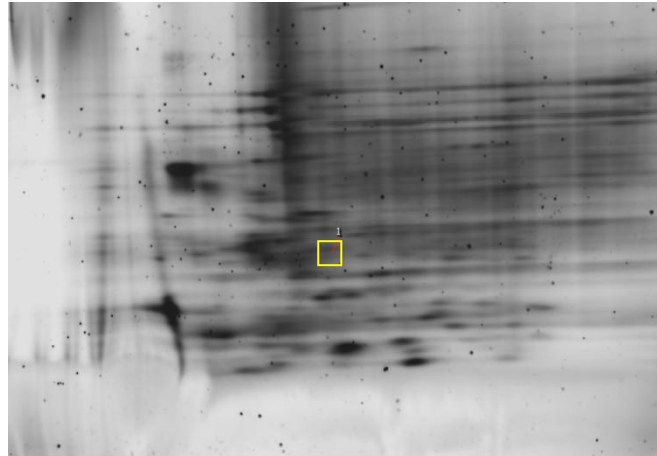
Figure 6.1: 2-DE analysis following centrifugation for removal of TiO₂ from cell lysates resulted in areas of protein loss from gels. BEAS-2B were cultured under submerged conditions at 1×10^5 cells/ well in a non-collagen-coated 24 well plate. Once confluent cells were treated with 100 μ g/ml TiO₂ in quiescent media, or quiescent media alone (not shown), for 24 hours at 37°C. Cells were then lysed with 1% (v/v) TritonX-100 with 1% (v/v) protease inhibitor cocktail. Lysates were cleared by centrifugation at 14000xg for 30 minutes; 50 μ g lysate was then rehydrated onto a 3-10pH range IPG strip overnight at 20°C. Samples were focused in a Protean IEF cell at 500V for 500Vh, 3500V for 3500Vh and finally 3500V for 90kVh. After focusing gels were equilibrated and focused in the 2nd dimension on 4-20% gradient Tris HCl gels at 90V for 150 minutes. Proteins were then fixed and stained with Flamingo™ protein stain overnight. Gels were scanned on a Pharos FX™ Plus Molecular Imager. n=1. The boxed area indicates an example of a protein-free area.

6.4.3: Proteomic analysis of lysates from TiO₂ and UFTiO₂-treated BEAS-2B results in poorly resolved gels.

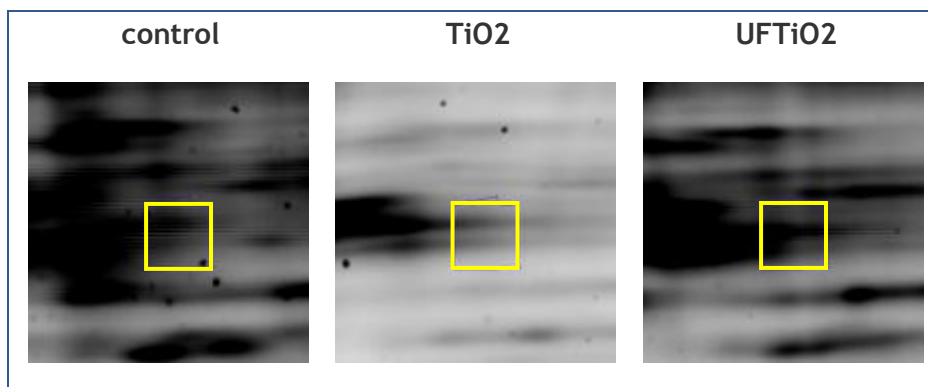
After a method of particle clearance from lysates that would allow for iso-electric focussing was obtained, cell lysates from TiO₂, UFTiO₂ or control-treated differentiated BEAS-2B were analysed using 2-D electrophoresis to investigate whether particle-treatment alters the cell proteome. IPG-strips with a narrower pH range (pH 4-7) were used to further improve resolution of proteins (Figure 6.2). Protein spots between treatments were then analysed for statistical significance using Progenesis Same Spots software.

Although iso-electric focussing occurred normally without electrical resistance separation of proteins was poor in the 1st dimension of electrophoresis as large streaks were evident across the gels (Figure 6.2A). Large areas of unresolved proteins were also evident (these areas were cropped from the gels during analysis). As protein resolution was poor analysis of the proteins with Progenesis Same Spots did not result in accurate matched protein spots between gels, and consequently spot matching was carried out manually. In total 35 spots were identified across the 3 groups (control, TiO₂ and UFTiO₂), however only 1 protein spot, spot 327, showed a statistically significant difference, ANOVA $p < 0.05$ and statistical power > 0.8 . (Figure 6.2A shows the spot position and expression profile from Progenesis SameSpots). The analysis of this spot (Figure 6.2B, outlined by the square) shows this spot to be poorly matched across treatment groups, since the gels were of poor quality regarding 1st dimension separation of the proteins, identification of the protein within this spot by mass spectrometry was not pursued.

A)



B)



C)

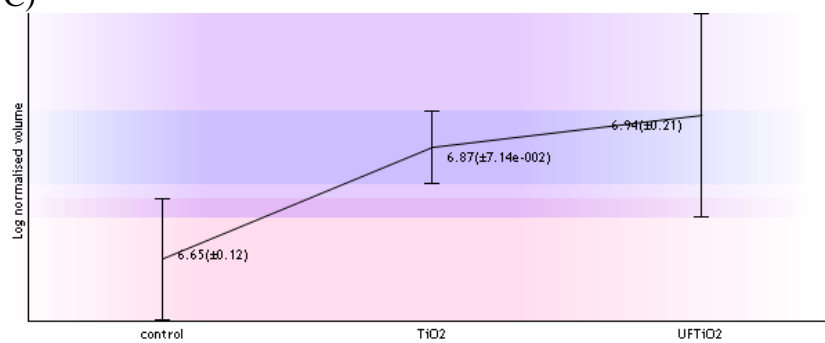
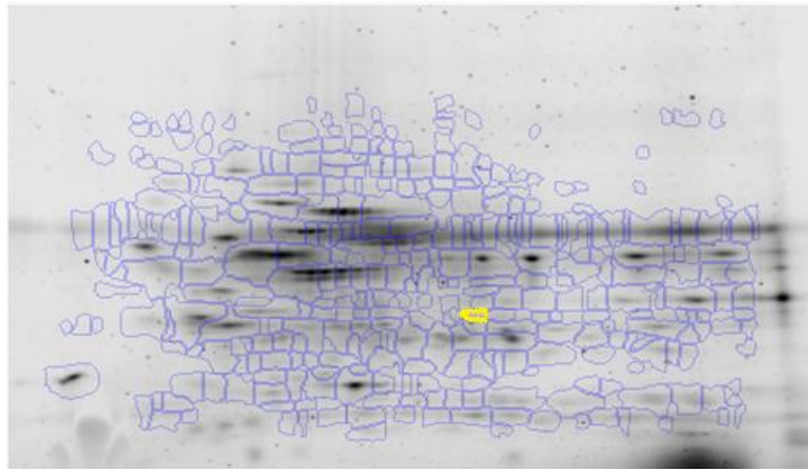


Figure 6.2: Proteomic analysis of lysates from TiO₂ and UFTiO₂-treated BEAS-2B resulted in poorly resolved gels. 2D gels of BEAS-2B on Transwell[®] inserts treated with 100µg/ml particles for 24 hours. Lysates were focused on IPG strips with a pH range of 4-7. Proteins were then resolved in the second dimension and stained with Flamingo[™] protein stain. Spots were manually matched across gels and analysed for statistically significant changes in expression using Progenesis Same Spots software. Significantly up- or down-regulated proteins (ANOVA $p < 0.05$ statistical power > 0.8) were identified. A) reference gel identifying significantly altered spots, (B) representative image of the significantly altered spot across treatment groups (C) graphical representation of normalised spot expression profile for the significantly altered spot. A is a representative gel from the control group, Lysates from 3 individual experiments were pooled and 2 gels were run per pool.

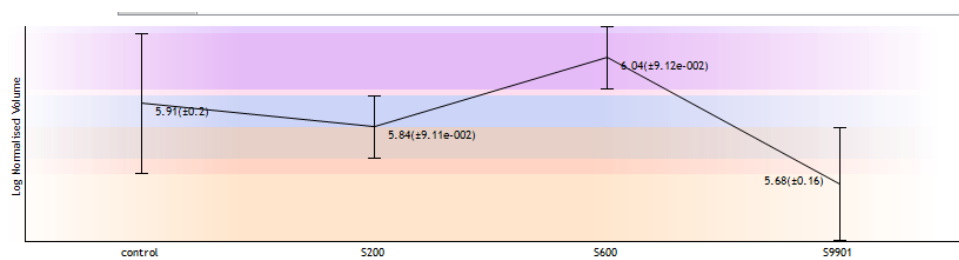
6.4.4: Proteomic analysis of particle-treated BEAS-2B cultured at ALI

Particles S2219200, S2218600 and S2429901 are non-toxic (as measured by CellTiter-Blue[®], (see chapter 2.2.6) to BEAS-2B at ALI. S2219200 and S2218600 are non-inflammatory to BEAS-2B whilst S2429901 induced IL-6 secretion from these cells. Proteomic analysis was undertaken on lysates from particle-treated BEAS-2B at ALI to determine any biomarkers of exposure or response. In total 337 confirmed protein spots were identified. Statistical analysis spot expression profiles for all particles and control determined that only spot 583 (Figure 6.3A, highlighted by a yellow border) was significantly altered between treatments. However, 3-dimensional representation of this spot shows it to be in an area poorly focused and is a “smear” rather than an individual protein spot (Figure 6.3C), protein identification of this spot was therefore not carried out.

A)



B)



C)

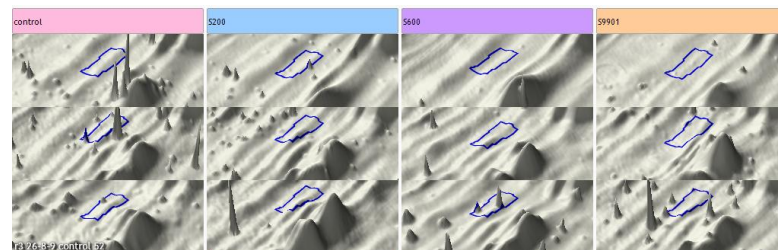


Figure 6.3: Proteomic analysis of particle-treated BEAS-2B cultured at ALI. 2D gels of BEAS-2B on Transwell® inserts treated with 100µg/ml particles for 24 hours. Lysates for each treatment were pooled and focused on IPG strips with a pH range of 4-7. Proteins were then focused in the second dimension and stained with Flamingo™ protein stain. Gels were analysed using Progenesis Same Spots software. Significantly up- or down-regulated proteins (ANOVA $P < 0.05$ statistical power > 0.8) were identified. A) reference gel showing all identified spots. The yellow border outlines spot 583. B) normalized expression profile of spot 583. C) three dimensional representation of spot 583 in all gels. Lysates from 3 individual experiments were pooled and three gels were run per pooled lysate.

6.4.5: 2-DE analysis of pooled plasmas identified a total of 80 spots with differential expression

In order to determine whether biomarkers of exposure could be determined from *in vivo* experiments, plasmas from rats exposed to polymer 020310 or MM/EM/BA (Carthew et al., 2006) were depleted of albumin and analysed by 2-DE. Despite albumin depletion of rat plasma samples, the 2D gels showed intense staining in areas with a pH and molecular weight consistent with albumin staining patterns. Mass spectrometry analysis confirmed this area as albumin. Progenesis SameSpots identified 362 spots in total across all 20 gels, 80 of which were confirmed as protein spots by visual inspection (Figure 6.4). Spot areas containing speckles, or spots in areas of protein streaks were excluded.

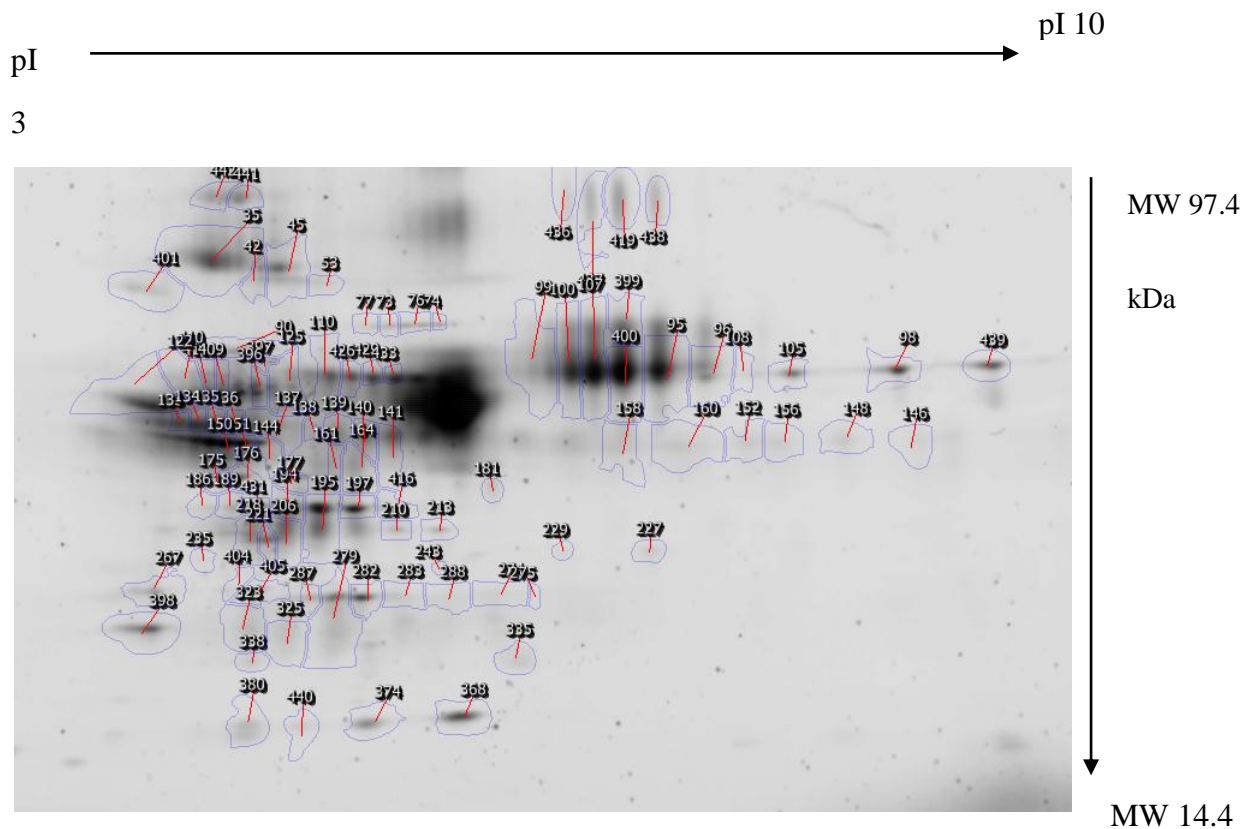


Figure 6.4: 2-DE analysis of pooled plasmas identified a total of 80 spots with differential expression. Plasma samples were grouped according to treatment and albumin depleted with ammonium sulphate, 50µg plasma was then rehydrated onto IPG strips (pH3-10) and rehydrated overnight. The protein-loaded rehydrated strips were focused by isoelectric point in a Protean IEF Cell (BioRad, Hertfordshire, UK). Gels were then equilibrated and proteins were separated by molecular weight on 4-20% Tris-glycine gradient gels for 150 minutes at 90V and detected using Flamingo™ fluorescent gel stain. Gels were scanned on a Pharos FX™ Plus Molecular Imager (BioRad, Hertfordshire, UK) and protein spots were analysed by Progenesis SameSpots software (Nonlinear Dynamics, Newcastle upon Tyne, UK). The large dark area in the centre of the gel has a staining pattern consistent with albumin staining patterns (confirmed by LC-MS/MS) and was therefore ignored during analysis.

6.4.6: Analysis of protein spots from plasmas of rats in polymer treatment groups

Analysis was undertaken on the plasma samples from polymer 020310, MM/EM/BA or saline treated rats between treatment groups by time and dose of polymer exposure. All treatments were analysed against experiment 1, the negative control at 9 weeks; and each treatment group at 22 weeks recovery, was compared against the corresponding negative control at 22 weeks. All treatments at 9 weeks were compared to the corresponding treatment at 22 weeks. Table 6.4 details those spots that were identified as both significant in volume by ANOVA, and for further confidence in results, spots that also had a statistical power analysis of >0.8 . Analysis of experiment 1 (negative control, 9 week recovery) versus 5 (mid dose polymer 020310 treatment, 9 week recovery) did not show any significantly altered spots.

Table 6.4: Polymer 020310 treatment-sensitive spots from plasma that showed a significant expression change by ANOVA (P<0.05) and statistical power analysis (>0.8). Plasma samples were grouped, albumin-depleted 50µg plasma and focused by 2-DE. Proteins were detected using Flamingo™ fluorescent gel stain. Gels were scanned on a Pharos FX™ Plus Molecular Imager (BioRad, Hertfordshire, UK) and protein spots were analysed by Progenesis SameSpots software (Nonlinear Dynamics, Newcastle upon Tyne, UK). Significantly up- or down-regulated spots were identified using ANOVA (p<0.05) and with a statistical power of >0.8 (high statistical power). Up-regulated spots are in bold font, down-regulated spots are in normal font. The fold change in protein expression for each spot is in brackets.

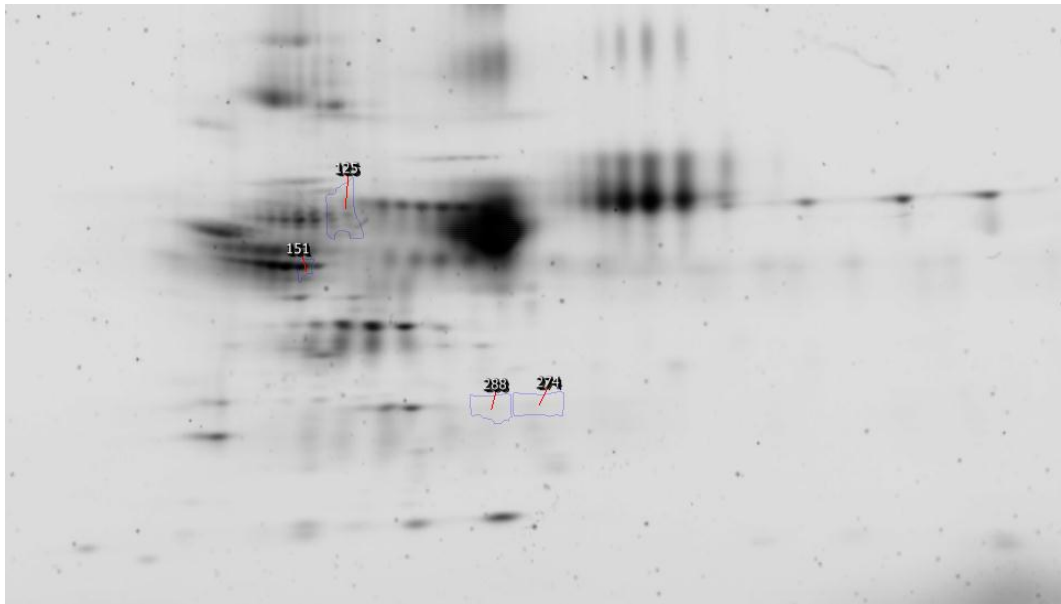
Experiment	ANOVA p<0.05, plus statistical power>0.8
Negative control 9 week recovery versus negative control 22 week recovery	323 (1.2), 275 (1.1) , 416 (1.3)
Negative control 9 week recovery versus low dose polymer 9 week recovery	323 (1.4)
Negative control 9 week recovery versus low dose polymer 22 week recovery	275 (2.6), 186 (1.4)
Negative control 9 week recovery versus mid dose polymer 22 week recovery	181 (2.1), 275 (1.3)
Negative control 9 week recovery versus high dose polymer 9 week recovery	156 (2.3)
Negative control 9 week recovery versus high dose polymer 22 week recovery	243 (3.3)
Negative control 9 week recovery versus MM/EM/BA 9 week recovery	275 (2.7) , 368 (1.3), 274 (3.3), 156 (1.9)
Negative control 9 week recovery versus MM/EM/BA 22 week recovery	416 (1.4)
Negative control 22 week recovery versus MM/EM/BA 22 week recovery	125 (1.5), 426 (1.9)
High dose polymer 9 week recovery versus high dose polymer 22 week recovery	243 (4.8), 74 (1.4)
MM/EM/BA 9 week recovery versus MM/EM/BA 22 week recovery	194 (1.4), 134 (1.8), 151 (1.9), 426 (1.4)

6.4.7: Differentially expressed protein spots in positive control MM/EM/BA-treated animals compared to negative control animals

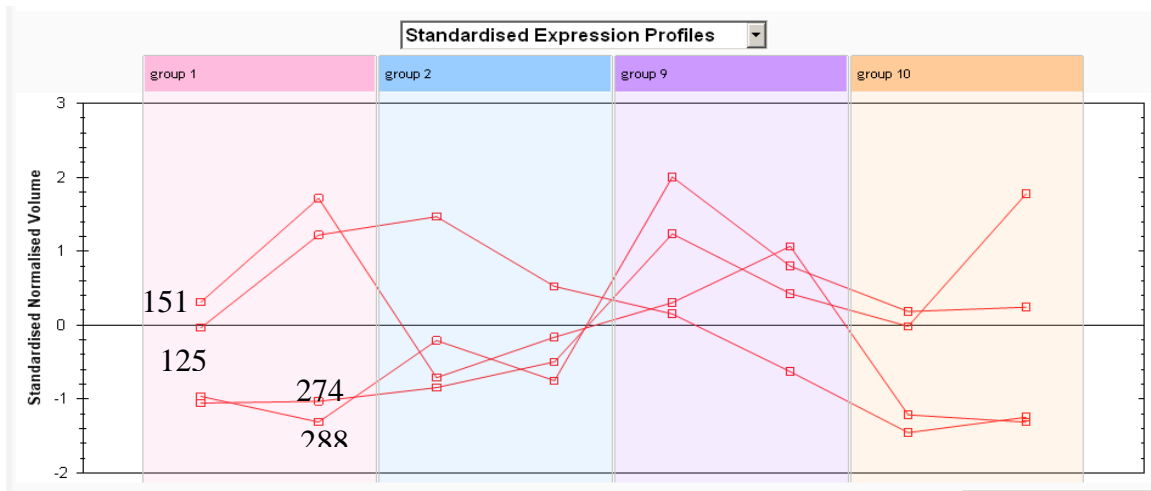
Analysis of treatment groups allows dose-response or time-related effects to be investigated. Progenesis SameSpots performs this analysis by PCA and results are presented as the log normalised volumes for significantly altered spots across various treatment groups, and shows the volume of spot obtained from each of the duplicate gels (samples were pooled and then 2 gels were run from the pool) for each treatment. In this view, gel outliers (when one of the replica gels is a poor match for the rest of the gels within a given treatment group) and expression levels of all the spots across the experiment can be examined.

PCA analysis was undertaken on the plasma protein spots from negative controls and MM/EM/BA-treated animals in order to investigate the effects of polymer treatment on the plasma proteome. In negative control versus MM/EM/BA analysis, a total of 4 protein spots were identified as being significantly altered in volume (spots 288, 151, 274 and 125). Spot 151 expression is high in both negative control and MM/EM/BA-treated animals at 9 weeks (groups 1 and 9 respectively) with a 2 fold lower expression in negative controls and MM/EM/BA-treated animals at 22 weeks (groups 2 and 10, Figure 6.5). Spots 274 (2.4 fold expression change) and 288 (3fold expression change) both show increased expression with MM/EM/BA positive control treatment regardless of recovery time (Figure 6.5), whilst spot 125 (1.5 fold expression change) shows decreased expression with polymer at 9 and 22 weeks after treatment (Figure 6.5).

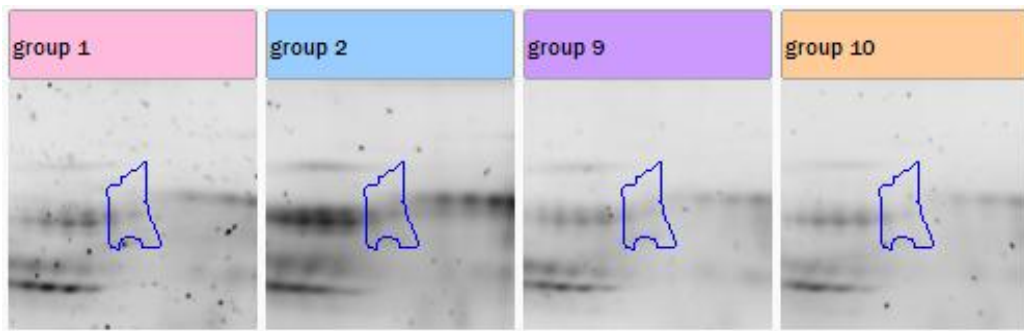
A)



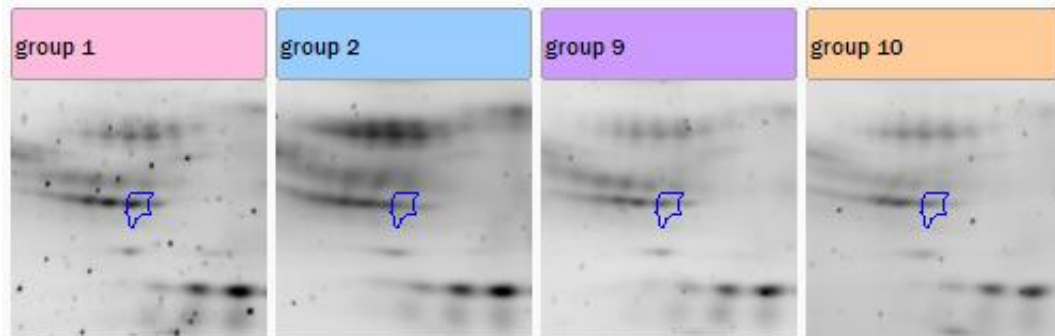
B)



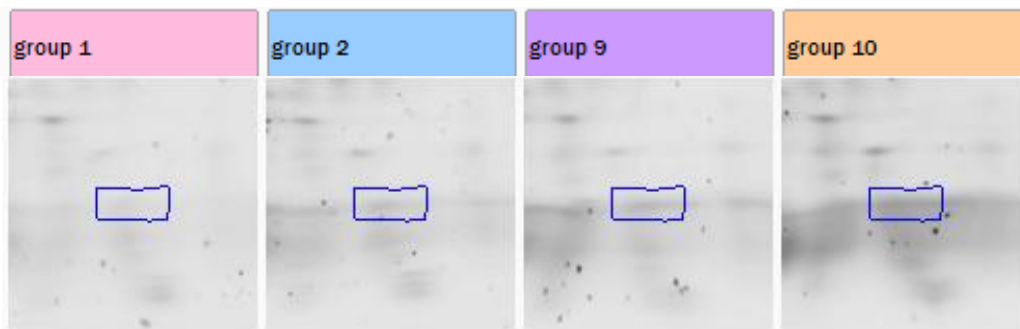
C)



D)



E)



F)

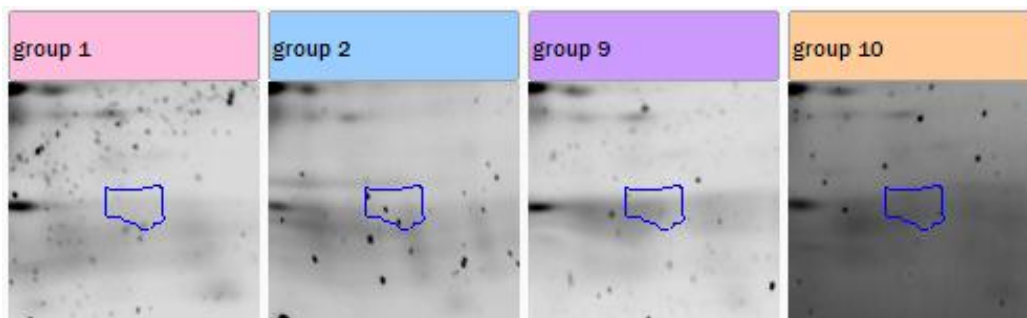


Figure 6.5: Differentially expressed protein spots in positive control MM/EM/BA-treated animals compared to negative control animals. Progenesis SameSpots group analysis of albumin-depleted pooled-plasma from rats 9 and 22 weeks post-lung instillation with negative control or MM/EM/BA. A) reference gel is shown which identifies the position of significantly altered spots B) graphical representation of log normalised volumes for each spot. C) representative image of spot 125 across treatments, D) representative image of spot 151 across treatments. E) representative image of spot 274 across treatments. F) representative image of spot 288 across treatments. Group 1 is negative control at 9 week recovery, group 2 is negative control at 22 weeks recovery, group 9 is MM/EM/BA 9 weeks recovery, group 10 is MM/EM/BA at 22 weeks recovery.

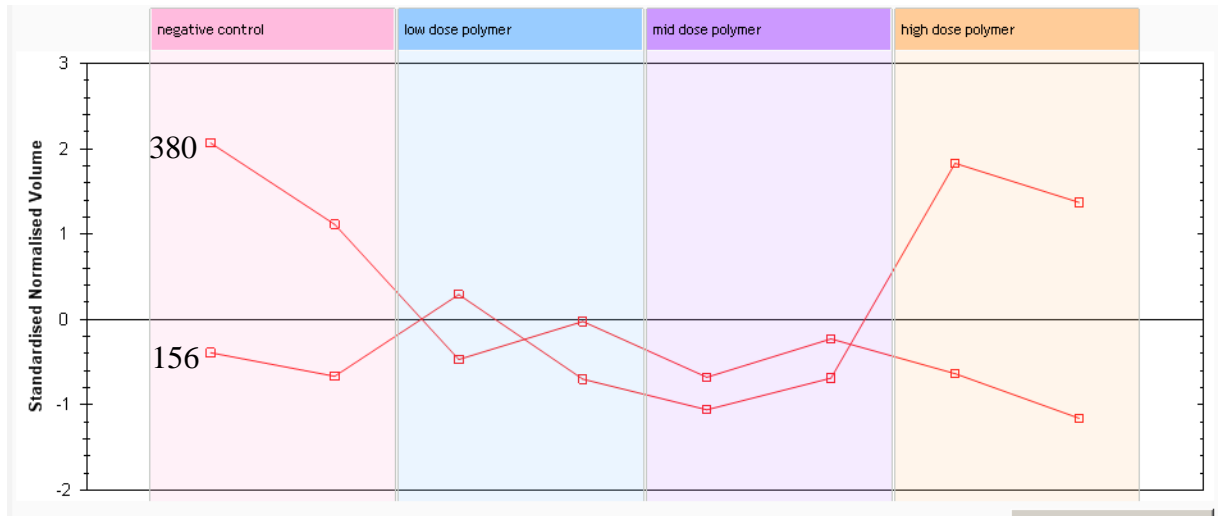
6.4.8: Effect of polymer 020310-dose on the rat plasma proteome following 9 weeks recovery or 22 weeks recovery

In order to investigate whether dose-response effects on the rat plasma proteome are observed following 020310 polymer treatment, independent group analyses of spot volume were undertaken on all 2D gels from rats receiving low, mid and high polymer 020310 doses compared to negative control at 9 weeks recovery; and 22 weeks recovery.

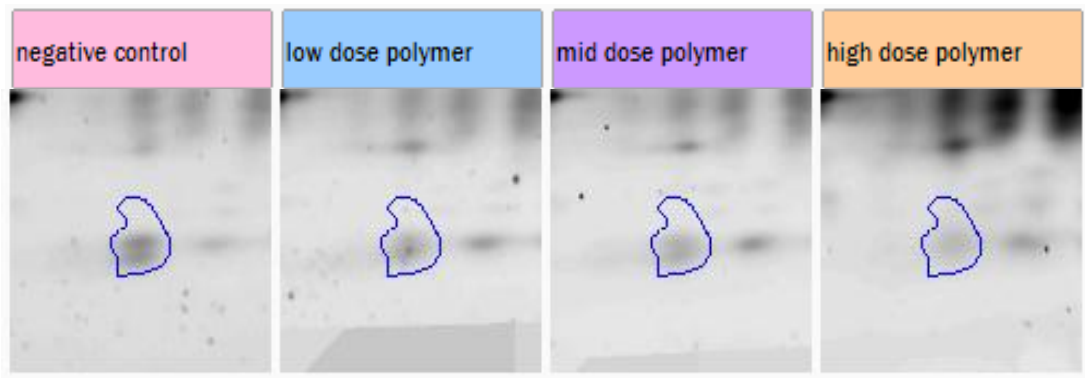
At 9 weeks recovery two proteins spots were identified as being significantly altered in volume with polymer 020310 treatment (spots 156 and 380, Figure 6.6A). Expression of protein 380 (3.8 fold expression change) was decreased in a dose-dependent manner with polymer 020310 treatment (Figure 6.6A). Expression of protein spot 156 (2.9 fold expression change) was increased in high dose polymer 020310 treatment compared to negative control, however, the response did not show a trend towards a dose-dependent increase (Figure 6.6A).

At 22 weeks recovery, a single protein spot showed significant alteration in volume with polymer 020310-treatment (Figure 6.6B). Spot 151 (1.8 fold expression change) showed increased expression in low-dose polymer 02031-treatment compared to negative control, expression then decreased to below negative control levels for high-dose polymer treatment (Figure 6.6B).

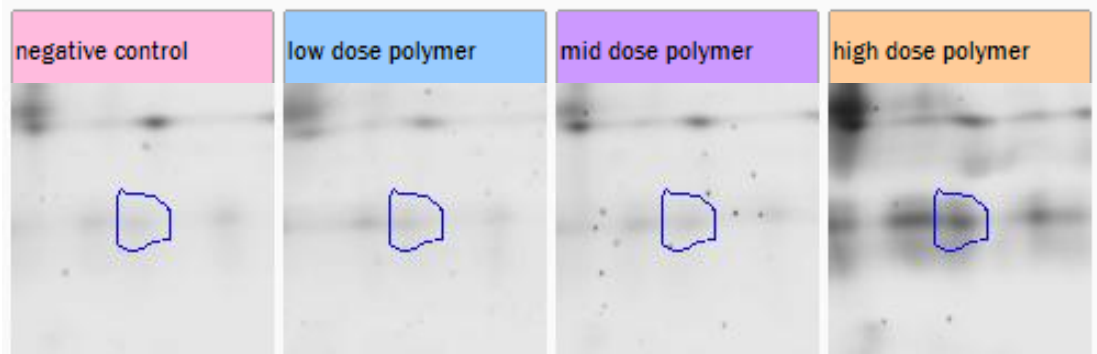
A)



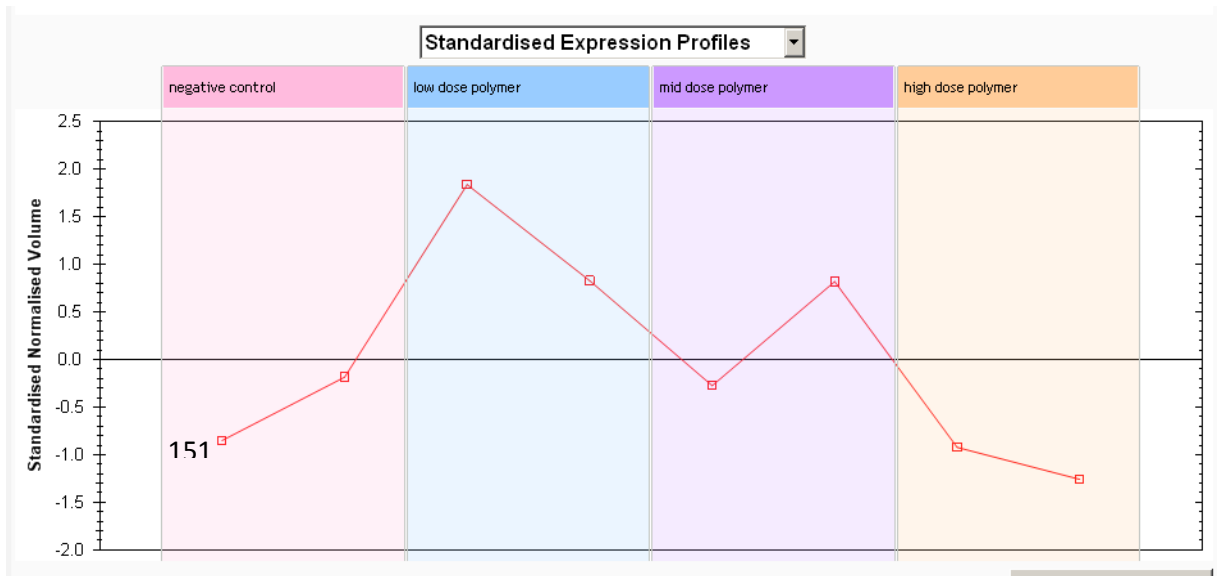
B)



C)



D)



E)

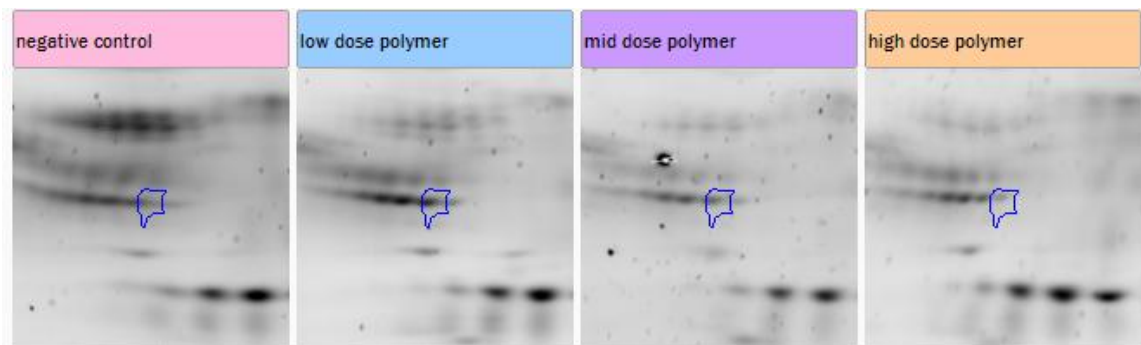


Figure 6.6: Effect of polymer 020310-dose on the rat plasma proteome following 9 weeks recovery (A) or 22 weeks recovery (B) after lung instillation. PCA analysis was undertaken on albumin depleted pooled-plasma from rats treated with negative control or increasing doses of 020310 polymer. (A) Spot volume profiles for those plasma protein spots showing dose-dependent effect of polymer 020310 treatment at 9 weeks recovery, B) representative image of spot 380, C) representative image of spot 156. D) spot volume profile for spot 151, E) representative image of spot 151.

6.4.9: MS/MS identification of significantly altered spots from polymer-treated rats

As many of the spots that were identified by PCA as being significantly altered in response to polymer are low abundant spots, two test spots were selected for mass spectrometry analysis to test the sensitivity of peptide detection from tryptic digests. The non-significantly altered spot, spot 45 (Figure 6.7, arrow head) was chosen as a spot with high abundance and the significantly altered spot, spot 274 (Figure 6.7, arrow) was chosen as a spot with low abundance. Spot 45 was identified as ceruloplasmin by mass spectrometry whilst spot 274 was unidentified. Due to lack of identification of low abundant spots, only spots with a similar abundance to spot 45 (426, 125, 134, 151 and 368) were selected for analysis by mass spectrometry. Tables 6.5-9 show the proteins identified for these spots by MS/MS.

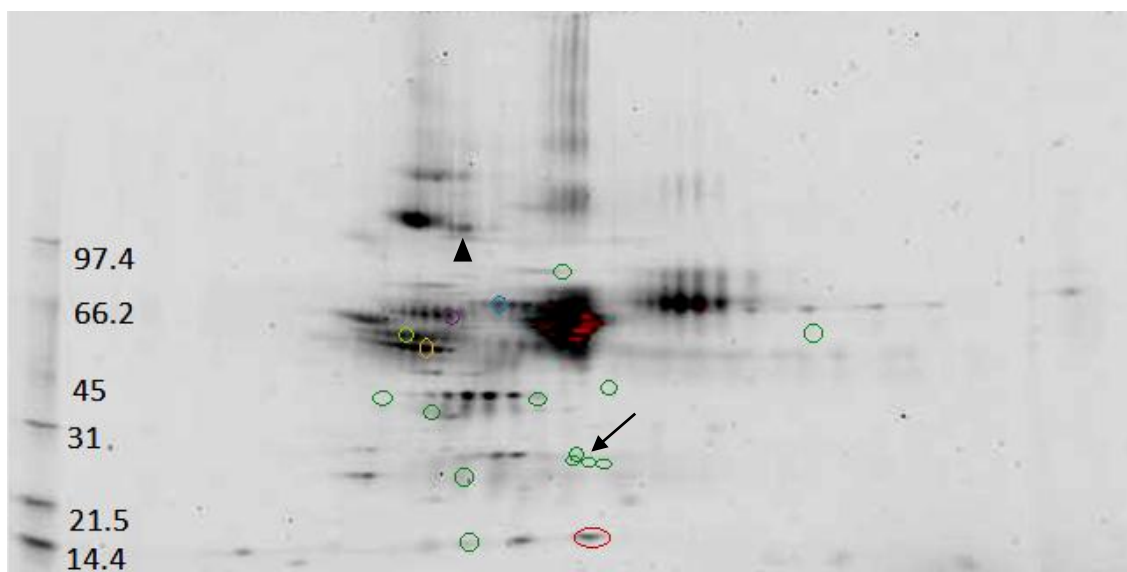


Figure 6.7: MS/MS identification of significantly altered spots from polymer-treated rats. Reference gel showing significantly altered spots detected by Progenesis Same Spots analysis of albumin-depleted pooled-plasma from rats. Spots from all sets of analysis are depicted. The blue circle borders spot 426, the yellow circle borders spot 134, the orange circle borders spot 151, the purple circle borders spot 125 the red circle borders spot 368. All other significantly altered spots are highlighted with a green circle. The arrowhead highlights spot 45 and arrow highlights spot 274.

Table 6.5: Protein identifications for Spot 134. Protein identifications for Spot 134 which showed a 1.8 fold decrease in expression in positive control at 22 weeks recovery compared to positive control 9 weeks recovery. E-Value is statistical representation of the sequence coverage of blast search to identified protein. The score is an indication of the sequence similarity of the blast search and the identified protein.

Accession	Name	Function	MW (kDa)	Length	Score	E Value
P24090	Alpha-2-HS-glycoprotein	Inhibits insulin receptor tyrosine kinase, and insulin stimulated receptor auto-phosphorylation	38	352	126	6×10^{-7}
P05544	Serine protease inhibitor	Inhibits serine proteases	68.2	413	175	3×10^{-13}
Q5PQU1	Kininogen 1	Thiol protease inhibitor	47.7	430	135	1×10^{-8}
P14046	Alpha-1-inhibitor 3	Wide spectrum protease inhibitor	163	1477	148	3×10^{-8}
P17475	Alpha-1-antitrypsin precursor	Inhibits serine proteases, primary target is elastase	45.8	411	205	9×10^{-15}
P09006	Serine peptidase inhibitor A3N	Inhibits serine proteases	45.5	418	134	1×10^{-6}
P01015	Angiotensinogen	Inhibits serine proteases	51.9	477	91	7×10^{-3}
P97569	Kallistatin	Inhibits serine type endopeptidases	48.3	423	129	5×10^{-6}
Q62930	Complement component C9	Complement cascade	62.2	554	139	4×10^{-7}
Q5EBC0	Inter alpha-trypsin inhibitor CRA_B	Inhibits serine type endopeptidases	78.4	933	85	7×10^{-2}

Table 6.6: Protein identification for spot 125. Spot 125 showed a 1.5 fold decrease in expression in positive control 9 and 22 weeks recovery compared to negative control 9 and 22 weeks recovery. E-Value is statistical representation of the sequence coverage of blast search to identified protein. The score is an indication of the sequence similarity of the blast search and the identified protein.

Accession	Name	Function	MW (kDa)	length	Score	E Value
Q5BJP7	AFM protein		52.6	464	105	3×10^{-4}
Q63041	Alpha-1-macroglobulin	Inhibits all classes of proteinases	167	1500	85	7×10^{-2}
Q64268	Heparin cofactor 2	Thrombin inhibitor (serpin d1)	54.5	479	194	9×10^{-16}
P14046	Alpha-1-inhibitor 3	Wide spectrum protease inhibitor	163.7	1477	288	2×10^{-24}
P17475	Alpha-1-antitrypsin precursor	Inhibits serine proteases, primary target is elastase	45.8	411	145	2×10^{-9}
Q62930	Complement component C9	Complement cascade	62.5	554	108	1×10^{-3}
Q5EBC0	Inter alpha-trypsin inhibitor CRA_B	Inhibits serine type endopeptidases	78.4	933	106	1×10^{-4}
P01048	T Kininogen-1	Inhibitor of thiol proteases	47.7	430	122	7×10^{-7}
P01026	Complement component C3	Complement cascade	186.2	1663	94	5×10^{-3}
P20059	Hemopexin precursor	Iron transport	51.3	460	110	5×10^{-6}
Q99PS8	Histidine rich glycoprotein	Cysteine/thiol protease inhibitor	59	525	122	1×10^{-6}

Table 6.7: Protein identification for Spot 426: Spot 426 showed a 1.9 fold decrease in expression in positive control 22 weeks recovery compared to negative control 22 weeks recovery and positive control 9 weeks recovery. E-Value is statistical representation of the sequence coverage of blast search to identified protein. The score is an indication of the sequence similarity of the blast search and the identified protein.

Accession	Name	Function	MW (kDa)	Length	Score	E Value
Q6IE52	Murinoglobulin 2	Serine type endopeptidase (serpin)	161.5	148	176	2×10^{-11}
Q7TMC7	Ab2-417	Iron binding protein Acute phase response	107.3	979	91	1.2×10^{-2}
P04276	Vitamin D binding protein	Associates with B&T lymphocytes	53.5	476	96	4×10^{-3}
P01026	Complement component C3	Complement cascade	186.2	1663	116	2×10^{-4}
P20059	Hemopexin precursor	Iron transport	51.3	460	113	1×10^{-5}
Q99PS8	Histidine rich glycoprotein	Cysteine/thiol protease inhibitor	59	525	122	1×10^{-3}
P17475	Alpha-1-antitrypsin precursor	Inhibits serine proteases, primary target is elastase	45.8	411	109	9×10^{-5}
P02767	Transferrin chain A	Thyroid hormone binding protein	15.72	147	187	3×10^{-15}

Table 6.8: Protein identification for spot 368. Spot 368 showed a 1.3 fold decrease in expression in positive control 9 weeks recovery compared to negative control 9 weeks recovery. E-Value is statistical representation of the sequence coverage of blast search to identified protein. The score is an indication of the sequence similarity of the blast search and the identified protein.

Accession	Name	Function	MW (kDa)	Length	Score	E Value
Q4QQR7	DSP	Wound healing	69.75	635	83	8.5×10^{-2}
P01835	Ig kappa chain C	Antigen binding	11.6	106	82	0.12
Q6POK8	Junction Plakoglobin	Cell-cell adhesion	81.8	745	127	5×10^{-7}
P23764	Glutathione peroxidase 3	Protects against oxidative damage	25.4	222	105	2×10^{-4}
P17475	Alpha-1-antitrypsin precursor	Inhibits serine proteases, primary target is elastase	45.8	411	109	8×10^{-5}
P02767	Transythyretin	Thyroid hormone binding protein	15.72	147	190	5×10^{-15}

Table 6.9: Protein identification of spot 151: Spot 151 showed a 1.9fold decrease in expression in positive control 22 weeks recovery compared to positive control 9 week recovery, and PCA group analysis for all doses of 010310. E-Value is statistical representation of the sequence coverage of blast search to identified protein. The score is an indication of the sequence similarity of the blast search and the identified protein.

Accession	Name	Function	MW (kDa)	Length	Score	E Value
P02651	Apolipoprotein A IV	Lipid transport	44.4	391	298	1×10^{-25}
P05545	Serine protease inhibitor A3K	Inhibits serine proteases	45.5	416	121	1×10^{-6}
Q5M7T5	Serine peptidase inhibitor	Inhibits serine proteases	49.1	465	144	3×10^{-9}
Q6MG90	Complement C4	Complement cascade Endopeptidase inhibitor	192	1737	118	3×10^{-9}
Q6IRK9	Plasma glutamate carboxy peptidase	Hydrolysis of circulating peptides	52	472	104	3×10^{-4}
P17475	Alpha-1-antitrypsin precursor	Serine protease inhibitor, primary target elastase	45.8	411	118	8×10^{-3}
P01048	T Kininogen	Thiol protease inhibitor	47.7	430	154	7×10^{-9}
P01046	Alpha-1-inhibitor 3	Wide spectrum protease inhibitor	78.8	1477	258	6×10^{-21}
P09006	Serine protease inhibitor	Serine protease inhibitor	45.5	418	99	7×10^{-4}
Q5EBC0	Inter alpha-trypsin inhibitor CRA_b	Serine type endopeptidase inhibitor	78.4	933	140	4×10^{-9}

Q62930	Complement component C9	Complement cascade	62.2	567	158	2×10^{-11}
P01015	Angiotensinogen	Serine protease inhibitor	51.9	477	89	2.3×10^{-2}
P01026	Complement component C3	Complement cascade	186.3	1663	104	3×10^{-4}

6.5: Discussion

Proteomics, the study of all the proteins within a cell, tissue or physiological fluid at a particular time, allows for analysis of expression changes, such as up- or down-regulation and posttranslational modifications of proteins, which cannot be identified with other approaches such as genomics. As proteomics allows for global protein changes within a proteome to be observed it has potential to be a powerful tool in identification of early biomarkers of disease. In the current study proteomic analysis was undertaken on; TiO₂, UFTiO₂, S2219200, S2218600, S2429901 or control treated BEAS-2B cultured at ALI. Proteomics was also undertaken on plasma from 10 week old male Wistar rats that had polymer 020310, MM/EM/BA positive control or saline as a negative control instilled intratracheally into the lungs, via the oropharynx. Recovery periods of either 9 or 22 weeks followed the final treatment.

A previous proteomic study on submerged cultures of BEAS-2B treated with TiO₂, has shown the pro-inflammatory cytokine macrophage migration-inhibitory factor (MIF) to be up-regulated (Cha *et al.*, 2007) indicating the inflammatory potential of TiO₂ to the airways epithelium. Proteomic analysis on BEAS-2B cultured at ALI (where the morphology of BEAS-2B mimics the airway epithelium *in vivo* more closely than submerged cultures) was undertaken to investigate global protein changes in response to both UFTiO₂ and TiO₂. High electrical resistance, resulting in gel melting, was observed during the iso-electric focussing stage of proteomic analysis. Filtration was undertaken to remove particles from lysates in a bid to prevent electrical resistance, however, during optimisation, protein loss was observed which was not recovered by inclusion of detergent and reducing agent DTT. Wang *et al.*, (2005) employed a proteomic approach of analysis after diesel exhaust particle (DEP) challenge of BEAS-2B cells whereby lysates were centrifuged at 23,800xg for 8 minutes to remove particles. Centrifugation of lysates from submerged BEAS-2B treated with TiO₂ with this method failed to remove particles from lysates and electrical resistance was still a problem resulting in occurrence of gel melting.

Adoption of the centrifugation method of Cha *et al.*, (2006) allowed the proteomic procedure to be completed, with evidence of melting (areas where there appeared to be loss of the the gel on the IPG strip), spots were visible on the gels. To improve spot resolution particle-cleared samples were analysed using a narrower pH range. Although spots were evident on gels, there were areas where the strips had melted and the replication of gels was poor making matching of the gels with Progenesis Same Spots software difficult. Indeed, only 1 spot was identified with statistically significant differences between treatment groups, the 3-dimensional analysis of the spot shows that the reproducibility is poor between the gels. By eye, the spot does not appear to be the same in each gel, indicating poor matching. Due to this poor reproducibility and the electrical resistance issue, caution is needed in the analysis of this result and protein identification of this spot was not pursued.

Cha *et al.*, (2006) observed that 20 protein spots were up- or down-regulated by more than 2-fold between control and TiO₂ treated groups. These findings were not replicated here, possibly because Cha *et al.*, (2006) used 1mg of protein for 2DE whilst in this thesis only 50µg of protein was used. It is possible that by using an increased concentration of protein, the loss observed here may be overcome, however Transwell[®] inserts do not allow for large scale cell culture so it would be difficult to obtain 1mg of protein per sample (a typical protein yield for a Transwell[®] insert with BEAS-2B culture conditions outlined in 2.2.1.1 is 0.08mg/well). Further, Cha *et al.*, (2006) used the rutile form of TiO₂ in their study, whilst in this thesis, the TiO₂ used is in the anatase form. Anatase TiO₂ is not as stable as the rutile form and has more free flowing electrons (Murugessan *et al.*, 2007; Sotter *et al.*, 2007) which may also lend explanation as to why electrical resistance impeded protein separation and resolution here.

S2219200 and S2218600 are non-cytotoxic and non-inflammatory to BEAS-2B cultured at ALI. S2429901 is also non-cytotoxic to BEAS-2B at ALI, but did induce increased IL-6 release indicating that this particle is inflammatory to BEAS-2B. Other inflammatory proteins may therefore show expression changes in S2429901 treated BEAS-2B. Proteomic analysis of lysates from these S2219200, S2218600, S2429901 or control cells was undertaken and revealed 1 significantly altered spot in the proteome.

However, this spot was in an area containing protein streaking and poor resolution and was therefore deemed a false positive. Triplicate gels of each particle treatment (containing pooled lysate from 3 individual experiments) were run, however as poor protein resolution was observed in some areas of the gels. Increasing the number of replicates would increase the confidence in results and may identify additional protein spots with expression changes between treatments and control

S2429901 increased the IL-6 secretory response in BEAS-2B, however, no change in the cell proteome was observed. Cytokines are rarely detected in 2-DE proteomic analysis due to their low abundance (Grant *et al.*, 2011). Supernatants and lysates were collected after 24 hour particle exposure, however, increased IL-6 secretion from airway epithelial cells can be observed as early as 2 hour post treatment (Carter *et al.*, 1997). Carter *et al.*, 1997 report that 2 hour challenge with 50µg ROFA induced IL-6 secretion significantly from submerged cultures of NHBE cells. Investigation into the effect of S2429901 on the BEAS-2B proteome after a shorter incubation may identify biomarkers on inflammation.

Histopathological and transcriptomic analyses of polymer 020310 and MM/EM/BA treated rats were undertaken by Carthew *et al.*, 2006 and plasma proteomic analysis was undertaken here. Polymer treatments were first compared against negative control at 9 weeks recovery (experiment 1) independently, to investigate the effect of individual treatments on the rat plasma proteome. Several proteins were significantly altered by particle treatment compared to negative control, after 9 weeks recovery. A total of 5 protein spots were down-regulated after polymer treatment compared with the negative control, after 9 weeks recovery post- polymer instillation (spots; 323, 181, 243, 368 and 416) with a range in fold expression change of 1.3-3.3. Four spots which showed a statistically significant up-regulation in treatment compared to negative control, 9 weeks recovery (spots; 275, 186, 156, and 274) with a range in fold expression change of 1.1-2.7). Spots 125 (1.5 fold change) and 426 (1.9 fold change) were down-regulated in MM/EM/BA treated animals at 22 weeks compared to negative control at 22 weeks.

To assess the effect of recovery time on rat plasma-proteome after various treatments plasma obtained at 9 week recovery were compared to 22 week recovery, i.e. are any proteins indicative of chronic effect of exposure up/down-regulated at 22 weeks recovery compared to 9 week recovery. As expected, the MM/EM/BA had the greatest effect on the plasma-proteome with 4 proteins being significantly altered (spots; 194, 134, 151 and 426). These spots were all down regulated (with a range of expression of 1.4-1.9 fold) in 9 weeks recovery compared to 22 weeks recovery. Carthew *et al* (2006) noted several mRNA species showed increased expression 9 weeks following particle 020310 exposure, but appeared to be switched off by 22 weeks and these findings are consistent with observations reported here.

A limitation of the current study is that many of the spots identified above as potential biomarkers of polymer 020310 or MM/EM/BA inhalation are low abundant proteins and below the level of detection by mass spectrometry after 50µg total protein loading. Flamingo™ fluorescent protein stain was used to visualise protein spots on the 2D-gels, and has a linear detection range of 0.5-1000ng. LTQ-orbitrap mass spectrometers have a sensitivity of femtomolar (Yates *et al.*, 2009), so the low abundant proteins should be detected by ms/ms analysis, indicating that the failure to detect protein spots of low abundance maybe due digestion procedure. Inclusion of ProteaseMAX™ Surfactant, Trypsin enhancer (Promega) failed to improve protein recovery from the gels. Future work would include optimisation of protein recovery techniques, or increasing the loading concentration of protein during the 1st dimensional focusing to yield spots with higher protein concentrations. Nevertheless, sensitivity studies were carried out (data not shown) from which the following protein spots were selected for protein identification by mass spectrometry; 368, 151, 125, 426 and 134.

Table 6.10: spots chosen for protein identification. Fold expression changes for each spot are given in brackets.

Spot	Analysis	Result
368 (1.3)	Negative control 9 week recovery versus positive control 9 week recovery	Decreased expression in positive control
151 (1.9)	Negative and positive control 9 week recovery versus negative and positive control 22 week recovery	Decreased expression in 22 week recovery
125 (1.5)	Negative control 9 and 22 weeks recovery versus positive control 9 and 22 weeks recovery	Decreased expression with positive control
426 (1.9)	Negative control 22 weeks recovery versus positive control 22 weeks recovery	Decreased expression in positive control
134 (1.8) & 426 (1.4)	Positive control 9 week recovery versus positive control 22 week recovery	Decreased expression in 22 week recovery

For each spot several potential proteins were identified. Several proteins may occur in the same spot for a number of reasons including poor resolution of the proteins or post-translational modifications to a protein causing a pI shift for example phosphorylation of a protein results in a change in pI with a shift in the acidic direction (Zhu *et al.*, 2005).

Protease inhibitors and serine protease inhibitors (serpins) were identified within spots 125, and 134 with the highest statistical confidence (Spot 125, Alpha-1-inhibitor 3 (protease inhibitor) E score of 9×10^{-16} , spot 134 Alpha-1-antitrypsin E score of 9×10^{-15}) and are protein hits with high statistical confidence in spots 134, 368 and 151. These results suggest a role for serine proteases in the inflammatory state observed in these animals. Carthew *et al.*, (2006) report that MM/ME/BA treated rats exhibited granulomas located in the alveoli and interstitium consisting of foamy and occasional necrotic alveolar macrophages. Interstitial fibrosis and alveolitis also occurred. There was no progression of disease or recovery in the 22 week recovery group compared to 9 week recovery. Serine proteases are implicated in the pathogenesis of numerous airway inflammatory conditions such as COPD (Wang *et al.*, 2006; Zabel *et al.*, 2005) and have been shown to induce secretion of the inflammatory mediator IL-8 (Wang *et al.*, 2006) and induce inflammatory cell recruitment to the site of tissue damage (Zabel *et al.*, 2005). Serine proteases themselves are also capable of inducing tissue damage

(Barnes *et al.*, 2003). The decrease in serpins identified by 2-DE/ MS proteomics suggests a mechanism whereby increased presence of serine proteases allows for inflammatory cell migration resulting in macrophage containing granulomas, and tissue damage. Further, transcriptomic analysis conducted on lung tissue (Carthew *et al.*, 2006) indicated alteration in genes involved in cell adhesion including cadherin II, alpha-3-type IV collagen, E-selectin and K-kininogen indicative of tissue damage; a kininogen spot was changed (down-regulation) in the rat plasma as determined here by proteomics.

Several proteins can exist in a given spot due to protein iso-electric point (pI) shifts from post-translational modifications. Further experimental approaches can be conducted to identify which of these proteins are responsible for the change in spot expression, such a SDS-PAGE and western blotting using antibodies targeted to specific proteins, or ELISA. Future work could include investigations into protease activity in rat plasma samples by ELISA. Using a data-base approach to identify possible candidates for inducing a change in protein intensity, the location of the spots here were matched against rat plasma gels obtained by Gianazza *et al.*, (2002) for control or inflamed rats. Inflammation was induced in rats exposed to turpentine or heat-killed *M. tuberculosis*, and these gels have been cited by other authors studying rat plasma proteomics (Linke *et al.*, 2007). Blast E-value and scores from uniprot.org were also considered. Alpha-1-antiproteinase appears in all protein spots chosen for LC-MS/MS analysis (151, 368, 426, 125 and 134). Alpha-1-antiproteinase is a high abundant plasma protein and is often depleted to aid detection of low abundant proteins (Linke *et al.*, 2007).

The localisation of the protein in control rat plasma gels obtained by Gianazza *et al.*, (2002) is in the position of spot 151 in gels obtained in the current study. Poor separation of proteins in the 1st dimensional or pI shifts due to PTM may result in this protein focussing to positions near spot 125 and 134, however, its MW (45.8) is smaller than that of spot 426 (around 66kDa on the gels) and much greater than that of spot 368 (which separated in the second dimension in a position near to the 14.4kDa protein marker). It is possible that this high abundant protein has contaminated the digest

samples at the LC stage of protein identification. If this were the case the densitometry analysis from Progenesis SameSpots would not be due to this protein.

Spot 151 showed a 1.9 fold decrease in expression in negative and positive control 22 week recovery compared to negative and positive control 9 week recovery, and is therefore not a biomarker of MM/EM/BA treatment. As this spot showed decreased expression in older animals it is an attractive biomarker for aging. However a protein hit with an exceptionally high score and low E-value for this spot was apolipoprotein A-IV (score 298, E value 1×10^{-25}). Apolipoprotein A-IV displays anti-atherogenic properties (Culnan *et al.*, 2008). Atherosclerosis events occur with aging (Walter., 2009) supporting reduction in plasma apolipoprotein A-IV as a biomarker of aging.

Spot 368 when compared to the reference gels by Gianazza *et al.*, (2002) matches transthyretin. By mass spectrometry transthyretin was identified as a protein hit for this spot with a high score (190) and low E-value (5×10^{-15}) with a 1.3 fold decrease in expression in positive control animals with 9 week recovery compared negative control 9 week recovery. Transthyretin is a negative acute phase protein showing decreased expression in acute inflammation, (Dickson *et al.*, 1985; Gianazza *et al.*, 2002) supporting its identification here. Transthyretin loss is a potential biomarker of MM/ME/BA exposure in rats.

Spot 426 showed a 1.9 fold decreased expression in positive control 22 weeks recovery compared positive control 9 week recovery and negative control 22 week recovery indicating its potential as a biomarker of prolonged inflammation. One of the protein hits for this spot was hemopexin precursor (score 113, E value 1×10^{-5}), the location of this spot matches hemopexin in the reference gels by Gianazza *et al.*, (2002), however, they report an increase in this protein during inflammation. The protein hit within spot 436 with the highest statistical confidence is transthyretin (3×10^{-15}). Uniprot reports transthyretin as a protein with a molecular mass of 15.72kDa, further the hit for spot 368 was transthyretin and this spot focused between the molecular weight markers with weights of 21.5 and 14.4kDa. Literature reports transthyretin as a 55kDa protein which

exists as a heterotetramer Dickson *et al.*, (1985) so a possible explanation is both the heterotetramer and individual chains have been separated.

Histidine rich glycoprotein is another protein identified in spot 426 (score 122 E value 1×10^{-3}), this protein was also identified in spot 125 (decreased expression in positive control at both 9 and 22 week recovery compared to negative control at both 9 and 22 weeks recovery) with a score of 122 and E value of 1×10^{-6} . Histidine rich glycoprotein is structurally related to alpha₂-HS glycoprotein a protein which was observed in spot 134 (decreased expression in positive control 22 week recovery compared to positive control 9 weeks recovery, score 126, E value 6×10^{-7}). The location of this spot matches that in the reference gels by Gianazza *et al.*, (2002) where the expression of this protein decreases in inflammation. Histidine rich glycoprotein has a role in opsonisation of necrotic cells and inhibition of fibrosis (Jones *et al.*, 2005), similarly alpha₂-HS glycoprotein aids in removal of necrotic neutrophils by macrophages (Jersmann *et al.*, 2003). Carthew *et al.*, (2006) report fibrosis and granulomas consisting of necrotic macrophages with MM/EM/BA treated rats at both 9 and 22 week recovery supporting the result observed here. These results suggest that decreased plasma levels of histidine rich glycoprotein and alpha₂-HS glycoprotein may be worthy of investigations as biomarkers of prolonged lung injury due to inhalation of MM/EM/BA. Histidine rich glycoprotein undergoes several posttranslational modifications such as glycosylation and sulfation (Jahen-Dechant *et al.*, 1994) which may explain how this protein is observed in spot 426 as well as 125 which has a more acidic pH and lower molecular weight.

6.6: Conclusion

Particles S2219200, S2218600 and S2429901 did not alter the proteome of BEAS-2B at ALI after at 24 hour exposure, suggesting that exposure of these particles at the concentrations and times used in the current study. However, the following study had several limitations including sensitivity imposed by 50µg protein and recovery of peptides from gels. Improved separation of proteins in the 1st dimension for these samples would provide further confidence in this result. The 2D-separation of cell lysates after TiO₂ treatment requires further optimization for biomarkers of exposure to be identified.

Several potential biomarkers of polymer 020310 exposure have been highlighted as being significantly up- or down-regulated in the plasmas obtained from rats after recovery from lung instillation with various polymer 020310 doses. Identification of all protein spots was limited due to sensitivity. In spite of this, 3 potential biomarkers of MM/EM/BA treatment were identified (decreased plasma concentrations of the negative acute phase proteins transthyretin, histidine-rich glycoprotein and alpha₂-HS glycoprotein). Several serpins were also shown to be down-regulated with MM/EM/BA treatment. Further work into the expression of these proteins specifically, in MM/EM/BA rats is warranted to definitively identify these proteins as biomarkers of MM/EM/BA exposure. As complementary gross histological changes were observed in MM/EM/BA treated rats (Carthew *et al.*, 2006) these biomarkers have potential use screening of new cosmetic compounds for acute lung injury.

Chapter 7: Discussion

7.1: Discussion

The objectives of the current study were to develop an *in vitro* co-culture model of the human airways comprising human airway epithelial cells cultured at ALI and human pulmonary microvascular endothelial cells. The inflammatory response to model airway challenges (LPS and PM) was investigated along with barrier integrity, cell viability and GSH status. A proteomic analysis approach was also undertaken to investigate identification of potential biomarkers of exposure. Proteomic analysis was also undertaken on rat plasma samples to identify biomarkers of polymer exposure.

The main results of this thesis are:

- identification of ZO-1 staining indicative of tight junction formation in BEAS-2B cultured at ALI (to the authors knowledge, this is the first time this result has been shown)
- BEAS-2B barrier was maintained when co-cultured with HPMEC in HPMEC growth media.
- *E. coli* LPS treatment of BEAS-2B ALI mono-cultures resulted in disrupted ZO-1 localisation, and a directional increase in IL-6 secretion.
- Increased secretion of IL-6 was observed from acrylate particle S2429901-treated BEAS-2B, and a decrease in cellular GSH and viability was observed in UFTiO₂-treated BEAS-2B.
- Co-culture of BEAS-2B with HPMEC resulted in a reduction in IL-6 secretion after LPS and S2429901 particle challenge, and protected against loss of cell viability after UFTiO₂-treatment.
- Separately, proteomic analysis undertaken on plasma samples from MM/EM/BA polymer treated rats identified a significant down-regulation in serpins, histidine rich glycoprotein, α_2 -HS-glycoprotein and transthyretin, with treatment compared to saline treated control animals.

If inhaled material such as bacteria breach the airways mucosa, the innate immune system mounts an inflammatory response which aims to neutralise and remove the

threat (Smith, 1994). Briefly; airway epithelial cells respond to insult by increasing secretion of cytokines and chemokines (Bals & Hiemstra, 2004; Polito & Proud, 1998). Some of the released inflammatory mediators are sequestered by the ECM in order to maintain a chemotactic gradient (Vaday & Lider, 2000), whilst some of the chemokines and cytokines activate the airways endothelium. Upon activation, the endothelial cells themselves release cytokines to initiate proliferation and differentiation of circulating leukocytes and chemokines in order to attract leukocyte migration (Daneese *et al.*, 2007). Once activated the endothelial cells also up-regulate expression of adhesion molecules in order to allow leukocyte diapedesis (Rafiee *et al.*, 2003; Yan *et al.*, 2010). Serine proteases are also released which aid in leukocyte migration (Zabel *et al.*, 2005). The leukocytes migrate to the site of insult via the chemotactic gradient and phagocytose the offending material. If this inflammatory response is not tightly regulated tissue damage and airway remodelling may occur. To prevent airways damage, the inflammatory response decreases after the threat has been removed (Parihar *et al.*, 2010). Cytokines and chemokines are no longer released by epithelial and endothelial cells, so there is no activation signal for circulating leukocytes. Leukocytes revert back to having short half-lives and their numbers are controlled by apoptosis (Parihar *et al.*, 2010). Growth factors sequestered by the ECM are released and aid in tissue repair (Schulz & Wyoski, 2009), damaging serine proteases are inhibited by serpins, and necrotic and apoptotic leukocytes are removed from sites of inflammation (Jersmann *et al.*, 2003; Jones *et al.*, 2005).

Proteomic analysis suggests that there was a failure to resolve the inflammatory response mounted after MM/EM/BA treatment in rats. The results obtained show a 1.9 fold decrease in expression of histidine rich glycoprotein in MM/EM/BA challenged rats compared to saline treated rats, after 22 week post treatment recovery (spot 426). A 1.8 fold decrease in expression of Alpha₂-HS-glycoprotein was observed in MM/EM/BA polymer-treated rats after 22 weeks recovery compared to MM/EM/BA polymer-treated rats after 9 weeks recovery (spot 134). Histidine rich glycoprotein and Alpha₂-HS-glycoprotein have roles in removal of necrotic cells and inhibition of fibroblast proliferation (and therefore may have a role in limiting fibrosis) (Jersman *et al.*, 2003; Jones *et al.*, 2005). Proteomic results of MM/EM/BA treated rats also showed decreased levels of serine protease inhibitors. Serine proteases induce leukocyte

migration (Zabel *et al.*, 2005) and endothelial cell apoptosis (Yang *et al.*, 1996). Gross histological changes were observed in these rats, including granulomas and fibrosis in the lungs (Carthew *et al.*, 2006). These results highlight strong support between proteomic and histological analysis, and indicate the potential of proteomics for identification of biomarkers of lung exposure and response to injury. The proteomic results also highlight the mechanisms involved in lung inflammation after toxic exposure.

Multi-cell models of the airways that encompass epithelial and endothelial cells, and ECM and leukocytes may allow for investigations of these mechanisms *in vitro*, and help to consolidate results from *in vivo* and *in vitro* studies. This study aimed to develop a multi-cell model of the airways comprising airway epithelial cells on a collagen basement membrane (to represent the ECM) with HPMEC. The first step in doing so was the development of a robust airway epithelial monoculture which is representative of the airways epithelium *in vivo*. To this end, BEAS-2B or NHBE were cultured at ALI, and their barrier formation investigated by TER, paracellular permeability and expression of ZO-1.

Initial studies identified that NHBE failed to form tight junctions, and showed no resistance to ion flow (as measured by TER) or solutes (as measured by FITC-dextran permeability). The presence of mesenchymal cells, with limited epithelial cells, was also identified (by immunohistochemical analysis). As NHBE were not robust in culture under the current studies culture conditions, BEAS-2B were used for the remainder of the study.

BEAS-2B cultured at ALI contained cytokeratin 5 and 8 positive epithelial cells, which are typical of stratified epithelial cells of the trachea (Moll *et al.*, 1982). Measurement of tight junction formation by ion and solute conductance is problematic as TER does not directly correlate with ion permeability and epithelial cells have different ion conducting properties (Tang & Goodenough, 2003). Importantly, BEAS-2B expressed the tight junction protein ZO-1 at the sites of cell-cell contact. TER increased during

culture at ALI and permeability to 40kDa FITC-dextran decreased indicating the presence of a restrictive barrier. Under unstimulated conditions IL-8 secretion in ALI cultures is greater than in submerged conditions; submerged total control IL-8 125.53 ± 38.1 pg compared to ALI total control IL-8 368.61 ± 44.75 pg (apical compartment IL-8 148.71 ± 27.55 pg, basolateral compartment IL-8 291.29 ± 58.20 pg). IL-8 gene expression increases during primary HBEC differentiation (Ross *et al.*, 2007), the increased expression of IL-8 by BEAS-2B cultured at ALI may therefore be favourable and representative of a phenotype similar to that *in vivo*.

The BEAS-2B ALI monoculture was exposed to LPS or PM to evaluate the inflammatory response and viability after challenge. After *E. coli* LPS-challenge a significant increase in IL-8 secretion was observed, along with a directional increase in IL-6 towards the basolateral compartment. Leukocyte derived IL-6 induces up-regulation of endothelial cells adhesion molecules (Zhang *et al.*, 2011). The pro-inflammatory cytokines TNF α and IL-1 β induce up-regulation of human umbilical cord endothelial cell (HUVEC) adhesion molecule and cytokine expression in HUVEC via NF- κ B/p38 MAPK signalling (Kuldo *et al.*, 2005). Further, IL-6 induces up-regulation of ICAM-1 expression in intestinal epithelial cells via NF- κ B signalling (Wang *et al.*, 2003). Taken together, it is possible that secretion of IL-6, from LPS-stimulated BEAS-2B, into the basolateral compartment is physiologically relevant and may induce endothelial cell adhesion molecule and cytokine expression via NF- κ B signalling. Watson *et al.*, (1996), determined that IL-6 treatment of HUVEC resulted in increased adhesion of lymphocytes but not leukocytes, however, large experimental variation was observed in this study. Further, cytokine secretion profiles vary between LPS- or TNF α -stimulated HPMEC compared to HUVEC (Beck *et al.*, 1999), as does polymorphonuclear cell adhesion during flow conditions and TNF α stimulation (Otto *et al.*, 2001), highlighting the importance of using relevant cell lines in *in vitro* models. Further work could investigate the effect of BEAS-2B derived IL-6 (possibly by conditioned media treatment with or without IL-6 neutralising antibodies) on HPMEC adhesion molecule expression.

In vitro studies have identified TiO₂, in particular UFTiO₂, to be cytotoxic (Gurr *et al.*, 2005), result in oxidative stress (Gurr *et al.*, 2005) and inflammation in airway epithelial cells (Singh *et al.*, 2007). The current study identified a loss of cellular GSH and viability in BEAS-2B treated with UFTiO₂. The loss of cell viability may be due to inflammation induced damage, as observed *in vivo* during chronic inflammation. Due to binding of IL-8 to UFTiO₂, measuring the inflammatory response after exposure was problematic.

Inclusion of HMPEC cells to the BEAS-2B ALI monolayers resulted in decreased IL-6 secretion from BEAS-2B after LPS or S2429901-treatment, and decreased the toxicity of UFTiO₂ to BEAS-2B. *E. coli* LPS (1000ng/ml for 24 hours) inducing a significant 1.8 fold increase in IL-6 secretion to the basolateral compartment of BEAS-2B monocultures, which was reduced to 1.2 fold (and no-longer significant) in the co-culture. For S2429901-treatment; the 14 fold increase in IL-6 secretion to the apical compartment of BEAS-2B mono-cultures was reduced to 4 fold in co-cultures (although the response remains significant). The 2 fold significant increase in IL-6 secretion to the basolateral compartment of BEAS-2B mono-cultures was reduced to 1.9 fold in co-cultures and this marginal increase in IL-6 secretion was non-significant. UFTiO₂-treated of BEAS-2B monocultures resulted in a significant decrease in viability to 69.1±8.8% of control. Viability of BEAS-2B from the co-culture model was not affected by UFTiO₂-treatment (viability was 88.7±5.6% of control).

The protective effect of the endothelial cell layer is suggestive of regulation of the inflammatory response to prevent against tissue damage. A possible mode of action may be that HPMEC secrete anti-inflammatory mediators which act upon the BEAS-2B. For example, HGF, which is expressed in lung microvascular endothelial cells (Morisako *et al.*, 2010), inhibits the airway inflammatory response of ovalbumin sensitised mice (Ito *et al.*, 2005), further HGF as be shown to suppress IL-6 production from macrophages (Coudriet *et al.*, 2010). HGF, or other endothelial cell derived anti-inflammatory mediators, may inhibit epithelial cell IL-6 production. HGF acts as an anti-apoptotic mediator in epithelial cells, inhibiting cigarette smoke extract induced apoptosis in human primary bronchial epithelial cells (Togo *et al.*, 2010) which could

also explain the protection from UFTiO₂ cell death (although the mechanism responsible for cell death (i.e. necrosis or apoptosis) was not determined). HGF secretion from HPMEC is induced by IL-1 β (Morisako *et al.*, 2001), so it is feasible that BEAS-2B derived cytokines up-regulate secretion of HGF from the endothelium, which in turns regulates the BEAS-2B inflammatory response.

Secretion of pro-survival cytokines such as vascular endothelial cell growth factor (VEGF) from endothelial cells may also act to protect the epithelium after insult .VEGF has been observed to promote nasal epithelial cells growth and inhibit apoptosis in nasal airway epithelial cells in an autocrine manner (Lee *et al.*, 2009). Further work could include investigation of HGF and VEGF expression/secretion from in HPMEC in mono- and co-culture conditions and the effect of these mediators on BEAS-2B mono-culture IL-6 secretion and viability after LPS, S2429901 and UFTiO₂-treatment.

The differences in physiology and immunology between humans and rodents (for example rats and mice do not express IL-8 (Tarrant, 2010)) cannot be overlooked. Nikula *et al.*, (2001) compared lung particle burdens and distribution of coal soot in exposed rats and humans, and identified differences in particle distribution. Rat exposure models (exposed to 0.35mg/m³, 3.5mg/m³ or 7mg/m³ for 7 hours a day, 5 days a week for 24 months) were compared to human workplace (coal mine) exposures in individuals who were exposed to low ambient dose of particles (\leq 2mg/m³ for a period of 10-20 years), high dose exposure levels (<10mg/m³ for a period of 30-50 years) or control individuals. The authors identified that in rats, particle burden was mainly in the alveolar ducts and lumen, with particles contained in alveolar macrophages (for all exposure doses, with increased particle burden correlating to exposure dose). In humans however, up to 91% of particles were found within the interstitium (irrespective of exposure levels), again with particle burden correlating to exposure (Nikula *et al.*, 2001).

The differing location of particles in rats and humans highlights the fundamental differences between species and the limitations of animal studies. Extrapolation

between studies therefore requires caution, for example in the current study S2429901 induced up-regulation of IL-6 and Gaiser, (2008) identified that this particle was inflammatory to rat airways. However Gaiser, (2008) showed that S2219200 and S2218600 were more potent inducers of inflammation, whilst in the current study had no effect on parameters measured.

Human studies of PM exposure have shown increased levels of IL-8 and GSH (18 hours after 2 hour exposure to $100\mu\text{g}/\text{m}^3$ DEP $\text{PM}_{2.5}$) in bronchial washings (Behndig *et al.*, 2006) and increased IL-6 in induced sputum (6 hour exposure to $300\mu\text{g}/\text{m}^3$ DEP PM_{10}) (Nordenhall *et al.*, 2000). Human studies of LPS inhalation identify increased neutrophil and lymphocyte numbers in blood, induced sputum (24 hours after exposure to $40\mu\text{g}$ *E. coli* 026:B6 LPS (Thorn & Rylander, 1998)) and bronchial lavage (24 hours after exposure to $4\text{ng}/\text{kg}$ *E. coli* 0:113 LPS (O'Grady *et al.*, 2001). Increased IL-6 concentration in bronchial lavage after 2 hour *E. coli* 0:113 LPS, with levels peaking at 6 hours post exposure, has also been observed (O'Grady *et al.*, 2001). Importantly the results of the current study are in agreement with human *in vitro* PM and LPS exposures where increases inflammatory mediator secretion and oxidative stress are observed. Work in this thesis has shown increased IL-6 secretion from LPS-and S2429901-challenged mono-cultures and S2429901-challenged co-cultures.

Despite the differences in immunology between rodents and humans, both exhibit airway inflammation after airways exposure to noxious material (Behndig *et al.*, 2006; Bermudez *et al.*, 2004; Carthew *et al.*, 2006; Nordenhall *et al.*, 2000; Thorn & Rylander, 1998). Notably, proteomic biomarker results obtained in the current study from plasmas collected from MM/EM/BA exposed rats identified a down-regulation of α_2 -HS-glycoprotein and the serpin α_1 -antitrypsin. Histologically, airway inflammation and fibrosis was observed in these animals (Carthew *et al.*, 2006). Bowler *et al.*, (2009) identified a decrease in expression of α_2 -HS-glycoprotein and α_1 -antitrypsin in BAL fluid (using proteomic analysis) from LPS challenged humans. As the serpin α_1 -antitrypsin can be produced by lung epithelial cells (Wang *et al.*, 2007) the potential for BEAS-2B to show altered secretion of these proteins in response to challenge should be studied. The agreement between results obtained from the BEAS-2B ALI model

compared to human *in vivo* studies, and the regulation of inflammation by HPMEC which suggests crosstalk between the two cell types as observed *in vivo*, highlights the significance of the model developed in this thesis.

7.2: Conclusion

BEAS-2B mono-cultured cultured at ALI produce tight junctions, with ZO-1 localisation to the site of cell-cell contact, with low TER. To the author's knowledge this is the first time this result has been identified in BEAS-2B cultured at ALI. Tight junctions in epithelial cells *in vivo* function to maintain cellular homeostasis and provide a protective barrier against invading pathogens and inhaled toxicants, the presence of tight junctions in BEAS-2B ALI cultures provides evidence that these cells have a morphology resembling *in vivo* airway epithelial cell cultures. LPS and S2429901 induced IL-6 secretion from BEAS-2B mono-culture at ALI without compromising cell viability. LPS-stimulation of BEAS-2B ALI mono-cultures resulted in disruption of ZO-1 localisation, which may be the initiation of tight junction disruption. The presence of HPMEC resulted in a reduction of the BEAS-2B inflammatory response after LPS and S2429901 challenge, and HPMEC also protected against UFTiO₂ cytotoxicity in BEAS-2B. Importantly *in vitro* findings reported here, are in agreement with human *in vivo* studies. These results emphasise the importance for use of multi-cell *in vitro* models of the airways to investigate the inflammatory and toxicity potential of particulates and pathogens *in vivo*.

Analysis of TiO₂ induced inflammation, and identification of biomarkers or response to exposure was inconclusive due to assay interference. Identification of biomarkers of response to exposure with polymer 020310 or MM/EM/BA was limited due to lack of protein recovery from tryptic digests, however, 4 potential response biomarker of MM/EM/BA exposure in rats (where gross histopathological changes were also observed, Carthew *et al.*, (2006)) were identified; serpins/ α_1 -antitrypsin, transthyretin, histidine rich glycoprotein and alpha₂-HS glycoprotein. Specific analysis of expression for these proteins in rat plasma samples is required to confirm these as biomarkers of response to inhalation toxicity. However, down-regulation of expression of alpha₂-HS

glycoprotein and the serpin α_1 -antitrypsin has been identified in BAL from LPS challenged humans, again highlighting how results of the current study on airways inflammation in rats, and human cell *in vitro* studies, may be used to understand human *in vivo* inflammatory critical pathways and for identification of biomarkers or response.

Chapter 8: Future Work

The overall aim of this thesis is to develop a co-culture of the human airways for toxicity testing and identification of novel biomarkers of response to particles, with specific objectives including;

- 1) Characterisation of BEAS-2B morphology at ALI compared to NHBE
- 2) Development of an epithelial/endothelial co-culture model
- 3) Investigations into inflammatory mediator secretions from this model after challenge with LPS or PM
- 4) Determination of GSH oxidation and cell viability after LPS/PM challenge
- 5) Identification of biomarkers of response using proteomics and LC-MS/MS

The above objectives were carried out; however, several small investigations are required to clarify results of the current study. For example; do BEAS-2B cultured at ALI form cilia and express the tight junction protein claudin. BEAS-2B cultured at ALI should be challenged with increasing doses of LPS from the respiratory pathogens *P. aeruginosa* 5ODR and *B. cepacia* to investigate the hypothesis that airway epithelial cells do not produce an inflammatory response after challenge with low respiratory LPS concentrations, probably as a protective mechanism. Of importance is further investigation into the IL-8 response of TiO₂ and UFTiO₂ challenged BEAS-2B. Since UFTiO₂ interferes with IL-8 detection by ELISA, a functional assay (the neutrophil respiratory burst assay) was conducted for investigations into IL-8. However, it is unknown as to whether cells respond to UFTiO₂ challenge by up-regulation of IL-8. Investigations into IL-8 mRNA levels would give insight into the IL-8 response of UFTiO₂ challenge. *In vitro* models allow translation of results from animal toxicity studies to human diseases. Clarification of the results obtained in the current study would allow for further comparisons of the model to validated *in vivo* animal models.

Biomarkers of toxicity were not identified in the current study due to assay interference. Future work would focus on optimisation of the iso-electric focussing method for samples from TiO₂-treated cells. Carthew *et al.*, (2006) identified gross histological

changes in the lungs of MM/EM/BA treated rats, whilst the proteomic work undertaken in the current study on plasma samples from these rats identified changes in expression of the following proteins; α_1 -antitrypsin, transthyretin, histidine rich glycoprotein and α_2 -HS glycoprotein. Transthyretin, histidine rich glycoprotein and α_2 -HS glycoprotein are produced in the liver, so investigations into the expression of these proteins in the model developed in the current study cannot be undertaken. Protein identification in the rat plasma proteomic studies was limited due to poor recovery of peptides from trypsin-digests, an improved digestion method would allow for identification of these lower-abundant significantly altered spots, some of which may be epithelium or endothelium derived. Future work would therefore also include LC-MS/MS identification of the lower abundant-significantly altered spots identified in plasma from MM/EM/BA treated rats. The serpin α_1 -antitrypsin is secreted by the epithelium, investigation into the expression of this protein in PM treated BEAS-2B should also be considered to along with investigations into α_1 -antitrypsin, transthyretin, histidine rich glycoprotein and α_2 -HS glycoprotein mRNA levels and protein expression levels directly (by ELISA for example) in plasmas from MM/EM/BA treated rats. These studies would give insight into the potential of these proteins as biomarkers of response to inhalation exposure of toxic PM.

Optimisation of NHBE culture at ALI and proteomic analysis of TiO₂ and UFTiO₂ challenged BEAS-2B should also be undertaken to allow for identification of biomarkers of exposure and development of an airways epithelial-endothelial co-culture consisting of primary cells only. Primary cells have not undergone transformation and are taken from “normal” tissue and therefore more representative of *in vivo* cells.

A valuable line of enquiry would be to investigate monocyte adhesion to the endothelial cells after LPS or PM challenge of the co-culture, compared to stimulation of endothelial cells directly. This would give insight as to whether epithelial cell derived cytokine (with increased secretion after challenge) up regulate leukocyte adhesion to the endothelium, as observed *in vivo*. Philips *et al.*, (2003) investigate monocyte (U937) adhesion to LPS activated endothelium (HUVEC monolayers) by labelling the monocytes the fluorescent dye 2'-7' bis-2-carboxy-5-(6)-carboxyfluorescein-

acetoxymethylester (BCECF-AM). Labelled monocytes are added to LPS activated HUVEC cells for 30 minutes at 37°C. After incubation non-adhered cells are removed by washing, and adhered cells are lysed. The fluorescence of the resultant lysate is measured (Ex 485nm, Em 535nm) to give a measure of monocyte adherence.

This could be carried out after challenge of the co-culture with LPS or PM by removal of the Transwell® insert and addition of monocytes to the endothelial cell monolayer. Controls should include addition of challenge/control to the apical surface of a blank-collagen-coated Transwell® insert (Figure 8.1) as a control for non-direct stimulation of endothelial cells in the absence of epithelial cells. Endothelial cells should also be directly stimulated with LPS or PM. These controls will allow investigations into whether challenged epithelial cells respond by signalling up-regulation of endothelial cell adhesion molecules, whether enhanced adhesion is due to challenge of endothelial cells by particle translocation (by comparing adhesion of monocytes in the co-culture system to the blank-collagen-coated Transwell® insert) and whether the presence of an epithelial cells layer enhances monocyte adhesion to endothelium.

However, as the inflammatory response *in vivo* involves multiple cell types including leukocytes, fibroblasts and mast cells, further development of the current model would concentrate on inclusion of these cells into the model.

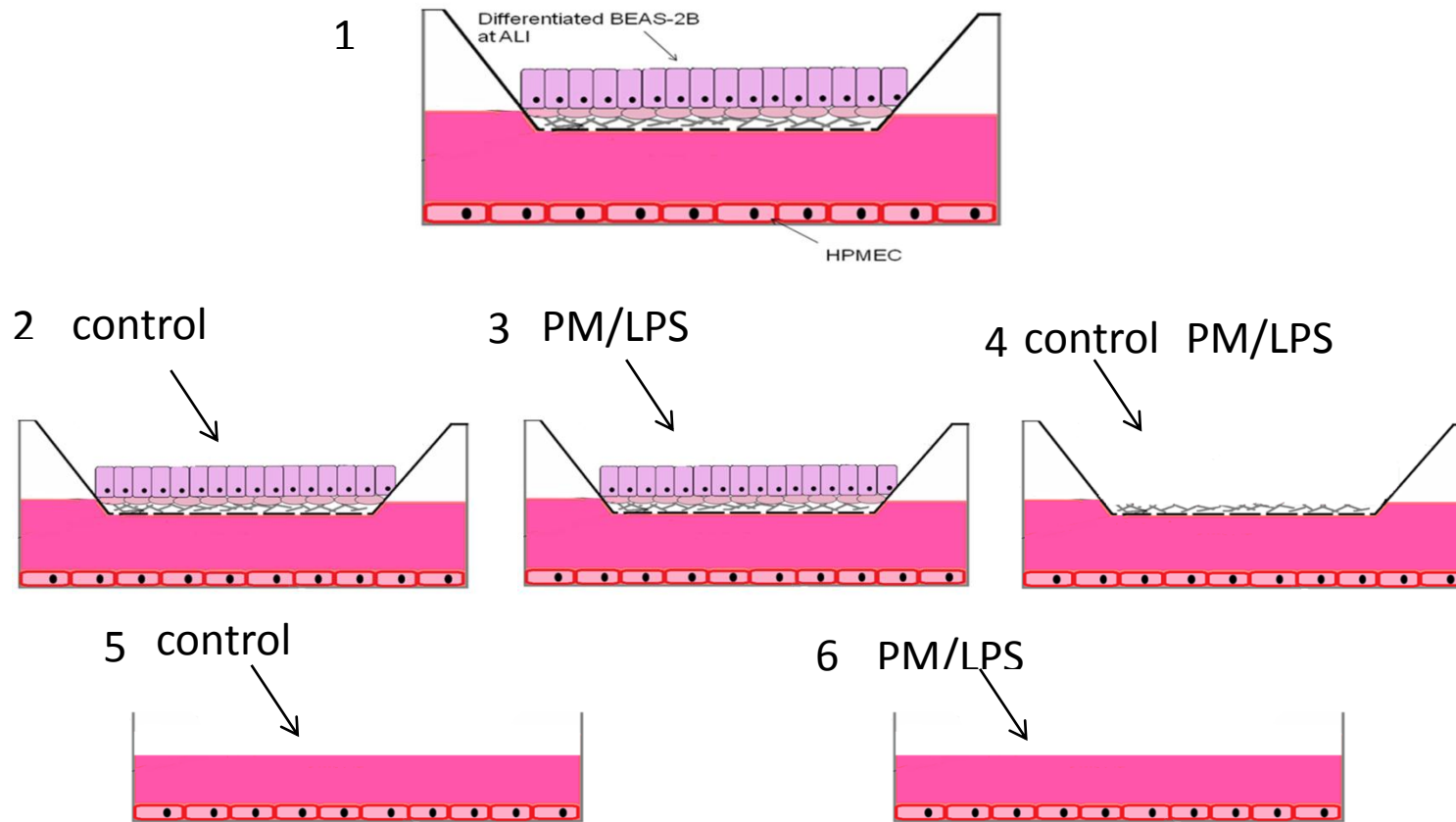


Figure 8.1 : Schematic diagram of proposed adhesion assay. 1) represents the co-culture model. 2) the co-culture treated with control (media alone). 3) the co-culture treated with LPS or PM. 4) Treatment in the absence of epithelial cells. Treatment given apical on a blank-collagen-coated Transwell® Insert as a control for in-direct exposure. 5) monocyte adhesion in the absence of epithelial cells or stimulus, 6) monocyte adhesion in the absence of epithelial cells, with direct stimulus of endothelial cells.

Chapter 9: References

Ahuja, M., Dhake, A.S., Sharma, S.K. & Majumder, D.K. (2008). Topical ocular delivery of NSAIDs. *The AAPS Journal*, **10(2)**; 229-241

Aldred, S., Grant, M.M. & Griffiths, H.R. (2004). The use of proteomics for the assessment of clinical samples in research. *Clinical Biochemistry*, **37(1)**; 943-952

7th Amendment of the European Cosmetic Directive (2003). Directive 2003/15/EC of the European Parliament and of the Council of 27 February 2003 Amending Council Directive 76/768/EEC on the approximation of the laws of the member states relating to cosmetic products. *Official Journal of the European Union*, **L66**; 26-35

Ammit, A.J., Moir, L.M., Oliver, B.G., Hughes, J.M., Allchouri, H., Ge, Q., Burgess, J.K., Black, J.L. & Roth, M. (2007). Effect of IL-6 *trans*-signalling on the pro-remodelling phenotype of airway smooth muscle. *American journal of Physiology, Lung Cellular and Molecular Physiology*, **292**; L199-L206

Andus, T., Geiger, T., Hirano, T., Northoff, H., Ganter, U., Bauer, J., Kishimoto, T. & Heinrich, P.C. (1987). Recombinant human B-cell stimulatory factor 2 (BSF-2/IFN-beta2) regulates beta fibrinogen and albumin mRNA levels in Fao-9 cells. *FEBS letters*, **22(1)**; 18-22

Asthma UK, www.asthma.org

Atsuta, J., Sterbinsky, S.A., Plitt, J., Schwiebert, L.M., Bochner, B.S. & Schleimer R.P. (1997). Phenotyping and Cytokine Regulation of the BEAS-2B Human Bronchial Epithelial Cell: Demonstration of Inducible Expression of the Adhesion Molecules VCAM-1 and ICAM-1. *Am. J. Respir. Cell Mol. Biol*, **17**; 571-582

Auger, F., Gendron, M-C., Chamot, C. & Maranof, F. (2006). Responses of well-differentiated nasal epithelial cells exposed to particles: role of the epithelium in inflammation. *Toxicology and Applied Pharmacology*, **215**; 285-294

Baggiolini, M. & Clark-Lewis, I. (1992). Interleukin-8, a chemotactic and inflammatory cytokine, *FEBS*, **307(1)**; 97-101

Baggiolini, M., Walz, A. & Kunkel, S.L. (1989). Neutrophil-activating Peptide-1/Interleukin 8, a novel cytokine that activates neutrophils. *Journal of Clinical Investigations*, **84**; 1045-1049

Bals, R. & Hiemstra, P.S. Innate immunity in the lung: how epithelial cells fight against respiratory pathogens (2004). *European Respiratory Journal*, **23(2)**; 327-333

Barnes, P.J. (2009). The cytokine network in chronic obstructive pulmonary disease. *American Journal of Respiratory Cellular and Molecular Biology*, **41**; 631-638

Barnes, P.J., Shapiro, S.D. & Pauwels, R.A. (2003). Chronic obstructive pulmonary disease: molecular and cellular mechanisms. *European Respiratory Journal*, **22**; 672-688

Barraza-Villarreal, A., Sunyer, J., Hernandez-Cadena, L., Escamilla-Nunez, M.C., Sienra-Monge, J.J., Ramirez-Aguilar, M., Cortez-Lugo, M., Holguin, F., Diaz-Sanchez,

- D., Olin, A.C. & Romieu, I. (2008). Air pollution, airway inflammation and lung function in a cohort study of Mexico city schoolchildren. *Environmental Health Perspectives*, **116**; 832-838
- Barton, G.M. (2008). A calculated response: control of inflammation by the innate immune system. *The Journal of Clinical Investigation*, **118**; 413-420
- Beck-Schimmer, B., Schimmer, R.C. & Pasch, T. (2004). The airway compartment: Chamber of secrets. *Physiology*, **19**; 129-132
- Bermudez, e., Mangum, J.B., Wong, B.A., Asgharian, B., Hext, P.M., Warheit, D.B. & Everitt, J.I. (2004). Pulmonary responses of mice, rats and hamsters to subchronic inhalation of ultrafine titanium dioxide particles. *Toxicological Sciences*, **77**; 347-357
- Bharti, A., Ma, P.C. & Salgia, R. (2007). Biomarker discovery in lung cancer- promises and challenges of clinical proteomics. *Mass Spec Reviews*, **26(3)**; 451-466
- Bhattacharya, K., Davoren, M., Boertz, J., Schins, R.P.F., Hoffmann, E. & Dopp, E. (2009). Titanium dioxide nanoparticles induce oxidative stress and DNA-adduct formation but not DNA-breakage in human lung cells. *Particle and Fibre Toxicology*, **16**; 17-28
- BioRad, Flamingo™™ Fluorescent Gel Stain, literature/bulletin 5346 www.bio-rad.com
- Biswas, S.K. & Rahman, I. (2009). Environmental toxicity, redox signalling and lung inflammation. The role of glutathione. *Molecular Aspects of Medicine*, **30**; 60-76
- Blackwell, T.S. & Christman, J.W. (1997). The role of nuclear factor-κB in cytokine gene regulation. *American Journal of Respiratory Cellular and Molecular Biology*, **17**; 3-9
- Blank, F., Rothen-Rutishauser, B. & Gehr, P. (2007). Dendritic Cells and Macrophages Form A Transepithelial Network against Foreign Particulate Antigens. *American Journal of Respiratory Cellular and Molecular Biology*, **36**; 669-677
- Boffeta, P., Soutar, A., Cherrie, J.W., Granath, F., Andersen, A., Anttila, A., Blettner, M., Gaborieau, V., Klug, S.J., Langard, S., Luce, D., Merletti, F., Miller, B., Mirabelli, D., Pukkala, E., Adami, H-O & Weiderpass, E. (2004). Mortality among workers employed in the titanium dioxide production industry in Europe. *Cancer Causes and Control*, **15**; 697-706
- Bonnans, C., Fukanga, K., Levy, M.A. & Levy, B.D. (2006). Lipoxin A₄ Regulates Bronchial Epithelial Cell Responses to Acid Injury. *Cardiovascular, Pulmonary and Renal Pathology*, **168**; 1064-1072
- Brook, R.D., Brook, J.R., Urch, B., Vincent, R., Rajagopalan, S. & Silverman, F. (2002). Inhalation of fine particulate and ozone causes acute arterial vasoconstriction in healthy adults. *Circulation*, **105**; 1534-1536
- Canas, B., Lopez-Ferrer, D., Ramos-Fernandez, A., Camafeita, E. & Calvo, E. (2006). Mass spectrometry technologies for proteomics. *Briefings in Functional Genomics and Proteomics*, **4(4)**; 295-320

- Caraballo, J.C., Yshii, C., Westphal, W., Moninger, T. & Comellas, A.P. (2011). Ambient particulate matter affects occluding distribution and increases alveolar transepithelial electrical conductance. *Respirology*, **16**; 340-349
- Carter, J.D., Ghio, A.J., Samet, J.M. & Devlin, R.B. (1997). Cytokine Production by Human Airway Epithelial Cells after Exposure to an Air Pollution Particle in Metal-Dependent. *Toxicology and Applied Pharmacology*, **146**; 180-188
- Carthew, P., Fletcher, S., White, A., Harries, H. & Weber, K. (2006). Transcriptomic and Histopathology Changes in Rat Lung After Intratracheal Instillation of Particles. *Inhalation Toxicology*, **18**; 227-245
- Casale, T.B. & Carolan, E.J. (1999). Cytokine-induced sequential migration of neutrophils through endothelium and epithelium. *Inflammation research*, **48**; 22-27
- Cascao, R., Rosario, C.R. & Fonseca, J.E. (2009). Neutrophils: warriors and commanders in immune mediated inflammatory diseases. *Acta Reumatol Port*, **34**; 313-326
- Castillon, N., Avril-Delplanque, A., Coraux, C., Delandra, C., Peult, B., Danos, O. & Puchelle, E. (2004). Regeneration of a well-differentiated human airway surface epithelium by spheroid and lentivirus vector-transduced airway cells. *The Journal of Gene Medicine*, **6**; 846-856.
- Cha, M-H., Rhim, T.Y., Kim, K.H., Jang, A-S., Paik, Y-K. & Park, C-S. (2007). Proteomic identification of macrophage migration-inhibitory factor upon exposure to titanium dioxide particles. *Molecular and Cellular Proteomics*, **6**; 56-63
- Chen, E.Y.T., Garnica, M., Wang, Y.C., Chen, C.S. & Chin, W.C. (2010). Mucin secretion induced by titanium dioxide nanoparticles. *PLoS ONE*, **6**(1); e16198
- Choe, M.M., Sporn, P.H.S. & Swartz, M.A. (2006). Extracellular Matrix Remodelling by Dynamic Strain in a Three-Dimensional Tissue Engineered Human Airway Wall Model. *American Journal of Respiratory Cellular and Molecular Biology*, **35**; 306-313
- Choi, J.K. (1961). Light and electron microscopy of the toad urinary bladder. *The Anatomical Record*, **139**; 214 (abstract)
- Chow, A.W-M., Liang, J.F-T., Wong, J.S-C., Fu, Y., Tang, N.L-S. & Ko, W-H. (2008). Polarised Secretion on Interleukin (IL)-6 and IL-8 by Human Airway Epithelia 16HBE14o⁻ cells in Response to Cationic Polypeptide Challenge. *PLoS one*, **5**(8); e1209-1219
- Chowdhury, F., Howat, W.J. Phillips, G.J. & Lackie, P.M. (2010) Interactions between endothelial cells and epithelial cells in a combined model of airway mucosa: effects of tight junction permeability. *Experimental Lung Research*, **36**(1); 1-11
- Chung, K.F. (2001). Cytokines in chronic obstructive pulmonary disease. *European Respiratory Journal*, (**18: suppl 34**); 50-59
- Churg, A., Gilks, B. & Dai, J. (1999). Induction of fibrogenic mediators by fine and ultrafine titanium dioxide in rat tracheal explants. *American Journal of Physiology; Lung Cellular and Molecular Physiology*, **277**; 975-982

Coudriet, G.M., He, J., Trucco, M., Mars, W.M. & Paganelli, J.D. (2010). Hepatocyte Growth Factor modulates Interleukin-6 production in bone marrow derived macrophages: implications for inflammatory mediated diseases. *PLoS ONE*, **5(11)**; e15384

Coyne, C.B, Vanhook, M.K., Gambling, T.M., Carson, J.L., Boucher, R.C. & Johnson, L.G. (2002). Regulation of Airway Tight Junctions by Proinflammatory Cytokines. *Molecular Biology of the Cell*, **13**; 3218-3234

Culnan, D.M., Cooney, R.N., Stanley, B. & Lynch, C.J. (2008). Apolipoprotein A-IV a Putative Satiety/Antiatherogenic Factor, Rises After Gastric Bypass. *Obesity*, **17(1)**; 46-52

Cystic Fibrosis Trust UK, www.cftrust.org.uk

Danese, S., Dejana, E. & Fiocchi, C. (2007). Immune regulation by microvascular endothelial cells: directing innate and adaptive immunity, coagulation, and inflammation. *Journal of Immunology*, **178**; 6017-6022

Dausend, J., Musyanovych, A., Dass, M., Walther, P., Schrezenmeier, H., Landfester, K & Mailander, V. (2008). Uptake mechanism of oppositely charged fluorescent nanoparticles in HeLa Cells. *Macromolecular Biosciences*, **8(12)**; 1135-1143

Davis, D.J. (2002). Regulation of mucin secretion from *In Vitro* cellular models. *In Vitro Models*, 113-131.

De Jong, P.M., van Sterkenburg, M.A., Hesseling, S.C., Kempenaar, J.A., Mulder, A.A., Mommass, A.M., Dijkman, J.H. & Ponc, M. (1994). Ciliogenesis in human bronchial epithelial cells cultured at the air-liquid interface. *American Journal of Respiratory Cell and Molecular Biology*, **10(3)**; 271-277

De Jong, P.M., van Sterkenburg, M.A., Kempenaar, J.A., Dijkman, J.H. & Ponc, M. (1993). Serial culturing of human bronchial epithelial cells derived from biopsies. *In Vitro Cell Dev Biol Anim*, **29A(5)**; 379-387

DEFRA Department for Environmental, Food and Rural Affairs, The environment/ environmental quality and pollution. www.defra.gov.uk

Delfino, R.J., Staimer, N., Tjoa, T., Polidori, A., Arhami, M., Gillen, D.L., Kleinman, M.T., Vaziri, N.D., Longhurst, J., Zaldivar, F. & Siouta, C. (2008). Circulating biomarkers of inflammation, antioxidant activity, and platelet activation are associated with primary combustion aerosols in subjects with coronary artery disease. *Environmental Health Perspectives*, **116**; 898-906

Deslee, D., Dury, S., Perotin, J.M., Alam, D.A., Vitry, F., Boxio, R., Gangloff, S.C., Guenounou, M., Lebargy, F. & Belaouaj, A. (2007). Bronchial epithelial spheroids: an alternative culture model to investigate inflammation-mediated COPD. *Respiratory Research*, **8**; 86-98

Dias, I.H., Marshall, L., Lambert, P.A., Chapple, I.L., Matthews, J.B. & Griffiths, H.R. (2008). Gingipains from *Porphyromonas gingivalis* increase the chemotactic and respiratory burst-priming properties of the 77-amino acid interleukin-8 variant. *Infection and Immunity*, **76(1)**; 317-323

- Dicksen, P.W., Howlett, G.J. Schreiber, G. (1985). Rat Transthyretin (Prealbumin). MOLECULAR CLONING NUCLEOTIDE SEQUENCE AND GENE EXPRESSION IN LIVER AND BRAIN. *The Journal of Biological Chemistry*, **260**(13); 8214-8219
- Doerner, A.M. & Zuraw, B.L. (2009). TGF- β_1 induced epithelial to mesenchymal transition (EMT) in human bronchial epithelial cells is enhanced by IL-1 β but not abrogated by corticosteroids. *Respiratory Research*, **10**; 100-115.
- Drakatos, P., Lykouras, D., Sampsonas, f., Karkoulas, K. & Spiropoulos, K. (2009). Targeting leukotrienes for the treatment of COPD. *Inflammation and Allergy Drug Targets*, **8**(4); 297-306
- Drukarch, B., Schepens, E., Jongenelen, C.A.M., Stoof, J.C. & Langeveld, C.H. (1997). Astrocyte-mediated enhancement of neuronal survival is abolished by glutathione deficiency. *Brain Research*, **770**; 123-130
- Duffin, R., Mills, N.L. & Donaldson, K. (2007). Nanoparticles-A thoracic toxicology perspective. *Yonsei Medical Journal*, **48**(4); 561-572
- Dunston, C.R. & Griffiths, H.R. (2010). The effect of aging on macrophage Toll-like receptor-mediated responses in the fight against pathogens. *Clinical and Experimental Immunology*, **161**(3); 407-416
- Dvork, A., Tilley, A.E., Shaykhiev, R., Wang, R. & Crystal, R.G. (2011). Do airway epithelium ALI cultures represent the *in vivo* airway epithelium transcriptome. *American Journal of Respiratory Cell and Molecular Biology*, **44**(4); 465-73.
- Elson, G., Dunn-Siegrist, I., Daubeuf, B. & Pugin, J. (2007). Contribution of Toll-like receptors to the immune response to Gram-negative and Gram-positive bacteria. *Blood*, **109**(4); 1574-1583
- Endres, M., Leinhase, I., Kaps, C., Wentges, M., Unger, M., Olze, H., Ringe, J., Sittinger, M. & Rotter, N. (2005). Changes in the gene expression pattern of cytokeratins in human respiratory epithelial cells during culture. *Eur Arch Otorhinolaryngol*, **262**; 390-396
- Erjefalt, J.S., Sundler, F. & Persson, C.G.A. (1997). Epithelial Barrier Formation by Airway Basal Cells. *Thorax*, **52**; 213-217
- Fahy, J.V. & Dickey, B.F. (2010). Airway mucus function and dysfunction. *The New England Journal of Medicine*, **363**(23); 2233-2247
- Farquhar, M.G. & Palade, G.E. (1963). Junctional complexes of various epithelia. *The Journal of Cell Biology*, **17**; 375-412
- Fitzgerald, K.A., Rowe, D.c., Golebock, D.T (2004). Endotoxin recognition and signal transduction by the TLR4/MD-2 complex. *Microbes and infection*, **6**; 1361-1367
- Fitzpatrick, A.M., Higgins, M., Holguin, F., Brown, L.A.S. & Teague, W.G. (2010). The molecular phenotype of severe asthma in children. *Journal of Allergy and Clinical Immunology*, **125**; 851-857

- Flynn, A.N., Itani, O.A., Moninger, T.O. & Welsh, M.J. (2009). Acute regulation of tight junction ion selectivity in human airway epithelia. *Proceedings of the National Academy of Sciences*, **106** (9); 3591-3596
- Forbes, B. & Ehrhardt, C. (2005). Human respiratory epithelial cell culture for drug delivery applications. *European Journal of Pharmaceutics and Biopharmaceutics*, **60**; 193-205
- Forman, H.J., Zhang, H. & Rinna, A. (2009). Glutathione: Overview of its protective roles measurement and biosynthesis. *Molecular Aspects of Medicine*, **30**; 1-12
- Freyre-Fonseca, V., Delgado-Buenrostro, N.L., Gutierrez-Cirlos, E.B., Calderon-Torres, C.M., Cabellos-Avelar, T., Sanchez-Perez, Y., Pinzon, E., Torres, I., Molina-Jijon, E., Zazueta, C., Pedraza-Chaverri, J., Garcia-Cuellar, C.M. & Chirino, Y.I. (2011). Titanium dioxide nanoparticles impair mitochondrial function. *Toxicology Letters*, **202**; 111-119
- Fujii, T., Hayashi, S., Hogg, J.C., Mukae, H., Suwa, T., Goto, Y., Vincent, R. & Van Eeden, S.F. (2002). Interaction of Alveolar Macrophages and Airway Epithelial Cells Following Exposure to Particulate Matter Produces Mediators that Stimulate the Bone Marrow. *American Journal of Respiratory Cell and Molecular Biology*, **27**; 34-41
- Furuse, M., Furuse, K., Sasaki, H. & Tsukita, S. (2001). Conversion of Zonulae Occludentes from tight to leaky strand type by introducing Claudin-2 into Madin-Darby canine kidney 1 cells. *The Journal of Cell Biology*, **153**(2); 263-272
- Furuse, M., Hirase, T., Itoh, M., Nagafuchi, A., Yonemura, S., Tsukita, S. & Tsukita, S. (1993). Occludin: a novel integral membrane protein localising at tight junctions. *The Journal of Cell Biology*, **123**(6 pt2); 1777-1788
- Gaiser, B.K. (2008). In vitro models to predict toxicity and fibrogenicity of organic polymers. *Thesis for the degree of Doctor of Philosophy, University of Edinburgh, School of Medicine and Veterinary Medicine.*
- Galan, I., Tobias, A., Benegas, J.R. & Aranguiz, E. (2003). Short-term effects of air pollution on daily asthma emergency room admissions. *European Respiratory Journal*; **22**; 802-808
- Garcia-Rio, F., Miravittles, M., Soriano, J.B., Munoz, L., Duran-Tauleria, E., Sanchez, G., Sobradillo, V., Ancochea, J & EPI-SCAN Steering Committee. (2010). Systemic inflammation in chronic obstructive pulmonary disease: a population-based study. *Respiratory Research*, **11**; 63-78
- Ge, Y., Bruno, M., Wallace, K., Winnik, W. & Prasad, R.Y (2001). Proteome profiling reveals potential toxicity and detoxification pathways following exposure of BEAS-2B cells to engineered nanoparticles titanium dioxide. *Proteomics*, **11**; 2406-2422
- Geiser, M., Rothen-Rutishauser, B., Kapp, N., Schurch, S., Kreyling, W., Schulz, H., Semmler, M., Hof, V.I., Heyder, J. & Gehr, P. (2005). Ultrafine Particles Cross Cellular Membranes by Nonphagocytic Mechanisms in Lungs and in Cultured Cells. *Environmental Health Perspectives*, **113**; 1555-1560

- Gianazza, E., Eberini, I., Villa, P., Fratelli, M., Pinna, C., Wait, R., Gemeiner, M. & Miller, I. (2002). Monitoring the effects of drug treatment in rat models of disease by serum protein analysis. *Journal of Chromatography B*, **771**; 107-130
- Godfrey R.A.A. (1997). Human Airway Epithelial Tight Junctions. *Microscopy research and technique*, **38**; 488-499
- Gojova, A., Guo, B., Kota, R.S., Rutledge, J.C., Kennedy, I.M. & Barakat, A.B. (2007). Induction of Inflammation in Vascular Endothelial Cells by Metal Oxide Nanoparticles: Effects of Particle Composition. *Environmental Health Perspectives*, **115**; 403-409
- Gorbet, M.B & Sefton, M.V. (2005). Endotoxin: The uninvited guest. *Biomaterials*, **26**; 6811-6817
- Gorg, A., Weiss, W. & Dunn, M.J. (2004). Current two-dimensional electrophoresis technology for proteomics. *Proteomics*, **4**; 3665-3685
- Goss, C.H., Newsom, S.E., Schildcrout, J.S., Sheppard, L. & Kauffman, J.D. (2004). Effect of ambient air pollution on pulmonary exacerbations and lung function in cystic fibrosis. *American Journal of Critical Care Medicine*, **169**; 816-821
- Grainger, C.I., Greenwell, I.I., Lockley, D.J., Martin, G.P. & Forbes, B. (2006). Culture of Calu-3 cells at the Air Interface Provides a Representative Model of the Airway Epithelial Barrier. *Pharmaceutical Research*, **23**; 1482-1490
- Granger, J., Siddiqui, J., Copeland, S. & Remick, D. (2005). Albumin depletion of human plasma also removes low abundance proteins including the cytokines. *Proteomics*, **5**; 4713-4718
- Gray, T.E., Guzman, K., Davis, C.W., Abdullah, A.H. & Netteshei, P. (1996). Mucociliary Differentiation of Serially Passaged Normal Human Tracheobronchial Epithelial Cells. *American Journal of Respiratory Cellular and Molecular Biology*, **14**; 104-112
- Greening, D.W. & Simpson, R.J. (2011). Low-molecular weight plasma proteome analysis using centrifugal ultrafiltration. *Methods in Molecular Biology*, **728(1)**; 109-124
- Griffiths, H.R. (2007). In, Peptidomics: methods and applications. **Eds:** Solovieve, M., Andron, P. & Shaw, C. *Wiley-Interscience*.
- Gruenert, D.C., Finkbeiner, W.,E. & Widdicombe, J.H. (1995). Culture and transformation of human airway epithelial cells. *American Journal of Physiology, Lung Cellular and Molecular Physiology*, **268 (12)**; L347-360
- Guarino, M., Tosoni, A. & Nebuloni, M. (2009). Direct contribution of epithelium to organ fibrosis: epithelial-mesenchymal transition. *Human Pathology*, **40**; 1365-1376
- Guillot, L., Medjane, S., Le-Barille, K., Balloy, V., Danel, C., Chigard, M. Si-Tahar, M. (2004). Response of human pulmonary epithelial cells to lipopolysaccharide involves Toll-like Receptor 4 (TLR4)-dependent signalling pathways. Evidence for an intracellular compartmentalization of TLR4. *The Journal of Biological Chemistry*, **279(4)**; 2712-2718

- Gurr, J-R., Wang, A.S.S., Chen, C-H & Jan, K-Y (2005). Ultrafine titanium dioxide particles in the absence of photoactivation can induce oxidative damage to bronchial epithelial cells. *Toxicology*, **213**; 66-73
- Haeffner-Cavaillo, H., Carreno, M.P., Aussel, L. & Caroff, M. (1998). Molecular aspects of endotoxins relevant to their biological functions. *Nephrology Dialysis Transplantation*, **14**; 853-860
- Haley, P.J. (2003). Species differences in the structure and function of the immune system. *Toxicology*, **188**; 49-71
- Harvey, C.J., Thimmulappa, R.K., Singh, A., Blanke, D.J., Ling, G., Wakabayashi, N., Fujji, J., Myers, A. & Biswal, S. (2009). Nrf2-regulated glutathione recycling independent of biosynthesis is critical for cell survival during oxidative stress. *Free Radical Biology and Medicine*, **46**; 443-453
- He, D., Su, Y., Usatyuk, P.V. Spannhake, E.W., Kogut, P., Solway, J., Natarajan, V. & Zhao, Y. 2009. Lysophosphatidyl acid enhances pulmonary epithelial barrier integrity and protects endotoxin induced epithelial barrier disruption and lung injury. *Journal of Biological Chemistry*,
- Heijink, I.H., Brandenburg, S.M., Noordhoek, J.A., Postma, D.S., Slebos, D-J. & van Oosterhout, A.J.M. (2009). Characterization of cell adhesion in airway epithelial cell types using ECIS. *European Respiratory society*,
- Heinrich, P.C., Behrmann, I., Haan, S., Hermanns, H.M., Muller-Newen, G. & Schaper, F. (2003). Principle of interleukin (IL)-6-type cytokine signalling and its regulation. *Biochemical Journal*, **374**; 1-20
- Hext, P.M., Tomenson, J.A. & Thompson, P. (2005). Titanium dioxide: inhalation toxicology and epidemiology. *Annals of Occupational Hygiene*, **49(6)**; 461-472
- Heyder, J. (2004). Deposition of inhaled particles in the human respiratory tract and consequence for regional targeting in respiratory drug delivery. *Proceedings of the American Thoracic Society*, **1**; 315-320
- Hirakata, Y., Yano, H., Arai, K., Endo, S., Kanamori, H., Aoyagi, T., Hiratani, A., Kitagawa, M., Hatta, M., Yamamoto, N., Kunishima, H., Kawakami, K. & Kakil M. (2010). Monolayer culture systems with respiratory epithelial cells for evaluation of bacterial invasiveness. *The Tohoku Journal of Experimental Medicine*, **220**; 15-19
- Hirano, T., Yasukawa, K., Harada, H., Taga, T., Matsuda, T., Kashiwamura, S., Nakiyama, F., Koyama, K., Iwamatsu, A., Tsunasawa, S., Sakiyama, F., Matsui, H., Takahara, Y., Taniguchi, T. & Kishimoto, T. (1986). Complementary DNA for a novel human interleukin (BSF-2) that induces B lymphocytes to produce immunoglobulins. *Nature*, **324(73)**; Abstract
- Hoffmann, E., Dittrich-Breiholz, O., Holtmann, H. & Kracht, M. (2002). Multiple control of Interleukin-8 gene expression. *Journal of leukocyte biology*, **72**; 847-855
- Holgate, S.T., Peters-Golden, M., Panettieri, R.A. & Henderson, W.R. (2003). Roles of cysteinyl leukotrienes in airway inflammation, smooth muscle function, and remodelling. *Journal of Allergy and Clinical Immunology*, **111**; S18-36

- Holguin, F., Flores, S., Ross, Z., Cortez, M., Molina, M., Molina, L., Rincon, C., Jerrett, M., Berhane, K., Granados, A. & Romieu, I. (2007). Traffic-related exposures, airway function, inflammation, and respiratory symptoms in children. *American Journal of Respiratory Critical Care Medicine*, **176**; 1236-1242
- Hong, K.U., Reynolds, S.D., Watkins, S., Fuchs, E. & Stripp, B.R. (2004). Basal Cells are a Multipotent Progenitor Capable of Renewing the Bronchial Epithelium. *American Journal of Pathology*, **164** (2); 577-588
- Hussain, S., Boland, S., Baeza-Squiban, A., Hamel, R., Thomassen, L.C.J., Martens, J.A., Billon-Galland, M.A., Fleury-Feith, J., Moisan, F., Pairon, J.C. & Marano, F. (2009). Oxidative stress and proinflammatory effects of carbon black and titanium dioxide nanoparticles: Role of particle surface area and internalised amount. *Toxicology*, **260**; 142-149
- Hussain, S., Thomassen, L.C.J., Ferecatu, I., Borot, M-C., Andreau, K., Martens, J.A., Fleury, J., Baeza-Squiban, A., Marano, F & Boland, S (2010). Carbon black and titanium dioxide nanoparticles elicit distinct apoptotic pathways in bronchial epithelial cells. *Particle and Fibre Toxicology*, **7**(10);
- Ito, W., Kanehiro, A., Matsumoto, K., Hirano, A., Ono, K., Maruyama, H., Kataoka, M., Nakamura, T., Gelfand, E.W. & Tanimoto, M. (2005). Hepatocyte Growth factor attenuates airway hyperresponsiveness, inflammation and remodelling. *American Journal of Respiratory Cell and Molecular Biology*, **32**; 268-280
- Ishii, H., Fuji, T., Hogg, J.C., Hayashi, S., Mukae, H., Vincent, R. & Van Eden, S.F. (2004). Contribution of IL-1 beta and TNF-alpha to the initiation of the peripheral lung response to atmospheric particles (PM10). *American Journal of Physiology, Lung Cellular and Molecular Physiology*, **287**; L176-83
- Ishii, H., Hayashi, S., Hogg, J.C., Fujii, T., Goto, Y., Sakamoto, N., Mukae, H., Vincent, R. & van Eeden. Alveolar macrophage-epithelial cell interaction following exposure to atmospheric particles induces the release of mediators involved in monocyte mobilization and recruitment. *Respiratory Research*, **6**; 87-98
- Issaq, H.J. & Veenstra, T.D. (2008). Two-dimensional polyacrylamide gel electrophoresis (2D-PAGE): advances and perspectives. *Biotechniques*, **44**; 697-700
- Iyanoaga, K., Miyajima, M., Suga, M., Saita, N. & Ando, M. (1997). Alterations in cytokeratin expression by the alveolar lining epithelial cells in lung tissues from patients with idiopathic pulmonary fibrosis. *Journal of Pathology*, **182**; 217-224
- Jang, H., Kim, H.S., Moon, S.L., Lee, Y.R., Yu, K.Y., Lee, B.K., Youn, H.Z., Jeong, Y.J., Kim, B.S., Lee, S.H. & Kim, J.S. (2009). Effects of protein concentration and detergent on endotoxin reduction by ultra-filtration. *BMB reports*, **42**(7); 462-466
- Jatakanon, A., Uasuf, C., Maziak, W., Lim, S, Chung, K.F. & Barnes, P.J. (1999). Neutrophilic inflammation in severe persistent asthma. *American Journal of Respiratory and Critical Care Medicine*, **160**; 1532-1539
- Jeffery, P.K. (1997). Airway mucosa: secretory cells, mucus and mucin genes. *European Respiratory Journal*, **10**; 1655-1662

- Jersmann, H.P.A., Dransfield, I. & Hart, S.P. (2003). Fetuin/alpha₂-HS glycoprotein enhances phagocytosis of apoptotic cells and macropinocytosis of human macrophages. *Clinical Science*, **105**; 273-278
- Johnson, J.R., Roos, A., Berg, T., Nord, M. & Fuxe, J. (2011). Chronic Respiratory aeroallergen exposure in mice induces epithelial-mesenchymal transition in the large airways. *PLoS ONE*, **6**(1); e16175
- Johnson, J.R., Wiley, R.E., Fattouh, R., Swirski, F.K., Gajewska, B.U., Coyle, A.J., Gutierrez-Ramos, J.K., Ellis, R., Inman, M.D. & Jordana, M. (2004). Continuous exposure to house dust mite elicits chronic airway inflammation and structural remodelling. *American Journal of Respiratory Critical Care Medicine*, **169**; 378-385
- Jones, S.A. (2005). Directing transition from innate to acquired immunity: defining a role for IL-6. *The Journal of Immunology*, **175**; 3463-3468
- Jones, A.L., Hulett, M.D. & Parish, C.R. (2005). Histidine-rich glycoprotein: A novel adaptor protein in plasma that modifies the immune, vascular and coagulation systems. *Immunology and Cell Biology*, **83**; 106-118
- Karoly, E.D., Li, Z., Dailey, L.A., Hyseni, X. & Huang, Y.C.T. (2007). Up-regulation of tissue factor in human pulmonary artery endothelial cells after ultrafine particle exposure. *Environmental Health Perspectives*, **115**; 535-540
- Kesimer, M., Kirkham, S., Pickles, P.J., Henderson, A.G., Alexis, N.E., DeMaria, G, Knight, D., Thornton, D.J. & Sheehan, J.K. (2009). Tracheobronchial air-liquid interface cell culture: a model for innate mucosal defence of the upper airways? *American Journal of Physiology: Lung cellular and Molecular Physiology*, **296**; L92-L100.
- Khair, O., Davies, R. & Devalia, J.L. (1996). Bacterial-induced release of inflammatory mediators by bronchial epithelial cells. *European Respiratory Journal*, **9**(9); 1913-1922
- Kim, K.H. & Ramaswamy. (2009). Electrochemical surface modification of titanium in dentistry. *Dental Materials Journal*, **28**(1); 20-36
- Kim, S.W., Hong, J.S., Ryu, S.H., Chung, W.C., Yoon, J.H. & Koo, J.S. (2007). Regulation of mucin gene expression by CREB via a non-classical retinoic acid signalling pathway. *Mol Cell Biol*, **27**; 6933-6947
- Kim, Y.J., Sajjan, V.S., Krasan, G.P. & LiPuma, J.J. (2005). Disruption of Tight Junctions during Traversal of the Respiratory Epithelium by Burkholderia Cenocepacia. *Infection and Immunity*, **73**(11); 7107-7112
- Kishimoto, T. (2010). IL-6: from its discovery to clinical applications. *International Immunology*, **22**(5); 347-352
- Kishimoto, T. & Ishizaka, K. (1973). Regulation of antibody response in vitro V. Effect of carrier-specific Helper cells on generation of hapten specific memory cells of different immunological classes. *Journal of Immunology*, **111**; Abstract
- Klotz, S.A., Penn, C.C., Negvesky, G.J. & Butrus, S.I. (2000). Fungal and parasitic infections of the eye. *Clinical Microbiology Reviews*, **13**(4); 662-685

- Knowles, M.R. & Boucher, R.C. (2002). Mucus clearance as a primary innate defence mechanism for mammalian airways. *Journal of Clinical Investigation*, **109(5)**; 571-577
- Kong, X., Thimmulappa, R., Kombairaju, P. & Biswal, S. (2010). NADPH oxidase dependant reactive oxygen species mediate amplified TLR4 signalling and sepsis induced mortality in Nrf2-deficient mice. *The Journal of Immunology*, **185**; 569-577
- Koyama, S., Sato, E., Nomura, H., Kubo, K., Miura, M., Yamashita, T., Nagai, S. & Izumi, T. (2000). The potential of various lipopolysaccharides to release IL-8 and G-CSF. *American journal of Physiology. Lung Cellular and Molecular Physiology*. **278**; L658-L666
- Kreda, S.M., Okada, S.F., van Heusden, C.A., O'Neil, W., Gabriel, S., Abdullah, L., Davis, C.W., Boucher, R.C. & Lazarowski, E.R. (2007). Coordinated release of nucleotides and mucin from human epithelial Calu-3 cells. *The Journal of Physiology*, **584(1)**; 2245-259
- Kuntz, E., Hoeller, U., Greatrix, B., Lankin, C., Seifert, N., Acharya, S., Riss, G., Buchwald-Hunziker, P., Hunziker, W., Goralczyk, R. & Wertz, K. (2006). B-Carotene and apocarotenals promote retinoid signalling in BEAS-2B human bronchioepithelial cells. *Archives of Biochemistry and Biophysics*, **455**; 48-60
- Laan, M., Bozinovski, S. & Anderson, G.P. (2004). Cigarette Smoke Inhibits Lipopolysaccharide-Induced Production of Inflammatory Cytokines by Suppressing the Activation of Activator Protein-1 in Bronchial Epithelial Cells. *The journal of immunology*, **173**; 4164-4170
- Langer, H.F. & Chavakis, T. (2009). Leukocyte-Endothelial interactions in inflammation, *Journal of Cellular and Molecular Medicine*, **13(7)**; 1211-1220
- Langeveld, C.H., Jongenelen, C.A.M., Schepens, E., Stoof, J.C., Bast, A. & Drularch, B. (1995). Cultured rat striatal and cortical astrocytes protect mesencephalic dopaminergic neurons against hydrogen peroxide toxicity independent of their effect on neuronal development. *Neuroscience Letters*, **192**; 13-16
- Lavorini, F., Levy, M.L., Corrigan, C., Crompton, G. (2010). The ADMIT series – issues in inhalation therapy. 6) Training tools for inhalation devices. *Primary Care Respiratory Journal*, **19(4)**; 335-341
- Lazard, D.S., Moore, A., Huperton, V., Martin, C., Escabasse, V., Drefus, P., Burgel, P-R., Amselem, S., Escudier, E. & Coste, A. (2009). Muco-Ciliary differentiation of nasal epithelial cells is decreased after wound healing. *In Vitro. Allergy*, **64**; 1136-1143
- LeBlanc, a.J., Moseley, A.M., Chen, B.T., Frazer, D., Castranova, V. & Nurkiewicz, T.R. (2010). Nanoparticle inhalation impairs coronary microvascular reactivity via a local reactive oxygen species-dependent mechanism. *Cardiovascular Toxicology*, **10(1)**; 27-36
- Lee, H.S., Myers, A. & Kim, J. (2009). Vascular endothelial cell growth factor drives autocrine epithelial cell proliferation and survival in chronic rhinosinusitis with nasal polyposis. *American Journal of Respiratory Critical Care Medicine*, **180**; 1056-1067

- Liao, C-M., Chiang, Y-H & Chio, P-C (2008), Assessing the airborne titanium dioxide nanoparticle-related exposure hazard at workplace. *Journal of Hazardous Materials*
- Lim, M.S. & Elenitoba-Johnson, K.S.J. (2004). Proteomics in Pathology Research. *Laboratory Research*, **84(10)**; 1227-1244
- Lin, H., Cho, H-J., Bian, S., Roh, H-J., Lee, M-K., Kim, J.S., Chung, S-J., Shim, C-K. & Kim, D-D. (2007). Air-Liquid Interface (ALI) Culture of Human Bronchial Epithelial Cell Monolayers as an *In Vitro* Model for Airway Drug Transport Studies. *Journal of Pharmaceutical Sciences*, **96 (2)**; 341-350
- Ling, S.H. & van Eeden, S.F. (2009). Particulate matter air pollution exposure: role in the development and exacerbation of chronic obstructive pulmonary disease. *International Journal of Chronic Obstructive Pulmonary Disease*, **4**; 233-243
- Linke, T., Doraiswamy, S. & Harrison, E.H. (2007). Rat plasma proteomics: Effects of abundant protein depletion on proteomic analysis. *Journal of Chromatography B*, **849**; 273-281
- Lomer, M.C.E., Thompson, R.P.H. & Powell, J.J. (2002). Fine and ultrafine particles of the diet. Influence on the mucosal immune response and association with Crohn's disease. *Proceedings of the nutrition society*, **61**; 123-130
- Lu, Y.C., Yeh, W.C. & Ohashi, P.S (2008). LPS/TLR4 signal transduction pathway. *Cytokine*, **24**; 145-151
- Lundien, M.C., Mohammed, K.A., Nasreen, M., Tepper, R.S., Hardwick, J.A., Sanders, K.I., Van Horn, R.D. & Antony, V.B. (2002). Induction of MCP-1 Expression in Airway Epithelial Cells: Role of CCR2 receptor in Airway Epithelial Injury. *Journal of Clinical Immunology*, **22(3)**; 144-152
- MacGillivray, A.J. & Rickwood, D. (1974) The heterogeneity of mouse-chromatin nonhistone proteins as evidenced by two-dimensional polyacrylamide-gel electrophoresis and ion-exchanged chromatography. *European Journal of Biochemistry*, **41**; 181-190
- Magalhaes, P.O., Lopes. A.M., Mazzola, P.G., Rangel-Yagui, C., Penna, T.C. & Pessoa, A. Jr. (2007). Methods of endotoxin removal from biological preparations: a review. *Journal of Pharmacy and Pharmaceutical sciences*, **10(3)**; 388-404
- Maryanoff, B.E., de Garavilla, L., Greco, M.N., Haertlein, B.J., Wells, G.I., Andrade-Gordon, P. & Abraham, W.M. (2010). Dual Inhibition of Cathepsin G and Chymase is effective in Animal Models of Pulmonary Inflammation. *American Journal of Respiratory Critical Care Medicine*, **181**; 247-253
- Matt, P., Fu, Z., Fu, Q. & Van Eyk, J.E. (2008). Biomarker discovery; proteome fractionation and separation in biological samples. *Physiological Genomics*, **33(1)**; 12-17
- McIntyre, T.M., Prescott, S.M., Weyrich, A.S. & Zimmerman, G.A. (2003). Cell-Cell interactions: leukocyte-endothelial interactions. *Current Opinions in Haematology* **10**; 150-158

- Medina-Raman, M., Zock, J., Kogevinas, M., Sunyer, J., Torralba, Y., Borrell, A., Burgo, F. & Anto, J. (2005). Asthma, chronic bronchitis, and exposure to irritant agents in domestic cleaning. *Occupational and Environmental Medicine*, **62(9)**; 598-606
- Mestas, J. & Hughes, C.C.W. (2004). Of mice and not men: differences between mouse and human immunology. *Journal of Immunology*, **172**; 2731-2738
- Middleton, J., Americh, L., Gayon, R., Julien, D., Mansat, M., Mansat, P., Anract, P., Cantagrel, Q., Cattan, P., Reimund, J.M., Aguilar, L., Amalrich, F. & Girard, J.P. (2005). A comparative study of endothelial cell markers expressed in chronically inflamed human tissues: MECA-79, Duffy antigen receptor for chemokines, Von Willebrand factor, CD31, CD34, CD105 and CD146. *The Journal of Pathology*, **206**; 260-268
- Mikolajczyk-Pawlinska, J., Travis, J. & Potempa, J. (1998). Modulation of interleukin-8 activity by gingipains from *Porphyromonas gingivalis*: implications for pathogenicity of periodontal disease. *FEBS Letters*, **440**; 282-286
- Miller, I., Crawford, J. & Gianazza, E. (2006). Protein stains for proteomic applications: which, when, why? *Proteomics*, **6**;
- Mills, P.R., Davies, R.J. & Devalia, J.L. (1999). Airway epithelial cells, cytokines and pollutants. *American Journal of Respiratory and Critical Care Medicine*, **160**; S38-S43
- Mogel, M., Kruger, E., Krug, H.F. & Siedel, A. (1998). A new coculture system of bronchial epithelial and endothelial cells as a model for studying ozone effects on airway tissue. *Toxicology Letters*, **96(97)**; 25-32
- Moll, R., Franke, W.W. & Schiller, D.L. (1982). The Catalog of Human Cytokeratins: Patterns of Expression in Normal Epithelia, Tumours and Cultured Cells. *Cell*, **31**; 11-24
- Montuschi, P. (2010). Role of leukotrienes and leukotriene modifiers in asthma. *Pharmaceuticals*, **3**; 1792-1811
- Morris, A., Steinberg, M.L. & Defendi, V. (1985). Keratin gene expression in simian virus 40-transformed human keratinocytes. *Proceedings of the National Academy of Sciences of the United States of America*, **82(24)**; 8498-502
- Muhlfeld, C., Geiser, M., Kapp, N., Gehr, P. & Rothen-Rutishauser, B. (2007). Re-evaluation of pulmonary titanium dioxide nanoparticle distribution using the "relative deposition index": evidence for clearance through microvasculature. *Particle and Fibre Toxicology*, **4**; 7-15
- Mukaida, N. (2003). Pathophysiological roles of interleukin-8/CXCL8 in pulmonary diseases. *American Journal of Physiology; Lung Cellular and Molecular Biology*, **284**; L566-L577
- Mul, F.P., Zuubier, A.E.M., Janssen, H., Calafat, J., van Wetering, S., Hiemstra, P.S., Roos, D. & Hordijk, P.L. (2000). Sequential migration of neutrophils across monolayers of endothelial and epithelial cells. *Journal of Leukocyte Biology*, **68**; 529-537

- Mullol, J., Baraniuk, J.N., Logun, C. & Benfield, T. (1996). Endothelin-1 induces GM-CSF, IL-6 and IL-8 but not G-CSF release from a human bronchial epithelial cell line (BEAS-2B). *Neuropeptides*, **30(6)**; 551-556
- Murphey, D.M. & O'Byrne, P.M. (2010). Recent advances in the pathophysiology of Asthma. *Chest*, **137**; 1417-1426
- Murugesan, S., Kuppusami, P., Parvathavarthini, N. & Mohondas, E. (2007). Pulsed laser deposition of anatase and rutile TiO₂ thin films. *Surface and Coatings Technology*, **201**; 7713-1179
- Nakamura, T. & Minzuno, S. (2010). *Proceedings of the Japan Academy, Ser.B., Physical and Biological Sciences*, **86**; 588-610
- Nascimento, L.F.C. (2011). Air pollution and cardiovascular hospital admissions in a medium-sized city in Sao Paulo State, Brazil. *Brazilian Journal of Medical and Biological Research*, **44**; 720-724
- Nazil, A., Chan, O., Dobson-Belaire, W.N., Ouellet, M., Tremblay, M.J., Gray-Owen, S.D., Arsenault, A.L. & Kaushic, C. (2010). *PLoS PATHOGENS*, **6(4)**; e1000852
- Nazaroff, W.W. & Weschler, C.J. (2004). Cleaning products and air fresheners: exposure to primary and secondary air pollutants. *Atmospheric Environment*, **38**; 2841-2865
- Nenmar, A., Hoet, P.H.M., Vanquickenborne, B., Dinsdale, D., Thomeer, M., Hoylaerts, M.F., Vanbilloen, H., Mortelmans, L. & Nemery, B. (2002). Passage of Inhaled Particles Into the Blood Circulation in Humans. *Circulation*, **105**; 411-414
- Netteshiem, P., Seok Koo, J.A. & Gray, T. (2000). Regulation of Differentiation of the Tracheobronchial Epithelium. *Journal of Aerosol Medicine*, **13**; 207-218
- Nials, A.T. & Uddin, S. (2008). Mouse models of allergic asthma: acute and chronic allergin challenge. *Disease Models and Mechanisms*, **1(4-5)**; 213-220
- Niessen, C.M. (2007). Tight junctions/adherans junctions: basic structure and function. *Journal of Investigative Dermatology*, **127**; 2525-2532
- Nieto, M.A. (2002). The SNAIL superfamily of zinc-finger transcription factors. *Nature Reviews: Molecular Cell Biology*, **3**; 155-166
- Noah, T.L., Yankaskas, J.R., Carson, J.L., Gambling, T.M., Cazares, L.H., McKinnon, K.P. & Devlin, R.B. (1995). Tight junctions and mucin and mRNA in BEAS-2B cells. *In Vitro Cell. Dev. Biol-Animal*, **31**; 738-740
- Nohynek, G.J., Antignac, E., Re, T. & Tourain, H. (2010). Safety assessment of personal care product/cosmetics and their ingredients. *Toxicology & Applied Pharmacology*, **243**; 239-259
- Noushargh, S., Perkins, J.A., Showell, H.J., Matsushima, K., Williams, T.J. & Collins, P.D. (1992). A comparative study of the neutrophil stimulatory activity in vitro and pro-inflammatory properties in vivo of 72 amino acid and 77 amino acid IL-8. *The journal of Immunology*, **148**; 106-111

- Nurkiewicz, T.R., Porter, D.W., Barger, M., Millecchia, L., Rao, M.K., Marvar, P.J., Hubbs, A.F., Castranova, V. & Boegehold, M.A. (2006). Systemic microvascular dysfunction and inflammation after pulmonary particulate matter exposure. *Environmental Health Perspectives*, **114**; 412-419
- Ocak, S., Chaurand, P. & Massion, P.P. (2009). Mass Spectrometry-based Proteomic Profiling of Lung Cancer. *Proceedings of the American Thoracic Society*, **6(2)**; 159-170
- Ohnishi, T., M. Muroi, et al. (2007). The lipopolysaccharide-recognition mechanism in cells expressing TLR4 and CD14 but lacking MD-2. *FEMS Immunology & Medical Microbiology*, **51(1)**; 84-91
- Ostroff, R.M., Bigbee, W.L., Franklin, W., Gold, L., Mehan, M., Miller, Y.E., Pass, H.I., Rom, W.N., Siegfried, J.M., Stewart, A., Walker, J.J., Weissfeld, J.L., Williams, S., Zichi, D. & Brody, E. (2010). Unlocking biomarker discovery: large scale application of aptamer proteomic technology for early detection of lung cancer. *PLoS ONE*, **5(12)**; e15003
- O'Toole, T.E., Hellmann, J., Wheat, L., Haberzettl, P., Lee, J., Conklin, D.J., Bhatnager, A. & Pope, C.A. (2010). Episodic exposure to fine particulate air pollution decreases circulating levels of endothelial progenitor cells. *Circulation Research*, **107**; 200-203
- Parihar, A., Eubank, T.D. & Doseff, A.I. (2010). Monocytes and macrophages regulate immunity through dynamic networks of survival and cell death. *Journal of Innate Immunity*, **2**; 204-215
- Park, E-J., Yi, J., Chung, K-H., Ryu, D-Y., Choi, J. & Park, K. (2008). Oxidative stress and apoptosis induced by titanium dioxide nanoparticles in cultured BEAS-2B cells. *Toxicology Letters*, **180**; 222-229
- Park, J.H., Spiegelman, D.L., Burge, H.A., Gold, D.R., Chew, G.L. & Milton, D.K. (2000). Longitudinal study of dust and airborne endotoxin in the home. *Environmental Health Perspectives*, **108**; 1023-1028
- Pease, J.E. & Sabroe, I. (2002). The role of Interleukin-8 and its receptor in inflammatory lung disease: implications for therapy. *Am J Respir Med*, **1(1)**; 19-25
- Perry, A.K., Chen, G., Zheng, D., Tang, H. & Cheng, G. (2005). The host type I interferon response to viral and bacterial infections, *Cell Research*, **15(6)**; 407-422
- Petecchia, L., Sabatini, F., Varesio, L., Camoirano, A., Ysai, C., Pezzelo, A. & Rossi, G.A. (2009). Bronchial airway epithelial cell damage following exposure to cigarette smoke includes disassembly of tight junction components mediated by the extracellular signal-regulated kinase 1/2 pathway. *Chest*, **135(6)**; 1502-1512
- Phillips, D.C., Woollard, K.J. & Griffiths, H.R. (2003). The anti-inflammatory actions of methotrexate are critically dependent upon the production of reactive oxygen species. *British Journal of Pharmacology*, **138(3)**; 501-511
- Plopper, C., St George, J., Cardoso, W., Wu, R., Pinkerton, K. & Buckpitt, A. (1992). Development of Airway Epithelium. Patterns of expression for markers of differentiation. *Chest*, **101**; S2-S5

- Pohl, C., Hermanns, M.I., Uboldi, C., Bock, M., Fuchs, S., Dei-Anang, J., Mayer, E., Kehe, K., Kummer, W. & Kirkpatrick, C.J. (2009). Barrier functions and paracellular integrity in human cell culture models of the proximal respiratory unit. *European Journal of Pharmaceutics and Biopharmaceutics*, **72**; 339-349
- Polito, A.J. & Proud, D.P. (1998). Epithelial cells as regulators of airway inflammation. *Journal of Allergy and Clinical Immunology*, **102**; 714-718
- Pozharskaya, V., Torres-Gonzalez, E., Rojas, M., Gal, A., Amin, M., Dollard, S., Roman, J., Stecenko, A.A. & Mora, A.L. (2009). Twist: A Regulator of Epithelial-Mesenchymal Transition in Lung Fibrosis. *PlosOne*, **4 (10)**; 7559-7569
- Purkis, P.E., Steel, J.B., Mackenzie, I.C., Nathrath, W.B., Leigh, I.M. & Lane, E.B. (1990). Antibody markers of basal cells in complex epithelia, *Journal of Cell Science*, **97 (Pt 1)**; 39-50
- Qu, S., Liberda, E.N., Qu, Q. & Chen, L-C. (2010). *In vitro* assessment of the inflammatory response of respiratory endothelial cells exposed to particulate matter. *Journal of Toxicology and Environmental Health, Part A*, **73**; 1113-1121
- Quay, J.L., Reed, W., Samet, J. & Devlin, R.B. (1998). Air Pollution Particles Induce IL-6 Gene Expression in Human Airway Epithelial Cells via NF-kB Activation. *American Journal of Respiratory Cell and Molecular Biology*, **19(1)**; 98-106
- Rabilloud, T., Chevallet, M., Luche, S. & Lelong, C. (2010). Two-dimensional gel electrophoresis in proteomics: past present and future. *Journal of proteomics*, **73(11)**; 2064-77
- Rafiee, P., Ogawa, H., Heidemann, J., Li, M.S., Aslam, M. Lamirand, T.H., Fisher, P.J., Graewin, S.J., Dwinell, M.B., Johnson, C.P., Shaker, R. & Binion, D.G. (2003). Isolation and characterisation of human esophageal microvascular endothelial cells: mechanisms of inflammatory activation. *American Journal of Physiology, Gastrointestinal and Liver Physiology*, **285**; G1277-G1292
- Rahman, I. & Macnee, W. (2000). Oxidative stress and regulation of glutathione in lung inflammation. *European Respiratory Journal*, **16**; 534-554
- Ramage, L., Proudfoot, L. & Guy, K. (2004). Expression of C-reactive protein in human lung epithelial cells and upregulation by cytokines and carbon particles. *Inhalation Toxicology*, **16**; 607-13
- Randem, B.G., Ulvestad, B., Burstyn, I. & Kongerud, J. (2004). Respiratory symptoms and airflow limitations in asphalt workers. *Occupational and Environmental Medicine*, **61(4)**; 367-9
- Rao, R.M., Yang, L., Garcia-Cardena, G. & Luscinskas, F.W. (2007). Endothelial-dependent mechanisms of leukocyte recruitment to the vascular wall. *Circulation Research*, **101**; 234-247
- Raoust, E., Balloy, V., Garcia-Verdugo, I., Touqui, L., Ramphal, R. & Chigard, M. (2009). Pseudomonas aeruginosa LPS or flagellin are sufficient to activate TLR-dependant signalling in murine alveolar macrophages and airway epithelial cells. *PLoS ONE*, **4(10)**; e7259

Ratjen, F.A. (2009). Cystic Fibrosis: pathogenesis and future treatment strategies. *Respiratory Care*, **54(5)**; 595-606

Reibman, J., Hsu, T., Chen, L.C., Kumar, A., Su, W.C., Choy, W., Talbot, A. & Gordon, T. (2002). Size fractions of ambient particle matter induce granulocyte macrophage colony-stimulating factor in human bronchial epithelial cells by mitogen-activated protein kinase pathways. *American Journal of Respiratory Cellular and Molecular Biology*, **27**; 455-62

Relova, A-J., Shahana, S., Makeeva, N. & Roomans, G.M. (2005). Effects of cytokines on ICAM-1 and ZO-1 expression on human airway epithelial cells. *Cell Biology International*, **29**; 768-777

Renwick, L.C., Brown, D., Clouter, A. & Donaldson, K. (2004). Increased inflammation and altered macrophage chemotactic responses caused by two ultrafine particle types. *Occupational and Environmental Medicine*, **61(5)**; 442-447

Rietschel, E.T., Kirkae, T., Schade, U., Mamat, U., Schmidt, G., Loppnow, H., Ulmer, a.J., Zahringer, U., Seydel, U., Padova, F.D., Schreier, M. & Brade, H. (1994). Bacterial endotoxin: molecular relationships of structure to activity and function. *FASEB J*, **8**; 217-225

Riffo-Vasquez, Y. & Spina, D. (2002). Role of cytokines and chemokines in bronchial hyperresponsiveness and airway inflammation. *Pharmacology and Therapeutics*, **94**; 185-211

Riise, G.C., Ahlstedt, S., Larsson, S., Enander, I., Jones, I., Larsson, P. & Andersson, B. (1995). Bronchial inflammation in chronic bronchitis assessed by measurement of cell products in bronchial lavage fluid. *Thorax*, **50**; 360-365

Rogers, D.F. (2007). Physiology of airway mucus secretion and pathophysiology of hypersecretion. *Respiratory Care*, **52**; 1134-1146

Rosenberg, J.B., Greengard, J.S. & Montgomery, R.R. (2000). Genetic induction of a releasable pool of factor VIII in human endothelial cells. *Arteriosclerosis, thrombosis and vascular biology*, **20(12)**; 2689-95

Ross, A.J., Dailey, L.A., Brighton, L.E. & Devlin, R.B. (2007). Transcriptional profiling of mucociliary differentiation in human airway epithelial cells. *American Journal of Respiratory Cell and Molecular Biology*, **37**; 169-185

Rothen-Rutishauser, B., Muller, L., Blank, F., Brandenberger, C., Muhlfeld, C. & Gehr, P. (2008). A Newly Developed *In Vitro* Model of the Human Epithelial Airway Barrier to Study the Toxic Potential of Nanoparticles. *Altex*, **25(3)**; 191-6

Sajjan, V., Wang, Q., Zhao, Y., Gruenert, D.C. & Hershenson, M.B. (2008). Rhinovirus Disrupts the Barrier Function of Polarised Airway Epithelial Cells. *American Journal of Respiratory and Critical Care Medicine*, **178**; 1271-1281

Scarfman, A., Arora, S.K., Delmotte, P., Van Brussel, E., Mazurier, J., Ramphal, R. & Roussel, P. (2001). Recognition of Lewis X derivatives present on mucins by flagellar components of *Pseudomonas aeruginosa*. *Infection and Immunity*, **69(9)**; 5243-5248

- Schneeberger, E.E. & Lynch, R.D. (2004). The tight junction: a multifunctional complex. *American Journal of Physiology, Cell Physiology*, **286**; C1213-1228
- Schins, R.P.F. & Borm, P.J.A. (1999). Mechanisms and mediators in coal dust induced toxicity: a review. *Annual Occupational Hygiene*, **43(1)**; 7-33
- Schulz, C., Farkas, L., Wolf, K., Kratzel, K., Eissner, G. & Pfeifer, M. (2002). Differences in LPS-induced activation of bronchial epithelial cells (BEAS-2B) and Type II like pneumocytes (A-549). *Scandinavian Journal of Immunology*, **56**; 294-302
- Schulz, G.S. & Wysocki, A. (2009). Interactions between extracellular matrix and growth factors in wound healing. *Wound Repair and Regeneration*, **17**; 153-162
- Schwartz, D.A., Christ, W.J., Kleeberger, S.R. & Wohlford-Lenane, C.L. (2001). Inhibition of LPS-induced airway hyperresponsiveness and airway inflammation by LPS antagonists. *American Journal of Physiology, Lung Cellular and Molecular Physiology*, **280**; L771-L778
- Seagrave, J. C. (2008). Mechanisms and implications of air pollution particle associations with chemokines. *Toxicology and Applied Pharmacology*, **232**; 469-477
- Seydel, Y., Hawkins, L., Schrom, A.B., Heine, H., Scheel, O., Koch, M.H.J. & Brandenburg, K. (2003). The generalised endotoxic principle. *European Journal of Immunology*, **33**; 1586-92
- Sheikh, A. & Hurwitz, B. (2005). Topical antibiotics for acute bacterial conjunctivitis: Cochrane systematic review and meta-analysis update. *British Journal of General Practice*, 962-964
- Sheth, V.R., van Heeckeren, R.C., Wilson, A.G., van Heeckeren, A.M. & Pagel, M.D. (2008). Monitoring infection and inflammation in murine models of Cystic Fibrosis with magnetic resonance imaging. *Journal of Magnetic Resonance Imaging*, **28(2)**; 527-532
- Shi, y., Wang, F., He, J., Yadav, S. & Wang, H. (2010). Titanium dioxide nanoparticles cause apoptosis in BEAS-2B cells through the caspase 8/t-Bid-independent mitochondrial pathway. *Toxicology Letters*, **196**; 23-27
- Siepen, J.A., Keevil, E.J., Knight, D. & Hubbard, S.J. (2006). Prediction of missed cleavage sites in tryptic peptides aids protein identification in proteomics. *Journal of Proteome Research*, **6**; 399-408
- Sigaud, S., Goldsmith, A.A.W., Zhou, H., Yang, Z., Fedulov, A., Imrich, A. & Kobzik, L. (2007). Air pollution particles diminish bacterial clearance in the primed lungs of mice. *Toxicology and Applied Pharmacology*, **223**; 1-9.
- Singh, S., Shi, T., Duffin, R., Albrecht, C., van Berlo, D., Hohr, D., Fubini, B., Marta, G., Fenoglio, I., Borm, P.J.A & Schins, R.P.F. (2007). Endocytosis, oxidative stress and IL-8 expression in human lung epithelial cells upon treatment with fine and ultrafine TiO₂: role of the specific surface area and of surface methylation of the particles. *Toxicology and Applied Pharmacology*, **222**; 141-151

- Si-Tahar., M., Touqui, L. & Chignard, M. (2009). Innate immunity and inflammation-two facets of the same anti-infectious reaction. *Clinical and Experimental Immunology*, **156**; 194-198
- Skibinski, G., Elborn, J.S. & Ennis, M. Bronchial epithelial cell growth regulation in fibroblast cocultures: the role of hepatocyte growth factor. *American Journal of Physiology, Lung cellular and Molecular Physiology*, **293**; L69-76
- Smith, J.A. (1994). Neutrophils, host defence and inflammation: a double-edged sword, *Journal of Leukocyte Biology*, **56**; 672-686
- Smith, J.C., Lambert, J.P., Elisma, F. & Figeys, D. (2007). Proteomics in 2005/2006; Developments, Application and Challenges. *Analytical Chemistry*, **79**; 4325-4344
- Sotter, E., Vilanova, X., Llobet, E., Vasilev, E. & Correig, X. (2007). Thick film titania sensors for detecting traces of oxygen. *Sensors and Actuators B*, **127**; 567-579
- Stearns, R.C., Paulauskis, J.D. & Godleski, J.J. (2011). Endocytosis of ultrafine particles by A549 cells. *American Journal of Respiratory Cell and Molecular Biology*, **24**; 108-115
- Steed, E., Balda, M.S. & Matter, K. (2010). Dynamics and functions of tight junctions. *Trends in Cell Biology*, **20(3)**; 142-149
- Stevenson, B.R., Silicano, J.D., Mooseker, M.S. & Goodenough, D.A. (1986). Identification of ZO-1: a high molecular weight polypeptide associated with the tight junction (zonula occludens) in a variety of epithelia. *The Journal of Cell Biology*, **103**; 755-766
- Strieter, R.M., Gomperts, B.N. & Keane, M.P. (2007). The role of CXC chemokines in pulmonary fibrosis. *The Journal of Clinical Investigations*, **117(3)**; 549-558
- Stuart, B.O. (1984). Deposition and clearance of inhaled particles. *Environmental Health Perspectives*, **55**; 369-390
- Sun, T., Swindle, E.J., Collins, J.E., Holloway, J.A., Davies, D.E. & Morgan, H. (2010). On-chip epithelial barrier function assays using electrical impedance spectroscopy. *Lab on a Chip*
- Sun. Y., Wu. F., Sun.F. & Huang, P. (2008). Adenosine promotes IL-6 release in airway epithelia. *Journal of Immunology*, **180**; 4173-4181
- Swammy, M., Jamora, C., Havran, W. & Hayday, A. (2010). Epithelial decision-makers: in search of the epimmunome. *Nature Immunology*, **11(8)**; 656-665
- Sydlik, U., Bierhals, K., Soufi, M., Abel, J. & Schins, R.P.F. (2006). Ultrafine carbon particles induce apoptosis and proliferation in rat lung epithelial cells via specific signalling pathways both using EGF-R. *American Journal of Physiology, Lung Cellular and Molecular Physiology*, **291**; L725-L733
- Tamada T, Hug MJ, Frizzell RA, Bridges RJ.(2001) Microelectrode and impedance analysis of anion secretion in Calu-3 cells. *JOP*, **2(4 Suppl)**; 219-28

- Tamagawa, E., Bai, N., Morimoto, K., Gray, C., Mui, T., Yatera, K., Zhang, X., Xing, L., Li, Y., Laher, I., Sin, D.D., Man, S.F.P. & van Eeden, S.F. (2008). Particulate matter exposure induces persistent lung inflammation and endothelial dysfunction. *American Journal of Physiology; Lung Cellular and Molecular Physiology*, **295**; 79-85
- Tamaoki, J., Isono, K., Takeyama, K., Tagaya, E., Nakata, J. & Nagai, A. (2004). Ultrafine carbon particles stimulate proliferation of human airway epithelium via EGF receptor-mediated signalling pathway. *American Journal of Physiology, Lung Cellular and Molecular Physiology*, **287**; L1127-1133
- Tang, V.W. & Goodenough, D.A. (2003). Paracellular ion channel at the tight junction. *Biophysical Journal*, **84**; 1660-1673
- Tarran, R. (2004). Regulation of airway surface liquid volume and mucus transport by active ion transport. *Proceedings of the American Thoracic Society*, **1**; 42-46
- Tarrant, J.M. (2010). Blood cytokines as biomarkers of *in vivo* toxicity in preclinical safety assessment: considerations for their use. *Toxicological Sciences*, **117(1)**; 4-16
- Thebauld, B. (2010). Angiogenesis in lung development, injury and repair. *PVRI Reviews*, **2(2)**; 62-68
- Thompson, A.B., Robbins, R.A., Romberger, D.J., Sissom, J.H., Spurzem, J.R., Teschler, H. & Rennard, S.I. (1995). Immunological functions of the pulmonary epithelium. *European Respiratory Journal*, **8**; 127-149
- Tobias, P.S., Tapping, R.I. & Gegner, J.A. (1999). Endotoxin interactions with lipopolysaccharide-responsive cells. *Clinical Infectious Disease*, **28**; 476-481
- Tortora, G.J. & Grabowski, S.R. (1993). Principles of anatomy and physiology. **Seventh Edition**, 721-764
- Tschumperlin, D.J., Shively, J.D., Kikuchi, T. & Drazen, J.M. (2003). Mechanical Stress Triggers Selective Release of Fibrotic Mediators from Bronchial Epithelium. *American Journal of Respiratory Cell and Molecular Biology*, **28**; 142-149
- Vaday, G.G. & Lider, O. (2010). Extracellular matrix moieties, cytokines, and enzymes: dynamic effects on immune cell behaviour and inflammation. *Journal of Leukocyte Biology*, **67**; 149-159
- Val, S., Hussain, S., Boland, S., Hamen, R., Baeza-Squiban, A & Marano F. (2009). Carbon black and titanium dioxide nanoparticles induce pro-inflammatory responses in bronchial epithelial cells: Need for multiparametric evaluation die to adsorption artifacts. *Inhalation Toxicology*, **21(S1)**; 115-122
- Valderrey, A.D., Pozuela, M.J., Jimenez, P.A., Macia, M.D., Oliver, A. & Rotger, R. (2010). Chronic colonisation by pseudomonas aeruginosa if patients with obstructive lung diseases: cystic fibrosis, bronchiectasis and chronic obstructive pulmonary disease. *Diagnostic Microbiology and Infectious Disease*, **68**; 20-27
- Van den Biggelaar, M., Bouwens, E.A., Kootstra, N.A., Hebbel, R.P., Voorberg, J. & Merlens, K. (2009). Storage and regulated secretion of factor VIII in blood outgrowth endothelial cells. *Haematologica*, **94(5)**; 670-678

- Van Driessche, W., Kreindler, J.L., Malik, A.B., Margulies, S., Lewis, S.A. & Kim, K.-J. (2007). Interrelations/cross talk between transcellular transport function and paracellular tight junctional properties in lung epithelial and endothelial barriers. *American Journal of Physiology, Lung Cellular and Molecular Physiology*, **293**; L520-L524
- Veranth, J.M., Cutler, M.S., Kaser, E.G., Reilly, C.A. & Ypst, G.S. (2008). Effects of cell types and culture media on Interleukin-6 secretion in response to environmental particles. *Toxicology in vitro*, **22**; 498-509
- Veranth, J.M., Kaser, E.G., Veranth, M.M., Koch, M. and Yost, G.S. (2007). Cytokine response of human lung cells (BEAS-2B) treated with micron-sized and nanoparticles of metal oxides compared to soil dusts. *Particle and Fibre Toxicology*, **4**(2);
- Vivanco, F., Padial, L.R., Darde, V.M., de la Cuesta, F., Alvarez-Llamas, G., Diaz-Prieto, N. & Barderas, M.G. (2008). Proteomic biomarkers of atherosclerosis. *Biomarker Insights*, **3**; 101-113
- Walter, M. (2009). Interrelationships among HDL Metabolism, Aging and Atherosclerosis. *Atherosclerosis, Thrombosis and Vascular Biology*, **29**(9); 1244-1250
- Wan, H., Winton, H.L., Soeller, C., Stewart, G.A., Thompson, P.J., Gruenert, D.C., Cannell, M.B., Garrod, D.R. & Robinson, C. (2000). Tight junction properties of the immortalised human bronchial epithelial cell lines Calu-3 and 16HBEo⁻. *European Respiratory Journal*, **15**; 1058-1068
- Wang, H., Zheng, Y. & He, S. (2006). Induction of release and up-regulated gene expression of IL-8 in A549 by serine proteases. *BMC Cell Biology*, **7**(22);
- Wang, M., Xiao, G.G., Li, N., Xie, Y., Loo, J.A. & Nel, A. (2005). Use of a fluorescent phosphoprotein dye to characterise oxidative stress-induced signalling pathway components in macrophage and epithelial cultures exposed to diesel exhaust particle chemicals. *Electrophoresis*, **26**; 2092-2108
- Welsh, M.J. (1987). Electrolyte transport by airway epithelia. *Physiological Reviews*, **67**(4); 1143-1184
- West, A.P., Shadel, G.S. & Ghosh, S. (2011). Mitochondria in innate immune responses. *Nature Reviews, Immunology*, **11**; 389-402
- Westmoreland, C., Walker, T., Matthews, J. & Murdock, J. (1999). Preliminary Investigations into the Use of a Human Bronchial Cell Line (16HBE14o-) to Screen for Respiratory Toxins *In Vitro*. *Toxicology In Vitro*, **13**; 761-764
- Wientjes, F.B. & Segal, A.W. (2005). NADPH oxidase and the respiratory burst. *Seminars in Cell Biology*, **6**; 357-365
- Williams, O.W., Sharafkhaneh, A., Kim, U., Dickey, B.F. & Evans, C.M. (2006). Airway mucus; from production to secretion. *American Journal of Respiratory Cell and Molecular Biology*, **34**; 527-536
- Winton, H.L., Wan, H., Cannel, M.B., Gruenert, D.C., Thompson, P.J., Garrod, D.R., Stewart, G.A. & Robinson, C. (1998). Cell lines of pulmonary and non-pulmonary

origin as tools to study the effects of house dust mite proteinases on the regulation of epithelial permeability. *Clinical and Experimental Allergy*, **28**; 1273-1285

Woo, J., Chae, Y.K., Jang, S.J., Kim, M.S., Baek, J.H., Park, J.C., Trink, B., Ratovitski, E., Lee, T., Park, B., Park, M., Kang, J.H., Soria, J.C., Lee, J., Califano, J., Sidranski, D.J. & Moon, M. (2008). Membrane trafficking of AQP5 and cAMP dependant phosphorylation in bronchial epithelium. *Biochemical and Biophysical Research Communications*, **366**; 321-327

Wu, Q., Lu, Z., Verghese, M.W. & Randell, S.H. (2005). Airway epithelial cell tolerance to *Pseudomonas aeruginosa*. *Respiratory Research*, **6**; 26-41

Wu, R., Zhao, Y.H. & Chang, M.M.J. (1997). Growth and differentiation of conducting airway epithelial cells in culture. *European Respiratory Journal*, **10**; 2398-2403

Chapter 10:

10.1: Appendix one: Immunohistochemistry: method development and controls

10.1.1: Optimisation of Cytokeratin staining methods

BEAS-2B seeded onto human placental type IV collagen-coated ($10\mu\text{g}/\text{cm}^2$) 4-well slides at 5×10^4 cells/ml in 200 μl airway epithelial cell medium and cultured until confluent, or on Transwell[®] inserts as described above. Immunohistochemical staining on Transwell[®] inserts was undertaken when a differentiated monolayer was formed as indicated by TER measurements (when a TER of $>45 \Omega \times \text{cm}^2$ was reached). Cells on Transwell[®] inserts and 4 well slides were fixed with 100 μl 100% methanol (pre-cooled) for 20 minutes at -20°C and washed 3 times with 200 μl PBS. Cells were then permeabilised with 100 μl 0.1% (v/v) Triton X-100 in PBS for 30 minutes at room temperature followed by 3 washes with 200 μl PBS. Cells were then blocked with 100 μl 1% (v/v) normal goat serum in PBS for 1 hour at room temperature followed by an additional 3 washes with 200 μl PBS. Cells were incubated with 100 μl primary mouse monoclonal anti-cytokeratin antibodies, mouse monoclonal anti-fibroblast surface antigen, mouse monoclonal anti-muc5AC, mouse monoclonal anti-vimentin, mouse monoclonal anti-ZO-1 or isotype-matched control in 1% BSA (w/v) in PBS or 1% BSA in PBS alone overnight at 4°C . Cells were then washed 3 times with 200 μl PBS and incubated with 100 μl goat anti-mouse FITC-conjugated secondary antibody diluted 1:100 in 1% BSA in PBS for 1 hour at 4°C . Cells were washed a final 3 times with 200 μl PBS and mounted with hard set mounting medium containing DAPI (1 drop/well/insert) and left to set for 48 hours at 4°C in the dark. Images were taken on a Zeiss Axiovert 200M fluorescent microscope using objective 63 with a DAPI filter (exposures of 5-20ms) and a FITC filter (exposures of 50-150ms). ZO-1 images were taken at the most apical surface of cells.

10.1.2: Results

In order to determine the optimum conditions for immunohistochemical detection of cytokeratin in BEAS-2B and NHBE grown on Transwell[®] inserts, experiments were first conducted using different fixing and blocking conditions and a range of antibody concentrations (1:50, 1:100 and 1:250) on a basal, i.e. undifferentiated, BEAS-2B population in submerged culture. BEAS-2B cells were used for the initial method development as primary cells are expensive and have limited passage doublings.

10.1.2.1: Optimising antibody dilutions

In order to determine the optimum primary antibody concentration for cytokeratin 5 staining, BEAS-2B were seeded on uncoated glass coverslips and antibody dilutions of 1:50, 1:100 and 1:250 were tested. Cytokeratin 5 was detected in basal epithelial cells grown on glass coverslips at all antibody dilutions used (Figure 10.1A-C), however, there was noticeable cell loss from the coverslips (arrow head Figure 10.1A and C) in the majority of cases. Further experiments were conducted with primary cytokeratin antibody concentrations of 1:250 as this was sufficient to detect cytokeratin 5 (Figure 10.1C, arrows indicate clear staining of cytokeratin filaments). Further cytokeratin staining experiments on basal populations of BEAS-2B cells were conducted on collagen coated 4 well slides as these more closely replicate conditions used to culture cells at ALI and are easier to handle and therefore help to reduce cell loss.

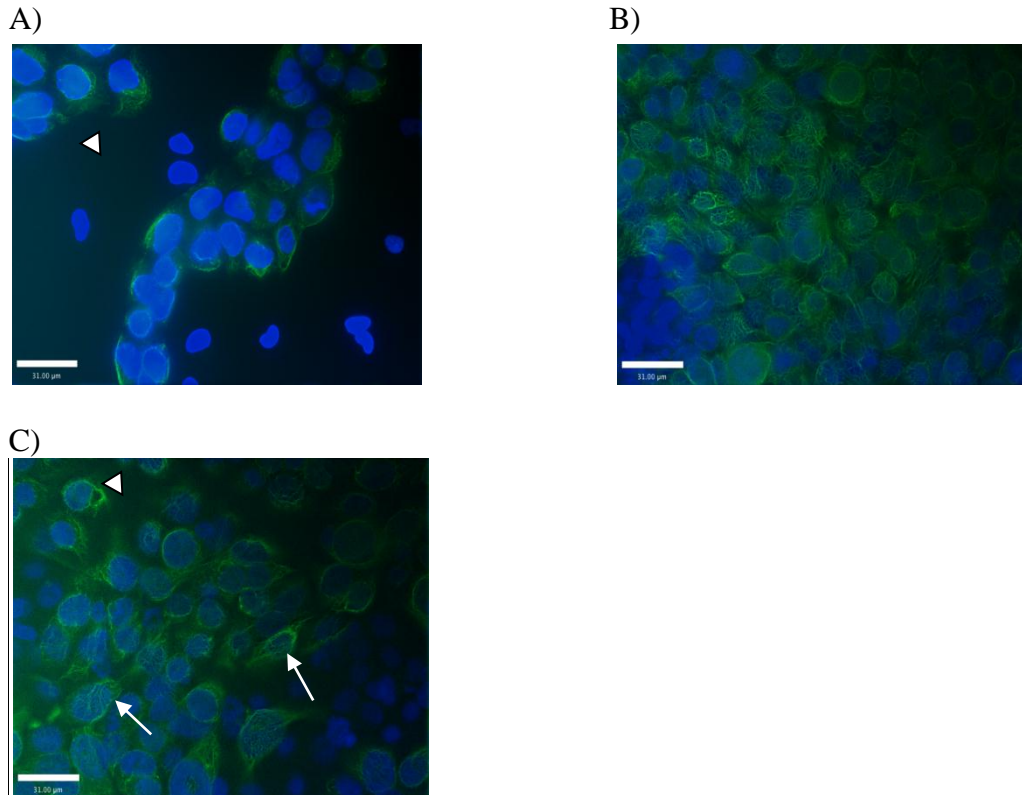


Figure 10.1: Cytokeratin 5 filaments are detected with an antibody dilution of 1:250. BEAS-2B were seeded on glass coverslips at a density of 1×10^5 cells/ml (200µl/well) and grown to confluence for 3 days. Cells were fixed with 200µl pre-cooled methanol at -20°C , blocked with 1% (v/v) normal goat serum in PBS and permeabilised with 0.1% (v/v) Triton-X-100 in PBS. Cells were then incubated with mouse-monoclonal anti-cytokeratin 5 antibody diluted 1:50 (A), 1:100 (B) or 1:250 (C) in 1% (w/v) BSA in PBS, overnight at 4°C . Cells were then washed and incubated with FITC-conjugated goat anti-mouse secondary antibody (1:100 in 1% (w/v) BSA in PBS) for 1 hour at room temperature. Cells were mounted in DAPI and images taken using a Zeiss Axiovert 200M fluorescent microscope, results are from a single experiment representative of 2 wells per antibody dilution. Scale bar indicates 31µm. Arrowheads indicate areas of cell loss and arrows indicate cytokeratin filaments.

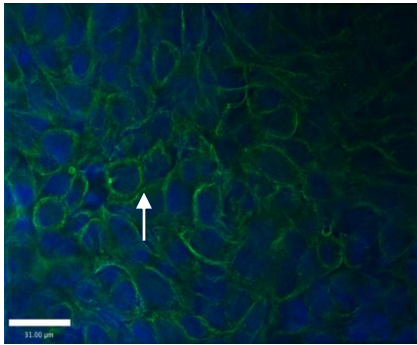
10.1.2.2: Optimising fixing and blocking conditions

In order to further optimise the cytokeratin staining method, a comparison was made between BSA and goat serum as blocking agents. In addition, fixing steps with methanol or paraformaldehyde were compared to define a protocol that produced minimal cell loss.

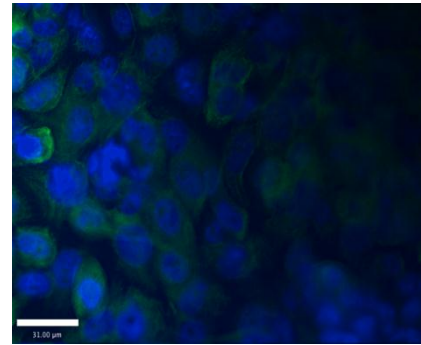
Cells were grown on collagen coated 4 well slides. The results show that following methanol fixation, cell loss was minimal and blocking with goat serum yielded a more defined cytokeratin staining pattern (Figure 10.2A, arrow) than BSA blocking (Figure 10.2B). Cells that had undergone paraformaldehyde PFA fixation appeared to have lost their cobblestone morphology and had a rounded appearance (Figure 10.2C and D arrowheads). With paraformaldehyde as a fixative there was little difference between goat serum block (Figure 10.2C) and BSA blocked (Figure 10.2D) experiments.

For further experiments methanol fixative and goat serum block were used as these conditions produced the clearest cytokeratin 5 staining with minimal cell loss.

A) Goat serum block

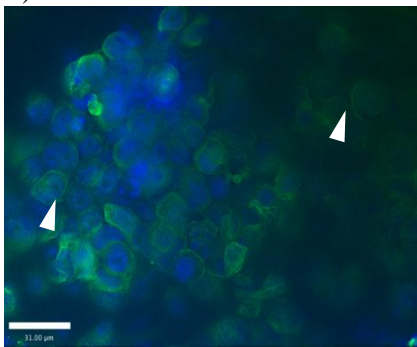


B) BSA block

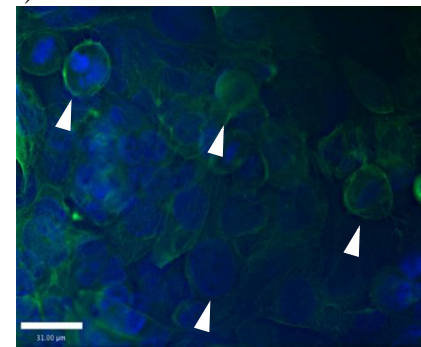


Methanol fix

C) Goat serum block



D) BSA block



PFA fix

Figure 10.2: Optimising fixing and blocking conditions BEAS-2B epithelial cells were seeded on collagen coated 4 well slides at a density of 1×10^5 cells/ml (200 μ l/well) and grown to confluence for 3 days. Cells were fixed with 200 μ l pre-cooled methanol at -20°C (A and B) or 4% (v/v) paraformaldehyde at room temperature (C and D), blocked with 1% (v/v) normal goat serum in PBS (A and C) or 1% BSA in PBS (B and D) and permeabilised with 0.1% (v/v) Triton-X-100 in PBS. Cells were then incubated with mouse-monoclonal anti-cytokeratin 5 antibodies diluted 1:250 in 1% (w/v) BSA in PBS, overnight at 4°C . Cells were washed and incubated with FITC conjugated goat anti-mouse secondary antibody (1:100 in 1% BSA in PBS) for 1 hour at room temperature. Cells were mounted in DAPI and images taken using Zeiss Axiovert 200M fluorescent microscope, images are from a 2 separate experiments. Scale bar indicates 31 μ m, arrow indicates cyokeratin filaments and arrow heads highlight cells with a rounded appearance.

10.1.2.3: Determining the specificity of the immunocytochemical method

In order to determine whether the staining is observed is specific for detection of bound primary antibodies, BEAS-2B cells were grown on collagen coated 4 well slides and incubated with either primary antibodies alone, no antibody, or isotype control (IgG1). Collagen coated slides without cells were also incubated with primary and secondary antibody to ascertain whether the primary antibody binds to the collagen. The cellular staining patterns observed with anti-cytokeratin 5 and cytokeatin 8 antibody (Figure 10.3A and B respectively) were not observed with either isotype control (Figure 10.3C) or with no primary antibody (Figure 10.3D). No staining was observed when collagen-coated slides in the absence of cells were incubated with antibodies to cytokeatin 5 (Figure 10.3E) of cytokeatin 8 (Figure 10.3F).

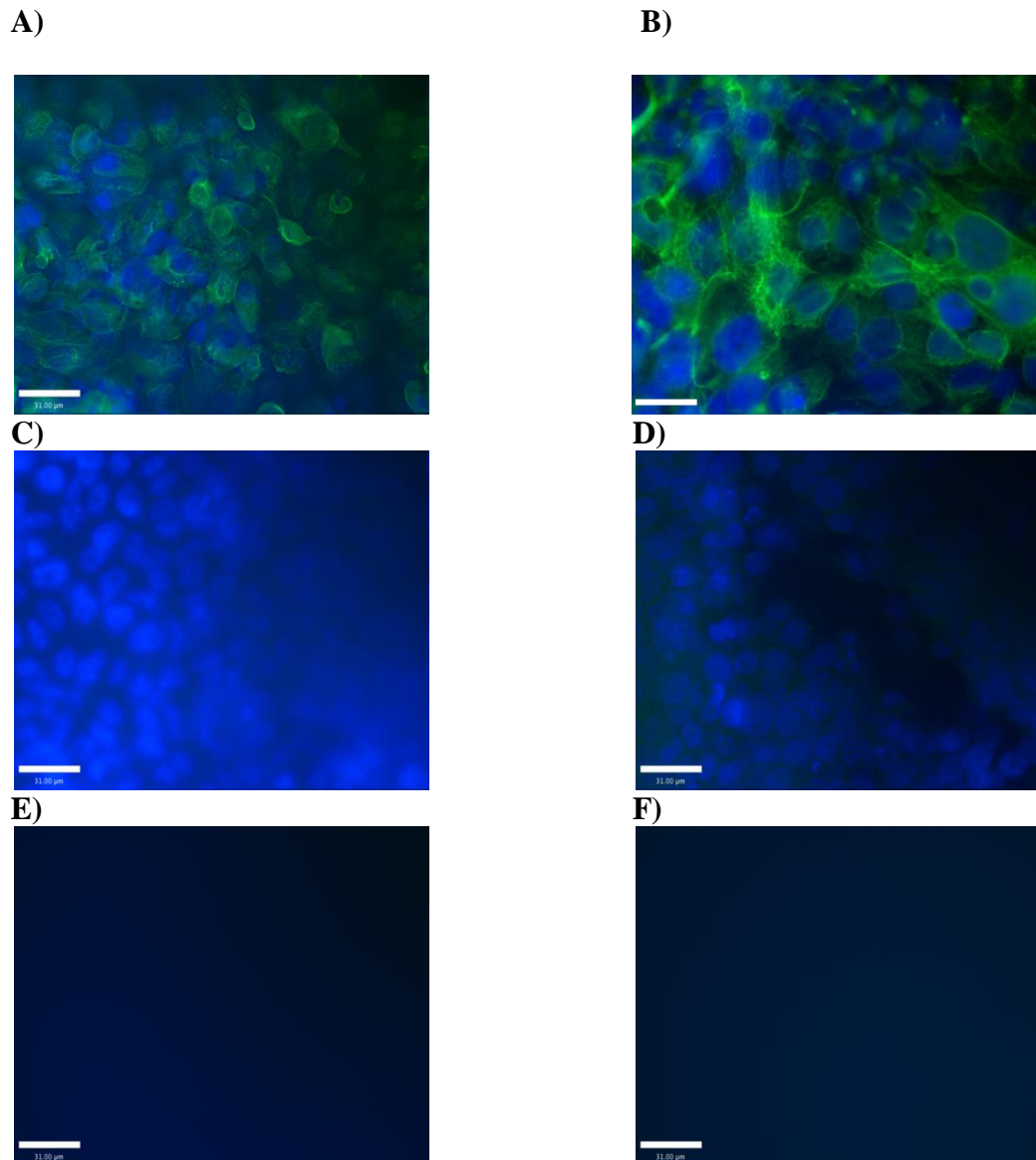


Figure 10.3: Determining the specificity of the immunocytochemical method. BEAS-2B epithelial cells were seeded on collagen coated 4 well slides at a density of 5×10^4 cells/ml (200 μ l/well) cell culture media alone (E and F) and cultured until slides with cells on had confluent cell populations. Slides were incubated with fix (200 μ l pre-cooled methanol at -20°C) and block (1% (v/v) normal goat serum in PBS) followed by permeabilising solution (0.1% (v/v) Triton X-100 in PBS). Slides were then incubated with mouse-monoclonal antibody to cytokeratin 5 (A and D), cytoekratin 8 (B and F), isotype control IgG1 (C) diluted 1:250 in 1% (v/v) BSA in PBS, or 1% (v/v) BSA in PBS alone (D) overnight at 4°C . Slides were then washed and incubated with FITC-conjugated goat anti-mouse secondary antibody (1:100 in 1% (v/v) BSA in PBS) for 1 hour at room temperature. Cells were mounted in DAPI and images taken using Zeiss Axiovert 200M fluorescent microscope, images are representative of 4 separate experiments. Scale bar indicates 31 μ m.

10.2: Appendix two: Development of a mucin dot blot

10.2.1: Mucin dot blot optimisation method

10.2.2: Results

Increased expression and secretion of the airways mucin muc5AC has been observed in ROFA PM (100µ/ml for 24 hours) challenged pulmonary mucoepidermoid carcinoma cells NCI-H292 (Longphre *et al.*, 200) In order to investigate mucous secretion from PM challenged NHBE and BEAS-2B a method to detect mucin using dot blots was developed.

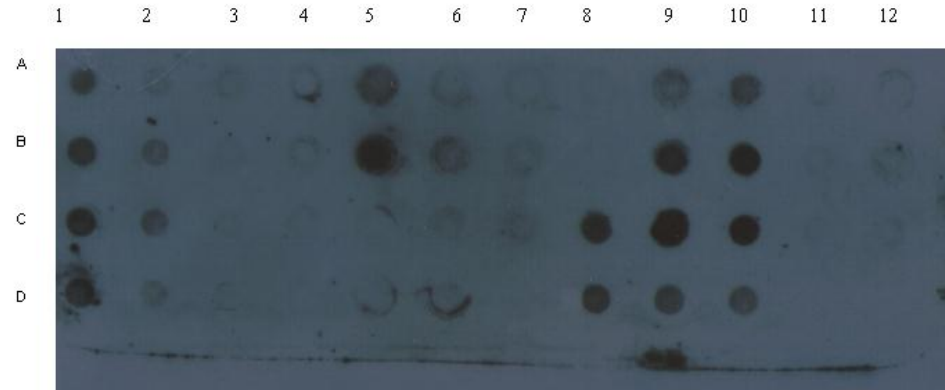
10.2.2.1: Heat denaturing or deglycosylation is not required for muc5AC detection by dot blot

The anti-Muc5AC antibody recognises the peptide core of the muc5AC protein. Since mucins are heavily glycosylated (oligosaccharides account for 65-50% of mucins molecular weight (Rose, 1992) the antibody may not be able to bind its target. Investigations were carried out to determine whether Muc5AC detection via the mouse monoclonal anti-Muc5AC primary antibody requires mucin to be denatured and/or deglycosylated. To this end, a dot blot of standard porcine mucin (which contains Muc5AC, Nordman *et al.*, 2002) under denaturing or deglycosylated conditions was compared to that of native mucin. Denaturing of the mucin may be required mucin is heavily glycosylated (~80%) which may prevent the anti-muc5AC antibody binding its target, the peptide core of mucin. BSA was used as a control for mucin detection via the anti-Muc5AC antibody.

The results indicate that the anti-muc5AC antibody detects mucin in its native form at concentrations of 5µg/well (Figure 10.4A5 and B5) and 1.25µg/well (Figure 10.4A6 and B6) but not at 0.6µg/well (Figure 10.4A7 and B7). Chemical and/or heat denaturation of the mucin standard did not prevent detection by the antibody (Figure 10.4 dots labelled A1, 2, B1, 2, show heat and chemical denatured samples and dots C1, 2, D1, 2, indicate heat denatured only). BSA was not detected by the anti-Muc5AC antibody at any of the concentrations tested (Figure 10.4C and D, 5-7).

To investigate whether the presence of lysis buffer (Triton X-100) affects mucin detection by anti-muc5AC, mucin (5µg/well) was applied to the membrane in different

concentrations of lysis buffer. The results (Figure 10.4) show that none of the concentrations of Triton X-100 used (Figure 10.4 1% A9 A10, 0.1% B9 B10, 0.5% C9 C10) affected mucin detection, and that lysis buffer alone was not detected by anti-muc5AC antibody at the concentrations tested (1% A11, 12, (0.1% Figure 10.4 B11,12 0.5% B11,12). However, the results also show that there is some cross-reaction with serum-free airway epithelial medium (QAEM, shown in C8 and D8).

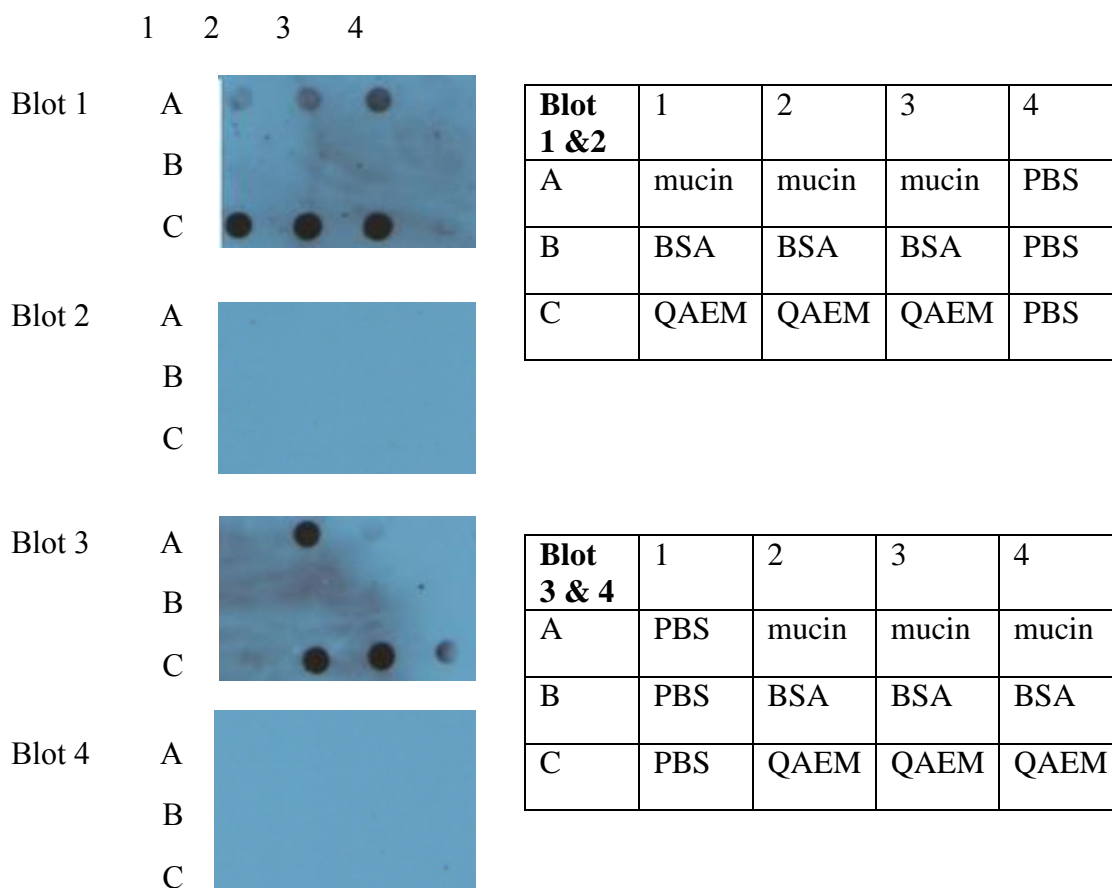


	1	2	3	4	5	6	7	8	9	10	11	12
A	5µg M D+ H+	1.25µg M D+ H+	0.6µg M D+ H+	PBS D+H+	5µg M D- H-	1.25µg M D- H-	0.6µg M D- H-	PBS D-H-	5µg M 1%T	5µg M 1%T	1% T	1% T
B	5µg M D+ H+	1.25µg M D+ H+	0.6µg M D+ H+	PBS D+H+	5µg M D- H-	1.25µg M D- H-	0.6µg M D- H-	PBS D-H-	5µg M 0.1%T	5µg M 0.1%T	0.1% T	0.1% T
C	5µg M D- H+	1.25µg M D- H+	0.6µg M D- H+	PBS D-H+	5µg BSA	1.25µg BSA	0.6µg BSA	QAEM	5µg M 0.5%T	5µg M 0.5%T	0.5% T	0.5% T
D	5µg M D- H+	1.25µg M D- H+	0.6µg M D- H+	PBS D-H+	5 µg BSA	1.25µg BSA	0.6µg BSA	QAEM	AEM 5%T	AEM 5%T		

Figure 10.4: Heat denaturing or deglycosylation is not required for muc5AC detection by dot blot. Standard porcine gastric mucin (M) and BSA (5µg 1.25µg, 0.6µg) in 50µl PBS were either denatured by boiling at 100°C for 10 minutes (H+), denatured by treatment with 2% octyl β-D-glucopyranoside with 100mM 2-mercaptoethanol and boiled at 100°C for 10 minutes (D+), or with no treatment(H-D). PBS samples were also denatured in the above manner as controls. Airway epithelial medium with 5% serum (AEM) or serum free (QAEM) along with mucin (5µg) in Triton X-100 (percentage of Triton indicated in the table) or Triton X-100 alone were also analysed. The samples were blotted onto nitrocellulose membrane under vacuum. The membrane was subsequently blocked and stained with primary mouse monoclonal anti-muc5AC antibody diluted 1:500, washed and treated with HRP-conjugated sheep anti-mouse antibody at 1: 1000. The scanned image is representative of two independent experiments.

10.2.2.2: HRP-conjugated sheep anti-mouse secondary antibody at a dilution of 1:1000 cross reacts with serum free airway epithelial cell medium.

In order to identify whether the mouse monoclonal anti-muc5AC antibody or HRP-conjugated sheep anti-mouse) cross-react with complete and serum-free airway epithelial cell medium (QAEM), a series of control dot blots were carried out (Figure 10.5). These results confirm that the HRP-conjugated sheep anti-mouse secondary antibody was cross reacting with serum free medium (Figure 10.5 blot 3 C2, 3 and 4).

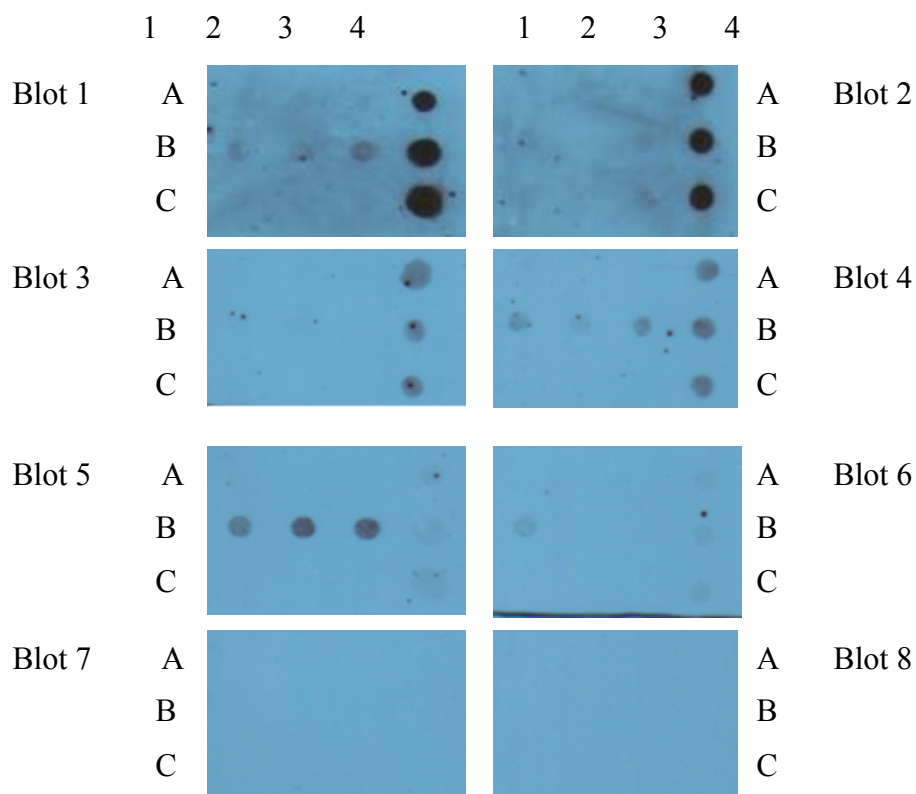


Blot	Mouse monoclonal anti-Muc5AC dilution	HRP-conjugated sheep anti-mouse antibody dilution
1	1:500	1:1000
2	1:500	No antibody
3	No antibody	1:1000
4	No antibody	No antibody

Figure 10.5: HRP-conjugated sheep anti-mouse secondary antibody at a dilution of 1:1000 cross reacts with serum free airway epithelial cell medium. Mucin standard and BSA (5µg in 50µl PBS) along with PBS or serum free airway epithelial cell medium (QAEM) were blotted onto nitrocellulose membrane. The membrane was subsequently blocked and treated with primary mouse monoclonal anti-muc5AC antibody diluted 1:500 (1 and 2) or with no antibody (3 and 4) washed and treated with horseradish peroxidase linked sheep anti-mouse antibody at 1: 1000 (1 and 3) or no secondary antibody (2 and 4).

10.2.2.3: HRP-conjugated sheep anti-mouse secondary antibody diluted 1:5000 shows minimal cross reaction with serum free airway epithelial cell medium

In order to determine a HRP sheep anti-mouse secondary antibody concentration that allows for specific muc5AC detection but does not cross react with serum free airway epithelial cell medium a series of antibody titrations was conducted. Results show that, secondary antibody concentrations of 1:1000 (Figure 10.6 blot 2) and 1:2500 (Figure 10.6 blot 4) show cross-reactivity with quiescent airway epithelial cell medium. A secondary antibody concentration of 1:5000 allows for muc5AC detection (Figure 10.6 blot 5) with minimal quiescent AEM cross reactivity (Figure 10.6 blot 6). No muc5AC was detected in either of the controls (Figure 10.6 blot 7; mouse monoclonal anti-muc5AC primary antibody without HRP-conjugated sheep anti-mouse secondary antibody, and blot 8, no antibodies).



Blot	Mouse monoclonal anti-muc5Ac antibody dilution	HRP-conjugated sheep anti-mouse antibody dilution
1	1:500	1:1000
2	No antibody	1:1000
3	1:500	1:2500
4	No antibody	1:2500
5	1:500	1:5000
6	No antibody	1:5000
7	1:500	No antibody
8	No antibody	No antibody

	1	2	3	4
A	PBS	PBS	PBS	QAEM
B	mucin	mucin	mucin	QAEM
C	BSA	BSA	BSA	QAEM

Figure 10.6: HRP-conjugated sheep anti-mouse secondary antibody diluted 1:5000 shows minimal cross reaction with serum free airway epithelial cell medium (QAEM). Mucin standard and BSA (5 μ g in 50 μ l PBS) along with PBS or QAEM were blotted onto nitrocellulose membrane. The membrane was subsequently blocked and treated with primary mouse monoclonal anti-muc5AC antibody at 1:500 or with no antibody, washed and treated with HRP-conjugated sheep anti-mouse antibody at the stated dilutions or without secondary antibody n=1.

10.2.2.4: HRP-conjugated sheep anti-mouse secondary antibody diluted 1:5000 allows for detection of 1.25 μ g muc5AC

Once conditions were defined that allowed specific detection of muc5AC, a dot blot was carried out with a range of standard porcine mucin concentrations. The results show that with a secondary antibody concentration of 1:5000 (Figure 10.7 blot 1) mucin was detected at the lowest concentration tested (1.25 μ g/well; Figure 10.7, blot 1 row F). However, with this secondary antibody concentration there is still cross-reaction with serum-free medium (Figure 10.7 rows A and L).

In an attempt to reduce cross reactivity whilst keeping the assay sensitivity, the dot blot was repeated with a secondary antibody dilution of 1:10,000. The results (Figure 10.7) show that the serum-free airway epithelial cell medium cross reactivity was nearly abolished (Figure 10.7, blot 2 rows column A and L) however the assay sensitivity was markedly reduced, with the lowest mucin concentration detected being 5 μ g/ml (Figure 10.7; Blot 2, row D). For further studies a dilution of 1:5000 for HRP-conjugated sheep anti-mouse secondary antibody was used to maintain assay sensitivity.

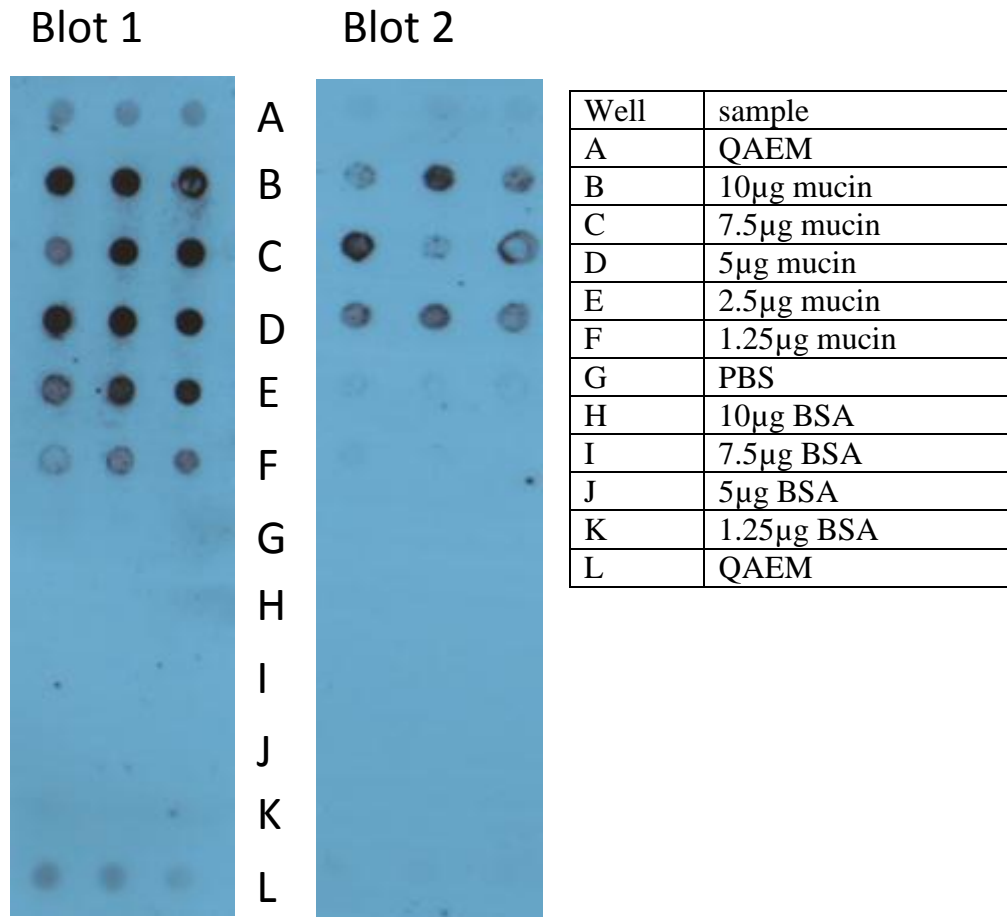


Figure 10.7: HRP-conjugated sheep anti-mouse secondary antibody diluted 1:5000 allows for detection of 1.25 μ g muc5AC. Standard porcine mucin and BSA (10 μ g-1.25 μ g in 50 μ l PBS) along with PBS or serum free airway epithelial cell medium (QAEM) were blotted onto nitrocellulose membrane. The membrane was subsequently blocked and treated primary mouse monoclonal anti-muc5AC antibody at 1:500, washed and treated with HRP-linked sheep anti-mouse antibody at 1:5000 (blot 1) or 1:10,000 (blot 2), n=1.

10.3: Appendix three: Particle method controls

10.3.1: Methods

10.3.1.1: IL-8/IL-6 ELISA

Standards IL-8/IL-6 was incubated with 100µg/ml particles at 37°C for 24hours. Samples were cleared by centrifugation at 295xg for 2 minutes. IL-8/IL-6 ELISA's were carried out as described in section 2.2.5.

10.3.1.2: CellTiter-Blue[®] viability assay

Un-converted CellTiter-Blue[®] reagent was incubated with 100µg/ml particles at 37°C for 4 hours, after which fluorescence was determined as described in section 2.2.6.

10.3.1.3: TER acquisition

TER was taken of a collagen coated Transwell[®] insert in the absence of cells with 600µl AEM in the basolateral compartment and 300µl AEM with or without 100µg/ml particles as described in 2.2.2.

10.3.1.4: Respiratory burst assay

Human recombinant IL-8 (10ng) was incubated with 100µg/ml particles at 37°C for 24 hours. Following incubation the respiratory burst assay was conducted in the absence of neutrophils as described in section 5.3.10.

10.3.1.5: GSH-Glo[™] assay

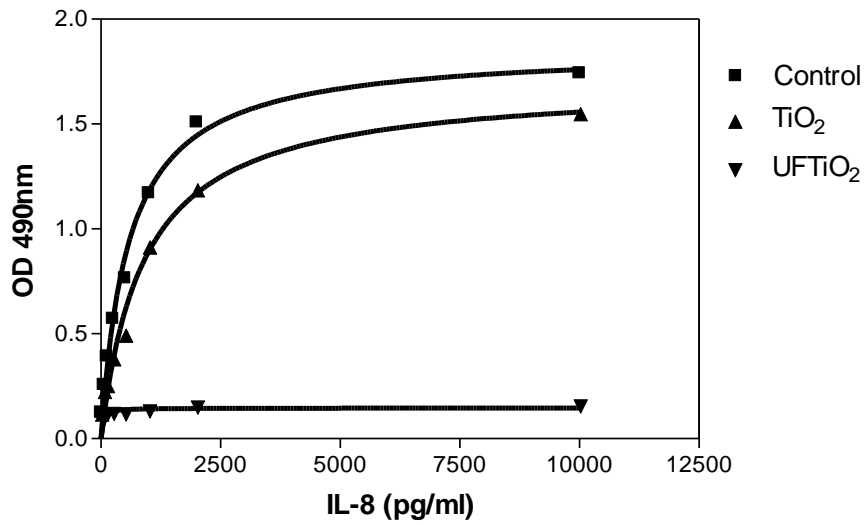
GSH-Glo[™] assay was conducted in the presence of 100µg/ml particles and absence of cells, as described in 5.3.12.

10.3.2: Results

10.3.2.1: UFTiO₂ treated IL-8 is not detected by IL-8 ELISA

IL-8 has been reported to adsorb onto DEP particle surface (Segrave 2008). To test for adsorption of IL-8 onto test particles IL-8 standards were incubated at 37°C for 24 hours with or without TiO₂, UFTiO₂ or S2219200, S2218600 and S2429901, and the IL-8 ELISA carried out. Figure 10.8A indicates that UFTiO₂ results in a loss of IL-8 detection but other particles did not interfere with IL-8 analysis using ELISA (Figure 10.8B).

A)



B)

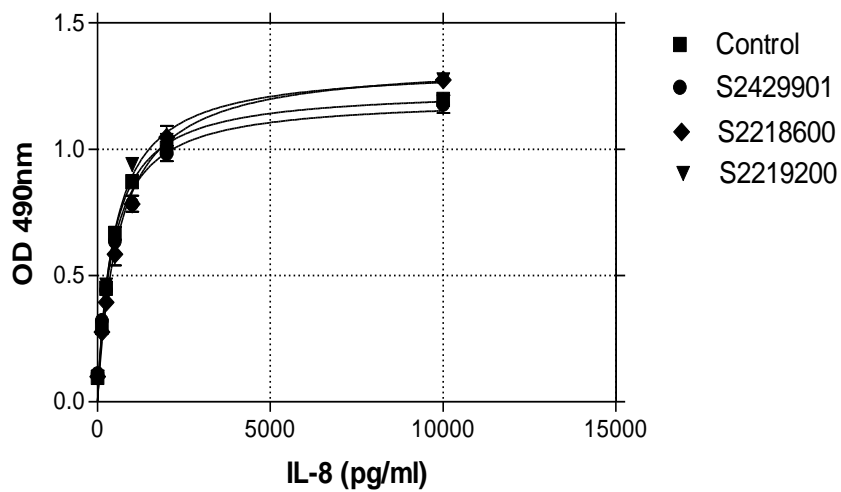
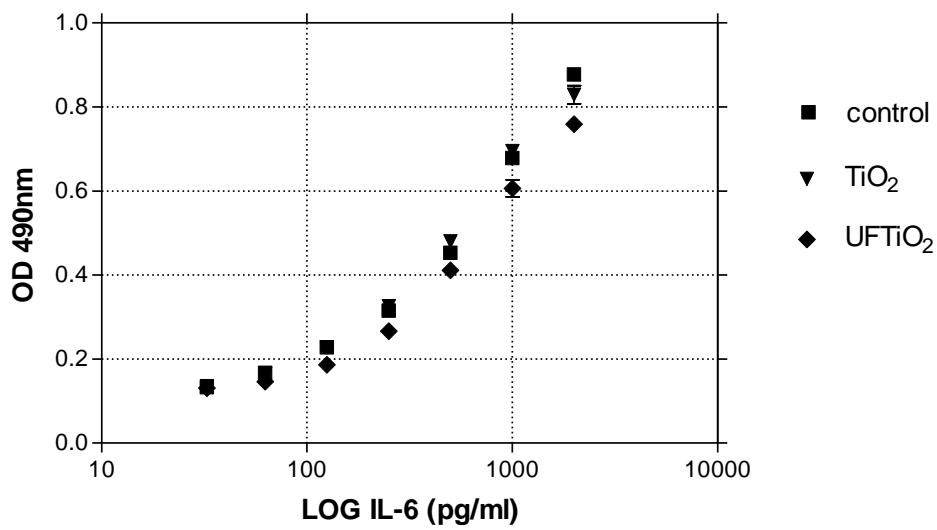


Figure 10.8: UFTiO₂ treated IL-8 is not detected by IL-8 ELISA. IL-8 ELISA standards were incubated for 24 hours at 37°C with 100µg/ml *particles* and analysed by ELISA. Results are expressed as mean ± SD of inter-assay duplicates and are representative of 3 individual experiments

10.3.2.2: PM/polymer-treated IL-6 is detected by IL-6 ELISA

To test for adsorption of IL-6 onto particles, IL-6 standards were incubated at 37°C for 24 hours with or without PM (100µg/ml). Samples were cleared by centrifugation at 295xg for 2 minutes. IL-6 ELISA was carried out with cleared IL-6 standards as above. Figure 10.9A and 10.9B indicate that particles treatment of standards does not result in a loss of IL-6 detection.

A)



B)

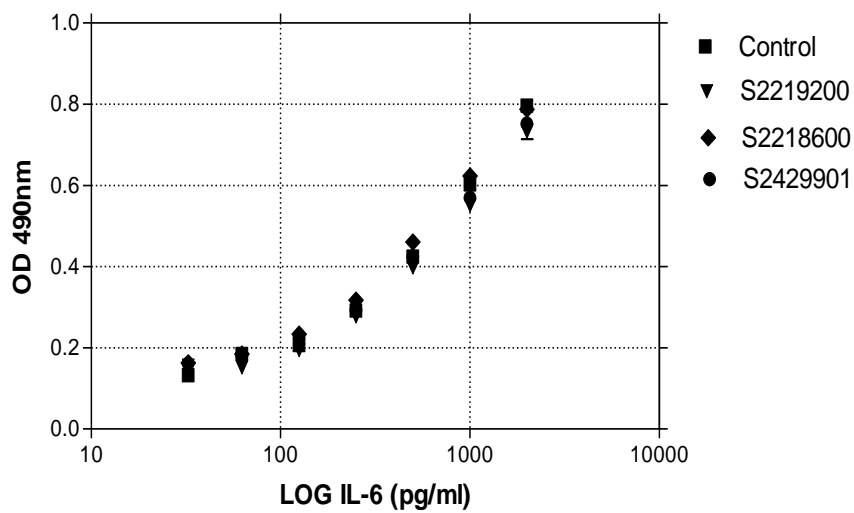


Figure 10.9: Particles -treated IL-6 is detected by IL-6 ELISA. IL-6 ELISA standards were incubated for 24 hours at 37°C with 100µg/ml particles and analysed by ELISA. Results are expressed as mean ± SD of inter-assay duplicates and are representative of 3 individual experiments.

10.3.2.3: S2218600 and S2429901 reduce the CellTiter-Blue® viability assay signal significantly.

In order to investigate interference of particles with CellTiter-Blue®, un-converted reagent was incubated for 4 hours with 100µg/ml PM in airway epithelial cell media and endothelial cell culture media, after which fluorescence was measured as above. S2218600 and S2429901 result in a slight, but significant reduction in fluorescence in airway epithelial cell media (Figure 10.10B).

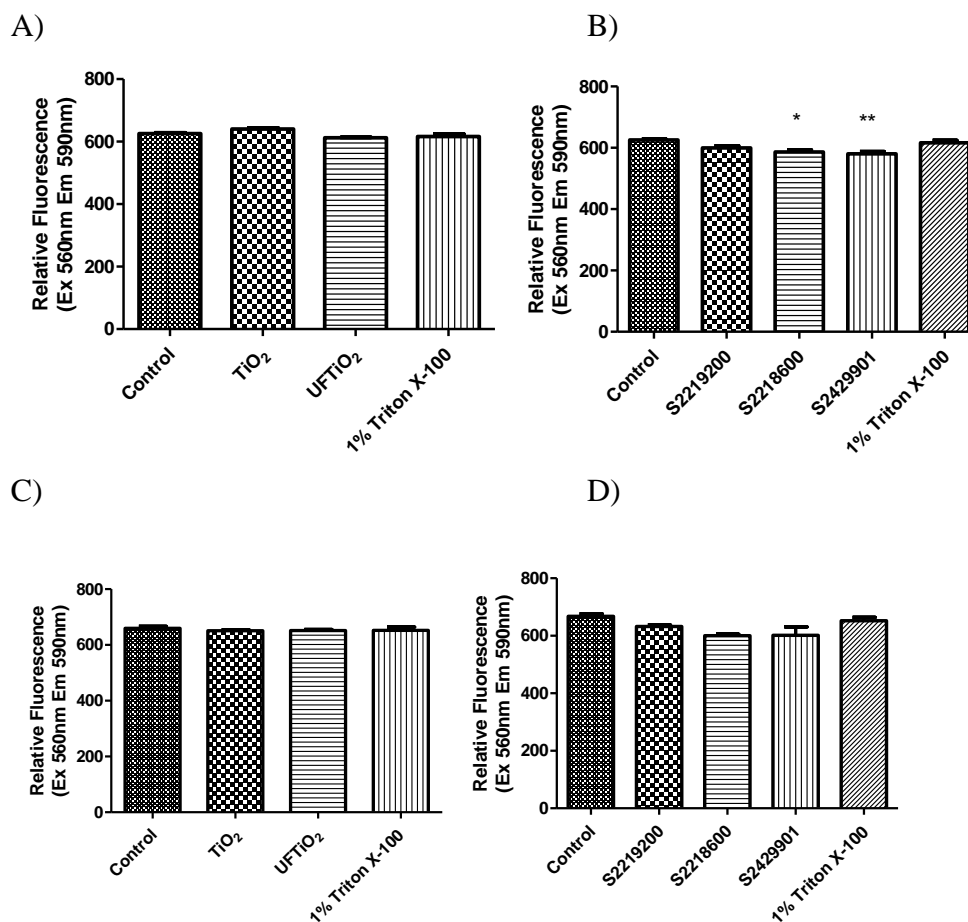


Figure 10.10: S2218600 and S2429901 reduce the CellTiter-Blue® signal significantly. CellTiter-Blue reagent was incubated with particles or 1% (v/v) Triton X-100 in the absence of cells in airway epithelial cell media (A and B) or endothelial cell culture media (C and D). After incubation fluorescence was measured at excitation 560nm emission 590nm. Results are expressed as mean \pm SEM, n=3, * $=P<0.05$ compared to control, ** $P<0.001$ compared to control.

10.3.2.4: The presence of particles do not affect TER acquisition

Westmoreland *et al.*, (1999) observed that sodium carbonate as a positive control for airway damage induced a significant time dependent reduction in TER, which correlated to loss of viability using MTT. TER was therefore used in the current study to investigate the effects of particles or LPS on the airways epithelium barrier. Triton X-100 was used as a positive control. To test for interference of particles on TER, TER of empty collagen coated Transwell[®] insert with 600µl airway epithelial cell media in the basolateral compartment and 100µg/ml particles in 300µl airway epithelial cell media, 1% (v/v) Triton X-100 in 300µl airway epithelial cell media or epithelial cell media alone in the apical compartment. TER was measured as above. Figure 10.11 shows that TER was unaffected by the presence of particles.

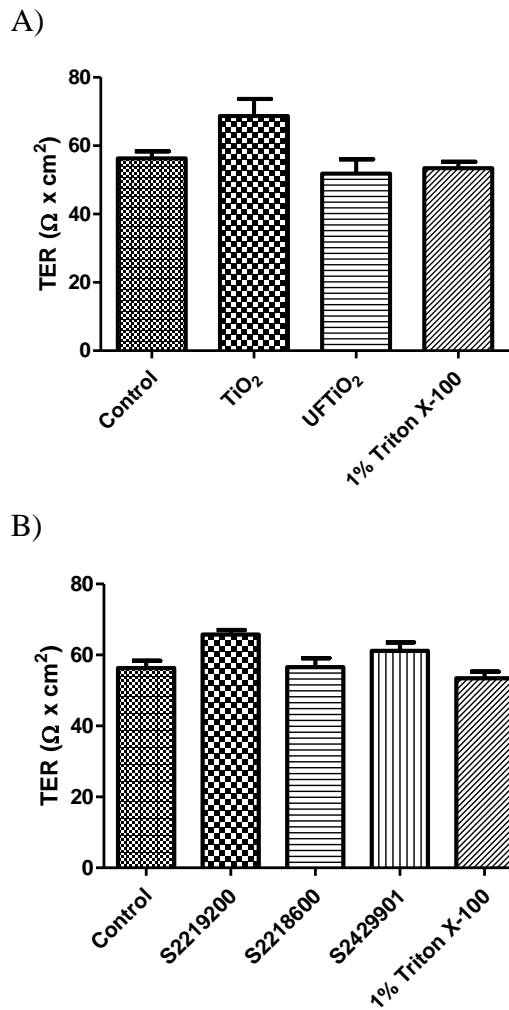


Figure 10.11: The presence of particles do not affect TER acquisition. TER of serum free airway epithelial cell media with or without 100 μ g/ml PM or 1% (v/v) Triton X-100 was taken using an empty collagen coated Transwell[®] insert. Results are expressed as mean \pm SEM, n=3 **.

10.3.2.5: The lucigenin signal is not affected by particles.

Control experiments were conducted to test for particle interference with the lucigenin signal. Figure 10.12 shows that there was no interference in luminescence with any of the test PM.

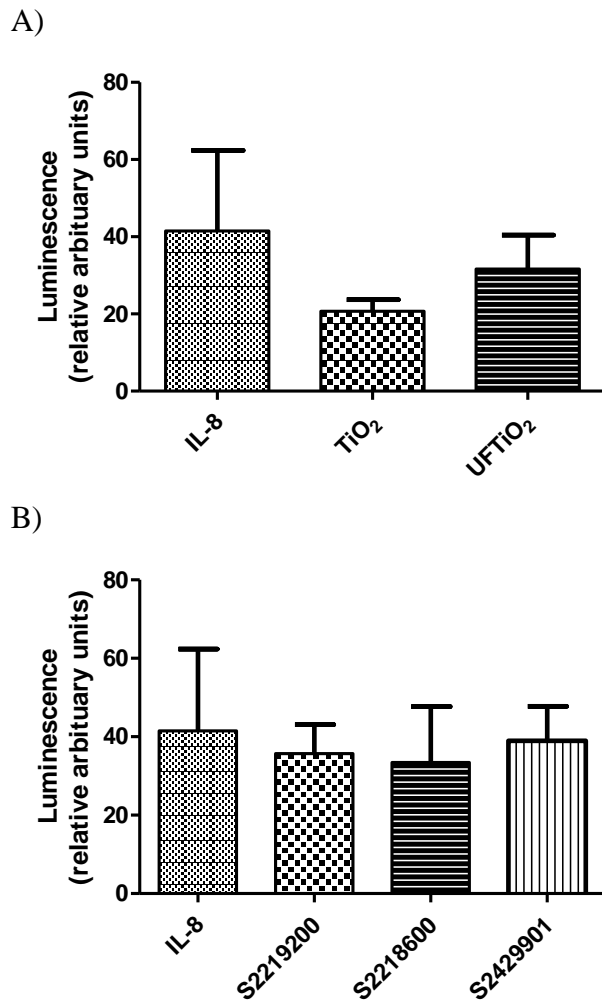
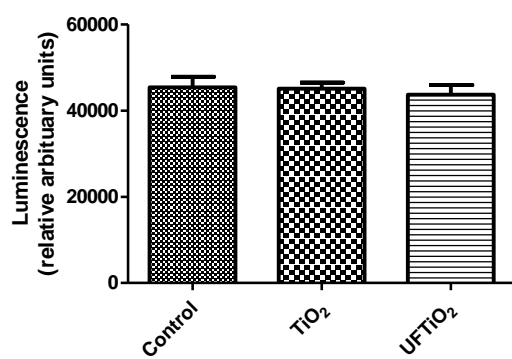


Figure 10.12: The lucigenin signal is not effected by particles. Lucigenin was incubated with particle bound IL-8 for 15 minutes during which time baseline luminescence was measured. Results are expressed as mean \pm SEM, n=3.

10.3.2.6: Effect of particles on the GSH-Glo™ assay

The ability of particles to induce oxidative damage in BEAS-2B and HPMEC was investigated with the GSH-GLO™ assay. To test for possible interference in signal by particles, the assay reagents were incubated with 100µg/ml particles in the absence of cells. Figure 10.13 shows that there was no interference with the assay by particles.

A)



B)

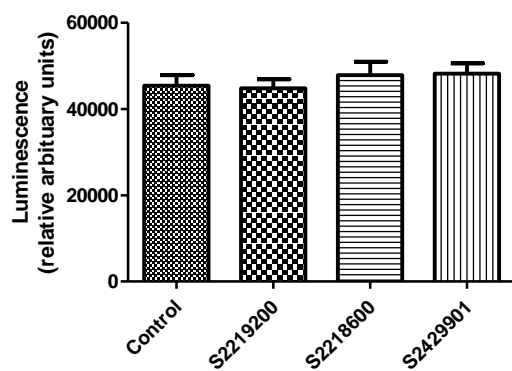


Figure 10.13: Effect of particles treatment on GSH-Glo™ GSH assay. GSH-Glo™ was conducted in a cell free system in the presence of 100µg/ml particles. Results are expressed as mean ± SEM n=3.